J/ψ production in deep inelastic scattering

Dissertation
zur Erlangung des Doktorgrades
des Fachbereichs Physik
der Universität Hamburg

vorgelegt von
Lennart Zwirner
aus Paderborn

Hamburg
2003

Gutachter der Dissertation: Prof. Dr. B.A.Kniehl
Prof. Dr. G.Kramer

Gutachter der Disputation: Prof. Dr. B.A.Kniehl
Prof. Dr. W.Buchmüller

Datum der Disputation: 28.10.2003

Vorsitzender des Prüfungsausschusses: Prof. Dr. G.Mack

Vorsitzender des Promotionsausschusses: Prof. Dr. R.Wiesendanger

Dekan des Fachbereichs Physik: Prof. Dr. G.Huber

Abstract

We investigate, at Born level, J/ψ inclusive production in $e^{\pm}p$ electromagnetic deep inelastic scattering (DIS) in the H1 experiment at DESY HERA as well as in νN neutral and charged current DIS in the CHORUS and NOMAD experiments at CERN, both within the color singlet model (CSM) and in the factorization formalism of nonrelativistic Quantum Chromodynamics (NRQCD). We find, that in case of the H1 experiment the data tend to support the NRQCD rather than the CSM predictions. Concerning the NOMAD and CHORUS experiments, only a measurement of the total cross section for J/ψ inclusive production in neutral current DIS is available. In addition to calculating the corresponding CSM and NRQCD predictions we also estimate the diffractive contribution within the Vector Dominance Model. Both, the CSM prediction together with the diffractive contribution as well as the NRQCD prediction together with the diffractive contribution are found to underestimate the measurement by more than one or nearly one order of magnitude, respectively. Finally, we calculate the ${}^1S_0^{(8)}$ part of the next leading order corrections to J/ψ inclusive production in $e^{\pm}p$ electromagnetic DIS.

Zusammenfassung

Wir untersuchen auf Born Niveau im Rahmen des Farbsingulett Modells (CSM) als auch des Faktorisierungsformalismus nichtrelativistischer Quantenchromodynamik (NRQCD) inklusive J/ψ Produktion in tief inelastischer $e^{\pm}p$ Streuung über die elektromagnetische Wechselwirkung im H1 Experiment bei DESY HERA und in tief inelastischer νN Streuung über die neutrale wie auch die geladene Strom Wechselwirkung in den CHORUS und NOMAD Experimenten bei CERN. Es zeigt sich, daß im Falle des H1 Experiments die Meßdaten die NRQCD Vorhersagen gegenüber den CSM Vorhersagen begünstigen. Im Falle der NOMAD und CHORUS Experimente existiert nur eine Messung des totalen Wirkungsquerschnitts für inklusive J/ψ Produktion in tief inelastischer νN Streuung über die neutrale Strom Wechselwirkung. Neben der Berechnung der entsprechenden CSM und NRQCD Vorhersagen schätzen wir auch den diffraktiven Beitrag im Vektor Dominanz Modell ab. Es stellt sich heraus, daß sowohl die CSM Vorhersage mit dem Diffraktionsbeitrag zusammengenommen wie auch die NRQCD Vorhersage mit dem Diffraktionsbeitrag zusammengenommen die Messung um mehr als eine bzw. ungefähr eine Größenordnung untertrifft. Wir berechnen auch den ${}^1S_0^{(8)}$ Anteil der Korrekturen nächstführender Ordnung zu inklusiver J/ψ Produktion in tief inelastischer $e^{\pm}p$ Streuung über die elektromagnetische Wechselwirkung.

Contents

1 Introduction **7**

2 NRQCD as an effective field theory of heavy quarkonia **13**
2.1 The effective lagrangian of NRQCD 14
2.2 The scaling rules of NRQCD 21
2.3 Decay and production of heavy quarkonia 23
2.4 Heavy quark spin symmetry and vaccuum saturation approximation 26

3 The short distance coefficients for heavy quarkonium production **29**
3.1 The covariant projection method 29
3.2 Derivation of the covariant projection method 31

4 J/ψ inclusive production in lN DIS at Born level **49**
4.1 The analytical calculations 49
4.1.1 Single J/ψ inclusive production in lN electromagnetic and neutral current DIS 50
4.1.2 J/ψ plus jet inclusive production in lN electromagnetic and neutral current DIS 58
4.1.3 J/ψ plus jet inclusive production in lN charged current DIS 63
4.2 Predictions for H1 at DESY HERA and CHORUS and NOMAD at CERN 67
4.2.1 Differential distributions for H1 71
4.2.2 Differential distributions for CHORUS and NOMAD 78
4.2.3 Estimation of the diffractive background in neutral current J/ψ production 84

5 Single J/ψ inclusive production in $e^{\pm}p$ electromagnetic DIS at next leading order **89**
5.1 The analytical calculation 89
5.1.1 The real corrections 92
5.1.2 The virtual corrections 99
5.1.3 The analytical total result 107
5.2 Numerical analysis 108

6 Summary and outlook **115**

A The short distance coefficients of the Born processes **117**
A.1 The processes $lN \to l(J/\psi)_{\rm prompt} jX$ with $l = \nu_e, \overline{\nu}_e, e^{\pm}$ 117
A.2 The process $\nu_e N \to e^-(J/\psi)_{\rm prompt} jX$ 126

B Formulae concerning the calculation of $\sigma\left(e^{\pm}p \to e^{\pm}J/\psi X'\right)$ at $o(\alpha^2\alpha_s^2)$ **141**
B.1 The integration measure $\frac{d^{D-1}\vec{p}'}{(2\pi)^{D-1}2p'^0}$ 141
B.2 ρ- and +-distributions 144
B.3 ϵ-expansion of $\frac{(16\pi)^\epsilon}{\Gamma(1-\epsilon)}(1-\mathrm{x})^{-1-2\epsilon}(1-\mathrm{y})^{-1-\epsilon}(1+\mathrm{y})^{-\epsilon}$ 144
B.4 $f_a\left[{}^1S_0^{(8)}\right]$ and $g\left[{}^1S_0^{(8)}\right]$ 147

Chapter 1

Introduction

Since its development in the early 1970s Quantum Chromodynamics (QCD)[1] is generally believed to be the fundamental theory of the strong interaction. Very convincing evidence for it is established, among other things, by the very precise agreement between the measurement and the QCD prediction of the running of the strong coupling constant g_s or the famous ratio R of the cross sections for e^+e^- annihilation into hadrons and into muons, respectively as well as by the noticeable success of QCD in quantitatively describing observed phenomena like the partonic structure of hadrons or the production of jets and heavy quarkonia. But it still remains a main task of elementary particle physics to test this theory in a growing field of experimental and accelerator technical possibilities. In this respect, very much attention is paid to the heavy quarkonia, whose first representative, the J/ψ meson, was discovered in 1974[2]. Heavy quarkonia are mesons, which contain a heavy quark $Q = c, b, t$ and its antiquark $\bar{Q}$. They can be characterized in the usual spectroscopic way by $n_r^{2S+1}L_J$ as well as by the parity $P = (-1)^{L+1}$ and the charge conjugation number $C = (-1)^{L+S}$. Here $n_r = 1, 2, ...$ is the radial excitation quantum number, $S = 0, 1$ is the total spin of the $Q\bar{Q}$ pair, $L = 1, 2, ...$ (or $L = S, P, D, F, ...$) is the orbital angular momentum and $J = |L - S|, |L - S| + 1, ..., L + S$ is the total angular momentum. It should be noted thereby, that in contrast to J, P and C, L and S are in principle no exactly conserved quantum numbers in QCD, but are approximately conserved for sufficiently large heavy quark mass m, for which the $Q\bar{Q}$ system becomes nonrelativistic. As the simplest bound systems of the strong interaction with a rich internal structure, the heavy quarkonia provide an excellent opportunity to test QCD both in its perturbative and in its nonperturbative regime. In table 1.1 an overview of the most important charmonia ($Q = c$) is given[3]. Especially the J/ψ meson attracted much interest in the past because of its very clean experimental signature of leptonic decay.

Most theoretical approaches to heavy quarkonium physics are based on a factorization of observables like production or decay rates in process dependent parts, which describe the dynamics at short distances of order $1/m$, and universal parts, which contain all the information on the nonperturbative dynamics related to the quarkonium bound state H at long distances comparable to the quarkonium size of order $1/mv$. Here m denotes the heavy quark mass and v is the heavy quark velocity in the quarkonium rest frame. While

Table 1.1: Important charmonia

charmonium	$n_r^{2S+1}L_J$	J^{PC}	Mass/GeV
η_c	1^1S_0	0^{-+}	2979.8 ± 1.8
J/ψ	1^3S_1	1^{--}	3096.87 ± 0.04
ψ'	2^3S_1	1^{--}	3685.96 ± 0.09
h_c	1^1P_1	1^{+-}	3526.14 ± 0.24
χ_{c0}	1^3P_0	0^{++}	3415.0 ± 0.8
χ_{c1}	1^3P_1	1^{++}	3510.51 ± 0.12
χ_{c2}	1^3P_2	2^{++}	3556.18 ± 0.13

the short distance parts can be calculated perturbatively, the universal long distance parts must be determined in some special measurement and can then be used to make predictions for other experiments. Such a factorization is of course only reliable, if v is nonrelativistic $v \ll 1$, since only then both distance scales are well separated

$$\frac{1}{m} \ll \frac{1}{mv} \ , \tag{1.1}$$

so that an interference of the process specific dynamics and the bound state dynamics becomes neglegible. From a simple virial satz argument one finds, that for m large enough v is proportional to the QCD fine structure constant $\alpha_s(m) \equiv g_s^2/4\pi$, that is v decreases with increasing m like $1/\ln m$. With $v^2 \approx 0.3$ the charmonia are the lightest quark antiquark systems, which satisfy the reliability criterion (1.1)[1]. First studies of heavy quarkonium production were performed within the Color Evaporation Model [4]. In this approach the production process is described up to a universal phenomenological factor by the cross section $\sigma_{Q\bar{Q}}$ for the perturbative creation of the $Q\bar{Q}$ pair at short distances in all possible spin and color configurations and with an invariant mass M between the thresholds for H and open Q production

$$\sigma_H \sim \int_{2m}^{2m_D} dM \frac{d\sigma_{Q\bar{Q}}}{dM} \ . \tag{1.2}$$

Here σ_H denotes the heavy quarkonium production cross section and m_D is the mass of the lightest meson, which can be built with the heavy quark Q. The underlying idea is, that the color of the generated $Q\bar{Q}$ pair is neutralized by the nonperturbative dynamics at long

[1]Alternatively, the long distance scale could also be estimated to be the inverse of the confinement scale Λ_{QCD}, resulting in $\frac{1}{m} \ll \frac{1}{\Lambda_{QCD}}$ as reliability criterion. This would not change the outcome, that the charmonia are the lightest $Q\bar{Q}$ systems, to which factorization approaches apply.

distances during the formation of the physical bound state H. Though not without any phenomenological success, the color evaporation model suffers from the crucial lack, that it doesn't allow for a distinction of the various quarkonium states, which differ in their spin and orbital angular momentum structure. This situation is improved in the Color Singlet Model (CSM) [5, 6], which claims, that the $Q\bar{Q}$ pair is produced at short distances in a color singlet Fock state with exactly the quantum numbers $^{2S+1}L_J$ of the physical quarkonium state H. While this process can be calculated within perturbation theory, all the nonperturbative effects of the transition of this $|Q\bar{Q}\rangle$ Fock state into the quarkonium H are factorized into a universal factor, which must be extracted from measurement. A similar factorization holds for heavy quarkonium decay. For more than one decade the CSM has been serving as the standard picture to describe the phenomenology of heavy quarkonia. But serious problems were encountered, when applying the CSM to P wave states. In cases like the h_c or the χ_{cJ} the production and decay rates were found to be plagued with unremovable infrared divergences[5, 7, 8], indicating, that the factorization, on which the CSM relies, is incomplete. This conceptional lack could be surmounted within Nonrelativistic Quantum Chromodynamics (NRQCD)[9], which was conceived as a rigorous effective field theory of heavy quarkonia, based on a nonrelativistic treatment of the heavy quark and antiquark. NRQCD provides factorization formulae for the production and decay rates, which correspond to a generalization of the CSM in the sense, that the $Q\bar{Q}$ pair at short distances is no longer restricted to the quantum numbers of the physical bound state H but may occur in all possible Fock states. In case that the $Q\bar{Q}$ pair is created or annihilated in a color octet state, the long distance dynamics is assumed to provide a mechanism of color compensation, for example through the emission of soft gluons. This is referred to as the Color Octet Mechanism and constitutes the most spectacular novelty compared to the CSM. The NRQCD factorization formulae explicitly read for the production cross section

$$\sigma_H = \sum_n \sigma_{Q\bar{Q}[n]} \, \langle O^H[n] \rangle \tag{1.3}$$

and for the total decay width Γ_H

$$\Gamma_H = \sum_n \Gamma_{Q\bar{Q}[n]} \, \langle O[n] \rangle_H \ . \tag{1.4}$$

Here the short distance coefficients $\sigma_{Q\bar{Q}[n]}$ account for the perturbative creation of a heavy quark pair in a quantum mechanical color singlet or color octet configuration n, and the $\langle O^H[n] \rangle$ are universal production matrix elements, which parametrize the nonperturbative evolution of this $Q\bar{Q}$ pair into the observed quarkonium H. Analogously, the $\langle O[n] \rangle_H$ are universal decay matrix elements, which correspond to the probability to meet the $Q\bar{Q}$ pair within the quarkonium H in a color singlet or color octet configuration n, while the coefficients $\Gamma_{Q\bar{Q}[n]}$ describe the annihilation of the $Q\bar{Q}$ pair in this configuration. While the coefficients are calculable in perturbation theory, the matrix elements have to be gained from fits to the data of a special experiment. Since the summation in (1.3), (1.4) extends over all possible configurations n, NRQCD predictions of production and decay rates in

principle depend on an infinite number of phenomenological input parameters. But due to a well defined scaling behaviour of the matrix elements with respect to the nonrelativistic heavy quark velocity v in the quarkonium rest frame, only a few leading ones of them are of practical importance, thus the predictive power of the theory being preserved. Those matrix elements, which are significant at the current level of accuracy of NRQCD analyses, can be labelled by $n = {}^{2S+1}L_J^{(c)}$, indicating the intermediate heavy quark pair to be in a configuration with definite spin S, orbital angular momentum L, total angular momentum J and color $c = 1, 8$, where $1, 8$ stands for color singlet and octet respectively. For instance the matrix elements relevant for $H = J/\psi, \psi'$ production (decay) are $\left\langle O^H \left[{}^3S_1^{(1)}\right]\right\rangle$, $\left\langle O^H \left[{}^1S_0^{(8)}\right]\right\rangle$, $\left\langle O^H \left[{}^3S_1^{(8)}\right]\right\rangle$ and $\left\langle O^H \left[{}^3P_J^{(8)}\right]\right\rangle$ $\left(\left\langle O \left[{}^3S_1^{(1)}\right]\right\rangle_H, \left\langle O \left[{}^1S_0^{(8)}\right]\right\rangle_H, \left\langle O \left[{}^3S_1^{(8)}\right]\right\rangle_H\right.$ and $\left.\left\langle O \left[{}^3P_J^{(8)}\right]\right\rangle_H\right)$ and the leading ones for χ_{cJ} production (decay) are $\left\langle O^{\chi_{cJ}} \left[{}^3P_J^{(1)}\right]\right\rangle$ and $\left\langle O^{\chi_{cJ}} \left[{}^3S_1^{(8)}\right]\right\rangle$ $\left(\left\langle O \left[{}^3P_J^{(1)}\right]\right\rangle_{\chi_{cJ}}\right.$ and $\left.\left\langle O \left[{}^3S_1^{(8)}\right]\right\rangle_{\chi_{cJ}}\right)$. Two crucial failings of the CSM have been resolved within NRQCD. First, in contrast to the CSM, NRQCD allows for the infrared safe calculation of P wave production and decay. The infrared divergences occuring in the color singlet channel (${}^1P_1^{(1)}$ for h_c and ${}^3P_J^{(1)}$ for χ_{cJ}) can be removed by renormalization of a color octet matrix element ($\left\langle O^{h_c} \left[{}^1S_0^{(8)}\right]\right\rangle$ or $\left\langle O \left[{}^1S_0^{(8)}\right]\right\rangle_{h_c}$ for h_c and $\left\langle O^{\chi_{cJ}} \left[{}^3S_1^{(8)}\right]\right\rangle$ or $\left\langle O \left[{}^3S_1^{(8)}\right]\right\rangle_{\chi_{cJ}}$ for χ_{cJ})[11, 15]. Secondly, the CSM underestimates the charmonium production rate for large transverse momenta P_T measured in $p\bar{p}$ collisions at the Fermilab Tevatron by more than one order of magnitude[12]. This discrepancy could be eliminated within NRQCD due to the additional color octet contributions [13, 14]. For large P_T, charmonium production at the Tevatron was found to be dominated by gluon fragmentation[14], which at leading order is a pure color octet process. However, in order to establish NRQCD as the correct description of heavy quarkonium physics, the color octet mechanism must also be identified in other processes. That means, it's to be tested, if based on the matrix elements fitted to the Tevatron data, NRQCD is also able to make reasonable predictions for charmonium production in other experiments. In this respect, there has been much research activity over the last years. NRQCD analyses have been carried out for charmonium hadroproduction[13, 15, 17, 18, 19], photoproduction [21, 22, 23, 24, 25, 26], charmonium production in e^+e^- annihilation [27], $\gamma\gamma$ collisions[28], Z-boson decays[29], B-meson decays [30], and lepton(l) nucleon(N) deep inelastic scattering (DIS)[8, 31, 32, 33, 34, 35]. J/ψ production in association with electroweak gauge bosons was investigated in [16] and in association with the standard model Higgs as well as its supersymmetric versions within the minimal supersymmetric standard model (MSSM) in [20], both in hadroproduction and in $\gamma\gamma$ collisions. Furthermore the polarization of charmonium, which is very sensitive to the color octet mechanism, was investigated in [18, 19, 25, 26, 31]. For comprehensive reviews of the current status of research in the topic of heavy quarkonium production see [36]. lN DIS is especially suited to probe the production mechanism of heavy quarkonia, since the virtuality Q^2 of the exchanged gauge boson provides a high scale, by which higher order corrections or nonperturbative contributions like higher twist effects are effectively suppressed. An additional advantage is, as far as the photon is concerned, that for high Q^2 the contribu-

tion of resolved photons becomes neglegible, rendering the predictions independent from uncertainties in the photon structure functions. On the other side heavy quarkonium production in lN electromagnetic and neutral current DIS is generally accompanied by a large background of diffractive production. In contrast to nondiffractive production, where the nucleon participates in the hard scattering via its parton content and is thus destroyed (DIS), in diffractive production the nucleon interacts with the rest of the process via the exchange of colourless objects of small spacelike virtualities and stays intact (elastic scattering) or turns into a hadronic system of small invariant mass (diffractive dissociation). Contributions from diffractive production can not be described within NRQCD and must therefore be carefully discriminated against by applying appropriate kinematical cuts. Very important in this respect is the inelasticity variable z, which is defined as the energy fraction, transferred from the photon or the Z boson to the produced heavy quarkonium in the nucleon rest frame. As diffractive production predominantly takes place at large z values close to 1, this variable allows for a clean separation of the regime of deep inelastic from that of diffractive production.

In this thesis we present CSM and NRQCD Born level calculations of (I) single and jet associated J/ψ inclusive production in electron (positron) proton ($e^{\pm}p$) electromagnetic DIS at DESY HERA[34], (II) single and jet associated prompt J/ψ inclusive production in neutrino (antineutrino) nucleon ($\nu(\overline{\nu})N$) neutral current DIS in the NOMAD and CHORUS experiments at CERN[8] and (III) jet associated prompt J/ψ inclusive production in $\nu(\overline{\nu})N$ charged current DIS in the NOMAD and CHORUS experiments at CERN[35]. Thereby prompt means, that besides direct J/ψ production also the contributions from the decay of the directly produced heavier charmonia ψ', χ_{c0}, χ_{c1} and χ_{c2} into the J/ψ plus rest are taken into account. In case I we also calculate the ${}^1S_0^{(8)}$ part of the corresponding next leading order corrections. In case II we additionally estimate the contribution from diffractive prompt J/ψ production within the Vector Dominance Model[37, 38, 39].

Before entering the calculations we first give a thorough presentation of NRQCD as an effective field theory of heavy quarkonia as well as of the projection formalism, which our calculations of the short distance coefficients for production are based on.

Chapter 2

NRQCD as an effective field theory of heavy quarkonia

NRQCD[9] is an effective field theory of heavy quarkonia, which is based on the assumption, that the heavy quark velocity v in the quarkonium rest frame is nonrelativistically small $v \ll 1$. It contains an ultraviolet cutoff Λ of the order m, which excludes relativistic heavy quarks as well as gluons and light quarks with momenta of the order m from the theory. Accordingly, NRQCD relies on an effective lagrangian, which treats the heavy quarks nonrelativistically, while the light quarks and the gluons are furtheron described full relativistically. Relativistic corrections are systematically taken into account order by order in $1/m$. The leading corrections can be identified with the QCD analogues of the magnetic dipole, the electric dipole, the spin orbit and the Darwin interaction in atom physics. The highly relativistic physics involved in quarkonium decay is reproduced on lagrangian level by effective local 4-fermion interactions. The complete dependence on the higher scales beyond the cutoff Λ is contained in the individual couplings (or coefficients) belonging to all the NRQCD interactions. In this way NRQCD is completely equivalent to full QCD, at least for onshell physical quantities. NRQCD provides a rigorously field theoretically based factorization approach to heavy quarkonium production and decay, which consists in a separation of the highly relativistic and perturbative physics of heavy quark pair annihilation or creation, related to the large scale m, or in production case all the large scales beyond the cutoff Λ, from the nonrelativistic and nonperturbative physics of quarkonium structure, involving all the lower scales like mv, mv^2 or the fundamental QCD scale Λ_{QCD}. Due to heavy quark velocity scaling rules, NRQCD allows furthermore for a clear separation of effects of different order in v. Therefore NRQCD predictions for production or decay rates take the form of consistent double expansions in α_s and v.

This chapter is devoted to a thorough presentation of NRQCD. All the results derived in this chapter are found to agree with Ref.[9].

2.1 The effective lagrangian of NRQCD

In deriving the effective NRQCD lagrangian we start from the lagrangian of full QCD

$$\mathcal{L}_{\rm QCD} = \bar{\Psi}(i\gamma^\mu D_\mu - m)\Psi + \sum_q \bar{q}\; i\gamma^\mu D_\mu\; q - \frac{1}{2}\; tr[G_{\mu\nu}G^{\mu\nu}]\;. \tag{2.1}$$

Here $D_\mu = \partial_\mu + ig_s A_\mu$ denotes the covariant derivative, A_μ and $G_{\mu\nu} = \partial_\mu A_\nu - \partial_\nu A_\mu + ig_s[A_\mu, A_\nu]$ are the lie algebra valued gluon field and the corresponding fieldstrength, respectively, Ψ is the heavy quark spinor field and q represents the spinor fields of the light quarks. As a crucial step towards NRQCD, we perform a nonrelativistic expansion of the first term in (2.1)

$$\mathcal{L}_\Psi = \bar{\Psi}(i\gamma^\mu D_\mu - m)\Psi \tag{2.2}$$

in powers of $1/m$ using the procedure of Foldy-Wouthuysen transformation. This consists in a successive decoupling of the large and the small spinor components, or, what's the same, the heavy quark and the heavy antiquark degrees of freedom in $\mathcal{L}_\Psi$ order by order in $1/m$ through appropriate unitary transformations U

$$\Psi \to \Psi' = U\Psi\;. \tag{2.3}$$

To this end, it is suitable to represent the dirac matrices by

$$\gamma^0 = \beta \qquad , \qquad \gamma^i = \beta\alpha^i \qquad ; \qquad i = 1,2,3 \tag{2.4}$$

with

$$\beta = \begin{pmatrix} 1 & 0 \\ 0 & -1 \end{pmatrix} \qquad , \qquad \alpha^i = \begin{pmatrix} 0 & \sigma^i \\ \sigma^i & 0 \end{pmatrix} \qquad ; \qquad i = 1,2,3\;, \tag{2.5}$$

where the σ^i are the Pauli matrices

$$\sigma^1 = \begin{pmatrix} 0 & 1 \\ 1 & 0 \end{pmatrix} \qquad , \qquad \sigma^2 = \begin{pmatrix} 0 & -i \\ i & 0 \end{pmatrix} \qquad , \qquad \sigma^3 = \begin{pmatrix} 1 & 0 \\ 0 & -1 \end{pmatrix}\;. \tag{2.6}$$

Choosing the notation

$$A^\mu = (\phi, \vec{A}) \quad , \quad \partial_\mu = (\partial_t, \vec{\nabla}) \quad \text{and} \quad D_\mu = (D_t, \vec{D}) \equiv (\partial_t + ig_s\phi, \vec{\nabla} - ig_s\vec{A}) \tag{2.7}$$

$\mathcal{L}_\Psi$ takes the form

$$\mathcal{L}_\Psi = \Psi^\dagger[i\partial_t - H]\Psi \tag{2.8}$$

with

$$H = \beta m + \mathcal{E} + \mathcal{O}\;, \tag{2.9}$$

where the operators $\mathcal{E}$ and $\mathcal{O}$ are defined by

$$\mathcal{E} = g_s\phi \qquad , \qquad \mathcal{O} = -i\vec{\alpha}\vec{D}\;. \tag{2.10}$$

Here and in the following we distinguish between "even" operators like $\mathcal{E} = g_s\phi$, which only relate large to large and small to small spinor components, and "odd" operators like

$\mathcal{O} = -i\vec{\alpha}\vec{D}$, which couple the large and the small spinor components. In the following we will make extensive use of the general property, that even operators commute with β, while odd operators anticommute with β

$$[\mathcal{E}, \beta] = \{\mathcal{O}, \beta\} = 0 \ . \tag{2.11}$$

After a first Foldy-Wouthuysen transformation

$$\Psi' = e^{iS}\Psi \qquad \text{with} \qquad S = -i\frac{\beta\mathcal{O}}{2m} = o\left(\frac{1}{m}\right) \tag{2.12}$$

$\mathcal{L}_\Psi$ reads

$$\begin{aligned}
\mathcal{L}_\Psi &= \Psi'^\dagger e^{iS}[i\partial_t - H]e^{-iS}\Psi' \\
&= \Psi'^\dagger \Big\{ i\partial_t - [S,\partial_t] - \frac{i}{2}[S,[S,\partial_t]] + \frac{1}{6}[S,[S,[S,\partial_t]]] \\
&\quad -H - i[S,H] + \frac{1}{2}[S,[S,H]] + \frac{i}{6}[S,[S,[S,H]]] \\
&\quad -\frac{1}{24}[S,[S,[S,[S,H]]]]\Big\}\Psi' \ ,
\end{aligned} \tag{2.13}$$

where in the second line we made use of the Haussdorff-Campbell formula

$$e^{iA}Be^{-iA} = B + i[A,B] + \frac{i^2}{2}[A[A,B]] + ... + \frac{i^n}{n!}[A,[A,...[A,B]]...] + ... \ , \tag{2.14}$$

and we neglected terms of order higher than $(1/m)^3$. For the commutators in (2.13) we find

$$\begin{aligned}
[S,\partial_t] &= -\partial_t S = i\frac{\beta\partial_t\mathcal{O}}{2m} \ , \\
[S,[S,\partial_t]] &= -\frac{1}{4m^2}[\mathcal{O},\partial_t\mathcal{O}] \\
[S,[S,[S,\partial_t]]] &= \frac{i\beta}{8m^3}[\mathcal{O},[\mathcal{O},\partial_t\mathcal{O}]] \\
[S,H] &= i\mathcal{O} - \frac{i\beta}{m}\mathcal{O}^2 - \frac{i\beta}{2m}[\mathcal{O},\mathcal{E}] \\
[S,[S,H]] &= \frac{\beta\mathcal{O}^2}{m} + \frac{\mathcal{O}^3}{m^2} + \frac{1}{4m^2}[\mathcal{O},[\mathcal{O},\mathcal{E}]] \\
[S,[S,[S,H]]] &= \frac{i}{m^2}\mathcal{O}^3 - \frac{i\beta}{m^3}\mathcal{O}^4 - \frac{i\beta}{8m^3}[\mathcal{O},[\mathcal{O},[\mathcal{O},\mathcal{E}]]] \\
[S,[S.[S,[S,H]]]] &= \frac{\beta\mathcal{O}^4}{m^3} + o\left(\frac{1}{m^4}\right) \ .
\end{aligned} \tag{2.15}$$

Hence it follows for $\mathcal{L}_\Psi$

$$\mathcal{L}_\Psi = \Psi'^\dagger[i\partial_t - H']\Psi' \tag{2.16}$$

with

$$H' = \beta m + \mathcal{E}' + \mathcal{O}' \ , \tag{2.17}$$

where the transformed even and odd operators $\mathcal{E}'$ and $\mathcal{O}'$ up to order $(1/m)^3$ are given by

$$\mathcal{E}' = \mathcal{E} + \beta\left(\frac{\mathcal{O}^2}{2m} - \frac{\mathcal{O}^4}{8m^3}\right) - \frac{1}{8m^2}[\mathcal{O}, i\partial_t\mathcal{O} + [\mathcal{O}, \mathcal{E}]] \tag{2.18}$$

$$\mathcal{O}' = \frac{\beta}{2m}(i\partial_t\mathcal{O} + [\mathcal{O}, \mathcal{E}]) - \frac{\mathcal{O}^3}{3m^2} - \frac{\beta}{48m^3}[\mathcal{O}, [\mathcal{O}, i\partial_t\mathcal{O} + [\mathcal{O}, \mathcal{E}]]] \ . \tag{2.19}$$

As a result of the transformation (2.12) the odd operator $\mathcal{O}'$ is reduced by one order in m compared to the original odd operator $\mathcal{O}$. In order to decouple the large and the small spinor components in $\mathcal{L}_\Psi$ up to order $(1/m)^3$, three further Foldy-Wouthuysen transformations are necessary. A second transformation

$$\Psi'' = e^{iS'}\Psi' \qquad \text{with} \qquad S' = -i\frac{\beta\mathcal{O}'}{2m} = o\left(\frac{1}{m^2}\right) \tag{2.20}$$

results in

$$\mathcal{L}_\Psi = \Psi''^\dagger[i\partial_t - H'']\Psi'' \tag{2.21}$$

with

$$H'' = \beta m + \mathcal{E}'' + \mathcal{O}'' \ , \tag{2.22}$$

where the transformed even and odd operators $\mathcal{E}''$ and $\mathcal{O}''$ up to order $(1/m)^3$ are now given by

$$\begin{aligned}\mathcal{E}'' &= \mathcal{E}' + \beta\frac{\mathcal{O}'^2}{2m} \\ &= \mathcal{E} + \beta\left(\frac{\mathcal{O}^2}{2m} - \frac{\mathcal{O}^4}{8m^3} - \frac{1}{8m^3}(i\partial_t\mathcal{O} + [\mathcal{O}, \mathcal{E}])^2\right) - \frac{1}{8m^2}[\mathcal{O}, i\partial_t\mathcal{O} + [\mathcal{O}, \mathcal{E}]]\end{aligned} \tag{2.23}$$

and

$$\begin{aligned}\mathcal{O}'' &= \frac{\beta}{2m}(i\partial_t\mathcal{O}' + [\mathcal{O}', \mathcal{E}']) \\ &= \frac{i}{4m^2}\partial_t\left(i\partial_t\mathcal{O} + [\mathcal{O}, \mathcal{E}] - \frac{2\beta\mathcal{O}^3}{3m}\right) + \frac{1}{4m^2}[i\partial_t\mathcal{O} + [\mathcal{O}, \mathcal{E}], \mathcal{E}] \\ &\quad -\frac{\beta}{8m^3}\{i\partial_t\mathcal{O} + [\mathcal{O}, \mathcal{E}], \mathcal{O}^2\} - \frac{\beta}{6m^3}[\mathcal{O}^3, \mathcal{E}] \ .\end{aligned} \tag{2.24}$$

After a third Foldy-Wouthuysen transformation

$$\Psi''' = e^{iS''}\Psi'' \qquad \text{with} \qquad S'' = -i\frac{\beta\mathcal{O}''}{2m} = o\left(\frac{1}{m^3}\right) \tag{2.25}$$

we find

$$\mathcal{L}_\Psi = \Psi'''^\dagger[i\partial_t - H''']\Psi''' \tag{2.26}$$

with

$$H''' = \beta m + \mathcal{E}''' + \mathcal{O}''' \ , \tag{2.27}$$

where the transformed even and odd operators $\mathcal{E}'''$ and $\mathcal{O}'''$ within the wanted order of accuracy now read

$$\mathcal{E}''' = \mathcal{E}'' \tag{2.28}$$

and

$$\begin{aligned} \mathcal{O}''' &= \frac{\beta}{2m}(i\partial_t \mathcal{O}'' + [\mathcal{O}'', \mathcal{E}'']) \\ &= \frac{i\beta}{8m^3}\partial_t^2(i\partial_t \mathcal{O} + [\mathcal{O}, \mathcal{E}]) + \frac{\beta}{8m^3}\partial_t[i\partial_t \mathcal{O} + [\mathcal{O}, \mathcal{E}], \mathcal{E}] \ . \end{aligned} \tag{2.29}$$

Performing a last Foldy-Wouthuysen transformation

$$\Psi'''' = e^{iS'''}\Psi''' \qquad \text{with} \qquad S''' = -i\frac{\beta \mathcal{O}'''}{2m} = o\left(\frac{1}{m^4}\right) \tag{2.30}$$

we end up with

$$\mathcal{L}_\Psi = \Psi''''^\dagger [i\partial_t - H'''']\Psi'''' \ , \tag{2.31}$$

where

$$H'''' = \beta m + \mathcal{E}'''' + \mathcal{O}'''' \tag{2.32}$$

with

$$\mathcal{E}'''' = \mathcal{E}''' = \mathcal{E}'' \tag{2.33}$$

and the odd part of H'''' being beyond the considered order of accuracy

$$\mathcal{O}'''' = o\left(\frac{1}{m^4}\right) \ . \tag{2.34}$$

Renaming Ψ'''' by Ψ the up to order $(1/m)^3$ decoupled heavy quark lagrangian $\mathcal{L}_\Psi$ reads

$$\begin{aligned} \mathcal{L}_\Psi = \Psi^\dagger \Bigg\{ & i\partial_t - \beta \left(m + \frac{\mathcal{O}^2}{2m} - \frac{\mathcal{O}^4}{8m^3} - \frac{1}{8m^3}(i\partial_t \mathcal{O} + [\mathcal{O}, \mathcal{E}])^2 \right) \\ & -\mathcal{E} + \frac{1}{8m^2}[\mathcal{O}, i\partial_t \mathcal{O} + [\mathcal{O}, \mathcal{E}]] \Bigg\} \Psi \ . \end{aligned} \tag{2.35}$$

In order to clarify the physical meaning of the different terms contributing to $\mathcal{L}_\Psi$, it is useful to eliminate the operators $\mathcal{E}$ and $\mathcal{O}$ in favour of the covariant derivative $D_\mu = (D_t, \vec{D}) = (\partial_t + ig_s\phi, \vec{\nabla} - ig_s\vec{A})$, the chromoelectric field

$$\vec{E} = \left(G^{i0}\right) = -\vec{\nabla}\phi - \partial_t \vec{A} - ig_s[\phi, \vec{A}] \tag{2.36}$$

and the chromomagnetic field

$$\vec{B} = \left(\frac{1}{2}\epsilon^{ijk}G^{kj}\right) = \vec{\nabla} \times \vec{A} - ig_s \vec{A} \times \vec{A} \ . \tag{2.37}$$

Note, that $[\phi, \vec{A}]$ and $\vec{A}\times\vec{A}$ do not necessarily vanish, since ϕ and $\vec{A}$ are lie algebra valued. Using the relation

$$\alpha^i\alpha^j = \delta^{ij} + i\epsilon^{ijk}\sigma^k \ , \tag{2.38}$$

which follows from $[\alpha^i, \alpha^j] = 2i\epsilon^{ijk}\sigma^k$ and $\{\alpha^i, \alpha^j\} = 2\delta^{ij}$, we find

$$\begin{aligned}
\frac{\mathcal{O}^2}{2m} &= -\frac{1}{2m}\alpha^i\alpha^j D_i D_j \\
&= -\frac{1}{2m}(\delta^{ij} + i\epsilon^{ijk}\sigma^k) D_i D_j \\
&= -\frac{1}{2m}\left[\vec{D}^2 + g_s\sigma^k\epsilon^{kij}(\partial_i A^j - ig_s A^i A^j)\right] \\
&= -\frac{1}{2m}\left[\vec{D}^2 + g_s\vec{\sigma}(\vec{\nabla}\times\vec{A} - ig_s\vec{A}\times\vec{A})\right] \\
&= -\frac{\vec{D}^2}{2m} - \frac{g_s}{2m}\vec{\sigma}\vec{B} \ ,
\end{aligned} \tag{2.39}$$

$$\frac{\mathcal{O}^4}{8m^3} = \frac{1}{2m}\left(\frac{\mathcal{O}^2}{2m}\right)^2 = \frac{1}{8m^3}\left[(\vec{D}^2)^2 + g_s^2(\vec{\sigma}\vec{B})^2 + \{\vec{D}^2, g_s\vec{\sigma}\vec{B}\}\right] \ , \tag{2.40}$$

$$\begin{aligned}
i\partial_t\mathcal{O} + [\mathcal{O}, \mathcal{E}] &= -ig_s\vec{\alpha}(\partial_t\vec{A} + [\vec{D}, \phi]) \\
&= -ig_s\vec{\alpha}(\partial_t\vec{A} + [\vec{\nabla}, \phi] - ig_s[\vec{A}, \phi]) \\
&= ig_s\vec{\alpha}(-\vec{\nabla}\phi - \partial_t\vec{A} - ig_s[\phi, \vec{A}]) \\
&= ig_s\vec{\alpha}\vec{E}
\end{aligned} \tag{2.41}$$

and

$$\begin{aligned}
[\mathcal{O}, i\partial_t\mathcal{O} + [\mathcal{O}, \mathcal{E}]] &= g_s[\vec{\alpha}\vec{D}, \vec{\alpha}\vec{E}] \\
&= g_s\alpha^i\alpha^j(D_i E^j - E^i D_j) \\
&= g_s(\delta^{ij} + i\epsilon^{ijk}\sigma^k)(D_i E^j - E^i D_j) \\
&= g_s(\vec{D}\vec{E} - \vec{E}\vec{D}) + ig_s\vec{\sigma}(\vec{D}\times\vec{E} - \vec{E}\times\vec{D}) \ .
\end{aligned} \tag{2.42}$$

Parametrizing furthermore Ψ by

$$\Psi = \begin{pmatrix} \psi\ e^{-imt} \\ \chi\ e^{imt} \end{pmatrix} \ , \tag{2.43}$$

where ψ and χ are two component spinors, which are easily seen to describe the heavy quark and the heavy antiquark, respectively, we arrive at

$$\begin{aligned}
\mathcal{L}_\Psi = \psi^\dagger\left[iD_t + \frac{\vec{D}^2}{2m}\right]\psi + \chi^\dagger\left[iD_t - \frac{\vec{D}^2}{2m}\right]\chi \\
+\frac{1}{2m}\left[\psi^\dagger g_s\vec{B}\vec{\sigma}\psi - \chi^\dagger g_s\vec{B}\vec{\sigma}\chi\right]
\end{aligned}$$

$$+\frac{1}{8m^2}\left[\psi^\dagger\left(\vec{D}g_s\vec{E}-g_s\vec{E}\vec{D}\right)\psi+\chi^\dagger\left(\vec{D}g_s\vec{E}-g_s\vec{E}\vec{D}\right)\chi\right]$$
$$+\frac{1}{8m^2}\left[\psi^\dagger\left(i\vec{D}\times g_s\vec{E}-g_s\vec{E}\times i\vec{D}\right)\vec{\sigma}\psi+\chi^\dagger\left(i\vec{D}\times g_s\vec{E}-g_s\vec{E}\times i\vec{D}\right)\vec{\sigma}\chi\right]$$
$$+\frac{1}{8m^3}\left[\psi^\dagger\left(\vec{D}^2\right)^2\psi-\chi^\dagger(\vec{D}^2)^2\chi\right]\ . \tag{2.44}$$

Thereby, in addition to orders higher than $(1/m)^3$ we have now also neglected terms of the order fieldstrength$/m^3$. Note the explicit decoupling of the heavy quark and the heavy antiquark degrees of freedom in (2.44). The interpretation of the different contributions to $\mathcal{L}_\Psi$ is now rather obvious. While the first (second) term on the right hand side of (2.44) describes the heavy quark (antiquark) by means of Schrödinger quantum mechanics, the subsequent terms represent, as the leading relativistic corrections, the chromomagnetic dipol, the chromoelectric dipol, the spin orbit and the Darwin interaction. As a consequence of charge conjugation symmetry, there exists to each term containing the heavy quark field ψ a similar term containing the heavy antiquark field χ. A temporary result for the NRQCD lagrangian $\mathcal{L}_{\rm NRQCD}$ is obtained by inserting the expansion (2.44) of $\bar{\Psi}(i\gamma^\mu D_\mu - m)\Psi$ in (2.1). $\mathcal{L}_{\rm NRQCD}$ is obviously symmetric under global $U(1)\times U(1)$ transformations

$$\begin{pmatrix}\psi\\ \chi\end{pmatrix}\to\begin{pmatrix}\psi'\\ \chi'\end{pmatrix}=\begin{pmatrix}e^{i\alpha}&0\\ 0&e^{i\beta}\end{pmatrix}\begin{pmatrix}\psi\\ \chi\end{pmatrix}\ , \tag{2.45}$$

implying separate conservation of the heavy quark and the heavy antiquark number. Thus the annihilation and creation of heavy quark antiquark pairs is not reproduced by $\mathcal{L}_{\rm NRQCD}$. This is in accordance with the ultraviolet cutoff Λ of the order m, which, as part of the definition of NRQCD, has been introducd, to exclude relativistic heavy quarks as well as light quarks and gluons with momenta of the order m from the theory. In order to implement heavy quarkonium decay on lagrangian level local 4-fermion operators are added to $\mathcal{L}_{\rm NRQCD}$, which describe $Q\bar{Q}\to Q\bar{Q}$ scattering and can be related to heavy quarkonium decay via the optical theorem. These operators are defined in the center of mass frame of the heavy quark and the heavy antiquark. A complete set of them is constructed on the basis of the requirement, that they must be invariant under spatial rotations and $SU(3)$ color transformations. The most important 4-fermion operators are

$$O\left[^1S_0^{(1)}\right]=\psi^\dagger\chi\chi^\dagger\psi \tag{2.46}$$
$$O\left[^3S_1^{(1)}\right]=\psi^\dagger\vec{\sigma}\chi\chi^\dagger\vec{\sigma}\psi \tag{2.47}$$
$$O\left[^1P_1^{(1)}\right]=\psi^\dagger\left(-\frac{i}{2}\overleftrightarrow{D}\right)\chi\chi^\dagger\left(-\frac{i}{2}\overleftrightarrow{D}\right)\psi \tag{2.48}$$
$$O\left[^3P_0^{(1)}\right]=\frac{1}{3}\psi^\dagger\left(-\frac{i}{2}\overleftrightarrow{D}\,\vec{\sigma}\right)\chi\chi^\dagger\left(-\frac{i}{2}\overleftrightarrow{D}\,\vec{\sigma}\right)\psi \tag{2.49}$$
$$O\left[^3P_1^{(1)}\right]=\frac{1}{2}\psi^\dagger\left(-\frac{i}{2}\overleftrightarrow{D}\times\vec{\sigma}\right)\chi\chi^\dagger\left(-\frac{i}{2}\overleftrightarrow{D}\times\vec{\sigma}\right)\psi \tag{2.50}$$
$$O\left[^3P_2^{(1)}\right]=\psi^\dagger\left(-\frac{i}{2}\overleftrightarrow{D}^{(i}\,\sigma^{j)}\right)\chi\chi^\dagger\left(-\frac{i}{2}\overleftrightarrow{D}^{(i}\,\sigma^{j)}\right)\psi \tag{2.51}$$

and

$$O\left[{}^1S_0^{(8)}\right] = \psi^\dagger T^a \chi \chi^\dagger T^a \psi \tag{2.52}$$

$$O\left[{}^3S_1^{(8)}\right] = \psi^\dagger \vec{\sigma} T^a \chi \chi^\dagger \vec{\sigma} T^a \psi \tag{2.53}$$

$$O\left[{}^1P_1^{(8)}\right] = \psi^\dagger \left(-\frac{i}{2} \overleftrightarrow{D}\right) T^a \chi \chi^\dagger \left(-\frac{i}{2} \overleftrightarrow{D}\right) T^a \psi \tag{2.54}$$

$$O\left[{}^3P_0^{(8)}\right] = \frac{1}{3}\psi^\dagger \left(-\frac{i}{2} \overleftrightarrow{D}\, \vec{\sigma}\right) T^a \chi \chi^\dagger \left(-\frac{i}{2} \overleftrightarrow{D}\, \vec{\sigma}\right) T^a \psi \tag{2.55}$$

$$O\left[{}^3P_1^{(8)}\right] = \frac{1}{2}\psi^\dagger \left(-\frac{i}{2} \overleftrightarrow{D} \times \vec{\sigma}\right) T^a \chi \chi^\dagger \left(-\frac{i}{2} \overleftrightarrow{D} \times \vec{\sigma}\right) T^a \psi \tag{2.56}$$

$$O\left[{}^3P_2^{(8)}\right] = \psi^\dagger \left(-\frac{i}{2} \overleftrightarrow{D}^{(i}\, \sigma^{j)}\right) T^a \chi \chi^\dagger \left(-\frac{i}{2} \overleftrightarrow{D}^{(i}\, \sigma^{j)}\right) T^a \psi \ . \tag{2.57}$$

Thereby $\overleftrightarrow{D}$ is defined as the difference of the covariant derivative acting on the spinor to the right and the covariant derivative acting on the spinor to the left

$$\psi^\dagger \overleftrightarrow{D} \chi = \psi^\dagger \vec{D} \chi - (\vec{D}\psi)^\dagger \chi \ , \tag{2.58}$$

brackets around pairs of indices have been used to indicate the traceless symmetric part of a tensor

$$T^{(ij)} = \frac{1}{2}(T^{ij} + T^{ji}) - \frac{1}{3} T^{ii} \ , \tag{2.59}$$

and the T^a , $a = 1, ..., 8$ denote the generators of the $SU(3)$ color symmetry. As is obvious from the behaviour of the operators $\chi^\dagger\psi$, $\chi^\dagger T^a \psi$, $\chi^\dagger \vec{\sigma} \psi$, $\chi^\dagger \vec{\sigma} T^a \psi$, ... or their hermitean conjugates, respectively, under spatial rotations and $SU(3)$ color transformations, the operators $O\left[{}^{2S+1}L_J^{(c)}\right]$ describe the scattering of a heavy quark antiquark pair in a Fock state with definite total spin S, orbital angular momentum L, total angular momentum J and color c, where $c = 1, 8$ stands for color singlet and octet, respectively. 4-fermion operators, which contain powers of D_t, are avoided in $\mathcal{L}_{\rm NRQCD}$ by exploiting the equations of motion

$$iD_t\psi = -\frac{\vec{D}^2}{2m}\psi + ... \qquad \text{and} \qquad iD_t\chi = \frac{\vec{D}^2}{2m}\chi + ... \ . \tag{2.60}$$

We are now in position to present our final result for the effective NRQCD lagrangian:

$$\mathcal{L}_{\rm NRQCD} = \mathcal{L}_{\rm heavy} + \delta\mathcal{L} + \delta\mathcal{L}_1 + \mathcal{L}_{\rm light} \ . \tag{2.61}$$

Here $\mathcal{L}_{\rm heavy}$ is the nonrelativistic Schrödinger lagrangian describing the heavy quark and the heavy antiquark

$$\mathcal{L}_{\rm heavy} = \psi^\dagger \left[iD_t + \frac{\vec{D}^2}{2m}\right] \psi + \chi^\dagger \left[iD_t - \frac{\vec{D}^2}{2m}\right] \chi \ . \tag{2.62}$$

$\delta\mathcal{L}$ contains all the higher relativistic corrections bilinear in ψ and χ

$$\begin{aligned}\delta\mathcal{L} = & \frac{c_1}{2m}\left[\psi^\dagger g_s\vec{B}\vec{\sigma}\psi - \chi^\dagger g_s\vec{B}\vec{\sigma}\chi\right] \\ & + \frac{c_2}{8m^2}\left[\psi^\dagger\left(\vec{D}g_s\vec{E} - g_s\vec{E}\vec{D}\right)\psi + \chi^\dagger\left(\vec{D}g_s\vec{E} - g_s\vec{E}\vec{D}\right)\chi\right] \\ & + \frac{c_3}{8m^2}\left[\psi^\dagger\left(i\vec{D}\times g_s\vec{E} - g_s\vec{E}\times i\vec{D}\right)\vec{\sigma}\psi + \chi^\dagger\left(i\vec{D}\times g_s\vec{E} - g_s\vec{E}\times i\vec{D}\right)\vec{\sigma}\chi\right] \\ & + \frac{c_4}{8m^3}\left[\psi^\dagger\left(\vec{D}^2\right)^2\psi - \chi^\dagger(\vec{D}^2)^2\chi\right] + \ldots\,, \end{aligned} \tag{2.63}$$

where the coefficients

$$c_i = 1 + o(\alpha_s) \tag{2.64}$$

have been introduced afterwards to take radiative corrections of full QCD properly into account. The local 4-fermion interactions are collected in $\delta\mathcal{L}_1$

$$\delta\mathcal{L}_1 = \sum_n f[n]\; O[n] + \ldots\,. \tag{2.65}$$

Thereby, the $f[n]$ are appropriate coupling constants and the summation extends over all 4-fermion operators $O[n]$, of which a few representatives have been given in (2.46)-(2.57). The dots stand for similar terms containing different types of effective interactions, such as possibly 5-,6-,7-... fermion operators, which in principle also may occur in the effective lagrangian, but are of no relevance for the here considered form of heavy quarkonium decay and production. The complete information on the highly relativistic dynamics associated with all the large scales beyond the ultraviolet cutoff Λ is exclusively contained in the coefficients c_i in $\delta\mathcal{L}$ and the couplings like the $f[n]$ in $\delta\mathcal{L}_1$. They are uniquely fixed by the condition, that NRQCD and full QCD must agree for all onshell Greens functions (this need not be the case for offshell Greens functions, since in deriving $\mathcal{L}_{\rm NRQCD}$ it was made use of the equations of motion). Λ adopts the role of a renormalization scale separating the large scale m from the lower scales mv, mv^2, ... By renormalizing NRQCD the operators in $\delta\mathcal{L}$ and in $\delta\mathcal{L}_1$ as well as the corresponding coefficients and couplings, respectively, become functions of Λ. The requirement, that $\mathcal{L}_{\rm NRQCD}$ as a whole must be independent of Λ, leads to renormalization group equations for the scaling of the NRQCD operators with respect to Λ. Finally, $\mathcal{L}_{\rm light}$ is the fully relativistic lagrangian of the light quarks and the gluons

$$\mathcal{L}_{\rm light} = \sum_q \bar{q} i\gamma^\mu D_\mu q - \frac{1}{2}\; tr[G_{\mu\nu}G^{\mu\nu}]\;. \tag{2.66}$$

2.2 The scaling rules of NRQCD

The QCD fine structure constant α_s as well as the fields and the operators entering $\mathcal{L}_{\rm NRQCD}$ exhibit a well defined scaling behaviour with respect to m and v, which is shown in table

Table 2.1: NRQCD scaling rules

object	scaling
α_s	v
ψ,χ	$(mv)^{\frac{3}{2}}$
D_t	mv^2
$\vec{D}$	mv
$g\phi$	mv^2
$g\vec{A}$	mv^3
$g\vec{E}$	m^2v^3
$g\vec{B}$	m^2v^4

2.1. These scaling rules can be used to estimate the relative importance of different NRQCD contributions. For example, the leading relativistic corrections in $\mathcal{L}_{\text{NRQCD}}$ - that are those terms in equation (2.63) for $\delta\mathcal{L}$, which are explicitly written out - are immediately seen to be suppressed by a factor v^2 compared to $\mathcal{L}_{\text{heavy}}$. The scaling rules are deduced from the heavy quark spinor normalizations, the virial theorem and the equations of motion encoded in $\mathcal{L}_{\text{NRQCD}}$, as we will now demonstrate in full detail.

The heavy quarks are limited to the volume V of the quarkonium state, which is given by $V \approx (1/mv)^3$, the cube of the inverse of the heavy quark momentum. The normalization of the heavy quark spinors to the value 1

$$1 = \int_V d^3\vec{x}\ \psi^\dagger\psi \approx \left(\frac{1}{mv}\right)^3 \psi^\dagger\psi \qquad \text{and} \qquad 1 = \int_V d^3\vec{x}\ \chi^\dagger\chi \approx \left(\frac{1}{mv}\right)^3 \chi^\dagger\chi \tag{2.67}$$

then results in

$$\psi, \chi \approx (mv)^{\frac{3}{2}}\ . \tag{2.68}$$

Assuming a coulomb like QCD potential $V(r) = \alpha_s(1/r)/r$ for (not too large) distance $r = 1/mv$ between the heavy quarks and estimating the heavy quark kinetic energy T to be of order mv^2, the virial theorem $T \approx V$ implies

$$\alpha_s(mv) \approx v\ . \tag{2.69}$$

The gluons and the light quarks in a heavy quarkonium all have momenta and energies similar to those of the heavy quark, from which they dynamically originate. As therefore

all spatial and time derivatives are related to the heavy quark momentum and energy, respectively, it follows

$$\vec{\nabla} \approx mv \qquad \text{and} \qquad \partial_t \approx mv^2 \ . \tag{2.70}$$

At leading order in g_s and $1/m$ $\vec{A}$ satisfies the equation of motion

$$(\partial_t^2 - \vec{\nabla}^2) g_s \vec{A} + \vec{\nabla}(\vec{\nabla} g_s \vec{A}) = \frac{g_s^2}{im}(\psi^\dagger \vec{\nabla}\psi - \chi^\dagger \vec{\nabla}\chi) - \frac{g_s^2}{2im}\vec{\nabla}(\psi^\dagger\psi - \chi^\dagger\chi) - \partial_t \vec{\nabla} g_s \phi \ . \tag{2.71}$$

Thereby, the light quarks have been neglected, since in a heavy quarkonium they first emerge through mechanisms of higher order in $\alpha_s \approx v$. Replacing the spinors, the spatial and the time derivatives as well as the squared QCD coupling $g_s^2 = 4\pi\alpha_s$ by their respective scaling behaviour according to (2.68)-(2.70) it follows

$$g_s \vec{A} \approx mv^3 - v g_s \phi \ . \tag{2.72}$$

At leading order in g_s and $1/m$ the equation of motion for ψ reads

$$\left[i\partial_t - g_s\phi + \frac{1}{2m}(\vec{\nabla}^2 - i g_s \vec{\nabla}\vec{A} - 2i g_s \vec{A}\vec{\nabla}) \right] \psi = 0 \ . \tag{2.73}$$

Making again use of the scaling behaviour given in (2.68)-(2.70) and inserting (2.72) for $g_s\vec{A}$, it is found for $g_s\phi$

$$g_s\phi \approx mv^2 \tag{2.74}$$

and hence

$$g_s \vec{A} \approx mv^3 \ . \tag{2.75}$$

From the above results one trivially obtains

$$\vec{D} \approx mv \qquad \text{and} \qquad D_t \approx mv^2 \ . \tag{2.76}$$

Finally, from the above results it is found for the scaling behaviour of the chromoelectric and the chromomagnetic field as defined in (2.36), (2.37)

$$g_s \vec{E} \approx m^2 v^3 \qquad \text{and} \qquad g_s \vec{B} \approx m^2 v^4 \ . \tag{2.77}$$

Therewith all the scaling rules stated in table (2.1) have been proved.

2.3 Decay and production of heavy quarkonia

The factorization formula (1.4) for the total decay width of heavy quarkonia

$$\Gamma_H = \sum_n \Gamma_{Q\bar{Q}[n]} \langle O[n] \rangle_H \tag{2.78}$$

follows directly from the NRQCD lagrangian $\mathcal{L}_{\rm NRQCD}$ as a consequence of the optical theorem. Thereby, the coefficients $\Gamma_{Q\bar{Q}[n]}$ are related to the imaginary part of the couplings $f[n]$ associated with the $O[n]$ through the equation

$$\Gamma_{Q\bar{Q}[n]} = 2 \text{ Im f[n]} \ , \tag{2.79}$$

while the decay matrix elements $\langle O[n]\rangle_H$ are given as expectation values of the 4-fermion operators $O[n]$ with respect to the quarkonium state $|H\rangle$

$$\langle O[n]\rangle_H = \langle H|O[n]|H\rangle \ . \tag{2.80}$$

Note thereby, that according to the usual conventions of NRQCD $|H\rangle \equiv |H(P)\rangle$ is understood to be nonrelativistically normalized

$$\langle H(P')|H(P)\rangle = (2\pi)^3\delta^3(\vec{P}-\vec{P}') \ , \tag{2.81}$$

where P and P' denote the heavy quarkonium momentum. Those matrix elements, which may contribute at the current level of accuracy of NRQCD calculations, are

$$\left\langle O\left[^{2S+1}L_J^{(c)}\right]\right\rangle_H = \langle H|O\left[^{2S+1}L_J^{(c)}\right]|H\rangle \tag{2.82}$$

with the operators $O\left[^{2S+1}L_J^{(c)}\right]$ given in (2.46)-(2.57). In combination with the short distance coefficients $\Gamma_{Q\bar{Q}[^{2S+1}L_J^{(c)}]}$ they correspond to quarkonium decay via intermediate heavy quark pairs in quantum states with definite color and spin orbital angular momentum quantum numbers $^{2S+1}L_J^{(c)}$. In contrast to the decay width the production cross section σ_H of heavy quarkonia can not be derived from $\mathcal{L}_{\rm NRQCD}$. The factorization formula (1.3) for σ_H

$$\sigma_H = \sum_n \sigma_{Q\bar{Q}[n]} \ \langle O^H[n]\rangle \tag{2.83}$$

must therefore be postulated. Here the $\langle O^H[n]\rangle \equiv \langle 0|O^H[n]|0\rangle$ are defined as vacuum expectation values of a new kind of 4-fermion operators $O^H[n]$ appropriate for heavy quarkonium production. A complete set of them is constructed in a similar way as that for the 4-fermion operators relevant for decay. Those production matrix elements, which may be significant at the current level of accuracy of NRQCD analyses, are

$$\left\langle O^H\left[^1S_0^{(1)}\right]\right\rangle = \langle 0|\chi^\dagger\psi\mathcal{P}^H\psi^\dagger\chi|0\rangle \tag{2.84}$$

$$\left\langle O^H\left[^3S_1^{(1)}\right]\right\rangle = \langle 0|\chi^\dagger\vec{\sigma}\psi\mathcal{P}^H\psi^\dagger\vec{\sigma}\chi|0\rangle \tag{2.85}$$

$$\left\langle O^H\left[^1P_1^{(1)}\right]\right\rangle = \langle 0|\chi^\dagger\left(-\frac{i}{2}\overleftrightarrow{D}\right)\psi\mathcal{P}^H\psi^\dagger\left(-\frac{i}{2}\overleftrightarrow{D}\right)\chi|0\rangle \tag{2.86}$$

$$\left\langle O^H\left[^3P_0^{(1)}\right]\right\rangle = \langle 0|\frac{1}{3}\chi^\dagger\left(-\frac{i}{2}\overleftrightarrow{D}\,\vec{\sigma}\right)\psi\mathcal{P}^H\psi^\dagger\left(-\frac{i}{2}\overleftrightarrow{D}\,\vec{\sigma}\right)\chi|0\rangle \tag{2.87}$$

$$\left\langle O^H\left[^3P_1^{(1)}\right]\right\rangle = \langle 0|\frac{1}{2}\chi^\dagger\left(-\frac{i}{2}\overleftrightarrow{D}\times\vec{\sigma}\right)\psi\mathcal{P}^H\psi^\dagger\left(-\frac{i}{2}\overleftrightarrow{D}\times\vec{\sigma}\right)\chi|0\rangle \tag{2.88}$$

$$\left\langle O^H\left[^3P_2^{(1)}\right]\right\rangle = \langle 0|\chi^\dagger\left(-\frac{i}{2}\overleftrightarrow{D}^{\,(i}\,\sigma^{j)}\right)\psi\mathcal{P}^H\psi^\dagger\left(-\frac{i}{2}\overleftrightarrow{D}^{\,(i}\,\sigma^{j)}\right)\chi|0\rangle \tag{2.89}$$

and

$$\left\langle O^H\left[{}^1S_0^{(8)}\right]\right\rangle = \langle 0|\chi^\dagger T^a\psi\mathcal{P}^H\psi^\dagger T^a\chi|0\rangle \tag{2.90}$$

$$\left\langle O^H\left[{}^3S_1^{(8)}\right]\right\rangle = \langle 0|\chi^\dagger \vec{\sigma} T^a\psi\mathcal{P}^H\psi^\dagger \vec{\sigma} T^a\chi|0\rangle \tag{2.91}$$

$$\left\langle O^H\left[{}^1P_1^{(8)}\right]\right\rangle = \langle 0|\chi^\dagger \left(-\frac{i}{2}\overleftrightarrow{D}\right) T^a\psi\mathcal{P}^H\psi^\dagger \left(-\frac{i}{2}\overleftrightarrow{D}\right) T^a\chi|0\rangle \tag{2.92}$$

$$\left\langle O^H\left[{}^3P_0^{(8)}\right]\right\rangle = \langle 0|\frac{1}{3}\chi^\dagger \left(-\frac{i}{2}\overleftrightarrow{D}\,\vec{\sigma}\right) T^a\psi\mathcal{P}^H\psi^\dagger \left(-\frac{i}{2}\overleftrightarrow{D}\,\vec{\sigma}\right) T^a\chi|0\rangle \tag{2.93}$$

$$\left\langle O^H\left[{}^3P_1^{(8)}\right]\right\rangle = \langle 0|\frac{1}{2}\chi^\dagger \left(-\frac{i}{2}\overleftrightarrow{D}\times\vec{\sigma}\right) T^a\psi\mathcal{P}^H\psi^\dagger \left(-\frac{i}{2}\overleftrightarrow{D}\times\vec{\sigma}\right) T^a\chi|0\rangle \tag{2.94}$$

$$\left\langle O^H\left[{}^3P_2^{(8)}\right]\right\rangle = \langle 0|\chi^\dagger \left(-\frac{i}{2}\overleftrightarrow{D}^{(i}\,\sigma^{j)}\right) T^a\psi\mathcal{P}^H\psi^\dagger \left(-\frac{i}{2}\overleftrightarrow{D}^{(i}\,\sigma^{j)}\right) T^a\chi|0\rangle\ . \tag{2.95}$$

Thereby,

$$\mathcal{P}^H = \sum_X \sum_{J_z=-J}^{J} |HX\rangle\langle XH| \tag{2.96}$$

is the projector on all states, which only contain the heavy quarkonium H inclusively soft hadronic rest X created by the long distance dynamics during the formation of the quarkonium bound state, and J_z denotes the z component of the total angular momentum J of H. In combination with the short distance coefficients $\sigma_{Q\bar{Q}[^{2S+1}L_J^{(c)}]}$ the above listed matrix elements correspond to quarkonium production via intermediate heavy quark pairs in quantum states with definite color and spin orbital angular momentum quantum numbers ${}^{2S+1}L_J^{(c)}$. Unlike the matrix elements $\langle O[n]\rangle_H$ and $\langle O^H[n]\rangle$, which contain the entire information on the nonrelativistic and highly nonperturbative dynamics of the quarkonium bound state and therefore can be reliably determined only from measurement, the coefficients $\Gamma_{Q\bar{Q}[n]}$ and $\sigma_{Q\bar{Q}[n]}$ are calculable in perturbation theory, as they only depend on the highly relativistic short distance dynamics of heavy quark pair annihilation and creation. However, it should be emphasised, that in contrast to the factorization of heavy quarkonium decay widths, which has been proven rigorously[9], the factorization of heavy quarkonium production cross sections is an assumption, which may be problematic. In fact circumstances of heavy quarkonium production are known, under which the factorization breaks down[9]. One method to determine the short distance coefficients $\Gamma_{Q\bar{Q}[n]}$ and $\sigma_{Q\bar{Q}[n]}$ consists in perturbative matching of NRQCD and full QCD. In case of quarkonium decay low energy $Q\bar{Q} \to Q\bar{Q}$ onshell scattering amplitudes are calculated both in perturbative NRQCD and in perturbative QCD. The $f[n]$ are then appropriately tuned, so that both calculations agree. The $\Gamma_{Q\bar{Q}[n]}$ are finally obtained from the $f[n]$ by using (2.79). Similarly, in case of production the $\sigma_{Q\bar{Q}[n]}$ are determined by matching the results for the cross sections for the production of an onshell heavy quark pair with small relative momentum in perturbative NRQCD and in perturbative QCD. The perturbative matching procedure is introduced in [9] and in case of production instructively demonstrated at simple examples in [10]. In this work an alternative method will be applied, which is based on the use of appropriate covariant color and spin projectors to take the Fock space

structure of the intermediate heavy quark pair adequately into account [15]. At least in four space time dimensions it can be shown to be equivalent to the perturbative matching method. For an extensive presentation of the covariant projection method it is referred to chapter 3.

2.4 Heavy quark spin symmetry and vaccuum saturation approximation

At leading order $\mathcal{L}_{\text{NRQCD}}$ exhibits heavy quark spin symmetry, which leads to simple relations between different production or decay matrix elements. For example among the matrix elements relevant for J/ψ, χ_{cJ}, η_c and h_c decay or production, respectively, there hold relations like

$$\left\langle O\left[{}^3S_1^{(1)}\right]\right\rangle_{J/\psi} = \left\langle O\left[{}^1S_0^{(1)}\right]\right\rangle_{\eta_c}\left(1+o(v^2)\right) \tag{2.97}$$

$$\left\langle O\left[{}^3P_J^{(8)}\right]\right\rangle_{J/\psi} = \left\langle O\left[{}^3P_0^{(8)}\right]\right\rangle_{J/\psi}\left(1+o(v^2)\right) \tag{2.98}$$

$$\left\langle O\left[{}^3P_J^{(8)}\right]\right\rangle_{\psi'} = \left\langle O\left[{}^3P_0^{(8)}\right]\right\rangle_{\psi'}\left(1+o(v^2)\right) \tag{2.99}$$

$$\begin{aligned}\left\langle O\left[{}^3P_J^{(1)}\right]\right\rangle_{\chi_{cJ}} &= \left\langle O\left[{}^3P_0^{(1)}\right]\right\rangle_{\chi_{c0}}\left(1+o(v^2)\right)\\ &= \left\langle O\left[{}^1P_1^{(1)}\right]\right\rangle_{h_c}\left(1+o(v^2)\right)\end{aligned} \tag{2.100}$$

$$\left\langle O\left[{}^3S_1^{(8)}\right]\right\rangle_{\chi_{cJ}} = \left\langle O\left[{}^3S_1^{(8)}\right]\right\rangle_{\chi_{c0}}\left(1+o(v^2)\right) \tag{2.101}$$

$$\left\langle O^{J/\psi}\left[{}^3S_1^{(1)}\right]\right\rangle = 3\ \left\langle O^{\eta_c}\left[{}^1S_0^{(1)}\right]\right\rangle\left(1+o(v^2)\right) \tag{2.102}$$

$$\left\langle O^{J/\psi}\left[{}^3P_J^{(8)}\right]\right\rangle = (2J+1)\ \left\langle O^{J/\psi}\left[{}^3P_0^{(8)}\right]\right\rangle\left(1+o(v^2)\right) \tag{2.103}$$

$$\left\langle O^{\psi'}\left[{}^3P_J^{(8)}\right]\right\rangle = (2J+1)\ \left\langle O^{\psi'}\left[{}^3P_0^{(8)}\right]\right\rangle\left(1+o(v^2)\right) \tag{2.104}$$

$$\left\langle O^{\chi_{cJ}}\left[{}^3P_J^{(1)}\right]\right\rangle = (2J+1)\ \left\langle O^{\chi_{c0}}\left[{}^3P_0^{(1)}\right]\right\rangle\left(1+o(v^2)\right) \tag{2.105}$$

$$\left\langle O^{\chi_{cJ}}\left[{}^3P_1^{(1)}\right]\right\rangle = \left\langle O^{h_c}\left[{}^1P_1^{(1)}\right]\right\rangle\left(1+o(v^2)\right) \tag{2.106}$$

$$\left\langle O^{\chi_{cJ}}\left[{}^3S_1^{(8)}\right]\right\rangle = (2J+1)\ \left\langle O^{\chi_{c0}}\left[{}^3S_1^{(8)}\right]\right\rangle\left(1+o(v^2)\right)\ . \tag{2.107}$$

Thereby the factors 3 and $2J+1$ are spin multiplicity factors originating from the sum over J_z in (2.96). For illustration purpose we will derive (2.97) and (2.102):

$$\begin{aligned}\left\langle O\left[{}^3S_1^{(1)}\right]\right\rangle_{J/\psi} &= \langle J/\psi|\psi^\dagger\vec{\sigma}\chi\chi^\dagger\vec{\sigma}\psi|J/\psi\rangle\\ &= \langle\eta_c|\psi^\dagger\chi\chi^\dagger\psi|\eta_c\rangle\left(1+o(v^2)\right)\\ &= \left\langle O\left[{}^1S_0^{(1)}\right]\right\rangle_{\eta_c}\left(1+o(v^2)\right)\end{aligned} \tag{2.108}$$

proves (2.97), and

$$\left\langle O^{J/\psi}\left[{}^3S_1^{(1)}\right]\right\rangle = \sum_X\sum_{J_z=-1}^{1}\langle 0|\chi^\dagger\vec{\sigma}\psi|J/\psi X\rangle\langle X J/\psi|\psi^\dagger\vec{\sigma}\chi|0\rangle$$

$$
\begin{aligned}
&= 3 \sum_X \langle 0|\chi^\dagger \vec{\sigma}\psi|J/\psi X\rangle\langle X J/\psi|\psi^\dagger\vec{\sigma}\chi|0\rangle \\
&= 3 \sum_X \langle 0|\chi^\dagger \psi|\eta_c X\rangle\langle X\eta_c|\psi^\dagger\chi|0\rangle \left(1+o(v^2)\right) \\
&= 3 \left\langle O^{\eta_c}\left[{}^1S_0^{(1)}\right]\right\rangle \left(1+o(v^2)\right) \qquad (2.109)
\end{aligned}
$$

proves (2.102). Moreover, the matrix elements for heavy quarkonium production can be related to those for heavy quarkonium decay by making use of the vacuum saturation approximation. Since the creation of soft hadronic states $|X\rangle$ in connection with the formation of the heavy quarkonium H only happens through NRQCD effects of higher order in v the projector $\sum_X |X\rangle\langle X|$ on all such states can be approximated by the vacuum projector $|0\rangle\langle 0|$

$$
\sum_X |X\rangle\langle X| = |0\rangle\langle 0| + o(v^4) \; . \qquad (2.110)
$$

Thus it follows for instance

$$
\begin{aligned}
\left\langle O^{J/\psi}\left[{}^3S_1^{(1)}\right]\right\rangle &= \sum_X \sum_{J_z=-1}^{1} \langle 0|\chi^\dagger\vec{\sigma}\psi|J/\psi X\rangle\langle X J/\psi|\psi^\dagger\vec{\sigma}\chi|0\rangle \\
&= \sum_{J_z=-1}^{1} \langle 0|\chi^\dagger\vec{\sigma}\psi|J/\psi\rangle\langle J/\psi|\psi^\dagger\vec{\sigma}\chi|0\rangle \left(1+o(v^4)\right) \\
&= 3\, \langle J/\psi|\psi^\dagger\vec{\sigma}\chi|0\rangle\langle 0|\chi^\dagger\vec{\sigma}\psi|J/\psi\rangle \left(1+o(v^4)\right) \\
&= 3 \sum_X \langle J/\psi|\psi^\dagger\vec{\sigma}\chi|X\rangle\langle X|\chi^\dagger\vec{\sigma}\psi|J/\psi\rangle \left(1+o(v^4)\right) \\
&= 3\, \langle J/\psi|\psi^\dagger\vec{\sigma}\chi\chi^\dagger\vec{\sigma}\psi|J/\psi\rangle \left(1+o(v^4)\right) \; , \qquad (2.111)
\end{aligned}
$$

and hence

$$
\left\langle O^{J/\psi}\left[{}^3S_1^{(1)}\right]\right\rangle = 3 \left\langle O\left[{}^3S_1^{(1)}\right]\right\rangle_{J/\psi} \left(1+o(v^4)\right) \; . \qquad (2.112)
$$

Note, that in the last line of (2.111) it was made use of the circumstance, that after annihilating the heavy quark pair from the quarkonium state only soft hadronic rest X remains. Analogously, to give a few more important examples, it is found

$$
\left\langle O^{J/\psi}\left[{}^3S_1^{(8)}\right]\right\rangle = 3 \left\langle O\left[{}^3S_1^{(8)}\right]\right\rangle_{J/\psi} \left(1+o(v^4)\right) \qquad (2.113)
$$

$$
\left\langle O^{\psi'}\left[{}^3S_1^{(8)}\right]\right\rangle = 3 \left\langle O\left[{}^3S_1^{(8)}\right]\right\rangle_{\psi'} \left(1+o(v^4)\right) \qquad (2.114)
$$

$$
\left\langle O^{\chi_{cJ}}\left[{}^3P_J^{(1)}\right]\right\rangle = (2J+1) \left\langle O\left[{}^3P_J^{(1)}\right]\right\rangle_{\chi_{cJ}} \left(1+o(v^4)\right) \; . \qquad (2.115)
$$

As becomes obvious from (2.97)-(2.107) and (2.112)-(2.115) the approximate heavy quark spin symmetry and the vacuum saturation approximation allow for a considerable reduction of the number of free parameters in NRQCD predictions.

In view of the calculations performed in this work we list in table 2.2 all the matrix elements, which are relevant for J/ψ, ψ' and χ_{cJ} production. The respective scaling

Table 2.2: Matrix elements relevant for J/ψ, ψ', χ_{cJ} production

matrix element	scaling
$O^{J/\psi,\psi'}\left[{}^3S_1^{(1)}\right]$	m^3v^3
$O^{J/\psi,\psi'}\left[{}^1S_0^{(8)}\right]$	m^3v^7
$O^{J/\psi,\psi'}\left[{}^3S_1^{(8)}\right]$	m^3v^7
$O^{J/\psi,\psi'}\left[{}^3P_0^{(8)}\right]$	m^5v^7
$O^{\chi_{c0}}\left[{}^3P_0^{(1)}\right]$	m^5v^5
$O^{\chi_{c0}}\left[{}^3S_1^{(8)}\right]$	m^3v^5

behaviour, quoted in the second column, is found from the scaling rules derived in section 2.3 and by noting, that a chromoelectric (chromomagnetic) dipole transition leads to an additional suppression factor v^2 (v^4).

Chapter 3

The short distance coefficients for heavy quarkonium production

3.1 The covariant projection method

In the following we will restrict ourselves to heavy quarkonium production. For that case we will now present the covariant projection method of NRQCD in D space time dimensions [15]. This method allows us to calculate those short distance coefficients $\sigma_{Q\bar{Q}[n]}$ in the factorization formula (1.3) for σ_H, which describe the creation of the heavy quark pair in configurations $n = {}^1S_0^{(c)}, {}^3S_1^{(c)}, {}^1P_1^{(c)}, {}^3P_{J=0,1,2}^{(c)}$, from amplitudes $\mathcal{M}[n]$, which are given by

$$\mathcal{M}\left[{}^1S_0^{(c)}\right] = tr\left[\mathcal{T}\Pi_0\mathcal{C}_c\right]\big|_{q=0} \ , \tag{3.1}$$

$$\mathcal{M}\left[{}^3S_1^{(c)}\right] = \epsilon_\alpha \, tr\left[\mathcal{T}\Pi_1^\alpha\mathcal{C}_c\right]\big|_{q=0} \ , \tag{3.2}$$

$$\mathcal{M}\left[{}^1P_1^{(c)}\right] = \epsilon_\alpha \, \frac{\partial}{\partial q_\alpha} tr\left[\mathcal{T}\Pi_0\mathcal{C}_c\right]\Big|_{q=0} \ , \tag{3.3}$$

$$\mathcal{M}\left[{}^3P_J^{(c)}\right] = \mathcal{E}_{\alpha\beta}^{(J)} \, \frac{\partial}{\partial q_\alpha} tr\left[\mathcal{T}\Pi_1^\beta\mathcal{C}_c\right]\Big|_{q=0} \ . \tag{3.4}$$

Here $\mathcal{T}$ is the heavy quark spinor amputated Feynman amplitude for the perturbative creation of a heavy quark Q with momentum

$$p = \frac{P}{2} + q \tag{3.5}$$

and a heavy antiquark $\bar{Q}$ with momentum

$$\bar{p} = \frac{P}{2} - q \tag{3.6}$$

in the corresponding hard scattering process. Thereby

$$P = p + \bar{p} \tag{3.7}$$

is the total momentum of the $Q\bar{Q}$ pair, and

$$q = \frac{1}{2}(p - \bar{p}) \tag{3.8}$$

becomes in the $Q\bar{Q}$ center of mass system

$$q_{CMS} = \begin{pmatrix} 0 \\ \vec{q}_{CMS} \end{pmatrix} \tag{3.9}$$

with $\vec{q}_{CMS}$ being the nonrelativistic heavy quark momentum in that frame. Throughout this work, in calculating $\mathcal{T}$, we employ the Feynman rules of the Standard Model in the conventions of [40]. Furthermore,

$$\Pi_0 = \frac{1}{\sqrt{8m^3}} \left(\frac{\not{P}}{2} - \not{q} - m \right) \gamma_5 \left(\frac{\not{P}}{2} + \not{q} + m \right) \tag{3.10}$$

and

$$\Pi_1^\alpha = \frac{1}{\sqrt{8m^3}} \left(\frac{\not{P}}{2} - \not{q} - m \right) \gamma^\alpha \left(\frac{\not{P}}{2} + \not{q} + m \right) \tag{3.11}$$

are projectors on $Q\bar{Q}$ configurations with total spin $S = 0$ and $S = 1$, respectively, and $\mathcal{C}_c$ with

$$\mathcal{C}_1 = \frac{1}{\sqrt{3}}\, 1 \qquad \text{and} \qquad \mathcal{C}_8 = \sqrt{2}\, T^a \tag{3.12}$$

are projectors on color singlet ($c = 1$) and color octet ($c = 8$) $Q\bar{Q}$ states, respectively. ϵ_α and $\mathcal{E}^{(J)}_{\alpha\beta}$ are the polarization vector and accordingly the polarization tensor of a $Q\bar{Q}$ configuration with total angular momentum J, which results from pure spin or pure orbital angular momentum in the former and from the composition of spin and orbital angular momentum in the latter case. ϵ_α and $\mathcal{E}^{(J)}_{\alpha\beta}$ satisfy the polarization sum relations

$$\sum_{J_z=-J}^{J} \epsilon^*_{\alpha'} \epsilon_\alpha = \Pi_{\alpha'\alpha} \ , \tag{3.13}$$

$$\sum_{J_z=-J}^{J} \mathcal{E}^{(J)*}_{\alpha'\beta'}\ \mathcal{E}^{(J)}_{\alpha\beta} = \Pi^{(J)}_{\alpha'\beta'\alpha\beta} \tag{3.14}$$

with

$$\Pi_{\alpha\beta} = -g_{\alpha\beta} + \frac{P_\alpha P_\beta}{M^2} \tag{3.15}$$

and

$$\Pi^{(J)}_{\alpha'\beta'\alpha\beta} = \begin{cases} \frac{1}{D-1} \Pi_{\alpha'\beta'} \Pi_{\alpha\beta} \ ; \ J = 0 \\ \frac{1}{2} [\Pi_{\alpha'\alpha} \Pi_{\beta'\beta} - \Pi_{\alpha'\beta} \Pi_{\beta'\alpha}] \ ; \ J = 1 \\ \frac{1}{2} [\Pi_{\alpha'\alpha} \Pi_{\beta'\beta} + \Pi_{\alpha'\beta} \Pi_{\beta'\alpha}] - \frac{1}{D-1} \Pi_{\alpha'\beta'} \Pi_{\alpha\beta} \ ; \ J = 2 \ . \end{cases} \tag{3.16}$$

Thereby $M = 2m$ is the mass of the heavy quarkonium. With the amplitudes $\mathcal{M}[n]$ in (3.1)-(3.4) the short distance coefficients relevant for heavy quarkonium production are given by

$$\sigma_{Q\bar{Q}[n]} = \frac{1}{F}\int dPS_{n+1}(p_1+p_2;P,k_1,k_2,...,k_n)\frac{\overline{\sum}|\mathcal{M}[n]|^2}{N_{\rm col}\ N_{\rm pol}}\ ;$$
$$n = {}^1S_0^{(c)}, {}^3S_1^{(c)}, {}^1P_1^{(c)}, {}^3P_{J=0,1,2}^{(c)}\ . \tag{3.17}$$

Here p_1, p_2 are the momenta of the particles in the initial state and k_1, k_2,..., k_n are the momenta of all the particles created together with the $Q\bar{Q}$ pair in the final state of the short distance process. F denotes the flux factor, which in case of massless initial state particles reads

$$F = 2s \qquad \text{with} \qquad s = (p_1+p_2)^2\ . \tag{3.18}$$

$dPS_{n+1}(p_1+p_2;P,k_1,k_2,...,k_n)$ is the D dimensional phase space measure, which in the here used conventions[40] for the normalizations of the states, spinors and gauge boson polarization vectors takes the form

$$dPS_{n+1}(p_1+p_2;P,k_1,k_2,...,k_n) = \frac{d^{D-1}\vec{P}}{(2\pi)^{D-1}2P^0}\frac{d^{D-1}\vec{k}_1}{(2\pi)^{D-1}2k_1^0}\frac{d^{D-1}\vec{k}_2}{(2\pi)^{D-1}2k_2^0}.....\frac{d^{D-1}\vec{k}_n}{(2\pi)^{D-1}2k_n^0}$$
$$\times\,(2\pi)^D\delta(p_1+p_2-P-k_1-k_2-...-k_n)\ . \tag{3.19}$$

$\overline{\sum}$ in (3.17) stands for the average (sum) over the spin and color degrees of freedom of the particles in the initial (final) state, whereby the $Q\bar{Q}$ pair is treated as a single particle with spin J_z and color $a = 1,2,...,8$ in case it is in a color octet and no color in case it is in a color singlet state. Finally, $N_{\rm col}$ and $N_{\rm pol}$ are defined by

$$N_{\rm col} = \begin{cases} 6\ ;\ c=1 \\ 8\ ;\ c=8 \end{cases} \qquad \text{and} \qquad N_{\rm pol} = 2J+1\ . \tag{3.20}$$

Without the summtion over J_z, (3.17) yields the short distance coefficients for polarized heavy quarkonium production.

3.2 Derivation of the covariant projection method

We now turn to the derivation of the projection formalism. In doing so, we are forced to confine us to $D = 4$ space time dimensions, since for $D \neq 4$ the role of higher dimensional representations of the spatial rotation group is not understood until now.

Let's consider a heavy quarkonium production process with two elementary (non composed) particles in the initial state and the inclusively with soft hadronic rest X produced quarkonium H and possibly further specified particles in the final state. If we assume, that the momenta p and $\bar{p}$ of the heavy quark Q and the heavy antiquark $\bar{Q}$ are distributed very sharply around half the quarkonium momentum P, a good approximation for the production amplitude $\mathcal{A}$ is

$$\mathcal{A} = \mathcal{T}_{i\bar{i};n\bar{n}}\ \langle HX|\bar{\Psi}_{in}\Psi_{\bar{i}\bar{n}}|0\rangle\ . \tag{3.21}$$

Thereby $\mathcal{T}_{i\bar{i};n\bar{n}}$ is the heavy quark spinor amputated Feynman amplitude for the production process with the nonperturbative state $|HX\rangle$ replaced by the perturbative Fock state $|prn;\bar{p}\bar{r}\bar{n}\rangle$ containing the heavy quark Q with momentum p, helicity r and color n and the heavy antiquark $\bar{Q}$ with momentum $\bar{p}$, helicity $\bar{r}$ and color $\bar{n}$. $\langle HX|\bar{\Psi}_{in}\Psi_{\bar{i}\bar{n}}|0\rangle$ is defined in terms of the spinors $u_{irn}(p)$, $v_{\bar{i}\bar{r}\bar{n}}(\bar{p})$ and the creation operators $c^\dagger_{rn}(p)$, $d^\dagger_{\bar{r}\bar{n}}(\bar{p})$ of the heavy quark and the heavy antiquark, respectively

$$\langle HX|\bar{\Psi}_{in}\Psi_{\bar{i}\bar{n}}|0\rangle = \int d\tilde{p}d\tilde{\bar{p}}\langle HX|\sum_r \bar{u}_{irn}(p)c^\dagger_{rn}(p)\sum_{\bar{r}} v_{\bar{i}\bar{r}\bar{n}}(\bar{p})d^\dagger_{\bar{r}\bar{n}}(\bar{p})|0\rangle \ . \tag{3.22}$$

Here i and $\bar{i}$ are dirac indices and $d\tilde{p}$ serves as an abbreviation for the integration measure

$$d\tilde{p} = \frac{d^3p}{(2\pi)^3 2p^0} \ . \tag{3.23}$$

According to the conventions of [40] we use for the normalizations of the spinors and the creation and annihilation operators of the heavy quark

$$\bar{u}_{rn}(p)u_{r'n'}(p) = 2m\delta_{rr'}\delta_{nn'} \tag{3.24}$$

$$\bar{v}_{\bar{r}\bar{n}}(\bar{p})v_{\bar{r}'\bar{n}'}(\bar{p}) = -2m\delta_{\bar{r}\bar{r}'}\delta_{\bar{n}\bar{n}'} \tag{3.25}$$

$$\{c_{rn}(p), c^\dagger_{r'n'}(p')\} = 2p^0\delta_{rr'}\delta_{nn'}\delta^3(\vec{p}-\vec{p'}) \tag{3.26}$$

$$\{d_{\bar{r}\bar{n}}(p), d^\dagger_{\bar{r}'\bar{n}'}(p')\} = 2p^0\delta_{\bar{r}\bar{r}'}\delta_{\bar{n}\bar{n}'}\delta^3(\vec{p}-\vec{p'}) \ . \tag{3.27}$$

In order to simplify the notation, for the time being, we will suppress the color indices n and $\bar{n}$. Choosing the quarkonium rest frame and inserting a sum over spin singlet and spin triplet Fock states $|Q\bar{Q}[^1S_0]\rangle$ and $|Q\bar{Q}[^3S_1]\rangle_l$ of the heavy quark pair (where Q carries the color n and $\bar{Q}$ carries the color $\bar{n}$), we get for the amplitude

$$\begin{aligned}\mathcal{A} &= \mathcal{T}_{i\bar{i}}\ \langle HX|Q\bar{Q}[^1S_0]\rangle\ \langle Q\bar{Q}[^1S_0]|\bar{\Psi}_i\Psi_{\bar{i}}|0\rangle + \mathcal{T}_{i\bar{i}}\sum_{l=1}^{3}\langle HX|Q\bar{Q}[^3S_1]\rangle_l\ {}_l\langle Q\bar{Q}[^3S_1]|\bar{\Psi}_i\Psi_{\bar{i}}|0\rangle \\ &= tr[\mathcal{T}\Pi_0]\ \langle HX|Q\bar{Q}[^1S_0]\rangle + \sum_{l=1}^{3} tr[\mathcal{T}\Pi_1^l]\ \langle HX|Q\bar{Q}[^3S_1]\rangle_l \ ,\end{aligned} \tag{3.28}$$

with the spin singlet and spin triplet projectors given by

$$\Pi_{0\bar{i}i} = \langle Q\bar{Q}[^1S_0]|\bar{\Psi}_i\Psi_{\bar{i}}|0\rangle \tag{3.29}$$

and

$$\Pi^l_{1\bar{i}i} = \ {}_l\langle Q\bar{Q}[^3S_1]|\bar{\Psi}_i\Psi_{\bar{i}}|0\rangle \tag{3.30}$$

and the index $l = 1, 2, 3$ labelling the three possible triplet states. While the terms $tr[\mathcal{T}\Pi_0]$ and $tr[\mathcal{T}\Pi_1^l]$ describe the perturbative creation of the heavy quark pair in an intermediate spin singlet and spin triplet state respectively, the matrix elements $\langle HX|Q\bar{Q}[^1S_0]\rangle$ and $\langle HX|Q\bar{Q}[^3S_1]\rangle^l$ contain the nonperturbative transition of these states into the observed quarkonium state. Parametrizing p and $\bar{p}$ by

$$p = P/2 + q \qquad , \qquad \bar{p} = P/2 - q \ , \tag{3.31}$$

the approximation, which underlies this factorization of $\mathcal{A}$, corresponds to putting q equal to zero in the short distance parts $tr[\mathcal{T}\Pi_0]$ and $tr[\mathcal{T}\Pi_1^l]$. Improving this approximation by including higher orders of the Taylor expansion of the short distance parts with respect to q brings additionally orbital angular momenta of the heavy quark pair into account, so that the sum in principle extends over all intermediate spin orbital angular momentum states. We will show this up to linear order in q, that means up to intermediate P wave states. In the quarkonium rest frame $\mathcal{A}$ reads up to this order in q

$$\begin{aligned}\mathcal{A} = tr[\mathcal{T}\Pi_0]|_{\vec{q}=0}\ \langle HX|Q\bar{Q}[^1S_0]\rangle + \sum_{i=1}^{3}\frac{\partial}{\partial q^i}\, tr[\mathcal{T}\Pi_0]|_{\vec{q}=0}\, q^i\langle HX|Q\bar{Q}[^1S_0]\rangle \\ + \sum_{l=1}^{3} tr[\mathcal{T}\Pi_1^l]\Big|_{\vec{q}=0}\langle HX|Q\bar{Q}[^3S_1]\rangle_l + \sum_{i,l=1}^{3}\frac{\partial}{\partial q^i}\, tr[\mathcal{T}\Pi_1^l]\Big|_{\vec{q}=0} q^i\langle HX|Q\bar{Q}[^3S_1]\rangle_l\ .\end{aligned} \tag{3.32}$$

To express the spin singlet and spin triplet projectors in terms of dirac matrices, we use for the heavy quark spinors the parametrization

$$u_1(p) = \frac{\not{p}+m}{\sqrt{p^0+m}}\begin{pmatrix}1\\0\\0\\0\end{pmatrix}\ ,\ u_2(p) = \frac{\not{p}+m}{\sqrt{p^0+m}}\begin{pmatrix}0\\-1\\0\\0\end{pmatrix}\ ,$$

$$v_1(p) = \frac{\not{\bar{p}}-m}{\sqrt{p^0+m}}\begin{pmatrix}0\\0\\1\\0\end{pmatrix}\ ,\ v_2(p) = \frac{\not{\bar{p}}-m}{\sqrt{p^0+m}}\begin{pmatrix}0\\0\\0\\1\end{pmatrix}\ , \tag{3.33}$$

which is consistent with (2.4) as choice for the representation of the dirac matrices and the normalization conditions (3.24), (3.25). Noting, that $u_1(p)$ represents a spin up and $u_2(p)$ a spin down quark but vice versa $v_1(\bar{p})$ a spin down and $v_2(\bar{p})$ a spin up antiquark, the heavy quark antiquark spin singlet state is given by

$$|Q\bar{Q}[^1S_0]\rangle = \frac{1}{\sqrt{2}}(|p1;\bar{p}1\rangle - |p2;\bar{p}2\rangle)\ , \tag{3.34}$$

and we will choose the following linear combinations of the standard spin triplet states

$$\begin{aligned}|Q\bar{Q}[^3S_1]\rangle_1 &= -\frac{1}{\sqrt{2}}(|Q\bar{Q}[^3S_1]\rangle_{S_z=+1} - |Q\bar{Q}[^3S_1]\rangle_{S_z=-1}) \\ &= -\frac{1}{\sqrt{2}}(|p1;\bar{p}2\rangle - |p2;\bar{p}1\rangle) \qquad (3.35)\\ |Q\bar{Q}[^3S_1]\rangle_2 &= \frac{i}{\sqrt{2}}(|Q\bar{Q}[^3S_1]\rangle_{S_z=+1} + |Q\bar{Q}[^3S_1]\rangle_{S_z=-1}) \\ &= \frac{i}{\sqrt{2}}(|p1;\bar{p}2\rangle + |p2;\bar{p}1\rangle) \qquad (3.36)\end{aligned}$$

$$|Q\bar{Q}[^3S_1]\rangle_3 = -|Q\bar{Q}[^3S_1]\rangle_{S_z=0}$$
$$= -\frac{1}{\sqrt{2}}(|p1;\bar{p}1\rangle + |p2;\bar{p}2\rangle) \ , \tag{3.37}$$

with S_z denoting the spin component in z-direction. From its definition (3.29), it follows now for the spin singlet projector in the quarkonium rest frame

$$\Pi_{0\bar{i}i} = \frac{1}{\sqrt{2}} \sum_{r',\bar{r}'} \int d\tilde{p}' d\tilde{\bar{p}}' v_{\bar{i}\bar{r}'}(\bar{p}') \bar{u}_{ir'}(p') \left[\langle p1;\bar{p}1|d^\dagger_{\bar{r}'}(\bar{p}')c^\dagger_{r'}(p')|0\rangle - \langle p2;\bar{p}2|d^\dagger_{\bar{r}'}(\bar{p}')c^\dagger_{r'}(p')|0\rangle \right]$$
$$= \frac{1}{\sqrt{2}} \left(v_{\bar{i}1}(\bar{p})\bar{u}_{i1}(p) - v_{\bar{i}2}(\bar{p})\bar{u}_{i2}(p) \right) \tag{3.38}$$

Using (3.31), (3.33), (2.4) and ignoring orders in $\vec{q}^2$, this becomes

$$\begin{aligned}
\Pi_{0\bar{i}i} &= \frac{1}{\sqrt{8m^2}} \left[(\not{\bar{p}} - m)_{\bar{i}3}(\not{p} + m)_{1i} + (\not{\bar{p}} - m)_{\bar{i}4}(\not{p} + m)_{2i} \right] \\
&= \frac{1}{\sqrt{8m^2}} \left[\left(\frac{P^0}{2}\gamma^0 + q^k\gamma^k - m \right)_{\bar{i}3} \left(\frac{P^0}{2}\gamma^0 - q^k\gamma^k + m \right)_{1i} \right. \\
&\qquad \left. + \left(\frac{P^0}{2}\gamma^0 + q^k\gamma^k - m \right)_{\bar{i}4} \left(\frac{P^0}{2}\gamma^0 - q^k\gamma^k + m \right)_{2i} \right] \\
&= \frac{m}{\sqrt{8}} \left[(\gamma^0 - 1)_{\bar{i}3}(\gamma^0 + 1)_{1i} + (\gamma^0 - 1)_{\bar{i}4}(\gamma^0 + 1)_{2i} \right. \\
&\qquad \left. + \frac{q^k}{m} \left(\gamma^k_{\bar{i}3}(\gamma^0 + 1)_{1i} - (\gamma^0 - 1)_{\bar{i}3}\gamma^k_{1i} + \gamma^k_{\bar{i}4}(\gamma^0 + 1)_{2i} - (\gamma^0 - 1)_{\bar{i}4}\gamma^k_{2i} \right) \right]
\end{aligned} \tag{3.39}$$

For the first part of this expression, we find

$$(\gamma^0 - 1)_{\bar{i}3}(\gamma^0 + 1)_{1i} + (\gamma^0 - 1)_{\bar{i}4}(\gamma^0 + 1)_{2i} = -4[\delta_{\bar{i}3}\delta_{i1} + \delta_{\bar{i}4}\delta_{i2}]$$
$$= -4 \begin{pmatrix} 0\,0 \\ 1\,0 \end{pmatrix}_{\bar{i}i} = [(\gamma^0 - 1)\gamma^5(\gamma^0 + 1)]_{\bar{i}i} \ . \tag{3.40}$$

Rotating the quarkonium rest frame in such a way, that the momentum $\vec{q}$ only has a component in z direction, we find for the second part up to linear order in $\vec{q}$

$$\begin{aligned}
&\frac{q^3}{m} \left(\gamma^3_{\bar{i}3}(\gamma^0 + 1)_{1i} + \gamma^3_{\bar{i}4}(\gamma^0 + 1)_{2i} - (\gamma^0 - 1)_{\bar{i}3}\gamma^3_{1i} - (\gamma^0 - 1)_{\bar{i}4}\gamma^3_{2i} \right) \\
&= \frac{2q^3}{m}[\delta_{\bar{i}1}\delta_{i1} - \delta_{\bar{i}2}\delta_{i2} + \delta_{\bar{i}3}\delta_{i3} - \delta_{\bar{i}4}\delta_{i4}] \\
&= \frac{2q^3}{m} \begin{pmatrix} \sigma^3 & 0 \\ 0 & \sigma^3 \end{pmatrix}_{\bar{i}i} \\
&= \frac{q^3}{m} \left(\gamma^3\gamma^5(\gamma^0 + 1) - (\gamma^0 - 1)\gamma^5\gamma^3 \right)_{\bar{i}i} \ .
\end{aligned} \tag{3.41}$$

Putting together both parts, the spin singlet projector reads in the quarkonium rest frame up to linear order in $\vec{q}$

$$\begin{aligned}\Pi_0 &= \frac{m}{\sqrt{8}}\left(\gamma^0 + \frac{q^3}{m}\gamma^3 - 1\right)\gamma^5\left(\gamma^0 - \frac{q^3}{m}\gamma^3 + 1\right) \\ &= \frac{1}{\sqrt{8m^2}}\left(\frac{\not{P}}{2} - \not{q} - m\right)\gamma^5\left(\frac{\not{P}}{2} + \not{q} + m\right) \ . \end{aligned} \tag{3.42}$$

Because the spin singlet projector behaves under a Lorentz transformation L like

$$\Pi_0 \to S(L)\Pi_0 S^{-1}(L) \ , \tag{3.43}$$

where $S(L)$ is the spinor representation of L, this result holds in any reference frame

$$\Pi_0 = \frac{1}{\sqrt{8m^2}}\left(\frac{\not{P}}{2} - \not{q} - m\right)\gamma^5\left(\frac{\not{P}}{2} + \not{q} + m\right) \ . \tag{3.44}$$

For the spin triplet projectors, we find in the quarkonium rest frame exactly as above

$$\begin{aligned}\Pi^1_{\bar{1}\bar{i}i} &= \frac{1}{\sqrt{2}}\left[v_{\bar{i}1}(\bar{p})\bar{u}_{i2}(p) - v_{\bar{i}2}(\bar{p})\bar{u}_{i1}(p)\right] \\ &= -\frac{1}{\sqrt{8m^2}}\left[(\not{\bar{p}} - m)_{\bar{i}3}(\not{p} + m)_{2i} + (\not{\bar{p}} - m)_{\bar{i}4}(\not{p} + m)_{1i}\right] \\ &= -\frac{1}{\sqrt{8m^2}}\left[\left(\frac{P^0}{2}\gamma^0 + q^k\gamma^k - m\right)_{\bar{i}3}\left(\frac{P^0}{2}\gamma^0 - q^k\gamma^k + m\right)_{2i}\right. \\ &\qquad \left. + \left(\frac{P^0}{2}\gamma^0 + q^k\gamma^k - m\right)_{\bar{i}4}\left(\frac{P^0}{2}\gamma^0 - q^k\gamma^k + m\right)_{1i}\right] \\ &= -\frac{m}{\sqrt{8}}\left[(\gamma^0 - 1)_{\bar{i}3}(\gamma^0 + 1)_{2i} + (\gamma^0 - 1)_{\bar{i}4}(\gamma^0 + 1)_{1i}\right. \\ &\quad \left. + \frac{q^k}{m}\left(\gamma^k_{\bar{i}3}(\gamma^0 + 1)_{2i} - (\gamma^0 - 1)_{\bar{i}3}\gamma^k_{2i} + \gamma^k_{\bar{i}4}(\gamma^0 + 1)_{1i} - (\gamma^0 - 1)_{\bar{i}4}\gamma^k_{1i}\right)\right] \ . \end{aligned} \tag{3.45}$$

For the first part of this expression we have

$$\begin{aligned}&(\gamma^0 - 1)_{\bar{i}3}(\gamma^0 + 1)_{2i} + (\gamma^0 - 1)_{\bar{i}4}(\gamma^0 + 1)_{1i} = -4[\delta_{\bar{i}3}\delta_{i2} + \delta_{\bar{i}4}\delta_{i1}] \\ &\qquad = -4\begin{pmatrix} 0 & 0 \\ \sigma^1 & 0 \end{pmatrix}_{\bar{i}i} = -[(\gamma^0 - 1)\gamma^1(\gamma^0 + 1)]_{\bar{i}i} \ , \end{aligned} \tag{3.46}$$

and again by choosing the rest frame in such a way, that the momentum $\vec{q}$ only has a component in z direction, it follows for the second part

$$\begin{aligned}&\frac{q^3}{m}\left(\gamma^3_{\bar{i}3}(\gamma^0 + 1)_{2i} - (\gamma^0 - 1)_{\bar{i}3}\gamma^3_{2i} + \gamma^3_{\bar{i}4}(\gamma^0 + 1)_{1i} - (\gamma^0 - 1)_{\bar{i}4}\gamma^3_{1i}\right) \\ &= \frac{2q^3}{m}[\delta_{\bar{i}1}\delta_{i2} - \delta_{\bar{i}3}\delta_{i4} - \delta_{\bar{i}2}\delta_{i1} + \delta_{\bar{i}4}\delta_{i3}]\end{aligned}$$

$$= i\frac{2q^3}{m}\begin{pmatrix}\sigma^2 & 0\\ 0 & -\sigma^2\end{pmatrix}_{\bar{i}i}$$
$$= \frac{q^3}{m}[(\gamma^0-1)\gamma^1\gamma^3-\gamma^3\gamma^1(\gamma^0+1)]_{\bar{i}i}\ . \tag{3.47}$$

Hence Π_1^1 reads in the quarkonium rest frame up to linear order in $\vec{q}$

$$\Pi_1^1 = \frac{1}{\sqrt{8m^2}}\left(\frac{P^0}{2}\gamma^0+q^3\gamma^3-m\right)\gamma^1\left(\frac{P^0}{2}\gamma^0-q^3\gamma^3+m\right)$$
$$= \frac{1}{\sqrt{8m^2}}\left(\frac{\not{P}}{2}-\not{q}-m\right)\gamma^1\left(\frac{\not{P}}{2}+\not{q}+m\right)\ . \tag{3.48}$$

For Π_1^2 we find

$$\Pi^2_{1\bar{i}i} = -\frac{i}{\sqrt{2}}[v_{\bar{i}1}(\bar{p})\bar{u}_{i2}(p)+v_{\bar{i}2}(\bar{p})\bar{u}_{i1}(p)]$$
$$= \frac{i}{\sqrt{8m^2}}\left[(\not{\bar{p}}-m)_{\bar{i}3}(\not{p}+m)_{2i}-(\not{\bar{p}}-m)_{\bar{i}4}(\not{p}+m)_{1i}\right]$$
$$= i\frac{m}{\sqrt{8}}\Big[(\gamma^0-1)_{\bar{i}3}(\gamma^0+1)_{2i}-(\gamma^0-1)_{\bar{i}4}(\gamma^0+1)_{1i}$$
$$+\frac{q^k}{m}\left(\gamma^k_{\bar{i}3}(\gamma^0+1)_{2i}-(\gamma^0-1)_{\bar{i}3}\gamma^k_{2i}-\gamma^k_{\bar{i}4}(\gamma^0+1)_{1i}+(\gamma^0-1)_{\bar{i}4}\gamma^k_{1i}\right)\Big]\ . \tag{3.49}$$

Writing for the first part of this expression

$$(\gamma^0-1)_{\bar{i}3}(\gamma^0+1)_{2i}-(\gamma^0-1)_{\bar{i}4}(\gamma^0+1)_{1i} = -4[\delta_{\bar{i}3}\delta_{i2}-\delta_{\bar{i}4}\delta_{i1}]$$
$$= -4i\begin{pmatrix}0 & 0\\ \sigma^2 & 0\end{pmatrix}_{\bar{i}i} = -i[(\gamma^0-1)\gamma^2(\gamma^0+1)]_{\bar{i}i} \tag{3.50}$$

and for the second one after an appropriate rotation of the rest frame

$$\frac{q^3}{m}\left(\gamma^3_{\bar{i}3}(\gamma^0+1)_{2i}-(\gamma^0-1)_{\bar{i}3}\gamma^3_{2i}-\gamma^3_{\bar{i}4}(\gamma^0+1)_{1i}+(\gamma^0-1)_{\bar{i}4}\gamma^3_{1i}\right)$$
$$= \frac{2q^3}{m}[\delta_{\bar{i}1}\delta_{i2}-\delta_{\bar{i}3}\delta_{i4}+\delta_{\bar{i}2}\delta_{i1}-\delta_{\bar{i}4}\delta_{i3}]$$
$$= \frac{2q^3}{m}\begin{pmatrix}\sigma^1 & 0\\ 0 & -\sigma^1\end{pmatrix}_{\bar{i}i}$$
$$= -i\frac{q^3}{m}[\gamma^3\gamma^2(\gamma^0+1)-(\gamma^0-1)\gamma^2\gamma^3]_{\bar{i}i}\ , \tag{3.51}$$

we find for Π_1^2 in the quarkonium rest frame up to linear order in $\vec{q}$

$$\Pi_1^2 = \frac{1}{\sqrt{8m^2}}\left(\frac{\not{P}}{2}-\not{q}-m\right)\gamma^2\left(\frac{\not{P}}{2}+\not{q}+m\right)\ . \tag{3.52}$$

Finally we get for Π_1^3

$$\begin{aligned}\Pi^3_{1\bar{i}i} &= -\frac{1}{\sqrt{2}}[v_{\bar{i}1}(\bar{p})\bar{u}_{i1}(p) + v_{\bar{i}2}(\bar{p})\bar{u}_{i2}(p)] \\ &= -\frac{1}{\sqrt{8m^2}}[(\bar{\not{p}} - m)_{\bar{i}3}(\not{p} + m)_{1i} - (\bar{\not{p}} - m)_{\bar{i}4}(\not{p} + m)_{2i}] \\ &= -\frac{m}{\sqrt{8}}\Big[(\gamma^0 - 1)_{\bar{i}3}(\gamma^0 + 1)_{1i} - (\gamma^0 - 1)_{\bar{i}4}(\gamma^0 + 1)_{2i} \\ &\quad + \frac{q^k}{m}\left(\gamma^k_{\bar{i}3}(\gamma^0 + 1)_{1i} - (\gamma^0 - 1)_{\bar{i}3}\gamma^k_{1i} - \gamma^k_{\bar{i}4}(\gamma^0 + 1)_{2i} + (\gamma^0 - 1)_{\bar{i}4}\gamma^k_{2i}\right)\Big] \ . \end{aligned} \tag{3.53}$$

With the first part of this expression yielding

$$\begin{aligned}(\gamma^0 - 1)_{\bar{i}3}(\gamma^0 + 1)_{1i} - (\gamma^0 - 1)_{\bar{i}4}(\gamma^0 + 1)_{2i} &= -4[\delta_{\bar{i}3}\delta_{i1} - \delta_{\bar{i}4}\delta_{i2}] \\ &= -4\begin{pmatrix} 0 & 0 \\ \sigma^3 & 0 \end{pmatrix}_{\bar{i}i} = -[(\gamma^0 - 1)\gamma^3(\gamma^0 + 1)]_{\bar{i}i}\end{aligned} \tag{3.54}$$

and the second one after an appropriate rotation of the rest frame

$$\begin{aligned}&\frac{q^3}{m}\left(\gamma^3_{\bar{i}3}(\gamma^0 + 1)_{1i} - (\gamma^0 - 1)_{\bar{i}3}\gamma^3_{1i} - \gamma^3_{\bar{i}4}(\gamma^0 + 1)_{2i} + (\gamma^0 - 1)_{\bar{i}4}\gamma^3_{2i}\right) \\ &= \frac{2q^3}{m}[\delta_{\bar{i}1}\delta_{i1} + \delta_{\bar{i}3}\delta_{i3} + \delta_{\bar{i}2}\delta_{i2} + \delta_{\bar{i}4}\delta_{i4}] = \frac{2q^3}{m}1_{\bar{i}i} \\ &= \frac{q^3}{m}\left[(\gamma^0 - 1)\left(\gamma^3\right)^2 - \left(\gamma^3\right)^2(\gamma^0 + 1)\right]_{\bar{i}i} \ ,\end{aligned} \tag{3.55}$$

we get for Π_1^3 in the quarkonium rest frame up to linear order in $\vec{q}$

$$\Pi_1^3 = \frac{1}{\sqrt{8m^2}}\left(\frac{\not{P}}{2} - \not{q} - m\right)\gamma^3\left(\frac{\not{P}}{2} + \not{q} + m\right) \ . \tag{3.56}$$

Defining

$$\Pi_1^0 = \frac{1}{\sqrt{8m^2}}\left(\frac{\not{P}}{2} - \not{q} - m\right)\gamma^0\left(\frac{\not{P}}{2} + \not{q} + m\right) \ , \tag{3.57}$$

which vanishes in the quarkonium rest frame, and noting the lorentz transformation behaviour of the spin triplet operators

$$\Pi_1^\mu \to L^\mu{}_\nu S(L)\Pi_1^\nu S^{-1}(L) \ , \tag{3.58}$$

where $S(L)$ is the spinor representation of the lorentz transformation L, the spin triplet projectors are given in an arbitrary reference frame up to linear order in $\vec{q}$ by

$$\Pi_1^\mu = \frac{1}{\sqrt{8m^2}}\left(\frac{\not{P}}{2} - \not{q} - m\right)\gamma^\mu\left(\frac{\not{P}}{2} + \not{q} + m\right) \ . \tag{3.59}$$

In order to relate the $|\langle Q\bar{Q}[n]|HX\rangle|^2$ to the standard NRQCD production matrix elements, we will express the spin singlet and spin triplet states in terms of nonrelativistic spinor fields. Note, that the heavy quark spinor parametrization (3.33) coincides with that one used in NRQCD

$$u_r(p)=\sqrt{p^0+m}\begin{pmatrix}\xi_r(p)\\ \frac{\vec{p}\vec{\sigma}}{p^0+m}\xi_r(p)\end{pmatrix}\ ,\ v_{\bar{r}}(\bar{p})=\sqrt{p^0+m}\begin{pmatrix}\frac{\vec{\bar{p}}\vec{\sigma}}{p^0+m}\eta_{\bar{r}}(\bar{p})\\ \eta_{\bar{r}}(\bar{p})\end{pmatrix}\ ,\ r,\bar{r}=1,2\ , \quad (3.60)$$

if we choose

$$\xi_1(p)=\begin{pmatrix}1\\0\end{pmatrix}\ ,\ \xi_2(p)=\begin{pmatrix}0\\-1\end{pmatrix}\ ,\ \eta_1(\bar{p})=\begin{pmatrix}-1\\0\end{pmatrix}\ ,\ \eta_2(\bar{p})=\begin{pmatrix}0\\-1\end{pmatrix}\ . \quad (3.61)$$

The nonrelativistic spinor fields ψ and χ in the quarkonium rest frame read according to the here used normalizations (3.24)-(3.27)

$$\begin{aligned}\psi(x)&=\sum_r\int\frac{d^3\vec{p}}{(2\pi)^3\sqrt{2p^0}}\xi_r(p)c_r(p)e^{-i(px-mx^0)}\\ \chi(x)&=\sum_{\bar{r}}\int\frac{d^3\vec{\bar{p}}}{(2\pi)^3\sqrt{2\bar{p}^0}}\eta_{\bar{r}}(\bar{p})d^\dagger_{\bar{r}}(\bar{p})e^{i(\bar{p}x-mx^0)}\quad ,\end{aligned} \quad (3.62)$$

where obviously ψ annihilates the heavy quark and χ creates the heavy antiquark. (3.62) is easily found from the defining equation (2.43) for ψ and χ

$$\begin{pmatrix}\psi e^{-imx^0}\\ \chi e^{imx^0}\end{pmatrix}=U\Psi\ , \quad (3.63)$$

where U denotes the Foldy Wouthuysen transformation and Ψ denotes the original four component Dirac field occuring in the fully relativistic lagrangian (2.1). Taking U into account only up to linear order in $1/m$ or equivalently v

$$U=1+\frac{\beta\vec{\alpha}}{2m}\frac{1}{i}\vec{\nabla}\ , \quad (3.64)$$

representing Ψ by

$$\Psi=\sum_r\int d\tilde{p}\{u_r(p)c_r(p)e^{-ipx}+v_r(p)d^\dagger_r(p)e^{ipx}\}\ , \quad (3.65)$$

which is in accordance with the normalization conditions (3.24)-(3.27), furthermore employing (3.60) for $u_r(p)$ and $v_r(p)$ and noting, that $p^0+m{=}2p^0+o(v^2)$, (3.63) becomes up to linear order in v

$$\begin{aligned}\begin{pmatrix}\psi e^{-imx^0}\\ \chi e^{imx^0}\end{pmatrix}&=\left(1+\frac{\beta\vec{\alpha}}{2m}\frac{1}{i}\vec{\nabla}\right)\sum_r\int\frac{d^3\vec{p}}{(2\pi)^3\sqrt{2p^0}}\begin{pmatrix}\xi_r(p)c_r(p)e^{-ipx}+\frac{\vec{p}\vec{\sigma}}{p^0+m}\eta_r(p)d^\dagger_r(p)e^{ipx}\\ \frac{\vec{p}\vec{\sigma}}{p^0+m}\xi_r(p)c_r(p)e^{-ipx}+\eta_r(p)d^\dagger_r(p)e^{ipx}\end{pmatrix}\\ &=\sum_r\int\frac{d^3\vec{p}}{(2\pi)^3\sqrt{2p^0}}\begin{pmatrix}\xi_r(p)c_r(p)e^{-ipx}+\frac{\vec{p}\vec{\sigma}}{p^0+m}\eta_r(p)d^\dagger_r(p)e^{ipx}-\frac{i\vec{\sigma}\vec{\nabla}}{p^0+m}\eta_r(p)d^\dagger_r(p)e^{ipx}\\ \frac{\vec{p}\vec{\sigma}}{p^0+m}\xi_r(p)c_r(p)e^{-ipx}+\eta_r(p)d^\dagger_r(p)e^{ipx}+\frac{i\vec{\sigma}\vec{\nabla}}{p^0+m}\xi_r(p)c_r(p)e^{-ipx}\end{pmatrix}\\ &=\sum_r\int\frac{d^3\vec{p}}{(2\pi)^3\sqrt{2p^0}}\begin{pmatrix}\xi_r(p)c_r(p)e^{-ipx}\\ \eta_r(p)d^\dagger_r(p)e^{ipx}\end{pmatrix}\ ,\end{aligned} \quad (3.66)$$

which immediately proves (3.62). Using this result, we find in the quarkonium rest frame (remember, that there holds $\vec{p} = -\vec{\bar{p}} = \vec{q}$)

$$\begin{aligned}\sum_{r,\bar{r}} |pr;\bar{p}\bar{r}\rangle\langle pr;\bar{p}\bar{r}|\psi^\dagger\chi|0\rangle &= -2m\sum_{r,\bar{r}} \xi_r^\dagger(p)\eta_{\bar{r}}(\bar{p})|pr;\bar{p}\bar{r}\rangle \\ &= \ 2m(|p1;\bar{p}1\rangle - |p2;\bar{p}2\rangle) \end{aligned} \tag{3.67}$$

$$\begin{aligned}\sum_{r,\bar{r}} |pr;\bar{p}\bar{r}\rangle\langle pr;\bar{p}\bar{r}|\psi^\dagger\sigma^l\chi|0\rangle &= -2m\sum_{r,\bar{r}} \xi_r^\dagger(p)\sigma^l\eta_{\bar{r}}(\bar{p})|pr;\bar{p}\bar{r}\rangle \\ &= \begin{cases} 2m(|p1;\bar{p}2\rangle - |p2;\bar{p}1\rangle) \ ; \ l=1 \\ -2mi(|p1;\bar{p}2\rangle + |p2;\bar{p}1\rangle) \ ; \ l=2 \\ 2m(|p1;\bar{p}1\rangle + |p2;\bar{p}2\rangle) \ ; \ l=3 \ . \end{cases} \end{aligned} \tag{3.68}$$

The right hand sides of (3.67), (3.68) can be identified with the heavy quark antiquark spin singlet state, given in (3.34), and the linear combinations of the standard spin triplet states, defined in (3.35)- (3.37). Hence (3.67), (3.68) imply for the representation of the spin singlet and spin triplet states in terms of the nonrelativistic spinor fields

$$|Q\bar{Q}[^1S_0]\rangle = \sum_{r,\bar{r}} |pr;\bar{p}\bar{r}\rangle\langle pr;\bar{p}\bar{r}|\frac{\psi^\dagger\chi}{\sqrt{8m^2}}|0\rangle \tag{3.69}$$

and

$$|Q\bar{Q}[^3S_1]\rangle_l = -\sum_{r,\bar{r}} |pr;\bar{p}\bar{r}\rangle\langle pr;\bar{p}\bar{r}|\frac{\psi^\dagger\sigma^l\chi}{\sqrt{8m^2}}|0\rangle \ . \tag{3.70}$$

Inserting (3.69) into the first and (3.70) into the third term of equation (3.32) and exploiting the fact, that the sum over the intermediate states also includes an integration over the heavy quark momenta, we get for the spin singlet part of the amplitude $\mathcal{A}$ in the quarkonium rest frame

$$\begin{aligned}\mathcal{A}\left[^1S_0\right] &= \langle HX|\int d\tilde{p}d\tilde{\bar{p}}\ |Q\bar{Q}[^1S_0]\rangle_{p\bar{p}}\underbrace{{}_{p\bar{p}}\langle Q\bar{Q}[^1S_0]|\Psi_{\bar{i}}\bar{\Psi}_i|0\rangle\mathcal{T}_{i\bar{i}}}_{tr[\mathcal{T}\Pi_0]} \\ &= \langle HX|\int d\tilde{p}d\tilde{\bar{p}}\sum_{r,\bar{r}} |pr;\bar{p}\bar{r}\rangle\langle pr;\bar{p}\bar{r}|\frac{\psi^\dagger\chi}{\sqrt{8m^2}}|0\rangle \times tr[\mathcal{T}\Pi_0] \ , \end{aligned} \tag{3.71}$$

hence

$$\mathcal{A}\left[^1S_0\right] = \langle HX|\frac{\psi^\dagger\chi}{\sqrt{8m^2}}|0\rangle\ tr[\mathcal{T}\Pi_0]\Big|_{\vec{q}=0} \ , \tag{3.72}$$

and analogously for the spin triplet part

$$\mathcal{A}\left[^3S_1\right] = \langle HX|\frac{\Psi^\dagger\sigma^l\chi}{\sqrt{8m^2}}|0\rangle\ tr[\mathcal{T}\Pi_1^l]\Big|_{\vec{q}=0} \ . \tag{3.73}$$

Thereby we used, that in the quarkonium rest frame there are only contributions from intermediate states with vanishing total momentum $\vec{p} + \vec{\bar{p}} = 0$. Derivating the short

distance parts in $\mathcal{A}\left[^1S_0\right]$ and $\mathcal{A}\left[^3S_1\right]$ with respect to q^i and replacing q^i in the matrix element by the covariant derivative, the second and fourth term in (3.32) take the form

$$\mathcal{A}\left[^1P_1\right] = \sum_{i=1}^{3} \langle HX| \frac{\Psi^\dagger (\frac{i}{2} \overleftrightarrow{D^i}) \chi}{\sqrt{8m^2}} |0\rangle \; \frac{\partial}{\partial q^i} tr[\mathcal{T}\Pi_0] \Big|_{\vec{q}=0} \tag{3.74}$$

and

$$\mathcal{A}\left[^3P_J\right] = \sum_{i=1}^{3} \langle HX| \frac{\Psi^\dagger (\frac{i}{2} \overleftrightarrow{D^i}) \sigma^l \chi}{\sqrt{8m^2}} |0\rangle \; \frac{\partial}{\partial q^i} tr[\mathcal{T}\Pi_1^l] \Big|_{\vec{q}=0} \tag{3.75}$$

where $\overleftrightarrow{D}$ is the difference between the covariant derivative acting on the spinor to the right and the spinor to the left: $\Psi^\dagger \overleftrightarrow{D^i} \chi = \Psi^\dagger D^i \chi - D^i \Psi^\dagger \chi$. By the transformation behaviour of the matrixelements under spatial rotations it is clear, that $\mathcal{A}\left[^1P_1\right]$ and $\mathcal{A}\left[^3P_J\right]$ correspond to quarkonium production via an intermediate $^1P_1$ state and ^3P_J states, respectively.

Until now, we have supressed the color indices. Writing out them explicitly, we have for instance for the $^1S_0$ part

$$\mathcal{A}\left[^1S_0\right] = \langle HX| \frac{\psi_n^\dagger \chi_{\bar{n}}}{\sqrt{8m^2}} |0\rangle \; tr\left[\mathcal{T}_{n\bar{n}} \Pi_0\right] \Big|_{\vec{q}=0} \; , \tag{3.76}$$

where n and $\bar{n}$ denote the color of the heavy quark and the heavy antiquark respectively. Introducing the color singlet and color octet projectors

$$C_1 = \frac{1}{\sqrt{3}} 1 \; ; \tag{3.77}$$

$$C_8^a = \sqrt{2} T^a \; ; \; a = 1, 2, ..., 8 \tag{3.78}$$

$\mathcal{T}_{n\bar{n}}$ can be written

$$\mathcal{T}_{n\bar{n}} = \frac{1}{\sqrt{3}} \; tr[\mathcal{T} C_1] \; \delta_{n\bar{n}} + \sqrt{2} \; tr[\mathcal{T} C_8^a] \; T_{n\bar{n}}^a \; , \tag{3.79}$$

where we have employed the normalisation condition of the color algebra

$$tr[T^a T^b] = \frac{1}{2} \delta^{ab} \tag{3.80}$$

and the vanishing of the trace of its elements

$$tr T^a = 0 \; . \tag{3.81}$$

Thus (3.76) becomes

$$\mathcal{A}\left[^1S_0\right] = \frac{1}{2m} \left\{ \frac{\langle HX|\psi^\dagger \chi|0\rangle}{\sqrt{6}} \; tr\left[\mathcal{T}\Pi_0 C_1\right] \Big|_{\vec{q}=0} \right.$$
$$\left. + \; \langle HX|\psi^\dagger T^a \chi|0\rangle \; tr\left[\mathcal{T}\Pi_0 C_8^a\right] \Big|_{\vec{q}=0} \right\} \; , \tag{3.82}$$

and analogously it follows for $\mathcal{A}\left[^3S_1\right]$, $\mathcal{A}\left[^1P_1\right]$ and $\mathcal{A}\left[^3P_J\right]$

$$\mathcal{A}\left[^3S_1\right] = \frac{1}{2m}\left\{\frac{\langle HX|\psi^\dagger\sigma^l\chi|0\rangle}{\sqrt{6}}\ tr\left[\mathcal{T}\Pi_1^l C_1\right]\Big|_{\vec{q}=0}\right.$$
$$\left. +\ \langle HX|\psi^\dagger\sigma^l T^a\chi|0\rangle\ tr\left[\mathcal{T}\Pi_1^l C_8^a\right]\Big|_{\vec{q}=0}\right\}\ , \tag{3.83}$$

$$\mathcal{A}\left[^1P_1\right] = \frac{1}{2m}\left\{\frac{\langle HX|\psi^\dagger\left(\frac{i}{2}\overleftrightarrow{D^i}\right)\chi|0\rangle}{\sqrt{6}}\ \frac{\partial}{\partial q^i}tr\left[\mathcal{T}\Pi_0 C_1\right]\Big|_{\vec{q}=0}\right.$$
$$\left. +\langle HX|\psi^\dagger\left(\frac{i}{2}\overleftrightarrow{D^i}\right)T^a\chi|0\rangle\ \frac{\partial}{\partial q^i}tr\left[\mathcal{T}\Pi_0 C_8^a\right]\Big|_{\vec{q}=0}\right\}\ , \tag{3.84}$$

$$\mathcal{A}\left[^3P_J\right] = \frac{1}{2m}\left\{\frac{\langle HX|\psi^\dagger\left(\frac{i}{2}\overleftrightarrow{D^i}\right)\sigma^l\chi|0\rangle}{\sqrt{6}}\ \frac{\partial}{\partial q^i}tr\left[\mathcal{T}\Pi_1^l C_1\right]\Big|_{\vec{q}=0}\right.$$
$$\left. +\langle HX|\psi^\dagger\left(\frac{i}{2}\overleftrightarrow{D^i}\right)\sigma^l T^a\chi|0\rangle\ \frac{\partial}{\partial q^i}tr\left[\mathcal{T}\Pi_1^l C_8^a\right]\Big|_{\vec{q}=0}\right\}\ . \tag{3.85}$$

By their color transformation behaviour, it's clear, that the first and the second part of the amplitudes (3.82)-(3.85) describe quarkonium production via an intermediate color singlet and color octet state, respectively. It is necessary to make a remark on the normalization of the quarkonium state $|H\rangle$. Calculating the production cross section, we will use for the quarkonium phase space the integration measure

$$d\tilde{P} = \frac{d^3\vec{P}}{(2\pi)^3 2P^0}\ , \tag{3.86}$$

according to a relativistic normalization of $|H\rangle$

$$\langle H(P)|H(P')\rangle = (2\pi)^3 2P^0\delta^3(\vec{P}-\vec{P}')\ . \tag{3.87}$$

Since the quarkonium states in the standard NRQCD matrix elements are nonrelativistically normalized according to (2.81), we have to rescale the matrix elements by a factor $\sqrt{2P^0} = 2\sqrt{m}$, that means, we replace $|HX\rangle$ by $2\sqrt{m}\ |HX\rangle$. The remaining global factor $\frac{1}{\sqrt{m}}$ in (3.82)-(3.85) is then shifted into the spin singlet and spin triplet projector, respectively. The total amplitude then finally reads

$$\mathcal{A} = \frac{\langle HX|\psi^\dagger\chi|0\rangle}{\sqrt{6}}\ tr\left[\mathcal{T}\Pi_0 C_1\right]\Big|_{\vec{q}=0} + \langle HX|\Psi^\dagger T^a\chi|0\rangle\ tr\left[\mathcal{T}\Pi_0 C_8^a\right]\Big|_{\vec{q}=0}$$

$$
\begin{aligned}
&+ \frac{\langle HX|\psi^\dagger \sigma^l \chi|0\rangle}{\sqrt{6}} tr\left[\mathcal{T}\Pi_1^l C_1\right]\Big|_{\vec{q}=0} + \langle HX|\psi^\dagger \sigma^l T^a \chi|0\rangle \; tr\left[\mathcal{T}\Pi_1^l C_8^a\right]\Big|_{\vec{q}=0} \\
&+ \frac{\langle HX|\psi^\dagger \left(\frac{i}{2} \overleftrightarrow{D}^i\right)\chi|0\rangle}{\sqrt{6}} \frac{\partial}{\partial q^i} tr\left[\mathcal{T}\Pi_0 C_1\right]\Big|_{\vec{q}=0} \\
&+ \langle HX|\psi^\dagger \left(\frac{i}{2} \overleftrightarrow{D}^i\right) T^a \chi|0\rangle \; \frac{\partial}{\partial q^i} tr\left[\mathcal{T}\Pi_0 C_8^a\right]\Big|_{\vec{q}=0} \\
&+ \frac{\langle HX|\psi^\dagger \left(\frac{i}{2} \overleftrightarrow{D}^i\right)\sigma^l \chi|0\rangle}{\sqrt{6}} \frac{\partial}{\partial q^i} tr\left[\mathcal{T}\Pi_1^l C_1\right]\Big|_{\vec{q}=0} \\
&+ \langle HX|\psi^\dagger \left(\frac{i}{2} \overleftrightarrow{D}^i\right) \sigma^l T^a \chi|0\rangle \; \frac{\partial}{\partial q^i} tr\left[\mathcal{T}\Pi_1^l C_8^a\right]\Big|_{\vec{q}=0}
\end{aligned}
\tag{3.88}
$$

with the spin singlet and spin triplet projectors now given by

$$
\Pi_0 = \frac{1}{\sqrt{8m^3}} \left(\frac{\not{P}}{2} - \not{q} - m\right) \gamma^5 \left(\frac{\not{P}}{2} + \not{q} + m\right) \tag{3.89}
$$

and

$$
\Pi_1^\mu = \frac{1}{\sqrt{8m^3}} \left(\frac{\not{P}}{2} - \not{q} - m\right) \gamma^\mu \left(\frac{\not{P}}{2} + \not{q} + m\right) \; . \tag{3.90}
$$

The last step, which remains to be done, is calculating the unpolarized quarkonium production cross section σ_H. Because of color, spatial rotation, parity (P) and charge conjugation (C) symmetry, within the here considered orders of q interferences between parts of the amplitude, which correspond to quarkonium production via intermediate $Q\bar{Q}$ states with different color or spin orbital angular momentum quantum numbers, do not contribute to σ_H. (Such interferences first appear after inclusion of the D wave contributions, for example between the ${}^3S_1$ and the ${}^3D_1$ channel, as they agree in the exactly conserved quantum numbers J, P and C.) Hence σ_H is a sum over cross sections $\sigma\left[{}^{2S+1}L_J^{(c)}\right]$, which describe unpolarized quarkonium production via intermediate $Q\bar{Q}$ pairs of definite color and spin orbital angular momentum

$$
\sigma_H = \sum \sigma\left[{}^{2S+1}L_J^{(c)}\right] \; . \tag{3.91}
$$

The $\sigma\left[{}^{2S+1}L_J^{(c)}\right]$ are given by

$$
\sigma\left[{}^{2S+1}L_J^{(c)}\right] = \frac{1}{F}\overline{\sum} \int dPS_{n+1}(p_1+p_2; P, k_1, k_2, ..., k_n) \left|\mathcal{A}\left[{}^{2S+1}L_J^{(c)}\right]\right|^2 \; , \tag{3.92}
$$

where F and p_1, p_2, k_1, k_2,...,k_n are as in (3.17). Similarly as in (3.17) $\overline{\sum}$ stands for the average (sum) over the spin and color degrees of freedom of the particles in the

initial (final) state. However $\overline{\sum}$ here does not contain the summation over the quarkonium spin J_z as this is already included in the definition of the NRQCD production matrix elements, as becomes clear soon. The adequately defined phase space measure $dPS_{n+1}(p_1+p_2;P,k_1,k_2,...,k_n)$ is given by (3.19) with $D=4$. The color spin orbital angular momentum parts $\mathcal{A}\left[^{2S+1}L_J^{(c)}\right]$ of the total amplitude $\mathcal{A}$ can be read off (3.88). With the standard NRQCD production matrix elements $\left\langle O^H\left[^{2S+1}L_J^{(c)}\right]\right\rangle$ introduced in section 2.4 we find

$$\left|\mathcal{A}\left[^1S_0^{(1)}\right]\right|^2 = \left|tr[\mathcal{T}\Pi_0 C_1]|_{q=0}\right|^2 \frac{\left\langle O^H\left[^1S_0^{(1)}\right]\right\rangle}{6} , \tag{3.93}$$

where here and in the following the $\left|\mathcal{A}\left[^{2S+1}L_J^{(c)}\right]\right|^2$ are understood to be already summed over J_z and X. Using color symmetry

$$\langle 0|\chi^\dagger T^a\psi\mathcal{P}^H\psi^\dagger T^b\chi|0\rangle = \langle 0|\chi^\dagger T^c\psi\mathcal{P}^H\psi^\dagger T^c\chi|0\rangle \frac{\delta^{ab}}{8} , \tag{3.94}$$

where $\mathcal{P}^H$ is defined in (2.96) and summation over double indices is understood, it follows

$$\left|\mathcal{A}\left[^1S_0^{(8)}\right]\right|^2 = \sum_a \left|tr[\mathcal{T}\Pi_0 C_8^a]|_{q=0}\right|^2 \frac{\left\langle O^H\left[^1S_0^{(8)}\right]\right\rangle}{8} . \tag{3.95}$$

$\left|\mathcal{A}\left[^3S_1^{(1)}\right]\right|^2$ reads in the quarkonium rest frame

$$\left|\mathcal{A}\left[^3S_1^{(1)}\right]\right|^2 = \left[tr[\mathcal{T}\Pi_1^k C_1]\Big|_{\vec{q}=0}\right]^* tr[\mathcal{T}\Pi_1^l C_1]\Big|_{\vec{q}=0} \frac{\langle 0|\chi^\dagger\sigma^k\psi\mathcal{P}^H\psi^\dagger\sigma^l\chi|0\rangle}{6} . \tag{3.96}$$

In an arbitrary frame it takes the form

$$\left|\mathcal{A}\left[^3S_1^{(1)}\right]\right|^2 = \left[tr[\mathcal{T}\Pi_1^\mu C_1]|_{q=0}\right]^* tr[\mathcal{T}\Pi_1^\nu C_1]|_{q=0} L^k{}_\mu L^l{}_\nu \frac{\langle 0|\chi^\dagger\sigma^k\psi\mathcal{P}^H\psi^\dagger\sigma^l\chi|0\rangle}{6} , \tag{3.97}$$

where we have exploited

$$\Pi_1^i = L^i{}_\mu S(L)\Pi_1^\mu S^{-1}(L) , \tag{3.98}$$

and L is understood to be the lorentz transformation back into the rest frame. Using spatial rotation symmetry

$$\langle 0|\chi^\dagger\sigma^k\psi\mathcal{P}^H\psi^\dagger\sigma^l\chi|0\rangle = \langle 0|\chi^\dagger\sigma^m\psi\mathcal{P}^H\psi^\dagger\sigma^m\chi|0\rangle \frac{\delta_{kl}}{3} \tag{3.99}$$

and

$$\delta_{kl}L^k{}_\mu L^l{}_\nu = -g_{\mu\nu} + \frac{P_\mu P_\nu}{P^2} \equiv \Pi_{\mu\nu} , \tag{3.100}$$

it follows

$$\left|\mathcal{A}\left[^3S_1^{(1)}\right]\right|^2 = \left[tr[\mathcal{T}\Pi_1^\mu C_1]|_{q=0}\right]^* tr[\mathcal{T}\Pi_1^\nu C_1]|_{q=0}\,\Pi_{\mu\nu} \frac{\left\langle O^H\left[^3S_1^{(1)}\right]\right\rangle}{6\times 3} . \tag{3.101}$$

The proof of (3.100) is the following. Consider the quarkonium momentum P and an arbitrary four vector k with $Pk = 0$ in the laboratory frame. $P'k' = 0$ and $P' = (M, \vec{0})$ with $P' = LP$, $k' = Lk$ and L being the lorentz transformation into the quarkonium rest frame then implies $k' = (0, \vec{k'})$. Thus, it follows ${L_i}^\mu {L^i}_\nu k^\nu = ({L^{-1}})^\mu{}_i \, k'^i = ({L^{-1}})^\mu{}_\nu \, k'^\nu = k^\mu$ and ${L_i}^\mu {L^i}_\nu P^\nu = 0$, indicating, that ${L_i}^\mu {L^i}_\nu$ is the projector onto the orthogonal complement of P. This proves (3.100).

For $\left|\mathcal{A}\left[{}^3S_1^{(8)}\right]\right|^2$ we get

$$\left|\mathcal{A}\left[{}^3S_1^{(8)}\right]\right|^2 = \sum_a \left[tr[\mathcal{T}\Pi_1^\mu C_8^a]|_{q=0}\right]^* tr[\mathcal{T}\Pi_1^\nu C_8^a]|_{q=0} \, \Pi_{\mu\nu} \frac{\left\langle O^H[{}^3S_1^{(8)}]\right\rangle}{8\times 3} \ , \tag{3.102}$$

where we have again exploited spatial rotation and color symmetry

$$\langle 0|\chi^\dagger \sigma^k T^a \psi \mathcal{P}^H \psi^\dagger \sigma^l T^b \chi|0\rangle = \langle 0|\chi^\dagger \vec{\sigma} T^c \psi \mathcal{P}^H \psi^\dagger \vec{\sigma} T^c \chi|0\rangle \ \frac{\delta^{ab}}{8}\frac{\delta_{kl}}{3} \tag{3.103}$$

and the lorentz transformation behaviour of the spin triplet projector as above. Using spatial rotation symmetry and noting, that $\frac{\partial}{\partial q_l} \, tr[\mathcal{T}\Pi_0 C_1]|_{\vec{q}=0}$ has the same lorentz transformation behaviour with respect to l as $tr[\mathcal{T}\Pi_1^l C_1]\Big|_{\vec{q}=0}$, we find for $\left|\mathcal{A}\left[{}^1P_1^{(1)}\right]\right|^2$

$$\left|\mathcal{A}\left[{}^1P_1^{(1)}\right]\right|^2 = \left[\frac{\partial}{\partial q_\mu} \, tr[\mathcal{T}\Pi_0 C_1]|_{q=0}\right]^* \frac{\partial}{\partial q_\nu} \, tr[\mathcal{T}\Pi_0 C_1]|_{q=0} \, \Pi_{\mu\nu} \, \frac{\left\langle O^H\left[{}^1P_1^{(1)}\right]\right\rangle}{6\times 3} \ . \tag{3.104}$$

Taking additionally the color symmetry into account, $\left|\mathcal{A}\left[{}^1P_1^{(8)}\right]\right|^2$ takes the form

$$\left|\mathcal{A}\left[{}^1P_1^{(8)}\right]\right|^2 = \sum_a \left[\frac{\partial}{\partial q_\mu} tr[\mathcal{T}\Pi_0 C_8^a]\Big|_{q=0}\right]^* \frac{\partial}{\partial q_\nu} tr[\mathcal{T}\Pi_0 C_8^a]\Big|_{q=0} \, \Pi_{\mu\nu} \, \frac{\left\langle O^H\left[{}^1P_1^{(8)}\right]\right\rangle}{8\times 3} \ . \tag{3.105}$$

The remaining two terms in the total amplitude $\mathcal{A}$ contain the matrix elements $\langle HX|\psi^\dagger\left(\frac{i}{2}\overleftrightarrow{D}^i\right)\sigma^l\chi|0\rangle$ and $\langle HX|\psi^\dagger\left(\frac{i}{2}\overleftrightarrow{D}^i\right)\sigma^l T^a\chi|0\rangle$, which transform under spatial rotations as direct product of a spin $S = 1$ and an orbital angular momentum $L = 1$ representation. A decomposition into irreducible representations, labelled by the total angular momentum $J = 0, 1, 2$, is given by

$$\begin{aligned}\langle HX|\psi^\dagger\left(\frac{i}{2}\overleftrightarrow{D}^i\right)\sigma^l\chi|0\rangle &= \frac{\delta^{il}}{3}\langle HX|\psi^\dagger\left(\frac{i}{2}\overleftrightarrow{D}\,\vec{\sigma}\right)\chi|0\rangle \\ &\quad + \frac{1}{2}\epsilon^{ilk}\langle HX|\psi^\dagger\left(\frac{i}{2}\overleftrightarrow{D}\times\vec{\sigma}\right)^k\chi|0\rangle \\ &\quad + \langle HX|\psi^\dagger\left(\frac{i}{2}\overleftrightarrow{D}^{(i}\,\sigma^{l)}\right)\chi|0\rangle \ ,\end{aligned} \tag{3.106}$$

where $\overleftrightarrow{D}^{(i}\,\sigma^{l)}$ is the symmetric, traceless part of $\overleftrightarrow{D}^i\,\sigma^l$

$$\overleftrightarrow{D}^{(i}\,\sigma^{l)} = \frac{1}{2}\left(\overleftrightarrow{D}^i\,\sigma^l + \overleftrightarrow{D}^l\,\sigma^i\right) - \frac{1}{3}\delta^{il}\,\overleftrightarrow{D}\,\vec{\sigma} \ . \tag{3.107}$$

In order to obtain (3.106) we simply used, that for two three vectors A and B, one can write

$$\begin{aligned} A^iB^j &= \frac{1}{3}\delta^{ij}AB + \frac{1}{2}(A^iB^j - A^jB^i) + \frac{1}{2}(A^iB^j + A^jB^i) - \frac{1}{3}\delta^{ij}AB \\ &= \frac{1}{3}\delta^{ij}AB + \frac{1}{2}\epsilon^{ijk}(A\times B)^k + A^{(i}B^{j)} \end{aligned} \tag{3.108}$$

with

$$A^{(i}B^{j)} = \frac{1}{2}(A^iB^j + A^jB^i) - \frac{1}{3}\delta^{ij}AB\ . \tag{3.109}$$

The first term on the right hand side of equation (3.106) transforms under spatial rotations as ${}^3P_0$, the second as ${}^3P_1$ and the third as ${}^3P_2$ representation. Exploiting rotational symmetry and neglecting interference terms, we get from (3.106)

$$\begin{aligned} &\langle 0|\chi^\dagger\left(-\frac{i}{2}\overleftrightarrow{D}^i\right)\sigma^l\psi\mathcal{P}^H\psi^\dagger\left(-\frac{i}{2}\overleftrightarrow{D}^{i'}\right)\sigma^{l'}\chi|0\rangle \\ &= \frac{1}{3}\delta^{il}\delta^{i'l'}\ \langle 0|\frac{1}{3}\chi^\dagger\left(-\frac{i}{2}\overleftrightarrow{D}\,\vec{\sigma}\right)\psi\mathcal{P}^H\psi^\dagger\left(-\frac{i}{2}\overleftrightarrow{D}\,\vec{\sigma}\right)\chi|0\rangle \\ &+\frac{1}{2}\epsilon^{ilk}\epsilon^{i'l'k'}\frac{\delta^{kk'}}{3}\langle 0|\frac{1}{2}\chi^\dagger\left(-\frac{i}{2}\overleftrightarrow{D}\times\sigma\right)\psi\mathcal{P}^H\psi^\dagger\left(-\frac{i}{2}\overleftrightarrow{D}\times\sigma\right)\chi|0\rangle \\ &+\frac{1}{5}\left[\frac{1}{2}(\delta^{ii'}\delta^{ll'}+\delta^{il'}\delta^{li'}) - \frac{1}{3}\delta^{il}\delta^{i'l'}\right]\langle 0|\chi^\dagger\left(-\frac{i}{2}\overleftrightarrow{D}^{(m}\,\sigma^{n)}\right)\psi\mathcal{P}^H\psi^\dagger\left(-\frac{i}{2}\overleftrightarrow{D}^{(m}\,\sigma^{n)}\right)\chi|0\rangle\ , \end{aligned} \tag{3.110}$$

hence

$$\begin{aligned} \langle 0|\chi^\dagger\left(-\frac{i}{2}\overleftrightarrow{D}^i\right)\sigma^l\psi\mathcal{P}^H\psi^\dagger\left(-\frac{i}{2}\overleftrightarrow{D}^{i'}\right)\sigma^{l'}\chi|0\rangle &= \frac{1}{3}\delta^{il}\delta^{i'l'}\ \left\langle O^H\left[{}^3P_0^{(1)}\right]\right\rangle \\ &+ \frac{1}{2}(\delta^{ii'}\delta^{ll'}-\delta^{il'}\delta^{li'})\ \frac{\left\langle O^H\left[{}^3P_1^{(1)}\right]\right\rangle}{3} \\ &+ \left[\frac{1}{2}(\delta^{ii'}\delta^{ll'}+\delta^{il'}\delta^{li'}) - \frac{1}{3}\delta^{il}\delta^{i'l'}\right]\frac{\left\langle O^H\left[{}^3P_2^{(1)}\right]\right\rangle}{5}\ . \end{aligned} \tag{3.111}$$

Thereby in the next to last line of (3.110) we used that symmetry under spatial rotations implies

$$\begin{aligned} &\langle 0|\chi^\dagger\left(-\frac{i}{2}\overleftrightarrow{D}\times\vec{\sigma}\right)^k\psi\mathcal{P}^H\psi^\dagger\left(-\frac{i}{2}\overleftrightarrow{D}\times\vec{\sigma}\right)^{k'}\chi|0\rangle \\ &= \frac{1}{3}\delta^{kk'}\langle 0|\chi^\dagger\left(-\frac{i}{2}\overleftrightarrow{D}\times\vec{\sigma}\right)\psi\mathcal{P}^H\psi^\dagger\left(-\frac{i}{2}\overleftrightarrow{D}\times\vec{\sigma}\right)\chi|0\rangle\ . \end{aligned} \tag{3.112}$$

In the last line of (3.110) we used that as a consequence of spatial rotation symmetry we have

$$\langle 0|\chi^\dagger\left(-\frac{i}{2}\overleftrightarrow{D}^{(i}\,\sigma^{j)}\right)\psi\mathcal{P}^H\psi^\dagger\left(-\frac{i}{2}\overleftrightarrow{D}^{(i'}\,\sigma^{j')}\right)\chi|0\rangle = a\delta^{ij}\delta^{i'j'} + b\delta^{ii'}\delta^{jj'} + c\delta^{ij'}\delta^{i'j}\ . \tag{3.113}$$

Symmetry in the first and last two indices demands $b = c$. The vanishing of the trace with respect to the first and last two indices requires $a + 2b = 0$, proving that $\langle 0|\chi^\dagger \left(-\frac{i}{2} \overset{\leftrightarrow}{D}^{(i} \sigma^{j)}\right) \psi \mathcal{P}^H \psi^\dagger \left(-\frac{i}{2} \overset{\leftrightarrow}{D}^{(i'} \sigma^{j')}\right) \chi|0\rangle$ is proportional to $\frac{1}{2}(\delta^{ii'}\delta^{jj'}+\delta^{ij'}\delta^{ji'})-\frac{1}{3}\delta^{ij}\delta^{i'j'}$. The proportionality constant is simply determined by putting $i = i'$ and $j = j'$ and summing over i and j.

Analogously it is found

$$\begin{aligned}\langle 0|\chi^\dagger \left(-\frac{i}{2} \overset{\leftrightarrow}{D}^{i}\right) \sigma^l T^a \psi \mathcal{P}^H \psi^\dagger \left(-\frac{i}{2} \overset{\leftrightarrow}{D}^{i'}\right) \sigma^{l'} T^b \chi|0\rangle = {} & \frac{1}{3}\delta^{il}\delta^{i'l'} \frac{\left\langle O^H\left[{}^3P_0^{(8)}\right]\right\rangle}{8} \\ & + \frac{1}{2}(\delta^{ii'}\delta^{ll'} - \delta^{il'}\delta^{li'}) \frac{\left\langle O^H\left[{}^3P_1^{(8)}\right]\right\rangle}{8\times 3} \\ & + \left[\frac{1}{2}(\delta^{ii'}\delta^{ll'} + \delta^{il'}\delta^{li'}) - \frac{1}{3}\delta^{il}\delta^{i'l'}\right] \frac{\left\langle O^H\left[{}^3P_2^{(8)}\right]\right\rangle}{8\times 5} ,\end{aligned} \tag{3.114}$$

where the additional factor 8 in the denominator comes again from the color symmetry. We are now in position to calculate the residual amplitude squares. From (3.111), we find for $\left|\mathcal{A}\left[{}^3P_0^{(1)}\right]\right|^2$

$$\begin{aligned}\left|\mathcal{A}\left[{}^3P_0^{(1)}\right]\right|^2 = {} & \left[\frac{\partial}{\partial q_\mu} tr[\mathcal{T}\Pi_1^\nu C_1]\Big|_{q=0}\right]^* \frac{\partial}{\partial q_{\mu'}} tr[\mathcal{T}\Pi_1^{\nu'} C_1]\Big|_{q=0} \\ & \times L^i{}_\mu L^l{}_\nu L^{i'}{}_{\mu'} L^{l'}{}_{\nu'} \ \frac{1}{3}\delta_{il}\delta_{i'l'} \frac{\left\langle O^H\left[{}^3P_0^{(1)}\right]\right\rangle}{6} ,\end{aligned} \tag{3.115}$$

hence

$$\begin{aligned}\left|\mathcal{A}\left[{}^3P_0^{(1)}\right]\right|^2 = {} & \left[\frac{\partial}{\partial q_\mu} tr[\mathcal{T}\Pi_1^\nu C_1]\Big|_{q=0}\right]^* \frac{\partial}{\partial q_{\mu'}} tr[\mathcal{T}\Pi_1^{\nu'} C_1]\Big|_{q=0} \ \frac{1}{3}\Pi_{\mu\nu}\Pi_{\mu'\nu'} \\ & \times \frac{\left\langle O^H\left[{}^3P_0^{(1)}\right]\right\rangle}{6} .\end{aligned} \tag{3.116}$$

We find for $\left|\mathcal{A}\left[{}^3P_1^{(1)}\right]\right|^2$

$$\begin{aligned}\left|\mathcal{A}\left[{}^3P_1^{(1)}\right]\right|^2 = {} & \left[\frac{\partial}{\partial q_\mu} tr[\mathcal{T}\Pi_1^\nu C_1]\Big|_{q=0}\right]^* \frac{\partial}{\partial q_{\mu'}} tr[\mathcal{T}\Pi_1^{\nu'} C_1]\Big|_{q=0} \\ & \times L^i{}_\mu L^l{}_\nu L^{i'}{}_{\mu'} L^{l'}{}_{\nu'} \ \frac{1}{2}(\delta^{ii'}\delta^{ll'} - \delta^{il'}\delta^{li'}) \frac{\left\langle O^H\left[{}^3P_1^{(1)}\right]\right\rangle}{6\times 3} ,\end{aligned} \tag{3.117}$$

hence

$$\left|\mathcal{A}\left[{}^3P_1^{(1)}\right]\right|^2 = \left[\frac{\partial}{\partial q_\mu} tr[\mathcal{T}\Pi_1^\nu C_1]\Big|_{q=0}\right]^* \frac{\partial}{\partial q_{\mu'}} tr[\mathcal{T}\Pi_1^{\nu'} C_1]\Big|_{q=0}$$

$$\times \frac{1}{2}\left(\Pi_{\mu\mu'}\Pi_{\nu\nu'} - \Pi_{\mu\nu'}\Pi_{\nu\mu'}\right) \frac{\left\langle O^H\left[{}^3P_1^{(1)}\right]\right\rangle}{6\times 3} . \tag{3.118}$$

Finally, we find for $\left|\mathcal{A}\left[{}^3P_2^{(1)}\right]\right|^2$

$$\left|\mathcal{A}\left[{}^3P_2^{(1)}\right]\right|^2 = \left[\frac{\partial}{\partial q_\mu} tr[\mathcal{T}\Pi_1^\nu C_1]\Big|_{q=0}\right]^* \frac{\partial}{\partial q_{\mu'}} tr[\mathcal{T}\Pi_1^{\nu'} C_1]\Big|_{q=0}$$
$$\times L^i{}_\mu L^l{}_\nu L^{i'}{}_{\mu'} L^{l'}{}_{\nu'} \left[\frac{1}{2}(\delta^{ii'}\delta^{ll'} + \delta^{il'}\delta^{li'}) - \frac{1}{3}\delta^{il}\delta^{i'l'}\right] \frac{\left\langle O^H\left[{}^3P_2^{(1)}\right]\right\rangle}{6\times 5} , \tag{3.119}$$

hence

$$\left|\mathcal{A}\left[{}^3P_2^{(1)}\right]\right|^2 = \left[\frac{\partial}{\partial q_\mu} tr[\mathcal{T}\Pi_1^\nu C_1]\Big|_{q=0}\right]^* \frac{\partial}{\partial q_{\mu'}} tr[\mathcal{T}\Pi_1^{\nu'} C_1]\Big|_{q=0}$$
$$\times \left[\frac{1}{2}\left(\Pi_{\mu\mu'}\Pi_{\nu\nu'} + \Pi_{\mu\nu'}\Pi_{\nu\mu'}\right) - \frac{1}{3}\Pi_{\mu\nu}\Pi_{\mu'\nu'}\right] \frac{\left\langle O^H[{}^3P_2^{(1)}]\right\rangle}{6\times 5} . \tag{3.120}$$

Analogously, we find for the octet parts $\left|\mathcal{A}\left[{}^3P_J^{(8)}\right]\right|^2$ from (3.114)

$$\left|\mathcal{A}\left[{}^3P_0^{(8)}\right]\right|^2 = \sum_a \left[\frac{\partial}{\partial q_\mu} tr[\mathcal{T}\Pi_1^\nu C_8^a]\Big|_{q=0}\right]^* \frac{\partial}{\partial q_{\mu'}} tr[\mathcal{T}\Pi_1^{\nu'} C_8^a]\Big|_{q=0} \frac{1}{3}\Pi_{\mu\nu}\Pi_{\mu'\nu'}$$
$$\times \frac{\left\langle O^H\left[{}^3P_0^{(8)}\right]\right\rangle}{8} , \tag{3.121}$$

$$\left|\mathcal{A}\left[{}^3P_1^{(8)}\right]\right|^2 = \left[\frac{\partial}{\partial q_\mu} tr[\mathcal{T}\Pi_1^\nu C_1]\Big|_{q=0}\right]^* \frac{\partial}{\partial q_{\mu'}} tr[\mathcal{T}\Pi_1^{\nu'} C_1]\Big|_{q=0}$$
$$\times \frac{1}{2}\left(\Pi_{\mu\mu'}\Pi_{\nu\nu'} - \Pi_{\mu\nu'}\Pi_{\nu\mu'}\right) \frac{\left\langle O^H\left[{}^3P_1^{(8)}\right]\right\rangle}{8\times 3} \tag{3.122}$$

and

$$\left|\mathcal{A}\left[{}^3P_2^{(8)}\right]\right|^2 = \left[\frac{\partial}{\partial q_\mu} tr[\mathcal{T}\Pi_1^\nu C_1]\Big|_{q=0}\right]^* \frac{\partial}{\partial q_{\mu'}} tr[\mathcal{T}\Pi_1^{\nu'} C_1]\Big|_{q=0}$$
$$\times \left[\frac{1}{2}\left(\Pi_{\mu\mu'}\Pi_{\nu\nu'} + \Pi_{\mu\nu'}\Pi_{\nu\mu'}\right) - \frac{1}{3}\Pi_{\mu\nu}\Pi_{\mu'\nu'}\right] \frac{\left\langle O^H\left[{}^3P_2^{(8)}\right]\right\rangle}{8\times 5} . \tag{3.123}$$

Inserting the above deduced results for the $\left|\mathcal{A}\left[{}^{2S+1}L_J^{(a)}\right]\right|^2$ in (3.92) and using (3.13), (3.14) proves the formulae for the short distance coefficients for unpolarized heavy quarkonium production in section 3.1. Therewith we have found agreement with Ref.[15].

Chapter 4

J/ψ inclusive production in lN DIS at Born level

Having prepared all the necessary tools, we will analyze in this chapter single and jet associated J/ψ inclusive production in lepton nucleon deep inelastic scattering (lN DIS) at Born level. Based on the obtained analytical results we make quantitative predictions for the H1 experiment at DESY HERA and the CHORUS and NOMAD experiments at CERN.

4.1 The analytical calculations

The here considered processes of single and jet associated J/ψ inclusive production in lN DIS can be symbollically written

$$lN \to l'H(j)X' \; . \tag{4.1}$$

Here l, l' and N denote the ingoing lepton, the outgoing lepton and the nucleon, respectively. j stands for the jet and we use brackets arround the symbol of a reaction product, if it only occurs in jet associated but not in single inclusive production. H is the J/ψ meson in case of direct J/ψ inclusive production, while in case of prompt J/ψ inclusive production H may also be one of the higher charmonia ψ' or χ_{cJ}, which is directly produced and subsequently decays into the J/ψ. X' symbolizes all the hadronic rest including the nucleon remnant as well as the soft hadronic rest X'', caused by the long distance dynamics involved in the formation of the H bound state. According to the parton model the production cross section $d\sigma(lN \to l'H(j)X')$ can be written

$$d\sigma(lN \to l'H(j)X') = \sum_a \int d\xi F_N^a\left(\xi, \mu_F^2\right) d\sigma(la \to l'H(a')X'') \; , \tag{4.2}$$

where $F_N^a\left(\xi, \mu_F^2\right)$ are the parton density functions of the nucleon, ξ is the longitudinal momentum fraction adopted by the parton a from the nucleon, μ_F is an appropriate factorization scale and $d\sigma(la \to l'H(a')X'')$ are the cross sections of the subprocesses

$la \to l'H(a')X''$. a is taken to be a gluon g or one of the light quarks u, d, s. The outgoing parton a' in the here discussed cases of J/ψ plus jet inclusive production may be a gluon g or one of the quarks u, d, s, c and, at leading order, can be identified with the jet j. Applying the NRQCD factorization formula (1.3), we find

$$d\sigma(lN \to l'H(j)X') = \sum_a \int d\xi F_N^a\left(\xi, \mu_F^2\right) \sum_n d\sigma(la \to l'c\bar{c}[n](a')) \left\langle O^H[n] \right\rangle \ , \tag{4.3}$$

where the only relevant NRQCD matrix elements $\left\langle O^H[n] \right\rangle$ are those, which belong to $n = {}^3S_1^{(1)}, {}^1S_0^{(8)}, {}^3S_1^{(8)}, {}^3P_J^{(8)}$ if $H = J/\psi, \psi'$ and to $n = {}^3P_J^{(1)}, {}^3S_1^{(8)}$ if $H = \chi_{cJ}$. The short distance coefficients $d\sigma_{c\bar{c}[n]} \equiv d\sigma(la \to l'c\bar{c}[n](a'))$, corresponding to the creation of the $c\bar{c}[n]$ state in the partonic subprocess $la \to l'c\bar{c}[n](a')$, are calculated within the projection formalism introduced in chapter 3. For $H = J/\psi$ (4.3) describes direct J/ψ inclusive production. With the branching ratios $B(\psi' \to J/\psi\ X_{\psi'})$ and $B(\chi_{cJ} \to J/\psi\ \gamma)$ for the decay of the ψ' into the J/ψ and hadronic rest $X_{\psi'}$ and of the χ_{cJ} into the J/ψ and a γ, respectively, the cross section for prompt J/ψ inclusive production reads

$$\begin{aligned} d\sigma(lN \to l'(J/\psi)_{\text{prompt}}(j)X) = & \quad d\sigma(lN \to l'J/\psi(j)X') \\ + & \quad d\sigma(lN \to l'\psi'(j)X')\ B(\psi' \to J/\psi\ X_{\psi'}) \\ + & \sum_{J=0}^{2} d\sigma(lN \to l'\chi_{cJ}(j)X')\ B(\chi_{cJ} \to J/\psi\ \gamma) \ . \end{aligned} \tag{4.4}$$

Thereby the $d\sigma(lN \to l'H(j)X')$ for $H = J/\psi$, ψ', χ_{cJ} are given in (4.3) and X denotes the hadronic rest, which besides the nucleon remnant and the soft hadronic rest X' now additionally includes the decay byproducts $X_{\psi'}$ or γ, respectively of the higher charmonium states ψ' and χ_{cJ}.

4.1.1 Single J/ψ inclusive production in lN electromagnetic and neutral current DIS

To start with, we investigate direct and prompt single J/ψ inclusive production in the process

$$lN \to lHX' \ , \tag{4.5}$$

where l is an electron $l = e^-$, which is scattered through the electromagnetic interaction, or a neutrino $l = \nu_e$, which is scattered through the neutral current interaction. Since the only contributing partonic subprocesses are the gluon initiated ones

$$lg \to lc\bar{c}[n] \ , \tag{4.6}$$

(4.3) for the direct H production cross section reduces to

$$d\sigma(lN \to lHX') = \int d\xi F_N^g\left(\xi, \mu_F^2\right) \sum_n d\sigma(lg \to lc\bar{c}[n]) \left\langle O^H[n] \right\rangle \ . \tag{4.7}$$

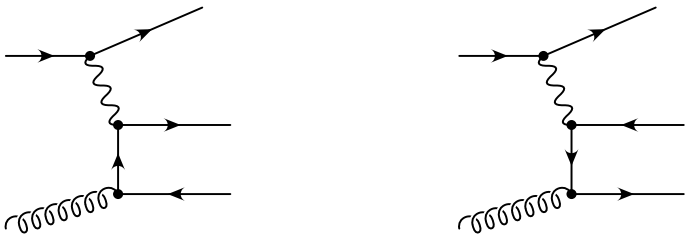

Figure 4.1: Feynman diagrams for the partonic subprocesses $lg \to lc\bar{c}[n]$.

The Feynman diagrams, which contribute to the short distance coefficients $d\sigma(lg \to lc\bar{c}[n])$ at Born level, are shown in Fig.4.1. Thereby, the gauge boson B exchanged between the lepton and the heavy quark is a photon in case of $l = e^-$ and a Z boson in case of $l = \nu_e$

$$B = \begin{cases} \gamma \text{ if } l = e^- \\ \\ Z \text{ if } l = \nu_e \ . \end{cases} \tag{4.8}$$

The only difference between the corresponding total amplitudes $\mathcal{M}[n] \equiv \mathcal{M}_{lg}[n]$ for $l = e^-$ and those for $l = \nu_e$ consists in the gauge boson mass m_B, which vanishes for $B = \gamma$ but does not for $B = Z$, and the structure of the gauge boson fermion vertex

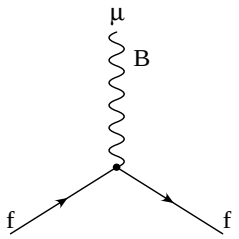

$$\leftrightarrow \qquad -iG\,\Gamma^{\mu}_{Bff} = -iG\left(V\gamma^{\mu} + A\gamma^5\gamma^{\mu}\right) \ , \tag{4.9}$$

where in case of $l = e^-$ and $B = \gamma$

$$V = \begin{cases} 1 \text{ if } f = e^- \\ \\ e_q \text{ if } f = q \end{cases} \qquad , \qquad A = 0 \qquad , \qquad G = e \tag{4.10}$$

with e in the last equation denoting the elementary charge and

$$e_q = \begin{cases} \frac{2}{3} \text{ if } q = u, c \\ \\ -\frac{1}{3} \text{ if } q = d, s \end{cases} \tag{4.11}$$

being the fractional charge of the quark $q = u, d, s, c$, while in case of $l = \nu_e$ and $B = Z$

$$V = \begin{cases} \frac{1}{2} \text{ if } f = \nu_e \\ \\ v_q \text{ if } f = q \end{cases} \quad , \quad A = \begin{cases} \frac{1}{2} \text{ if } f = \nu_e \\ \\ a_q \text{ if } f = q \end{cases} \quad , \quad G = g := 2^{\frac{1}{4}} G_F^{\frac{1}{2}} m_Z \tag{4.12}$$

with

$$v_q = \begin{cases} \frac{1}{2}\left(1 - \frac{8}{3}\,\sin^2\theta_W\right) \text{ if } q = u, c \\ -\frac{1}{2}\left(1 - \frac{4}{3}\,\sin^2\theta_W\right) \text{ if } q = d, s \end{cases} ,$$
$$a_q = \frac{1}{2} \text{ for } q = u, d, s, c \ , \tag{4.13}$$

G_F being the Fermi constant and θ_W being the weak mixing angle. In the following P_N, p, k, k' and $q_B = k - k'$ denote the momentum of the nucleon, the ingoing parton, the ingoing lepton, the outgoing lepton and the gauge boson B, respectively, while P stands for the charmonium momentum as before. Furthermore, throughout this work, we neglect the masses of the leptons, the light quarks u, d, s and, unless otherwise agreed, the nucleon. As kinematical invariants the total center of mass energy S

$$S = (P_N + k)^2 = 2P_N k \ , \tag{4.14}$$

the virtuality Q^2 of the exchanged gauge boson B

$$Q^2 = -q_B^2 = 2kk' \ , \tag{4.15}$$

and the energy fraction y transferred from the ingoing lepton to the gauge boson B in the nucleon rest frame

$$y = \frac{P_N q_B}{P_N k} \tag{4.16}$$

are introduced. Further useful variables are the center of mass energy squared $\hat{s}$ of the gauge boson B and the ingoing parton

$$\hat{s} = (p + q_B)^2 = \xi y S - Q^2 \ , \tag{4.17}$$

the center of mass energy W of the gauge boson B and the nucleon

$$W^2 = (P_N + q_B)^2 = yS - Q^2 \ , \tag{4.18}$$

as well as the inelasticity variable z, which was already mentioned in the introduction and which is defined as the energy fraction, transferred from the gauge boson B to the charmonium H in the nucleon rest frame

$$z = \frac{P_N P}{P_N q_B} \ . \tag{4.19}$$

The $\mathcal{M}_{lg}[n]$ can be decomposed into a hadronic part $h^\mu_{lg}[n]$ and a remaining leptonic one, according to

$$\mathcal{M}_{lg}[n] = \frac{G}{m_B^2 + Q^2} \bar{u}_{r'}(k') \Gamma^\mu_{Bll} u_r(k) h_{lg\,\mu}[n] \ . \tag{4.20}$$

This decomposition is obvious for $B = \gamma$. To obtain (4.20) in case of $B = Z$, we treated the Z boson propagator in the unitary gauge

$$\int d^4x \ \exp(iq_Z x)\langle 0|TZ^\mu(x)Z^\nu(0)|0\rangle = i\frac{-g^{\mu\nu} + \frac{q_Z^\mu q_Z^\nu}{m_Z^2}}{q_Z^2 - m_Z^2 + i\epsilon} \tag{4.21}$$

with Z_μ denoting the Z boson field, and exploited the Dirac equation for massless leptons $\not{k}u_r(k) = \bar{u}_{r'}(k')\not{k}' = 0$, implying

$$q_{Z\,\mu}\bar{u}_{r'}(k')\Gamma^\mu_{Z\nu_e\nu_e}u_r(k) = 0 \ . \tag{4.22}$$

From (4.20) it follows

$$d\sigma(lg \to lc\bar{c}[n]) = \frac{1}{2\xi S}dPS_2(p+k;P,k')\frac{G^2}{(m_B^2+Q^2)^2}l_l^{\mu\nu}H_{lg\,\mu\nu}[n] \ . \tag{4.23}$$

Here, the lepton tensor $l_l^{\mu\nu}$ is given by

$$\begin{aligned} l_l^{\mu\nu} &= \frac{1}{N_l}\sum_{r,r'}\bar{u}_r(k)\Gamma^\mu_{Bll}u_{r'}(k')\bar{u}_{r'}(k')\Gamma^\nu_{Bll}u_r(k) \\ &= \begin{cases} 2(k^\mu k'^\nu + k^\nu k'^\mu - \frac{Q^2}{2}g^{\mu\nu}) & \text{if} \quad l = e^- \\ 2(k^\mu k'^\nu + k^\nu k'^\mu - \frac{Q^2}{2}g^{\mu\nu} + i\epsilon^{\mu\nu\rho\sigma}k_\rho k'_\sigma) & \text{if} \quad l = \nu_e \end{cases} , \end{aligned} \tag{4.24}$$

where

$$N_l = \begin{cases} 2 & \text{if} \quad l = e^- \\ 1 & \text{if} \quad l = \nu_e \end{cases} \tag{4.25}$$

is the spin multiplicity of the ingoing lepton. The hadron tensor $H_{lg}^{\mu\nu}[n]$ is defined by

$$H_{lg}^{\mu\nu}[n] = \frac{1}{N_{\text{col}}N_{\text{pol}}}\overline{\sum}h_{lg}^{\dagger\mu}[n]h_{lg}^{\nu}[n] \tag{4.26}$$

with N_{col}, N_{pol} and $\overline{\sum}$ as in (3.17). In calculating $H_{lg}^{\mu\nu}[n]$ the gluon polarization sum can be replaced by $-g^{\mu\nu}$, as the gluon in the here contributing Feynman diagrams behaves photon like, and in case of a photon this replacement is well known to be justified due to the abelian gauge symmetry of QED. Performing the integration over $\vec{P}$, the phase space measure $dPS_2(p+k;P,k')$ becomes

$$dPS_2(p+k;P,k') = \frac{d^3\vec{k}'}{(2\pi)^2 2k'^0}\frac{1}{2P^0}\delta(p^0 + q_B^0 - P^0)\Big|_{\vec{p}+\vec{q}_B-\vec{P}=0} \ . \tag{4.27}$$

With

$$\begin{aligned} \frac{1}{2P^0}\delta(p^0+q_B^0-P^0) &= \frac{1}{2P^0}\left(\delta(p^0+q_B^0-P^0)+\delta(p^0+q_B^0+P^0)\right) \\ &= \delta\left((p^0+q_B^0)^2 - P^{0\,2}\right) \\ &= \delta\left((p+q_B)^2 - P^2 + (\vec{p}+\vec{q}_B)^2 - \vec{P}^2\right) \\ &= \delta\left(\hat{s} - M^2 + (\vec{p}+\vec{q}_B)^2 - \vec{P}^2\right) \end{aligned} \tag{4.28}$$

one obtains

$$\frac{1}{2P^0}\delta(p^0+q_B^0-P^0)\,\Big|_{\vec{p}+\vec{q}_B-\vec{P}=0} = \delta(\hat{s}-M^2)\ . \tag{4.29}$$

Thereby in the first line of (4.28) we used, that $p^0+q_B^0+P^0>0$ and consequently $\delta(p^0+q_B^0+P^0)$ doesn't contribute. For a further evaluation of the lorentz invariant measure $d^3\vec{k}'/(2\pi)^2 2k'^0$ it is useful to specify the lepton gluon center of mass frame and to express $d^3\vec{k}'$ in polar coordinates. Performing the integration over the azimuthal angle of the outgoing lepton, which for symmetry reasons results in a factor 2π, one finds

$$\frac{d^3\vec{k}'}{(2\pi)^2 2k'^0} = \frac{dk'^{0\,2}d\cos\theta}{8\pi}\ , \tag{4.30}$$

where $\theta=\measuredangle(\vec{k},\vec{k}')$ is the polar angle of the outgoing lepton. Noting, that $\vec{p}+\vec{k}=0$ together with $p^2=k^2=0$ implies $p^0=|\vec{p}|=k^0=|\vec{k}|=\sqrt{\xi S}/2$, we have

$$Q^2=\sqrt{\xi S}\ k'^0\ (1-\cos\theta)\ , \tag{4.31}$$

$$y=1-\frac{1}{\sqrt{\xi S}}\ k'^0\ (1+\cos\theta) \tag{4.32}$$

and consequently

$$dk'^{0\,2}d\cos\theta = dQ^2dy\ . \tag{4.33}$$

Hence, the phase space measure takes the form

$$dPS_2(p+k;P,k') = \frac{dQ^2dy}{8\pi}\delta(\hat{s}-M^2)\ . \tag{4.34}$$

It is advantageous to integrate out the azimuthal symmetry of the process in the center of mass system of the gauge boson B and the gluon g (Bg CMS) instead of that of the lepton and the gluon. For that purpose, we introduce on the right hand side of (4.34) the symbolic factor $d\phi/2\pi$, where ϕ is the azimuthal angle of the outgoing lepton in the Bg CMS. Performing the integration over ϕ before contracting the lepton tensor $l_l^{\mu\nu}$ with the hadron tensor $H_{lg}^{\mu\nu}[n]$ and noting, that due to the azimuthal symmetry of the process $H_{lg}^{\mu\nu}[n]$ doesn't depend on ϕ, (4.23) becomes

$$d\sigma(lg\to lc\bar{c}[n]) = \frac{dQ^2dy}{16\pi\xi S}\delta(\hat{s}-M^2)\frac{G^2}{(m_B^2+Q^2)^2}L_l^{\mu\nu}H_{lg\,\mu\nu}[n]\ , \tag{4.35}$$

where

$$L_l^{\mu\nu}=\int\frac{d\phi}{2\pi}\ l_l^{\mu\nu} \tag{4.36}$$

with $l_l^{\mu\nu}$ given in (4.24) is the integrated lepton tensor. Since in the Bg CMS the only vectors available for the construction of the tensor $L_l^{\mu\nu}$ are p and q_B, the very vectors, which serve for the definition of that frame, the most general ansatz for $L_l^{\mu\nu}$ is

$$L_l^{\mu\nu}=a_1g^{\mu\nu}+a_2p^\mu p^\nu+a_3q_B^\mu q_B^\nu+a_4(p^\mu q_B^\nu+p^\nu q_B^\mu)+a_5(p^\mu q_B^\nu-p^\nu q_B^\mu)+a_6\epsilon^{\mu\nu\rho\sigma}p_\rho q_{B\,\sigma}\ . \tag{4.37}$$

Note, that for symmetry reasons a_5 and a_6 vanish in case of $l = e^-$. The contraction of both sides of (4.37) with each of the six basis tensors on the right hand side yields six equations for the determination of the six unknowns a_1, a_2,..., a_6. In this way it is found for $L_l^{\mu\nu}$

$$L_l^{\mu\nu} = \begin{cases} \frac{Q^2}{y}\left[\frac{1+(1-y)^2}{y}\epsilon_T^{\mu\nu} - \frac{4(1-y)}{y}\epsilon_L^{\mu\nu}\right] & \text{if } \; l = e^- \\ \frac{Q^2}{y}\left[\frac{1+(1-y)^2}{y}\epsilon_T^{\mu\nu} - \frac{4(1-y)}{y}\epsilon_L^{\mu\nu} + (2-y)\epsilon_A^{\mu\nu}\right] & \text{if } \; l = \nu_e \end{cases} , \tag{4.38}$$

where

$$\epsilon_T^{\mu\nu} = -g^{\mu\nu} + \frac{1}{pq_B}(p^\mu q_B^\nu + p^\nu q_B^\mu) - \frac{q_B^2}{(pq_B)^2}p^\mu p^\nu \ , \tag{4.39}$$

$$\epsilon_L^{\mu\nu} = \frac{1}{q_B^2}\left(q_B - \frac{q_B^2}{pq_B}p\right)^\mu \left(q_B - \frac{q_B^2}{pq_B}p\right)^\nu \ , \tag{4.40}$$

$$\epsilon_A^{\mu\nu} = -i\epsilon^{\mu\nu\rho\sigma}\frac{p_\rho q_{B\,\sigma}}{pq_B} \ , \tag{4.41}$$

and we adopted the convention $\epsilon_{\mu\nu\rho\sigma} = 1$. The contributions to $L_l^{\mu\nu}$ proportional to $\epsilon_T^{\mu\nu}$ and $\epsilon_L^{\mu\nu}$ can be assigned to transverse and longitudinal polarization of the exchanged gauge boson B, respectively. Note, that in case of electroproduction $l = e^-$ the QED Ward identity

$$q_B^\mu H_{l\,g\,\mu\nu}[n] = 0 \tag{4.42}$$

leads to a decisive simplification as (4.38) is inserted in (4.35).

It is interesting to study (4.35) for $l = e^-$ in the photoproduction limit $Q^2 \to 0$. The short distance coefficients $\sigma(\gamma g \to c\bar{c}[n])$ for H photoproduction read

$$\sigma(\gamma g \to c\bar{c}[n]) = \frac{1}{2\hat{s}}\int dPS_1(p+q_\gamma; P)\overline{\sum}\epsilon_\lambda^{\mu *}(q_\gamma)\epsilon_\lambda^\nu(q_\gamma)H_{e^-\,g\,\mu\nu}[n]\,\Big|_{Q^2\to 0} \ . \tag{4.43}$$

Here the $\epsilon_\lambda^\mu(q_\gamma)$ are the polarization vectors of the ingoing real photon with momentum q_γ, and $\overline{\sum}$ stands for the average over the transverse photon polarization degrees of freedom $\lambda = 1, 2$. Performing the integration over $\vec{P}$ and replacing $\overline{\sum}\epsilon_\lambda^{\mu *}(q_\gamma)\epsilon_\lambda^\nu(q_\gamma)$ in (4.43) by $-g^{\mu\nu}/2$, (4.43) takes the form

$$\sigma(\gamma g \to c\bar{c}[n]) = \frac{\pi}{2\hat{s}}\delta(\hat{s} - M^2)\left(-g^{\mu\nu}H_{e^-\,g\,\mu\nu}[n]\right)\Big|_{Q^2\to 0} \ . \tag{4.44}$$

A comparison of this result with (4.35) for $l = e^-$ shows, that (4.35) becomes in the limit $Q^2 \to 0$

$$\frac{d\sigma}{dQ^2dy}(e^-g \to e^-c\bar{c}[n])\Big|_{Q^2\to 0} = \frac{\alpha}{2\pi Q^2}\frac{1+(1-y)^2}{y}\sigma(\gamma g \to c\bar{c}[n]) \ , \tag{4.45}$$

where $\alpha = e^2/4\pi$ is Sommerfeld's finestructure constant. With the cross section for H photoproduction in the process $\gamma N \to HX'$

$$\sigma(\gamma N \to HX') = \int d\xi F_N^g(\xi, \mu_F^2)\sum_n \sigma(\gamma g \to c\bar{c}[n])\left\langle O^H[n]\right\rangle \tag{4.46}$$

(4.45) is equivalent to the following result for the electroproduction cross section $\sigma(e^-N \to e^-HX')$ in the limit $Q^2 \to 0$:

$$\frac{d\sigma}{dQ^2dy}(e^-N \to e^-HX') = \frac{\alpha}{2\pi Q^2}\frac{1+(1-y)^2}{y}\sigma(\gamma N \to HX') \; . \tag{4.47}$$

We end this section with a presentation of our final results for the $\sigma(lN \to lHX')$. Inserting (4.35) in (4.7), substituting $H_{lg\,\mu\nu}[n]$ by its concrete form, dictated by the Feynman rules of the Standard Model [40] and the projection formalism, and making use of the heavy quark spin symmetry relations (2.103), (2.104), we find for $l = e^-$ in agreement with [31]

$$\begin{aligned}\frac{d\sigma}{dQ^2dy}(e^-N \to e^-HX') = &\int_0^1 d\xi F_N^g(\xi,\mu_F^2)\delta(\xi yS - M^2 - Q^2) \\ &\times \frac{4\pi^2 e_c^2\alpha^2\alpha_s}{M(M^2+Q^2)Q^2}\left[\frac{1+(1-y)^2}{y}\left(\left\langle O^H\left[{}^1S_0^{(8)}\right]\right\rangle\right.\right. \\ &+ \left.\left.\frac{28M^2+12Q^2}{M^2+Q^2}\frac{\left\langle O^H\left[{}^3P_0^{(8)}\right]\right\rangle}{M^2}\right)\right. \\ &- \left. y\frac{32M^2Q^2}{(M^2+Q^2)^2}\frac{\left\langle O^H\left[{}^3P_0^{(8)}\right]\right\rangle}{M^2}\right]\end{aligned} \tag{4.48}$$

for $H = J/\psi, \psi'$ and

$$\frac{d\sigma}{dQ^2dy}(e^-N \to e^-\chi_{cJ}X') = 0 \; . \tag{4.49}$$

Making use of (4.47) we extract from (4.48), (4.49) for $\sigma(\gamma N \to HX')$ the formulae

$$\begin{aligned}\sigma(\gamma N \to HX') = &\int_0^1 d\xi F_N^g(\xi,\mu_F^2)\delta(\xi S_\gamma - M^2)\frac{8\pi^3 e_c^2\alpha\alpha_s}{M^3} \\ &\times\left(\left\langle O^H\left[{}^1S_0^{(8)}\right]\right\rangle + 28\frac{\left\langle O^H\left[{}^3P_0^{(8)}\right]\right\rangle}{M^2}\right)\end{aligned} \tag{4.50}$$

for $H = J/\psi, \psi'$ and

$$\sigma(\gamma N \to \chi_{cJ}X') = 0 \; , \tag{4.51}$$

in agreement with [21, 22, 23, 24]. Thereby, $S_\gamma = (P_N+q_\gamma)^2 = 2P_Nq_\gamma$ is the photon nucleon center of mass energy squared. In the same way, it is found for $l = \nu_e$ in agreement with [33]

$$\begin{aligned}\frac{d\sigma}{dQ^2dy}(\nu_eN \to \nu_eHX') = &\int_0^1 d\xi F_N^g(\xi,\mu_F^2)\delta(\xi yS - M^2 - Q^2) \\ &\times\frac{g^4\alpha_s}{6M(M^2+Q^2)(m_Z^2+Q^2)^2}\left\{\frac{3v_c^2Q^2}{2}\left[\frac{1+(1-y)^2}{y}\right.\right.\end{aligned}$$

$$\times \left(\left\langle O^H \left[{}^1S_0^{(8)} \right] \right\rangle + \frac{28M^2 + 12Q^2}{M^2 + Q^2} \frac{\left\langle O^H \left[{}^3P_0^{(8)} \right] \right\rangle}{M^2} \right)$$
$$- \; y \frac{32M^2Q^2}{(M^2 + Q^2)^2} \frac{\left\langle O^H \left[{}^3P_0^{(8)} \right] \right\rangle}{M^2} \Bigg]$$
$$+ \; a_c^2 \frac{Q^2[1 + (1-y)^2] + 4M^2(1-y)}{2y} \left\langle O^H \left[{}^3S_1^{(8)} \right] \right\rangle \Bigg\} \quad (4.52)$$

for $H = J/\psi, \psi'$ and

$$\frac{d\sigma}{dQ^2 dy}(\nu_e N \to \nu_e \chi_{cJ} X') = \int_0^1 d\xi F_N^g(\xi, \mu_F^2) \delta(\xi y S - M^2 - Q^2)$$
$$\times \frac{g^4 \alpha_s a_c^2}{12 y M (M^2 + Q^2)(m_Z^2 + Q^2)^2}$$
$$\times \left\{ Q^2[1 + (1-y)^2] + 4M^2(1-y) \right\} \left\langle O^{\chi_{cJ}} \left[{}^3S_1^{(8)} \right] \right\rangle \; . \quad (4.53)$$

The kinematically allowed ranges for S, Q^2 and y in the above formulae for the cross sections are

$$S \geq M^2 \quad , \quad 0 \leq Q^2 \leq S - M^2 \quad , \quad \frac{M^2 + Q^2}{S} \leq y \leq 1 \; . \quad (4.54)$$

The lower bound of Q^2 and the upper bound of y are easily found from (4.31) and (4.32), noting, that $k'^0 \geq 0$ and that $\cos\theta$ may assume its maximum value 1 in (4.31) and its minimum value -1 in (4.32), respectively. The upper bound of Q^2 and the lower bounds of y and S then immediately follow from the relation $\xi y S - M^2 - Q^2 = 0$, which is enforced by the δ distribution in the above formulae for the cross sections. Note, that, since the contributions of the axial part of the lepton tensor $L_{\nu_e \mu\nu}$ to (4.52) and (4.53) are all vanishing

$$\epsilon_A^{\mu\nu} H_{\nu_e g \, \mu\nu}[n] = 0 \; , \quad (4.55)$$

the cross sections for electroproduction (4.48), (4.49) are recovered from those for neutrinoproduction (4.52), (4.53) in the limit $a_c \to 0$, $v_c \to e_c$, $g \to e$, $m_Z \to 0$. From the Feynman diagrams in Fig.4.1 the vanishing of the color singlet contributions to the cross sections (4.48)-(4.53) as well as of the ${}^3S_1^{(8)}$ contributions to the cross sections (4.48)-(4.51) is seen to be a consequence of color conservation and of the Furry theorem, respectively.

Due to lepton universality the cross sections do not change, if the scattered electron (electron neutrino) is replaced by a muon (muon neutrino) or a tauon (tauon neutrino). Furthermore, they remain unchanged, if the electron (electron neutrino) is replaced by an anti electron, anti muon or anti tauon (anti electron neutrino, anti muon neutrino or anti tauon neutrino).

Though the processes, discussed in this section, at leading order exclusively proceed through the color octet channels, they are not well suited for testing the color octet mechanism, as the inelasticity variable z here assumes exactly the value 1. This means, that the kinematical regime of these processes coincides with that of diffractive production, so that a suppression of the diffractive background by applying kinematical cuts is impossible.

4.1.2 J/ψ plus jet inclusive production in lN electromagnetic and neutral current DIS

As next, we reanalyze the processes of section 4.1.1 with the only difference, that we now demand the final state to contain additionally a jet j

$$lN \to lHjX' \ . \tag{4.56}$$

There are two types of partonic subprocesses

$$la \to lc\bar{c}[n]a' \tag{4.57}$$

contributing to the cross sections $d\sigma(lN \to lHjX')$, the gluon initiated ones with $a = a' = g$ as well as the light quark (antiquark) initiated ones with $a = a' = q = u, d, s$ ($a = a' = \bar{q} = \bar{u}, \bar{d}, \bar{s}$). The corresponding short distance coefficients $d\sigma(la \to lc\bar{c}[n]a)$ occuring in equation (4.3) for $d\sigma(lN \to lHjX')$ are calculated at leading order from the Feynman diagrams shown in Fig.4.2 for $a = q = u, d, s$ and in Fig.4.3 for $a = g$. The

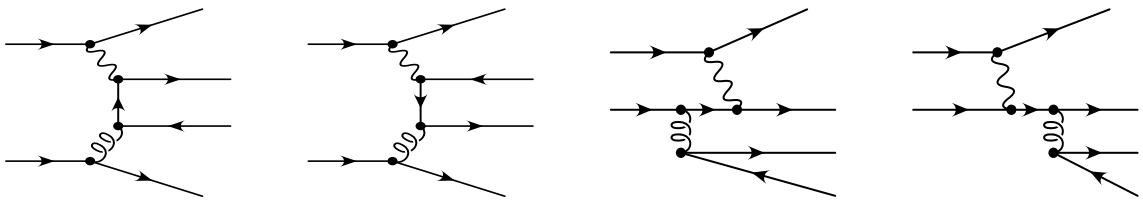

Figure 4.2: Feynman diagrams for the partonic subprocesses $lq \to lc\bar{c}[n]q$; q=u,d,s.

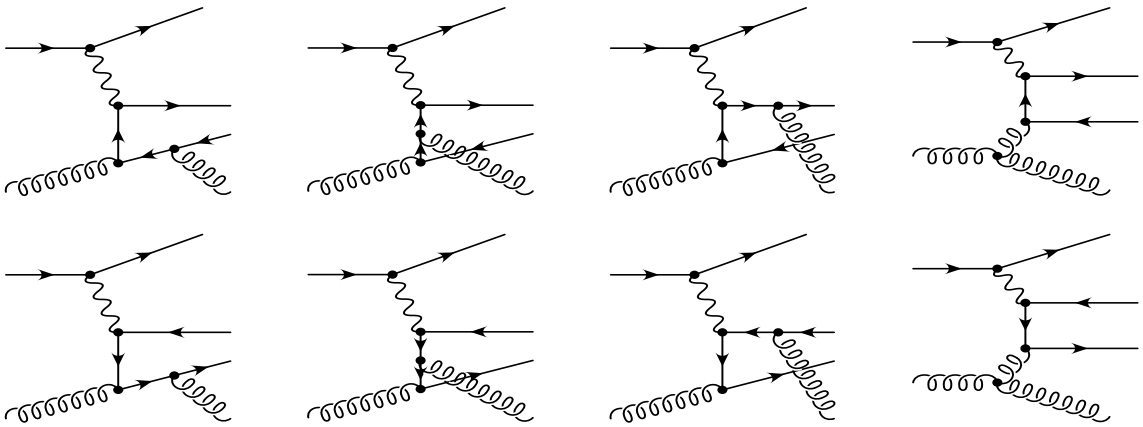

Figure 4.3: Feynman diagrams for the partonic subprocesses $lg \to lc\bar{c}[n]g$.

diagrams for $a = \bar{q} = \bar{u}, \bar{d}, \bar{s}$ agree with those for $a = q = u, d, s$ up to a reversal of the

arrow direction of the light quark line. As in section 4.1.1 the gauge boson B, exchanged between the lepton and the light or the heavy quark, is a photon if $l = e^-$ and a Z boson if $l = \nu_e$. The only difference between the corresponding total amplitudes $\mathcal{M}_{la}[n]$ for $l = e^-$ and those for $l = \nu_e$ furtheron consists in the deviating gauge boson masses and the different structure of the gauge boson fermion couplings Γ^μ_{Bff} given in (4.9). We enlarge the set of kinematical invariants defined in (4.14)-(4.19) by

$$\hat{t} = (p - p')^2 \ , \tag{4.58}$$

$$\hat{u} = (q_B - p')^2 \ . \tag{4.59}$$

Thereby p' denotes the momentum of the outgoing parton, while the other momenta are denoted as in section 4.1.1. Decomposing $\mathcal{M}_{la}[n]$ into a hadronic part $h^\mu_{la}[n]$ and a remaining leptonic one, exactly as before,

$$\mathcal{M}_{la}[n] = \frac{G}{m_B^2 + Q^2} \bar{u}_{r'}(k') \Gamma^\mu_{Bll} u_r(k) h_{la\,\mu}[n] \ , \tag{4.60}$$

$d\sigma(la \to lc\bar{c}[n]a)$ takes the form

$$d\sigma(la \to lc\bar{c}[n]a) = \frac{1}{2\xi S} dPS_3(p + k; P, k', p') \frac{G^2}{(m_B^2 + Q^2)^2} l_l^{\mu\nu} H_{la\,\mu\nu}[n] \ . \tag{4.61}$$

Thereby, $l_l^{\mu\nu}$ is the lepton tensor given in (4.24) and the hadron tensor is defined by

$$H_{la\,\mu\nu}[n] = \frac{1}{N_{\rm col} N_{\rm pol}} \overline{\sum} h^\dagger_{la\,\mu}[n] h_{la\,\nu}[n] \tag{4.62}$$

with $N_{\rm col}$, $N_{\rm pol}$, $\overline{\sum}$ as in (3.17). In case of $a = g$ the nonabelian gauge structure of QCD manifests itself through the occurence of diagrams containing the triple gluon vertex. Therefore, in calculating $H^{\mu\nu}_{lg}[n]$ the gluon polarization sum $\sum_{\lambda=1}^2 \epsilon^{\mu *}_\lambda(p_g) \epsilon^\nu_\lambda(p_g)$ with $p_g = p$ or $p_g = p'$ cannot be replaced anylonger by $-g^{\mu\nu}$, as this replacement corresponds to an inclusion of the unphysical scalar and longitudinal gluon polarization degrees of freedom, whose contributions only vanish for photon like gluons. Instead, we have to use

$$\sum_{\lambda=1}^2 \epsilon^{\mu *}_\lambda(p_g) \epsilon^\mu_\lambda(p_g) = -g^{\mu\nu} + \frac{p_g^\mu n^\nu + p_g^\nu n^\mu}{p_g n} \ , \tag{4.63}$$

where n^μ is an arbitrary lightlike four momentum. (4.63) is obtained from

$$\sum_{\lambda=1}^2 \epsilon^{\mu *}_\lambda(p_g) \ \epsilon^\nu_\lambda(p_g) = a_1 g^{\mu\nu} + a_2 p_g^\mu p_g^\nu + a_3 n^\mu n^\nu + a_4 p_g^\mu n^\nu + a_5 p_g^\nu n^\mu \tag{4.64}$$

as the most general ansatz for $\sum_{\lambda=1}^2 \epsilon^{\mu *}_\lambda(p_g) \ \epsilon^\nu_\lambda(p_g)$ by employing the transversality conditions

$$p_g \epsilon_\lambda(g) = n \epsilon_\lambda(g) = 0 \tag{4.65}$$

and the normalization condition

$$\sum_{\lambda=1}^{2} \epsilon_{\lambda}^{\mu *}(p_g)\ \epsilon_{\lambda\mu}(p_g) = -2 \tag{4.66}$$

to determine the unknowns a_1, a_2, ...,a_6. The term $(p_g^{\mu} n^{\nu} + p_g^{\nu} n^{\mu})/p_g n$ obviously can be understood to cancel the contributions of the unphysical gluon polarization degrees of freedom contained in $-g^{\mu\nu}$. For the sake of computational simplification we apply an equivalent alternative method, which is based on the Slavnov Taylor identities. Here, in calculating $\sum_{\lambda=1}^{2} |\mathcal{M}_{lg}[n]|^2$ the polarization sum $\sum_{\lambda=1}^{2} \epsilon_{\lambda}^{\mu *}(p_g)\epsilon_{\lambda}^{\nu}(p_g)$ is furtheron replaced by $-g^{\mu\nu}$, and in order to compensate for the unphysical polarization degrees of freedom twice the absolute square of the amplitude $\mathcal{M}_{l\tilde{g}}[n]$, which belongs to the diagrams containing the triple gluon vertex with the in and outgoing gluon replaced by Fadeev Popov ghosts $\tilde{g}$, is subtracted

$$\sum_{\lambda=1}^{2} |\mathcal{M}_{lg}[n]|^2 = \sum_{\lambda=1}^{2} |\mathcal{M}_{lg}[n]|^2 \Big|_{\sum_{\lambda=1}^{2} \epsilon_{\lambda}^{\mu *}(p_g)\epsilon_{\lambda}^{\nu}(p_g) \to -g^{\mu\nu}} - 2\,|\mathcal{M}_{l\tilde{g}}[n]|^2 \ . \tag{4.67}$$

The Feynman diagrams corresponding to the $\mathcal{M}_{l\tilde{g}}[n]$ are shown in Fig.4.4.

Figure 4.4: Feynman diagrams for the ghost contributions to the partonic subprocesses $lg \to lc\bar{c}[n]g$.

For later purposes we elaborate the phase space measure $dPS_3(p+k; P, k', p')$ for the more general case, that ${p'}^2 = {m'}^2 \geq 0$. Performing the integration over $\vec{P}$ we obtain

$$dPS_3(p+k; P, k', p') = \frac{d^3\vec{k}'}{(2\pi)^2 2k'^0} \frac{d^3\vec{p}'}{(2\pi)^3 2p'^0} \frac{1}{2P^0} \delta(p^0 + q_B^0 - P^0 - p'^0) \ . \tag{4.68}$$

$d^3\vec{k}'/(2\pi)^2 2k'^0$ has already been evaluated to be $dQ^2 dy/8\pi$, see (4.30), (4.33). Furthermore, it follows in exactly the same way as was derived (4.29)

$$\frac{1}{2P^0}\delta(p^0 + q_B^0 - P^0 - p'^0) = \delta(\hat{s} + \hat{t} + \hat{u} - M^2 - {m'}^2 + Q^2) \ . \tag{4.69}$$

For a further evaluation of $d^3\vec{p}'/(2\pi)^3 2p'^0$ we specify the center of mass frame of the gauge boson B and the ingoing parton and express $d^3\vec{p}'$ in polar coordinates. Performing the

integration over the azimuthal angle of the outgoing parton, which for symmetry reasons results in a factor 2π, we find

$$\frac{d^3\vec{p}'}{(2\pi)^3 2p'^0} = \frac{|\vec{p}'|^2 \, d\,|\vec{p}'| \, d\cos\theta}{(2\pi)^2 2p'^0} \ , \tag{4.70}$$

where $\theta = \angle(\vec{p}, \vec{p}')$ is the polar angle of the outgoing lepton. Noting, that $\vec{p} + \vec{q}_B = 0$ together with $p^2 = 0$ and $q_B^2 = -Q^2$ implies $p^0 = (\hat{s} + Q^2)/2\sqrt{\hat{s}}$ and $q_B^0 = (\hat{s} - Q^2)/2\sqrt{\hat{s}}$, we obtain

$$\hat{t} = m'^2 - \frac{\hat{s} + Q^2}{\sqrt{\hat{s}}} \left(\sqrt{m'^2 + \vec{p}'^2} - |\vec{p}'| \cos\theta \right) \tag{4.71}$$

$$\hat{u} = m'^2 - Q^2 - \frac{\hat{s} + Q^2}{\sqrt{\hat{s}}} \left(\frac{\hat{s} - Q^2}{\hat{s} + Q^2} \sqrt{m'^2 + \vec{p}'^2} + |\vec{p}'| \cos\theta \right) \tag{4.72}$$

and consequently

$$\frac{|\vec{p}'|^2 \, d\,|\vec{p}'| \, d\cos\theta}{p'^0} = \frac{d\hat{t} d\hat{u}}{2(\hat{s} + Q^2)} = \frac{d\hat{t} d\hat{u}}{2\xi y S} \ , \tag{4.73}$$

that is

$$\frac{d^3\vec{p}'}{(2\pi)^3 2p'^0} = \frac{d\hat{t} d\hat{u}}{16\pi^2 \xi y S} \ . \tag{4.74}$$

We therefore end up with

$$dPS_3(p + k; P, k', p') = \frac{dQ^2 dy d\hat{t} d\hat{u}}{128\pi^3 \xi y S} \delta(\hat{s} + \hat{t} + \hat{u} - M^2 - m'^2 + Q^2) \ , \tag{4.75}$$

where $m' = 0$ in the here considered processes. Treating the outgoing lepton in exactly the same way as in section 4.1.1 and performing the integration over $\hat{u}$, (4.61) becomes

$$\frac{d\sigma}{dQ^2 dy d\hat{t}}(la \to lc\bar{c}[n]a) = \frac{G^2}{256\pi^3 y \xi^2 S^2 (m_B^2 + Q^2)^2} L_l^{\mu\nu} H_{la\,\mu\nu}[n] \tag{4.76}$$

with the integrated lepton tensor $L_l^{\mu\nu}$ given in (4.38). We present our final results for the short distance coefficients in the form

$$\frac{d\sigma}{dQ^2 dy d\hat{t}}(la \to lc\bar{c}[n]a) = F_{la}[n] \left[\frac{1 + (1-y)^2}{y} T_{la}[n] - \frac{4(1-y)}{y} L_{la}[n] + (2-y) A_{la}[n] \right] \ , \tag{4.77}$$

where the $F_{la}[n]$, $T_{la}[n]$, $L_{la}[n]$ and $A_{la}[n]$ are functions of $\hat{s}$, $\hat{t}$, $\hat{u}(\equiv M^2 - Q^2 - \hat{s} - \hat{t})$ and Q^2, which are listed in appendix A.1. Thereby, we combined the results for $n = {}^3P_J^{(8)}$ with $J = 0, 1, 2$, exploiting the heavy quark spin symmetry relations (2.103), (2.104). The $A_{e^-a}[n]$ all vanish, as $L_{e^-}^{\mu\nu}$ has no axial part. In analogous way as was derived (4.47) we find for the $d\sigma(e^-a \to c\bar{c}[n]a)$ in the limit $Q^2 \to 0$

$$\left. \frac{d\sigma}{dQ^2 dy d\hat{t}}(la \to lc\bar{c}[n]a) \right|_{Q^2 \to 0} = \frac{\alpha}{2\pi Q^2} \frac{1 + (1-y)^2}{y} \frac{d\sigma}{d\hat{t}}(\gamma a \to c\bar{c}[n]a) \ , \tag{4.78}$$

where the $\sigma(\gamma a \to c\bar{c}[n]a)$ are the short distance coefficients for H photoproduction. Making use of (4.78), we reproduce, as an important test of our analytical results, the well known short distance coefficients corresponding to the color singlet [6] and the color octet [21, 25] partonic subprocesses of H photoproduction. We now compare our analytical results for electroproduction ($l = e^-$) with the literature. Formulae for the color singlet partonic subprocesses $e^-g \to e^-c\bar{c}\left[{}^3S_1^{(1)}\right]g$ may be found in Refs.[32, 41, 42, 43, 44]. In Ref.[32], also formulae for the color octet partonic subprocesses $e^-a \to e^-c\bar{c}[n]a$ with $a = g, q, \bar{q}$ and $n = {}^1S_0^{(8)}, {}^3S_1^{(8)}, {}^3P_J^{(8)}$ are listed. We agree with the result for $e^-g \to e^-c\bar{c}\left[{}^1S_0^{(8)}\right]g$ [32], but we disagree with all the other results. In particular, the results of Refs.[41, 43] and the residual results of Ref.[32] fail to reproduce the well established formulae of Refs.[6, 21, 25] in the photoproduction limit. It should be also remarked, that (A21) and (A35)-(A37) of Ref.[32] suffer from mass dimensional inconsistencies. Furthermore, we only find agreement with the result in equation (4) of Ref.[42] if we flip the overall sign of $L_{e^-g}\left[{}^3S_1^{(1)}\right]$ in (4.77). However, this causes $d\sigma(e^-g \to e^-c\bar{c}\left[{}^3S_1^{(1)}\right]g)$ to turn negative in certain regions of phase space, for instance at $y = 0.5$, $Q^2 = 25$ GeV^2, $\hat{s} = 100$ GeV^2 and $\hat{t} = -10$ GeV^2. Similarly, we only agree with the result in (2.49) of Ref.[44] if we include an overall factor of $4\pi\alpha$ on the right hand side of (4.77) and halve $L_{e^-g}\left[{}^3S_1^{(1)}\right]$.

The short distance coefficients $d\sigma(la \to lc\bar{c}[n]a)$ with $n = {}^1S_0^{(8)}, {}^3P_J^{(8)}$ exhibit collinear divergences in the limit $\hat{t} \to 0$. According to the factorization theorem of the QCD improved parton model the limiting expressions must coincide with the $d\sigma(lg \to lc\bar{c}[n])$ multiplied with the space like $a \to g$ splitting functions, where the $d\sigma(lg \to lc\bar{c}[n])$ can be read off (4.48) and (4.52), respectively. This provides another nontrivial test, which is satisfied by our analytical results, and among other things, this fixes the overall factor of the $L_{la}[n]$. For a more thorough discussion of this subject it is referred to chapter 5.

From (4.3) we find for the hadronic cross section

$$\frac{d\sigma}{dQ^2dy}(lN \to lHjX') = \int_{(M^2+Q^2)/(yS)}^1 d\xi \int_{-(\hat{s}+Q^2)(\hat{s}-M^2)/\hat{s}}^0 d\hat{t} \sum_a F_N^a(\xi, \mu_F^2) \sum_n \frac{d\sigma}{dQ^2dyd\hat{t}}(la \to lc\bar{c}[n]a) \left\langle O^H[n] \right\rangle \ , \quad (4.79)$$

where we have included the maximum boundaries of the integrations over ξ and $\hat{t}$, and the $\frac{d\sigma}{dQ^2dy}(la \to lc\bar{c}[n]a)$ are given in (4.77). The kinematically allowed ranges of S, Q^2 and y are furtheron described by (4.54). The derivation of the upper bound of y and the lower bound of Q^2 doesn't change with respect to that given in section 4.1.1, as (4.31), (4.32) remain valid. The upper bound of ξ is trivial. The upper bound of Q^2 and the lower bounds of S, y and ξ follow from $\xi yS - Q^2 = (p + q_B)^2 = (P + p')^2 \geq M^2$, noting, that p' may vanish. Finally, in order to derive the range of $\hat{t}$, we specify the center of mass frame of the gauge boson B and the ingoing parton a, where $\vec{p} + \vec{q}_B = \vec{P} + \vec{p}' = 0$, implying $p^0 = (\hat{s} + Q^2)/2\sqrt{\hat{s}}$, $p'^0 = (\hat{s} - M^2)/2\sqrt{\hat{s}}$ and therefore $\hat{t} = -2p^0p'^0(1 - \cos\theta) = -(\hat{s} + Q^2)(\hat{s} - M^2)(1 - \cos\theta)/2\hat{s}$ with $\theta = \angle(\vec{p}, \vec{p}')$. As $\cos\theta$ may assume its minimum value -1 as well as its maximum value 1, this proves $-(\hat{s} + Q^2)(\hat{s} - M^2)/\hat{s} \leq \hat{t} \leq 0$.

Note, that due to lepton universality, the cross section does not change if the scattered electron (electron neutrino) is replaced by a muon (muon neutrino) or a tauon (tauon neutrino). There is also no change, if the electron is replaced by an anti electron, anti muon or anti tauon. In case, that the electron neutrino is replaced by an anti electron neutrino, anti muon neutrino or anti tauon neutrino the axial part $A_{la}[n]$ in (4.77) changes its overall sign.

In order to avoid the collinear divergences in (4.79), values of $\hat{t}$ near to zero must be excluded from the integration by applying appropriate, experimentally controllable kinematical cuts. Let's consider the inelasticity variable z, defined in (4.19). z here satisfies the equation

$$z = 1 + \frac{\hat{t}}{\xi y S} \ , \tag{4.80}$$

and from the kinematical ranges of ξ, y, and $\hat{t}$, given above, it follows

$$\frac{M^2}{S} \leq z \leq 1 \tag{4.81}$$

for the kinematically allowed values of z. Due to (4.80) $z < 1$ implies $\hat{t} < 0$. Therefore, a cut on z according to $z < z_{\max}$ with $M^2/S < z_{\max} < 1$ prevents us from collinear divergences, and leads at the same time, for $z_{\max}$ not too close to 1, to an effective suppression of the diffractive background.

4.1.3 J/ψ plus jet inclusive production in lN charged current DIS

Jet associated J/ψ inclusive production can also proceed through the charged current interaction. We will in the following consider the process

$$\nu_e N \to e^- H j X' \ . \tag{4.82}$$

The involved partonic subprocesses are

$$\nu_e a \to e^- c\bar{c}[n] a' \tag{4.83}$$

with $(a, a') = (\bar{u}, \bar{d}), (d, u), (s, c)$. The Feynman diagrams relevant for calculating the corresponding short distance coefficients $d\sigma(\nu_e a \to e^- c\bar{c}[n] a')$ are shown in Fig.4.5 for $(a, a') = (\bar{u}, \bar{d})$, in Fig.4.6 for $(a, a') = (d, u)$ and in Fig.4.7 for $(a, a') = (s, c)$. For the sake of clarification, we labelled each external leg of the diagrams with the symbol of the respective particle together with the corresponding four momentum in brackets behind, whereby the momenta as well as the kinematical invariants are defined as in the sections before. The gauge boson B, exchanged between the lepton and the quark line, is now a W boson, giving rise to a change of flavour at the respective vertices. In the four diagrams in Fig.4.7, there are two c quarks in the final state. The c, which combines with the $\bar{c}$ to the $c\bar{c}[n]$ state, is of course the one, which carries the momentum $\frac{P}{2} + q$. Let us denote the

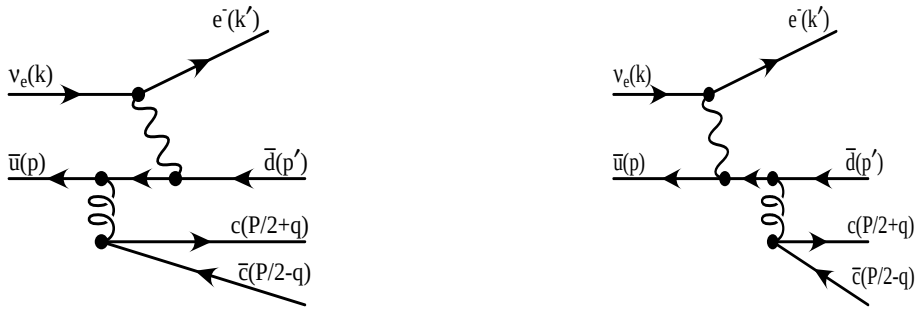

Figure 4.5: Feynman diagrams for the partonic subprocesses $\nu_e \bar{u} \to e^- c\bar{c}[n]\bar{d}$.

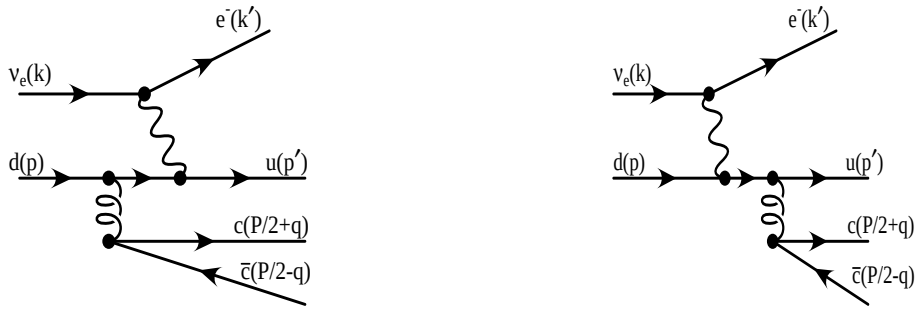

Figure 4.6: Feynman diagrams for the partonic subprocesses $\nu_e d \to e^- c\bar{c}[n]u$.

total amplitudes, belonging to the respective set of diagrams, by $\mathcal{M}_{\nu_e a}[n]$ with $a = \bar{u}, d, s$. Note, that for $a = s$ the third diagram in Fig.4.7 is obtained from the first and the fourth from the second by permuting the both outgoing c quarks. Therefore, as the c quarks obey Fermi Dirac statistics, in constructing $\mathcal{M}_{\nu_e s}[n]$ a relative minus sign between the single amplitudes corresponding to the first two and those corresponding to the second two diagrams is taken into account. As before, we decompose the $\mathcal{M}_{\nu_e a}[n]$ into a hadronic part $h^{\mu}_{\nu_e a}[n]$ and a remaining leptonic one, according to

$$\mathcal{M}_{\nu_e a}[n] = \frac{g'}{m_W^2 + Q^2} \bar{u}_{r'}(k') \Gamma^{\mu}_{W \nu_e e^-} u_r(k) h_{\nu_e a\, \mu}[n] \tag{4.84}$$

with $g' = 2^{\frac{3}{4}} G_F^{\frac{1}{2}} m_W$, $m_W = m_Z \cos\theta_W$ being the W mass, and the W boson fermion fermion vertex given by

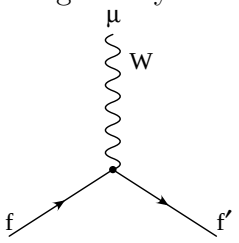

$$\leftrightarrow \qquad -ig'\, \Gamma^{\mu}_{W f f'} = -ig' \gamma^{\mu} \frac{1 - \gamma^5}{2} \ . \tag{4.85}$$

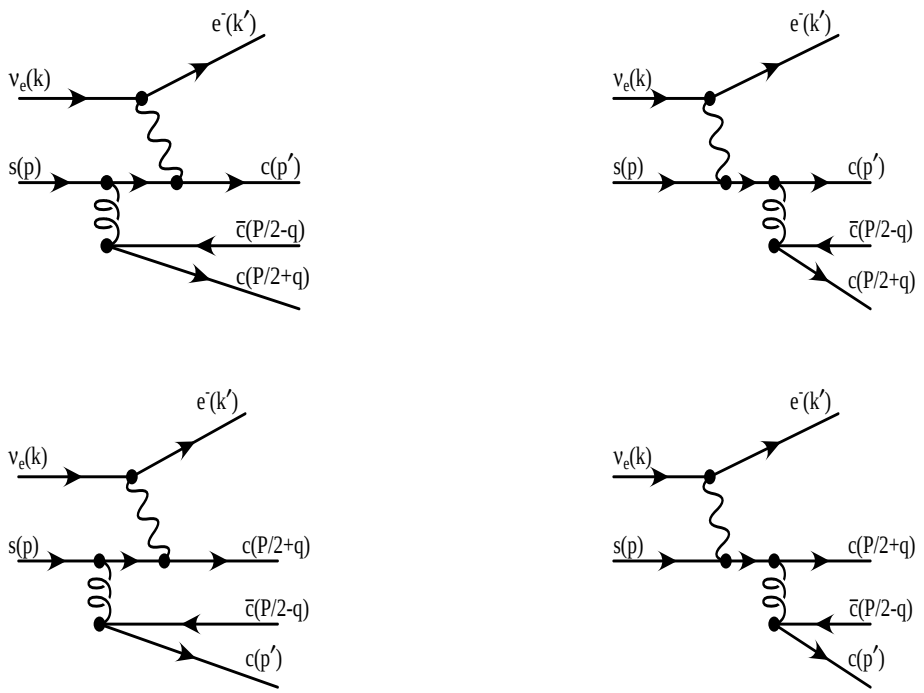

Figure 4.7: Feynman diagrams for the partonic subprocesses $\nu_e s \to e^- c\bar{c}[n]c$.

For $(f, f') = (d, u), (s, c)$ $\Gamma^{\mu}_{Wff'}$ principally contains as an additional factor the diagonal Cabbibo-Kobayashi-Maskawa mixing matrix element V_{ud} or V_{cs}, respectively. Here, as a good approximation, we put V_{ud} and V_{cs} equal to one. Performing the same steps as in the sections before, and using (4.75) for the phase space measure with

$$m' = \begin{cases} 0 & \text{if } a' = \bar{d}, u \\ m & \text{if } a' = c \end{cases} \quad , \tag{4.86}$$

where $m = M/2$ is the charm quark mass, we find from (4.84) for the short distance coefficients

$$\frac{d\sigma}{dQ^2 dy d\hat{t}}(\nu_e a \to e^- c\bar{c}[n]a') = \frac{g'^2}{256\pi^3 y \xi^2 S^2 (m_W^2 + Q^2)^2} L^{\mu\nu}_{\nu_e} H_{\nu_e a\,\mu\nu}[n] \ . \tag{4.87}$$

Thereby, the integrated lepton tensor $L^{\mu\nu}_{\nu_e}$ is given in (4.38) and the hadron tensor $H^{\mu\nu}_{\nu_e a}[n]$ is defined as in (4.26),(4.62). We again present our final results for the short distance coefficients in the form

$$\frac{d\sigma}{dQ^2 dy d\hat{t}}(\nu_e a \to e^- c\bar{c}[n]a') = F_{\nu_e a}[n] \left[\frac{1 + (1-y)^2}{y} T_{\nu_e a}[n] - \frac{4(1-y)}{y} L_{\nu_e a}[n] \right.$$
$$\left. + (2 - y) A_{\nu_e a}[n] \right] \ , \tag{4.88}$$

where the $F_{\nu_e a}[n]$, $T_{\nu_e a}[n]$, $L_{\nu_e a}[n]$ and $A_{\nu_e a}[n]$ are functions of $\hat{s}$, $\hat{t}$, $\hat{u}(\equiv M^2+m^2-Q^2-\hat{s}-\hat{t})$ and Q^2, which are listed in appendix A.2. Thereby, we again combined the results for $n = {}^3P_J^{(8)}$ with $J = 0, 1, 2$, exploiting the heavy quark spin symmetry relations (2.103), (2.104). From (4.3) we find for the hadronic cross section

$$\frac{d\sigma}{dQ^2dy}(\nu_e a \to e^- HjX') = \sum_a \int_{\xi_{min}}^{\xi_{max}} d\xi \int_{\hat{t}_{min}}^{\hat{t}_{max}} d\hat{t} F_N^a(\xi, \mu_F^2) \times \sum_n \frac{d\sigma}{dQ^2dyd\hat{t}}(\nu_e a \to e^- c\bar{c}[n]a') \left\langle O^H[n] \right\rangle \ , \tag{4.89}$$

where the maximum boundaries of the integrations over ξ and $\hat{t}$ are now given by

$$\xi_{min} = \frac{(M+m')^2+Q^2}{yS} \ , \tag{4.90}$$

$$\xi_{max} = 1 \ , \tag{4.91}$$

$$\hat{t}_{min} = \frac{2m'^2\hat{s} - (\hat{s}+Q^2)\left(\hat{s} - M^2 + m'^2 + \sqrt{(\hat{s}-M^2+m'^2)^2 - 4m'^2\hat{s}}\right)}{2\hat{s}} \ , \tag{4.92}$$

$$\hat{t}_{max} = \frac{2m'^2\hat{s} - (\hat{s}+Q^2)\left(\hat{s} - M^2 + m'^2 - \sqrt{(\hat{s}-M^2+m'^2)^2 - 4m'^2\hat{s}}\right)}{2\hat{s}} \ . \tag{4.93}$$

The kinematical allowed ranges of S, Q^2 and y read

$$S \geq (M+m')^2 \quad , \quad 0 \leq Q^2 \leq S - (M+m')^2 \quad , \quad \frac{(M+m')^2+Q^2}{S} \leq y \leq 1 \quad . \tag{4.94}$$

The ranges of ξ, $\hat{t}$, S, Q^2 and y given in (4.90)-(4.94) are obtained in the same way as in section 4.1.3, noting, that, as the only changes, the unequality $\xi yS - Q^2 \geq M^2$ is now replaced by $\xi yS - Q^2 = (p+q_W)^2 = (P+p')^2 \geq (M+m')^2$ with the lower bound being assumed for $\vec{P} = \vec{p}' = 0$, and that $\hat{t}$ in the center of mass frame of the W boson and the ingoing parton a now reads $\hat{t} = [2m'^2\hat{s} - (\hat{s}+Q^2)(\hat{s} - M^2 + m'^2 - \sqrt{(\hat{s}-M^2+m'^2)^2 - 4m'^2\hat{s}\cos\theta})]/2\hat{s}$ with $\theta = \angle(\vec{p}, \vec{p}')$. The latter formula for $\hat{t}$ follows from (4.71), noting, that $\vec{P} + \vec{p}' = 0$ implies $p'^0 = \sqrt{\vec{p}'^2 + m'^2} = (\hat{s} - M^2 + m'^2)/2\sqrt{\hat{s}}$. It should be remarked, that the cross section in (4.89) is free of infrared and collinear divergences, so that the integration over the whole phase space is well defined.

Formulae analogous to (4.89) also hold for the cross section $\frac{d\sigma}{dQ^2dy}(\bar{\nu}_e N \to e^+ HjX')$ of the process $\bar{\nu}_e N \to e^+ HjX'$. Due to charge conjugation symmetry the corresponding short distance coefficients $\frac{d\sigma}{dQ^2dyd\hat{t}}(\bar{\nu}_e a \to e^+ c\bar{c}[n]a')$ with $(a, a') = (u, d), (\bar{d}, \bar{u}), (\bar{s}, \bar{c})$ exactly agree with the $\frac{d\sigma}{dQ^2dyd\hat{t}}(\nu_e a \to e^- c\bar{c}[n]a')$ given in (4.88) with $(a, a') = (\bar{u}, \bar{d}), (d, u), (s, c)$. Furthermore, due to lepton universality, the respective cross sections do not change, if the ingoing electron neutrino (anti electron neutrino) and the outgoing electron (positron) are replaced by an ingoing muon neutrino (anti muon neutrino) and an outgoing muon (antimuon) or an ingoing tauon neutrino (anti tauon neutrino) and an outgoing tauon (anti tauon).

Experimentally, it is possible to decide, if the produced jet contains a c ($\bar{c}$) or if it doesn't. The corresponding cross sections are then obtained from (4.89) or the analogous equations by restricting the summation to $a = s(\bar{s})$ or $a = \bar{u}, d(u, \bar{d})$, respectively. As in the u, $\bar{u}$, d and $\bar{d}$ quark initiated partonic subprocesses the $c\bar{c}$ pair, as a consequence of color and angular momentum conservation, can only be produced in a ${}^3S_1^{(8)}$ state, those processes, where the jet doesn't contain a c or $\bar{c}$ quark, provide in principle an excellent test of the color octet mechanism.

4.2 Predictions for H1 at DESY HERA and CHORUS and NOMAD at CERN

In the following we will make quantitative predictions for the H1 experiment at DESY HERA and for the CHORUS and NOMAD experiments at CERN. In the HERA laboratory system electrons or, depending on the operation modus, positrons with energy E_e and protons with energy E_p coming from opposite directions are brought to collision. The CHORUS and NOMAD experiments are fixed target experiments, in which a lead or an iron target, respectively, is exposed to the wide band neutrino beam produced by protons from the CERN Super Proton Synchrotron (SPS). Concerning the H1 experiment, we will focus on direct J/ψ plus jet inclusive production in $e^{\pm}p$ DIS, while in case of the CHORUS and NOMAD experiments, we discuss single and jet associated prompt J/ψ inclusive production in νN neutral and, of course, only jet associated prompt J/ψ inclusive production in νN charged current DIS. Of great interest are, among others, the differential distributions with respect to the J/ψ transverse momentum P_T and the J/ψ rapidity $y_{J/\psi}$ in the center of mass system of the gauge boson B and the nucleon N (BN CMS) as well as in the respective laboratory frame. Let's concentrate on the kinematical situation of jet associated J/ψ production. In order to derive expressions for P_T and $y_{J/\psi}$ in the BN CMS we first specify the center of mass system of the gauge boson B and the ingoing parton a (Ba CMS). In the following quantities, which refer to the BN CMS, are indicated with an asterisk, while quantities, which refer to the Ba CMS, are indicated with a tilde. In the Ba CMS, we have

$$\left|\tilde{\vec{P}}\right| = \frac{\sqrt{(\hat{s} - M^2 + m'^2)^2 - 4\hat{s}m'^2}}{2\sqrt{\hat{s}}} \quad , \; \tilde{P}^0 = \frac{\hat{s} + M^2 - m'^2}{2\sqrt{\hat{s}}} \; ,$$
$$\tilde{P}^3 = \frac{2\hat{s}(\hat{t} - m'^2) + (\hat{s} + Q^2)(\hat{s} - M^2 + m'^2)}{2\sqrt{\hat{s}}(\hat{s} + Q^2)} \; , \tag{4.95}$$

where $m'^2 = p'^2$, and the coordinate axes have been chosen in such a way, that the z direction coincides with the direction of the momentum of the gauge boson B. The latter equation for $\tilde{P}^3$ is obtained from (4.71), using $\sqrt{m'^2 + \vec{p}'^2} \equiv p'^0 = (\hat{s} - M^2 + m'^2)/2\sqrt{\hat{s}}$ and $|\vec{p}'| \cos\theta = \left|\vec{P}\right| \cos\theta = P^3$. As the BN CMS and the Ba CMS are related to each other by a lorentz boost in longitudinal direction, under which transverse momentum components

are left unchanged, we have $P_T^* = \tilde{P}_T = \sqrt{\vec{\tilde{P}}^2 - \tilde{P^3}^2}$, yielding

$$P_T^* = \frac{\sqrt{\hat{t}(M^2Q^2 + \hat{s}\hat{u}) - m'^2(2M^2Q^2 + \hat{s}M^2 - Q^2\hat{u})}}{\hat{s} + Q^2} \ . \tag{4.96}$$

For $\tilde{y}_{J/\psi}$ it follows

$$\tilde{y}_{J/\psi} = \frac{1}{2}\ln\frac{\tilde{P}^0 + \tilde{P}^3}{\tilde{P}^0 - \tilde{P}^3} = \frac{1}{2}\ln\frac{\hat{s}(M^2 - \hat{u})}{\hat{s}(M^2 - \hat{t}) + Q^2(M^2 - m'^2)} \ . \tag{4.97}$$

Noting, that P_N and P in the Ba CMS and in the BN CMS are given by

$$\tilde{P}_N = \frac{W^2 + Q^2}{2\sqrt{\hat{s}}}\begin{pmatrix} 1 \\ 0 \\ 0 \\ -1 \end{pmatrix} \quad , \quad \tilde{P} = \begin{pmatrix} \widetilde{M}_T \cosh\tilde{y}_{J/\psi} \\ \tilde{P}^1 \\ \tilde{P}^2 \\ \widetilde{M}_T \sinh\tilde{y}_{J/\psi} \end{pmatrix} \tag{4.98}$$

and

$$P_N^* = \frac{W^2 + Q^2}{2W}\begin{pmatrix} 1 \\ 0 \\ 0 \\ -1 \end{pmatrix} \quad , \quad P^* = \begin{pmatrix} M_T^* \cosh y_{J/\psi}^* \\ P^{1*} \\ P^{2*} \\ M_T^* \sinh y_{J/\psi}^* \end{pmatrix} \ , \tag{4.99}$$

respectively, with $\widetilde{M}_T = \sqrt{M^2 + \tilde{P}_T^2} = \sqrt{M^2 + P_T^{*2}} = M_T^*$, and exploiting the equation $\tilde{P}_N\tilde{P} = P_N^*P^*$, we find for $y_{J/\psi}^*$

$$y_{J/\psi}^* = \frac{1}{2}\ln\frac{\hat{s}(M^2 - \hat{u})}{\hat{s}(M^2 - \hat{t}) + Q^2(M^2 - m'^2)} + \frac{1}{2}\ln\frac{W^2}{\hat{s}} \ . \tag{4.100}$$

As is clear from the derivation, $y_{J/\psi}^*$ is taken to be positive in the direction of the three momentum of the gauge boson B. We now derive expressions for P_T and $y_{J/\psi}$ in the laboratory frame of the H1 experiment and in that of the NOMAD and CHORUS experiments, which coincides with the nucleon rest frame. Choosing a suitable coordinate system in the BN CMS, we have

$$k^* = \frac{S - Q^2}{2W}\begin{pmatrix} 1 \\ \sin\psi^* \\ 0 \\ \cos\psi^* \end{pmatrix} \quad , \quad k'^* = \frac{S - W^2}{2W}\begin{pmatrix} 1 \\ \sin\theta^* \\ 0 \\ \cos\theta^* \end{pmatrix} \ ,$$

$$q_B^* = \frac{1}{2W}\begin{pmatrix} W^2 - Q^2 \\ 0 \\ 0 \\ W^2 + Q^2 \end{pmatrix} \quad , \quad P_N^* = \frac{W^2 + Q^2}{2W}\begin{pmatrix} 1 \\ 0 \\ 0 \\ -1 \end{pmatrix} \ ,$$

$$P^* = \begin{pmatrix} M_T^* \cosh y_{J/\psi}^* \\ P_T^* \cos\phi^* \\ P_T^* \sin\phi^* \\ M_T^* \sinh y_{J/\psi}^* \end{pmatrix} \ , \tag{4.101}$$

where

$$\cos\psi^* = \frac{2SW^2}{(S-Q^2)(W^2+Q^2)} - 1 \quad , \quad \cos\theta^* = 1 - \frac{2SQ^2}{(S-W^2)(W^2+Q^2)} \; . \tag{4.102}$$

The equations for q_B^* and P_N^* are clear, they immediately follow from $\vec{q}_B^* + \vec{P}_N^* = 0$, if the coordinate system is chosen in such a way, that the z axis is oriented in the direction of $\vec{q}_B^*$. In deriving k^* and k'^*, we use, that $k^{*^2} = k'^{*^2} = 0$ allows us to write $k^* = \alpha(1 \;\; \sin\psi^* \;\; 0 \;\; \cos\psi^*)$ and $k'^* = \alpha'(1 \;\; \sin\theta^* \;\; 0 \;\; \cos\theta^*)$, noting, that the vanishing of the y components can always be achieved by an appropriate rotation around the z axis. We then determine α and $\cos\psi^*$ from the equations $-Q^2/2 = k^* q_B^* = \alpha[W^2 - Q^2 - \cos\psi^*(W^2+Q^2)]/2W$ and $S/2 = k^* P_N^* = \alpha(W^2+Q^2)(1+\cos\psi^*)/2W$, α' from the equation $\alpha - \alpha' = k^{*0} - k'^{*0} = q_B^{*0} = (W^2-Q^2)/2W$ and $\cos\theta^*$ finally from the equation $(S-Q^2)\cos\psi^*/2W - (S-W^2)\cos\theta^*/2W = k^{*3} - k'^{*3} = q_B^{*3} = (W^2+Q^2)/2W$. On the other hand, we have in the HERA laboratory frame

$$\begin{aligned}
k &= E_e \begin{pmatrix} 1 \\ 0 \\ 0 \\ 1 \end{pmatrix} \quad , \quad k' = E'_e \begin{pmatrix} 1 \\ \sin\theta \\ 0 \\ \cos\theta \end{pmatrix} \; , \\
q_B &= \begin{pmatrix} q_B^0 \\ -|\vec{q}_B|\sin\psi \\ 0 \\ |\vec{q}_B|\cos\psi \end{pmatrix} \quad , \quad P_N = E_p \begin{pmatrix} 1 \\ 0 \\ 0 \\ -1 \end{pmatrix} \; , \\
P &= \begin{pmatrix} M_T \cosh y_{J/\psi} \\ P_T \cos\phi \\ P_T \sin\phi \\ M_T \sinh y_{J/\psi} \end{pmatrix}
\end{aligned} \tag{4.103}$$

with

$$\begin{aligned}
E'_e &= \frac{1}{4}\left(\frac{S-W^2-Q^2}{E_p} + \frac{Q^2}{E_e}\right) \quad , \quad \cos\theta = 1 - \frac{2SQ^2}{SQ^2 + 4E_e^2(S-W^2-Q^2)} \; , \\
q_B^0 &= \frac{1}{4}\left(\frac{W^2+Q^2}{E_p} - \frac{Q^2}{E_e}\right) \quad , \quad |\vec{q}_B| = \sqrt{Q^2 + (q_B^0)^2} \; , \\
\cos\psi &= \frac{1}{4\,|\vec{q}_B|}\left(\frac{W^2+Q^2}{E_p} + \frac{Q^2}{E_e}\right) \quad , \quad M_T = \sqrt{M^2 + P_T^2}
\end{aligned} \tag{4.104}$$

and in the nucleon rest frame

$$k = E_\nu \begin{pmatrix} 1 \\ 0 \\ 0 \\ 1 \end{pmatrix} \quad , \quad k' = E'_{\nu/e} \begin{pmatrix} 1 \\ \sin\theta \\ 0 \\ \cos\theta \end{pmatrix} \; ,$$

$$q_B = \begin{pmatrix} q_B^0 \\ -|\vec{q}_B|\sin\psi \\ 0 \\ |\vec{q}_B|\cos\psi \end{pmatrix} \quad , \quad P_N = m_N \begin{pmatrix} 1 \\ 0 \\ 0 \\ 0 \end{pmatrix} \ ,$$
$$P = \begin{pmatrix} M_T \cosh y_{J/\psi} \\ P_T \cos\phi \\ P_T \sin\phi \\ M_T \sinh y_{J/\psi} \end{pmatrix} \tag{4.105}$$

with

$$E'_{\nu/e} = \frac{S - W^2 - Q^2}{2m_N} \quad , \quad \cos\theta = 1 - \frac{2Q^2 m_N^2}{(S - m_N^2)(S - W^2 - Q^2)} \ ,$$
$$q_B^0 = \frac{W^2 + Q^2 - m_N^2}{2m_N} \quad , \quad |\vec{q}_B| = \sqrt{Q^2 + (q_B^0)^2} \ ,$$
$$\cos\psi = \frac{1}{2\,|\vec{q}_B|}\left(\frac{W^2 + Q^2 - m_N^2}{m_N} + \frac{Q^2}{E_\nu}\right) \quad , \quad M_T = \sqrt{M^2 + P_T^2} \ . \tag{4.106}$$

Thereby E_ν is the energy of the ingoing neutrino, m_N is the nucleon mass, which in defining the nucleon rest frame cannot be neglected, and ϕ^*, ϕ denote the J/ψ azimuthal angle in the respective frame. From (4.103), (4.105) it is apparent, that $y_{J/\psi}$ is defined to be positive in the direction of the three momentum of the ingoing lepton. Without loss of generality we may require, that $0 \leq \psi^*, \psi \leq \pi$, for, otherwise, we can achieve this by rotating the respective coordinate system by 180° around the z axis. The equations in (4.104) and (4.106) are derived as follows. $\cos\psi$ and q_B^0 are found from the equations $-Q^2/2 = kq_B = E_e(q_B^0 - |\vec{q}_B|\cos\psi)$ and $(W^2 + Q^2)/2 = q_B P_N = E_p(q_B^0 + |\vec{q}_B|\cos\psi)$ or $-Q^2/2 = kq_B = E_\nu(q_B^0 - |\vec{q}_B|\cos\psi)$ and $(W^2 + Q^2 - m_N^2)/2 = q_B P_N = q_B^0 m_N$, respectively. E'_e and $E'_{\nu/e}$ are then obtained from the equations $E_e - E'_e = k^0 - k'^0 = q_B^0$ or $E_\nu - E'_{\nu/e} = k^0 - k'^0 = q_B^0$, using, as the case may be, $S = (P_N + k)^2 = 4E_e E_p$ or $S = (P_N + k)^2 = m_N^2 + 2m_N E_\nu$. Finally, $\cos\theta$ is determined from the equation $Q^2/2 = kk' = E_e E'_e(1 - \cos\theta)$ or $Q^2/2 = kk' = E_\nu E'_{\nu/e}(1 - \cos\theta)$, respectively. Now, P_T, $y_{J/\psi}$ and $\cos\phi$ can be related to P_T^*, $y^*_{J/\psi}$ and $\cos\phi^*$, exploiting the equations $P_N^* P^* = P_N P$, $q_B^* P^* = q_B P$ and $k'^* P^* = k' P$ with k'^*, q_B^*, P_N^*, P^* given in (4.101) and k', q_B, P_N, P given in (4.103) or (4.105), respectively. Our final result for P_T, $y_{J/\psi}$ and $\cos\phi$ reads in the HERA laboratory frame

$$P_T = \sqrt{P_T^{*2} + A(A - 2P_T^*\cos\phi^*)} \ , \tag{4.107}$$
$$y_{J/\psi} = y^*_{J/\psi} + \ln\frac{(W^2 + Q^2)M_T^*}{\sqrt{S}WM_T} + \frac{1}{2}\ln\frac{E_e}{E_p} \ , \tag{4.108}$$
$$\cos\phi = \frac{P_T^*\cos\phi^* - A}{P_T} \tag{4.109}$$

with

$$A = \frac{M_T^*\sin\psi^*\exp y^*_{J/\psi}}{1 + \cos\psi^*} = \sqrt{\frac{Q^2(S - W^2 - Q^2)}{SW^2}}M_T^*\exp y^*_{J/\psi} \ , \tag{4.110}$$

and P_T^*, $y_{J/\psi}^*$ given in (4.96), (4.100). In the nucleon rest frame (4.108) changes to

$$y_{J/\psi} = y_{J/\psi}^* + \ln \frac{(W^2+Q^2)M_T^*}{\sqrt{S}WM_T} + \frac{1}{2}\ln\frac{S}{m_N^2} \;, \tag{4.111}$$

while (4.107),(4.109),(4.110) remain unchanged. In the limit $p' \to 0$ corresponding to single J/ψ production the formulae for P_T^*, $y_{J/\psi}^*$, P_T, $y_{J/\psi}$ and $\cos\phi$ drastically simplify to

$$P_T^* = 0 \quad , \quad y_{J/\psi}^* = \ln\frac{W}{M} \quad , \quad P_T = \sqrt{Q^2(1-y)} \quad , \quad \cos\phi = -1 \tag{4.112}$$

and

$$y_{J/\psi} = \ln\frac{2yE_e}{M_T} \quad \text{or} \quad y_{J/\psi} = \ln\frac{yS}{m_N M_T} \;, \tag{4.113}$$

respectively, where the first equation for $y_{J/\psi}$ refers to the HERA laboratory frame and the second to the nucleon rest frame. In calculating P_T, $y_{J/\psi}$ or ϕ distributions for jet associated J/ψ production we need to insert the symbolic factor $(1/2\pi)\int_0^{2\pi} d\phi^*$ on the right hand side of equation (4.79) with $l = e^\pm, \mu^\pm, \tau^\pm, \nu_e, \nu_\mu, \nu_\tau, \bar\nu_e, \bar\nu_\mu, \bar\nu_\tau$ as well as of equation (4.89) and the analogous ones corresponding to $(l,l') = (\nu_\mu,\mu^-), (\bar\nu_\mu,\mu^+), (\nu_\tau,\tau^-), (\bar\nu_\tau,\tau^+)$, since in that case P_T, $y_{J/\psi}$ and $\cos\phi$ depend on ϕ^*, so that the ϕ^* integration becomes nontrivial.

4.2.1 Differential distributions for H1

We now come to our predictions for direct J/ψ plus jet inclusive production in $e^\pm p$ DIS at DESY HERA. We compute differential distributions with respect to Q^2, z, W, P_T^*, $y_{J/\psi}^*$, P_T and $y_{J/\psi}$. Before presenting our results we first describe the theoretical input and the kinematical conditions, on which our numerical analysis is based. We use $m = (1.5\pm0.1)$GeV, $\alpha = 1/137.036$, and the leading order formula for $\alpha_s(\mu_R)$ with $n_f = 3$ active flavours[3]. As for the proton parton density functions, we employ the leading order set by Martin, Roberts, Stirling, and Thorne (MRST98LO)[45], with asymptotic scale parameter $\Lambda_{\rm QCD}^{(n_f=4)} = 174$ MeV, as our default and the leading order set by the CTEQ Collaboration (CTEQ5L) [46], with $\Lambda_{\rm QCD}^{(n_f=4)} = 192$ MeV, for comparison. The corresponding values of $\Lambda_{\rm QCD}^{(n_f=3)}$ are 204 MeV and 224 MeV, respectively. We choose the renormalization and factorization scales to be $\mu_R = \mu_F = \xi\sqrt{Q^2+M^2}$ and vary the scale parameter ξ between 1/2 and 2 around the default value 1. We adopt the NRQCD matrix elements from Table I of Ref. [19]. Specifically, they read $\left\langle O^{J/\psi}\left[{}^3S_1^{(1)}\right]\right\rangle = (1.3\pm0.1)$ GeV^3, $\left\langle O^{J/\psi}\left[{}^3S_1^{(8)}\right]\right\rangle = (4.4\pm0.7)\times10^{-3}$ GeV^3, and $M_{3.4}^{J/\psi} = (8.7\pm0.9)\times10^{-2}$ GeV^3 for set MRST98LO, where

$$M_r^H = \left\langle O^H\left({}^1S_0^{(8)}\right)\right\rangle + \frac{r}{m^2}\left\langle O^H\left({}^3P_0^{(8)}\right)\right\rangle. \tag{4.114}$$

The corresponding values for set CTEQ5L are (1.4 ± 0.1) GeV^3, $(3.9\pm0.7)\times10^{-3}$ GeV^3, and $(6.6\pm0.7)\times10^{-2}$ GeV^3, respectively. Since our analytical formulae for the production cross sections as given in the previous sections are sensitive to a different linear combination of $\left\langle O^{J/\psi}\left[{}^1S_0^{(8)}\right]\right\rangle$ and $\left\langle O^{J/\psi}\left[{}^3P_0^{(8)}\right]\right\rangle$ than appears in (4.114), we write $\left\langle O^{J/\psi}\left[{}^1S_0^{(8)}\right]\right\rangle =$

$\kappa_{J/\psi} M_r^{J/\psi}$ and $\left\langle O^{J/\psi}\left[{}^3P_0^{(8)}\right]\right\rangle = (1-\kappa_{J/\psi})\,(m^2/r)\,M_r^{J/\psi}$ and vary $\kappa_{J/\psi}$ between 0 and 1 around the default value 1/2. In order to estimate the theoretical uncertainties in our predictions, we vary the unphysical parameters ξ and $\kappa_{J/\psi}$ as indicated above, take into account the experimental errors on m and the default matrix elements, and switch from our default parton density function set to the CTEQ5L one, properly adjusting $\Lambda_{\rm QCD}^{(n_f=3)}$ and the matrix elements. We then combine the individual shifts in quadrature.

There are data of the H1 Collaboration on J/ψ plus jet inclusive and inelastic production in DIS[47, 48] available. These data were taken in collisions of positrons with $E_e = 27.5$ GeV and protons with $E_p = 820$ GeV in the HERA laboratory frame, so that $\sqrt{S} = 2\sqrt{E_e E_p} = 300$ GeV, and they refer to the kinematical region defined by $2 < Q^2 < 80$ GeV^2, $40 < W < 180$ GeV, and $z > 0.2$. In order to avoid the collinear divergences appearing in (4.79) for $l = e^+$ and to suppress the diffractive background we apply the cut $z < 0.9$. This cut on z is in accordance with the H1 data, which are presented in Ref. [47] and which we will use in the following for comparisons.

In Figs. 4.8–4.12, we confront the measured Q^2, P_T^2, z, $y_{J/\psi}^\star$, and W distributions, respectively, with our NRQCD predictions. For comparison, we also show the corresponding CSM predictions. In each case, the theoretical errors, evaluated as explained above, are indicated by the hatched areas. Instead of presenting our theoretical predictions as continuous curves, we adopt the binning pattern encoded in the experimental data, so as to facilitate quantitative comparisons. As for the Q^2 and P_T^2 distributions, the experimental data agrees rather well with the NRQCD predictions, both in normalization and shape, while it significantly overshoots the CSM predictions. In the case of the z distribution, the NRQCD prediction, in general, agrees better with the experimental data than the CSM one as far as the normalization is concerned. As for the shape, however, the experimental measurement favours the CSM prediction, while the NRQCD one exhibits an excess at large values of z, which is familiar from J/ψ inclusive photoproduction [21, 24]. As in the latter case, this rise in z is chiefly due to the ${}^1S_0^{(8)}$ and ${}^3P_J^{(8)}$ channels. It is known to be caused by a breakdown of the NRQCD expansion in the heavy quark velocity v near the boundaries of the phasespace and can be reduced by performing a resummation of large corrections of higher order in v[49]. In the case of the $y_{J/\psi}^\star$ distribution, the NRQCD prediction nicely agrees with the experimental data for $y_{J/\psi}^\star < 3$, while it appreciably overshoots the latter in the very forward direction. The CSM prediction roughly agrees with the experimental $y_{J/\psi}^\star$ distribution at the endpoints, while it significantly falls short of the latter in the central region. In the case of the W distribution, the experimental data mostly lie in the middle between the NRQCD and CSM predictions, slightly favouring the former. We conclude from Figs. 4.8–4.12 that the H1 data [47] tends to support the NRQCD predictions, while, in general, it overshoots the CSM predictions. In Figs. 4.13 and 4.14, we present our NRQCD and CSM predictions for the $(P_T^\star)^2$ and $y_{J/\psi}$ distributions, respectively, although there are no experimental data to compare them with.

At this point, we should compare our numerical results for the cross section of $e^\pm p \to e^\pm J/\psi j X'$ with the ones presented in Table II of Ref. [31]. To this end, we adopt the

theoretical input and kinematical conditions from Ref. [31]. Specifically, the authors of Ref. [31] evaluated $\alpha_s(\mu_R)$ at leading order with $n_f = 4$ and $\Lambda_{\rm QCD}^{(n_f=4)} = 130$ MeV, employed the leading order proton parton density function set by Glück, Reya, and Vogt [50], took the NRQCD matrix elements to be $\left\langle O^{J/\psi}\left[{}^3S_1^{(1)}\right]\right\rangle = 1.1$ GeV^3, $\left\langle O^{J/\psi}\left[{}^1S_0^{(8)}\right]\right\rangle = 1 \times 10^{-2}$ GeV^3, $\left\langle O^{J/\psi}\left[{}^3S_1^{(8)}\right]\right\rangle = 1.12 \times 10^{-2}$ GeV^3, and $\left\langle O^{J/\psi}\left[{}^3P_0^{(8)}\right]\right\rangle/m^2 = 5 \times 10^{-3}$ GeV^3, and required that $30 < W < 150$ GeV. All their other choices, except for the cuts on Q^2, P_T, $P_T^\star$, and z, coincide with our default settings. The outcome of this comparison is presented in Table 4.1. We are unable to determine the source of discrepancy.

Table 4.1: Comparison of our results for the color singlet (CS) and color octet (CO) contributions to $\sigma(e^\pm p \to e^\pm J/\psi j X')$ in DIS with the ones of Ref. [31].

Type	Cuts	Ref. [31]	Our result
CS	$Q^2 > 4$ GeV^2	89 pb	107 pb
CS	$Q^2, P_T^2 > 4$ GeV^2	40 pb	62 pb
CS	$Q^2 > 4$ GeV^2, $(P_T^\star)^2 > 2$ GeV^2, $z < 0.8$	13 pb	24 pb
CO	$Q^2 > 4$ GeV^2, $(P_T^\star)^2 > 2$ GeV^2, $z < 0.8$	8 pb	16 pb

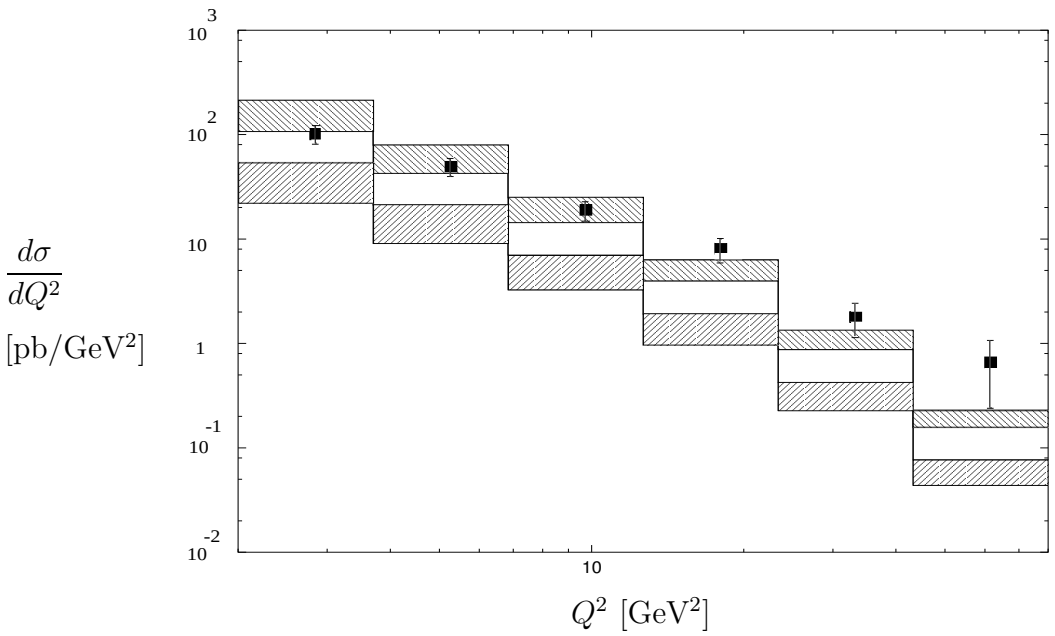

Figure 4.8: The Q^2 distribution of J/ψ inclusive production in e^+p DIS measured by the H1 Collaboration [47] is compared with the NRQCD (upper histogram) and CSM (lower histogram) predictions.

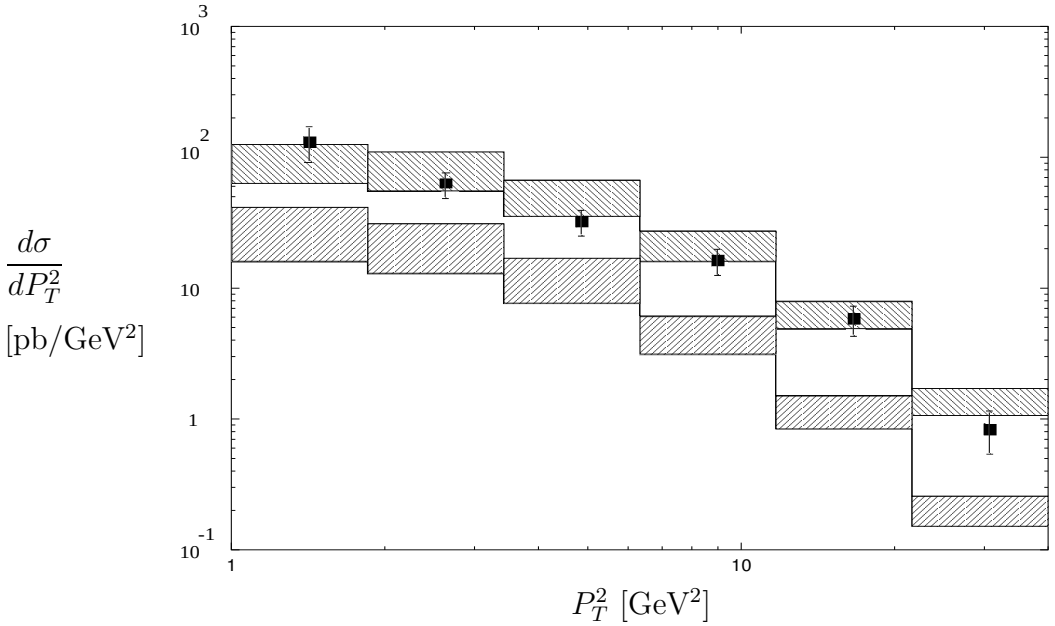

Figure 4.9: The P_T^2 distribution of J/ψ inclusive production in e^+p DIS measured by the H1 Collaboration [47] is compared with the NRQCD (upper histogram) and CSM (lower histogram) predictions.

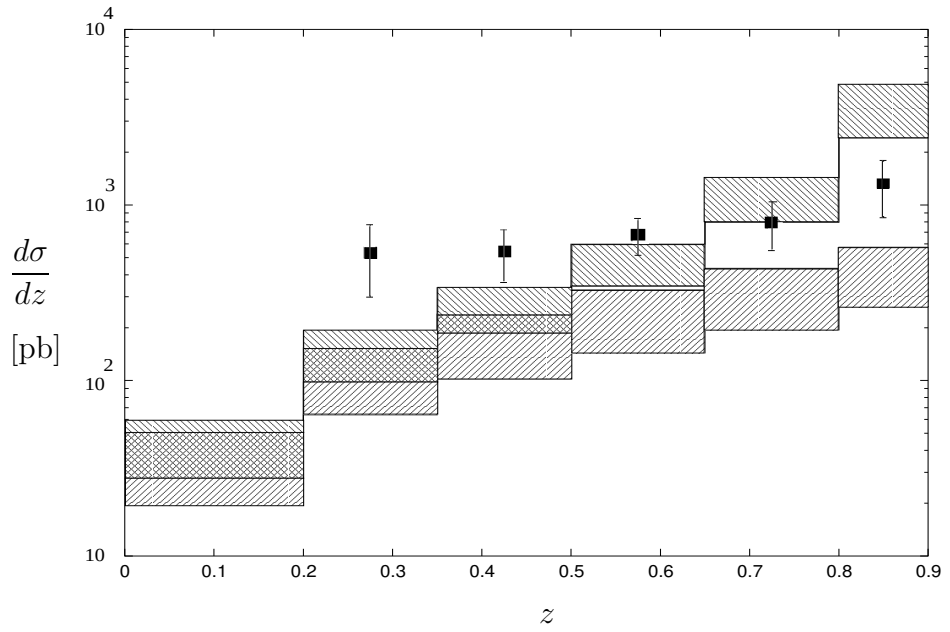

Figure 4.10: The z distribution of J/ψ inclusive production in e^+p DIS measured by the H1 Collaboration [47] is compared with the NRQCD (upper histogram) and CSM (lower histogram) predictions.

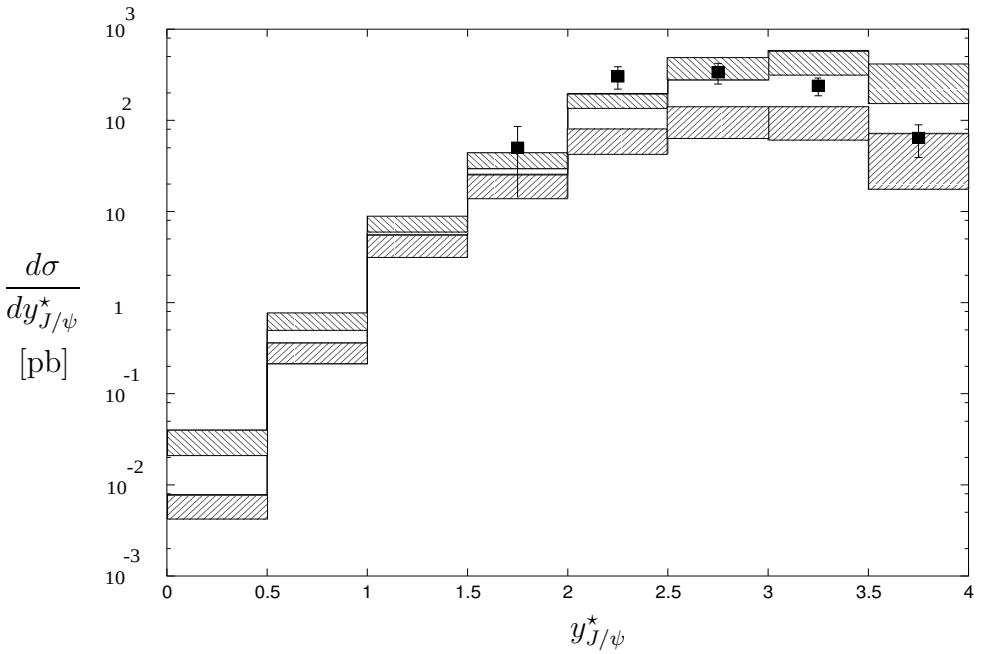

Figure 4.11: The $y^\star_{J/\psi}$ distribution of J/ψ inclusive production in e^+p DIS measured by the H1 Collaboration [47] is compared with the NRQCD (upper histogram) and CSM (lower histogram) predictions.

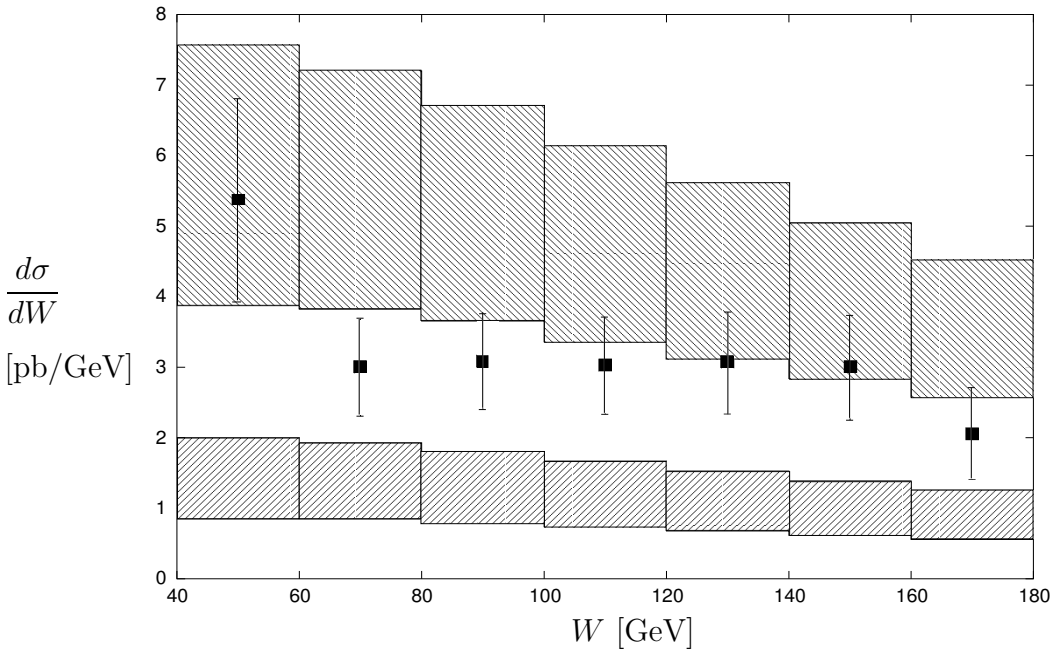

Figure 4.12: The W distribution of J/ψ inclusive production in e^+p DIS measured by the H1 Collaboration [47] is compared with the NRQCD (upper histogram) and CSM (lower histogram) predictions.

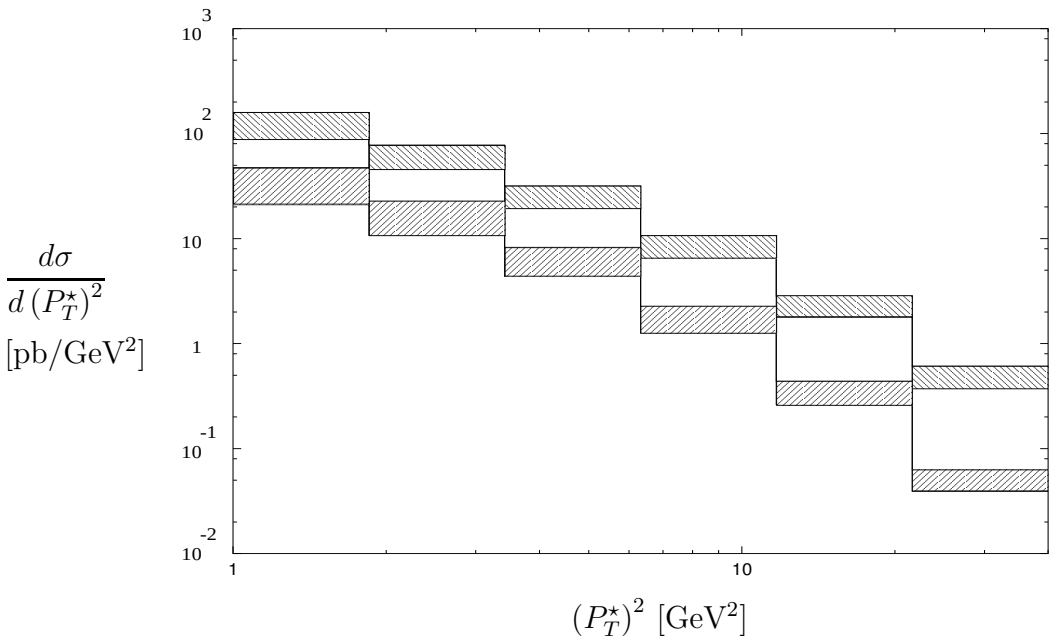

Figure 4.13: NRQCD (upper histogram) and CSM (lower histogram) predictions for the $(P_T^\star)^2$ distribution of J/ψ inclusive production in e^+p DIS.

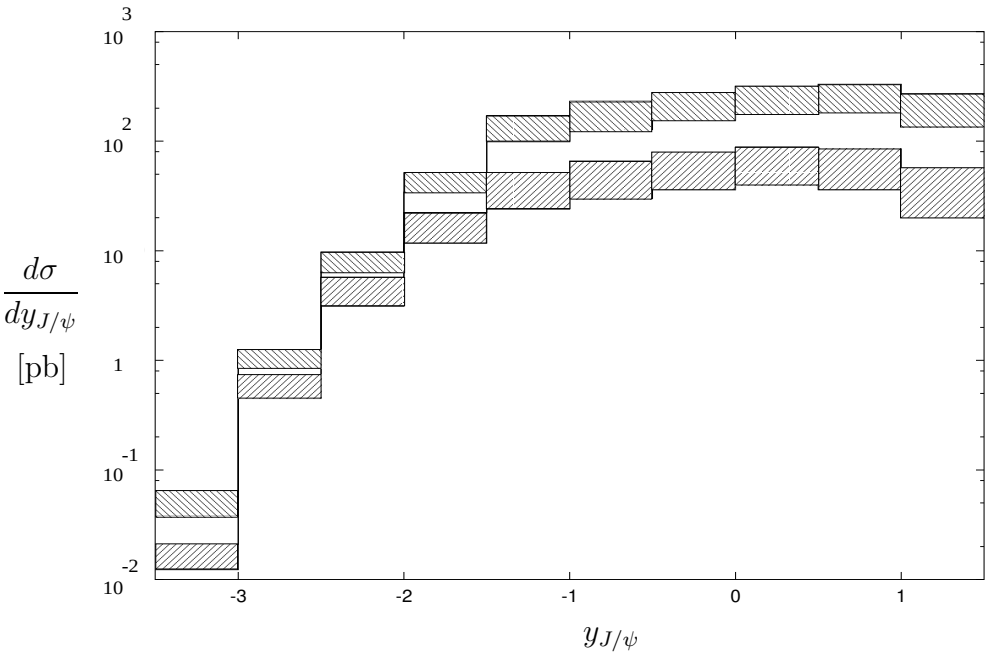

Figure 4.14: NRQCD (upper histogram) and CSM (lower histogram) predictions for the $y_{J/\psi}$ distribution of J/ψ inclusive production in e^+p DIS.

4.2.2 Differential distributions for CHORUS and NOMAD

In making theoretical predictions for the CHORUS and NOMAD experiments we have to account for a sizeable lack of kinematical information, due to the fact, that the four momenta of the in and outgoing neutrino are not measured and that CHORUS and NOMAD are at present not able to determine the four momentum of the proton remnant. Consequently, of all the kinematical quantities Q^2, z, W, P_T, $y_{J/\psi}$, P_T^* and $y_{J/\psi}^*$, which could be taken as experimentally controllable in case of the above analysis for DESY HERA, here only the J/ψ transverse momentum P_T and the J/ψ rapidity $y_{J/\psi}$ in the CHORUS and NOMAD laboratory frame satisfy this criterion. Particularly in case of J/ψ plus jet inclusive production through the neutral current interaction there are no longer proper cuts available to suppress the diffractive background or to get rid of the collinear divergences in the color octet channels of the relevant neutrino production cross sections given in (4.79) with $l = \nu, \bar{\nu} = \nu_e, \nu_\mu, \nu_\tau, \overline{\nu}_e, \overline{\nu}_\mu, \overline{\nu}_\tau$. In this case we therefore compute the P_T and $y_{J/\psi}$ distributions for jet associated J/ψ production only from the color singlet part of the respective production cross sections. For comparison we also compute these distributions for single J/ψ production, which, as already mentioned at the end of section 4.1.1, at Born level is a pure color octet process. The results of these both calculations can be understood to be the CSM and the leading order NRQCD prediction, respectively, for J/ψ production in νN neutral current DIS. In section 4.2.3, we will also give an estimation of the diffractive background, as this is now indispensible in order to compare with the experimental data. For J/ψ production through the charged current interaction the situation is less problematic, as this process is not accompagnied by diffraction and the corresponding cross sections like that given in (4.89) are free of infrared and collinear divergences. Therefore in computing the P_T and $y_{J/\psi}$ distributions for this process we can completely exploit our analytical NRQCD results. In performing the numerical calculations we adopt all the input for the non experiment specific parameters, the running QCD coupling constant and the proton parton density functions from the above analysis for DESY HERA. In addition, we use $m_N = 0.938\text{GeV}$, $m_Z = 91.1882\text{GeV}$, $m_W = 80.419\text{GeV}$, $\sin^2\theta_W = 1 - m_W^2/m_Z^2 = 0.22225$ and $G_F = 1.16639 \times 10^{-5}\text{GeV}^{-2}$. The CHORUS Collaboration [51] chose the target material to be lead (Pb), which in average consists of $A = 207.2$ nucleons, $Z = 82$ of them being protons. The NOMAD Collaboration [52] uses iron (Fe), with $A = 55.854$ and $Z = 26$. Leaving aside nuclear corrections and appealing to strong isospin symmetry, the effective nucleon parton density functions may be approximated by

$$\begin{aligned} F_N^a(\xi, \mu_F^2) &= \frac{1}{A}\left[ZF_p^a(\xi, \mu_F^2) + (A - Z)F_p^b(\xi, \mu_F^2)\right], \\ F_N^c(\xi, \mu_F^2) &= F_p^c(\xi, \mu_F^2), \end{aligned} \tag{4.115}$$

where $(a, b) = (u, d), (\overline{u}, \overline{d}), (d, u), (\overline{d}, \overline{u})$ and $c = s, \overline{s}, g$. We present the cross sections per nucleon, rather than per nucleus. The dependence of the cross section per nucleus, σ_A, on the number of nucleons, A, was studied experimentally for J/ψ inclusive photoproduction [53, 54] and muoproduction [55, 56]. The New Muon Collaboration (NMC)

[56], who performed the most recent of these experiments, was able to reconcile the seemingly inconsistent results of the previous experiments [53, 54, 55] by imposing appropriate cuts on z and P_T. Separating signal events of elastic (coherent) and deep inelastic (incoherent) scattering, the A dependences of the respective cross sections σ_A were found to differ significantly [54, 56]. Assuming that σ_A is related to the cross section per free nucleon (hydrogen), σ_1, by the simple power law $\sigma_A = A^\alpha \sigma_1$ [54, 57], with α being an A-independent number, we extract the values $\alpha_{\rm coh} = 1.19 \pm 0.02$ and $\alpha_{\rm in} = 1.05 \pm 0.03$ from the NMC results for coherent and incoherent scattering, respectively. For lead (iron) targets, this implies that the elastic and deep inelastic cross sections per (bound) nucleon, σ_A/A, are enhanced relative to the respective values of σ_1 by factors of $2.75^{+0.32}_{-0.27}$ ($2.15^{+0.18}_{-0.17}$) and $1.31^{+0.22}_{-0.20}$ ($1.22^{+0.16}_{-0.14}$), respectively. We note in passing that the above value of $\alpha_{\rm in}$ is in same ball park as those recently found for inclusive large P_T prompt photon and neutral pion hadroproduction in fixed target scattering, namely 1.04 and 1.08, respectively [57]. We assume that the power laws of J/ψ muoproduction, which dominantly proceeds via the electromagnetic current, carry over to νN neutral current DIS and employ them to determine the nuclear corrections. In this section, in which we only focus on nondiffractive deep inelastic neutrino nucleon scattering, only the values for $\alpha_{\rm in}$ are relevant. The values for $\alpha_{\rm coh}$ will be needed later, when we estimate the diffractive background for J/ψ production in neutral current DIS. As we now also consider contributions due to the feed down of the directly produced higher charmonium states ψ' and χ_{cJ}, we additionally adopt the matrix elements relevant for ψ' and χ_{cJ} production from Table I of Ref. [19]. Specifically, they read for the set MRST98LO $\left\langle O^{\psi'}\left[{}^3S_1^{(1)}\right]\right\rangle = (0.65\pm0.06)$ GeV^3, $\left\langle O^{\psi'}\left[{}^3S_1^{(8)}\right]\right\rangle = (4.2\pm1.0)\times10^{-3}$ GeV^3, $M_{3.5}^{\psi'} = (1.3\pm0.5)\times10^{-2}$ GeV^3, $\left\langle O^{\chi_{c0}}\left[{}^3P_0^{(1)}\right]\right\rangle = (8.9 \pm 1.3) \times 10^{-2}$ GeV^5, and $\left\langle O^{\chi_{c0}}\left[{}^3S_1^{(8)}\right]\right\rangle = (2.3 \pm 0.3) \times 10^{-3}$ GeV^3. The corresponding values for set CTEQ5L are (0.67 ± 0.07) GeV^3, $(3.7\pm0.9)\times10^{-3}$ GeV^3, $(0.78 \pm 0.36) \times 10^{-2}$ GeV^3, $(9.1 \pm 1.3) \times 10^{-2}$ GeV^5, and $(1.9 \pm 0.2) \times 10^{-3}$ GeV^3, respectively. Thereby M_r^H is defined in (4.114). For the same reasons as in section 4.2.1, we write $\left\langle O^{\psi'}\left({}^1S_0^{(8)}\right)\right\rangle = \kappa_{\psi'} M_r^{\psi'}$, $\left\langle O^{\psi'}\left({}^3P_0^{(8)}\right)\right\rangle = (1-\kappa_{\psi'})\,(m^2/r)\,M_r^{\psi'}$ and vary $\kappa_{\psi'}$ between 0 and 1 around the default value 1/2. Furthermore for the relevant charmonium decay branching fractions we use $B(\chi_{c0} \to J/\psi\,\gamma) = (0.66 \pm 0.18)\%$, $B(\chi_{c1} \to J/\psi\,\gamma) = (27.3 \pm 1.6)\%$, $B(\chi_{c2} \to J/\psi\,\gamma) = (13.5 \pm 1.1)\%$, and $B(\psi' \to J/\psi\,X_{\psi'}) = (55 \pm 5)\%$ [3]. The wide-band neutrino beam utilized in the CHORUS and NOMAD experiments mainly consists of ν_μ neutrinos and contains $\overline{\nu}_\mu$, ν_e, and $\overline{\nu}_e$ admixtures of about 6%, 1%, and below 1%, respectively. The average ν_μ energy is 27 GeV. Using accurate parameterizations for the energy spectra $\phi_\nu(E_\nu)$ of the individual neutrino species ν [52], we calculate the spectrum-averaged cross section as

$$\sigma = \frac{\sum_\nu \int dE_\nu\, \phi_\nu(E_\nu) \sigma_\nu(E_\nu)}{\sum_\nu \int dE_\nu\, \phi_\nu(E_\nu)}, \tag{4.116}$$

where the summation extends over $\nu = \nu_e, \overline{\nu}_e, \nu_\mu, \overline{\nu}_\mu$ and $\sigma_\nu(E_\nu)$ stands for the respective cross section $\sigma(\nu N \to l'(J/\psi)_{\rm promt} jX)$ as defined in (4.4) with the neutrino in the initial state having energy E_ν. In order to conform with the CHORUS analysis, we apply the

acceptance cut $20 < E_\nu < 200$ GeV. We estimate the theoretical uncertainties of our predictions in the same way as in case of the analysis for DESY HERA. However, we now vary the renormalization and the factorization scale independently, according to $\mu_i = \xi_i\sqrt{M^2+Q^2}$ with $\xi_i = 1$ as default and $\xi_i = 1/2, 2$ for comparison, where $i = R, F$. Moreover, we have now to take additionally into account the variation over $\kappa_{\psi'}$ as well as the experimental errors on α_{in}, the charmonium branching fractions and the additional matrix elements relevant for the production of the ψ' and the χ_{cJ} states. Finally, we now allow the upper half and the lower half errors to be different.

In Figs. 4.15 and 4.16, we present the P_T and $y_{J/\psi}$ distributions,respectively, for prompt J/ψ inclusive production in nondiffractive νN neutral current DIS under CHORUS experimental conditions. Specifically, the leading order NRQCD prediction (upper histogram) is shown in comparison with the CSM prediction (lower histogram). In each case, the theoretical errors, evaluated as explained above, are indicated by the hatched areas. Since the contributing partonic cross sections are all gluon initiated, our central predictions can be rendered appropriate for NOMAD by simply adjusting the nuclear correction factor, by multiplication with 0.94. Obviously the shapes of the color octet and color singlet distributions are very similar. However, the color octet distributions greatly exceed the color singlet ones in normalization. In fact, the integrated color octet and color singlet cross sections are $3.0^{+1.6}_{-1.7} \times 10^{-3}$ fb and $1.0^{+0.7}_{-0.5} \times 10^{-4}$ fb, respectively, the ratio of the central values being 30. The bulk parts, 72% in the color octet case and 78% in the color singlet case, are due to direct J/ψ production. In the first case, the fractions due to feed down from χ_{cJ} and ψ' mesons are each 14%, while, in the color singlet case, there is only feed down from ψ' mesons. Therefore, at first sight, the suppression of the CSM prediction seems to contradict the naïve expectation based on the NRQCD scaling rules (see Table 4.2). However, detailed inspection reveals that this suppression can be attributed

Table 4.2: Relative importance, measured in powers of α_s and $v^2 \approx \alpha_s$ (This esimation does not contradict (2.69). While (2.69) holds at long distances, α_s is of the order v^2 at short distances.) of the here considered nondiffractive J/ψ production channels according to the NRQCD scaling rules. The entries are normalized to the direct J/ψ plus jet color singlet contribution, which is of $o\left(\alpha^2\alpha_s^2 v^3\right)$. Note the abbreviations CS for color singlet, CO for color octet and LO for leading order.

	J/ψ, ψ'	χ_{cJ}
Single J/ψ CO (LO NRQCD)	$v^4/\alpha_s \approx \alpha_s$	$v^2/\alpha_s \approx 1$
J/ψ plus jet CS (CSM)	1	$v^2 \approx \alpha_s$

to the smallness of the effective value of $\sqrt{S}$, which affects the three particle phase space of the color singlet process more severely than the two particle phase space of the color octet processes. For a monoenergetic neutrino beam with $E_\nu = 27$ GeV, we just have $\sqrt{S} = 7.2$ GeV. For $E_\nu = 48$ TeV, so that $\sqrt{S} = 300$ GeV as for electron (positron) proton

collisions at DESY HERA, the color octet to color singlet ratio becomes 4.5. This should be compared with the corresponding analysis for direct J/ψ production in nondiffractive $e^{\pm}p$ DIS at HERA, with $Q^2 > 4$ GeV^2, which yields a color octet to color singlet ratio of 7.8[34]. A comparison of our theoretical predictions with the experimental data will be performed in the context of the estimation of the diffractive background in section 4.2.3.

In Figs. 4.17 and 4.18, we present the P_T and $y_{J/\psi}$ distributions, respectivly, for prompt J/ψ plus jet inclusive production in nondiffractive νN charged current DIS under CHORUS experimental conditions. Thereby the upper histogram shows the NRQCD prediction, while the lower one shows the corresponding color octet contribution in case, that the jet contains a charm or an anti charm quark. For comparison also the CSM prediction is shown in the middle histogram. Since the associated production of the J/ψ with an uncharmed jet only takes place through the ${}^3S_1^{(8)}$ channel, Figs. 4.17 and 4.18, respectively contain all the necessary information to obtain the color singlet and the color octet contributions to the P_T and $y_{J/\psi}$ distributions for charmed (uncharmed) jet associated J/ψ production. Specifically, they are given by the middle histogram (vanish) in the first and by the lower one (are found by subtracting the lower two histograms from the upper one) in the second case. Seeing, that until now there doesn't exist any data to compare with, we passed on a detailed error analysis. As we assumed the nuclear correction factor relevant for the here only contributing light quark initiated subprocesses to coincide with that relevant for gluon initiated subprocesses our predictions can be again rendered appropriate for NOMAD exactly as above by multiplication with 0.94. The CSM and the NRQCD result for the integrated cross section in case, that the jet is charmed (uncharmed) is $1.7^{+1.4}_{-0.8} \times 10^{-5}$ fb and $1.8^{+1.5}_{-0.9} \times 10^{-5}$ fb (0 fb and $4.9^{+3.4}_{-2.3} \times 10^{-5}$ fb), respectively. The fraction due to direct J/ψ production is 76.8% and 76.2% (not defined and 43.3%), respectively. The one due to the feed down from the ψ' meson is 21.1% and 21.0% (not defined and 22.7%), respectively. Finally the fraction due to the feed down from χ_{cJ} mesons is 2.1% and 2.8% (not defined and 34.0%), respectively. In particular, as was already mentioned at the end of section 4.1.3, the observation of uncharmed jet associated J/ψ production in νN charged current DIS would be a clear indication of the color octet mechanism.

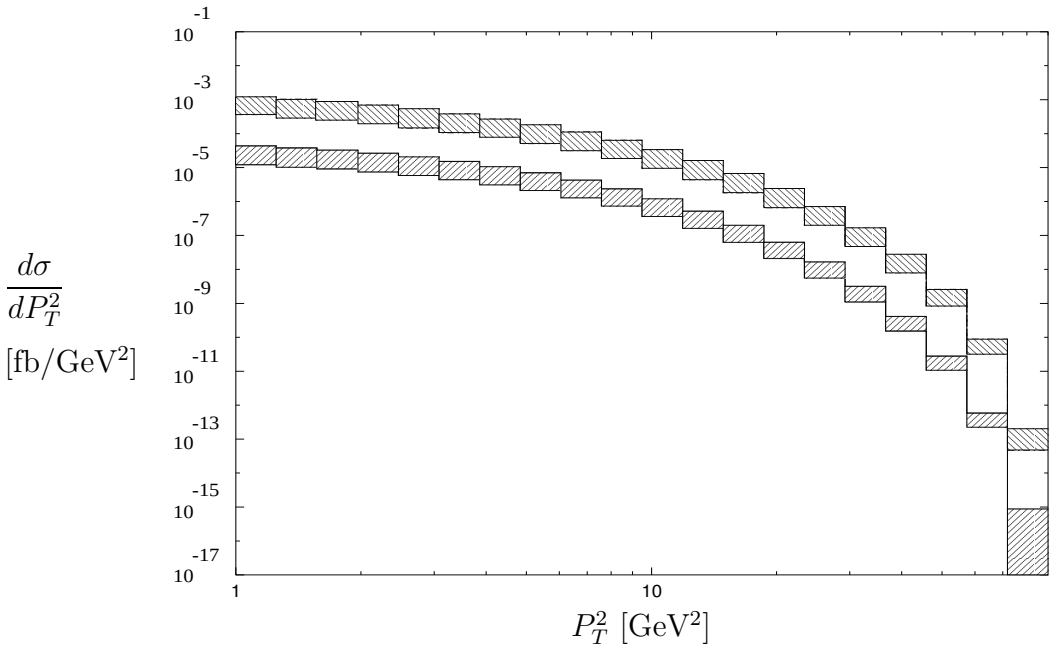

Figure 4.15: Leading order NRQCD (upper histogram) and CSM (lower histogram) predictions for the P_T^2 distribution of prompt J/ψ inclusive production in nondiffractive νN neutral current DIS appropriate for the CHORUS and NOMAD experiments.

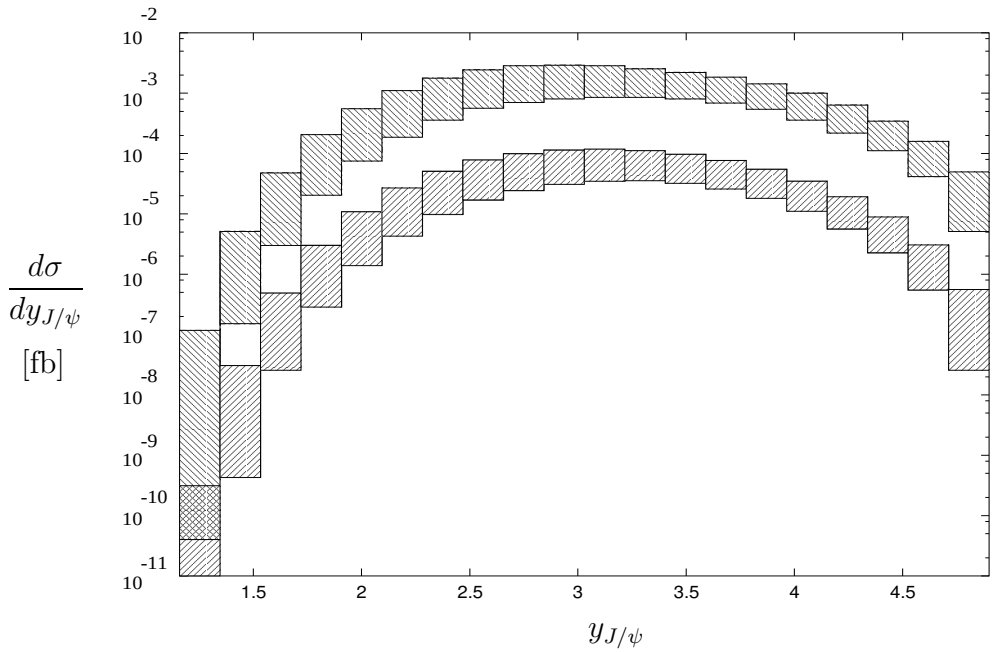

Figure 4.16: Leading order NRQCD (upper histogram) and CSM (lower histogram) predictions for the $y_{J/\psi}$ distribution of prompt J/ψ inclusive production in nondiffractive νN neutral current DIS appropriate for the CHORUS and NOMAD experiments.

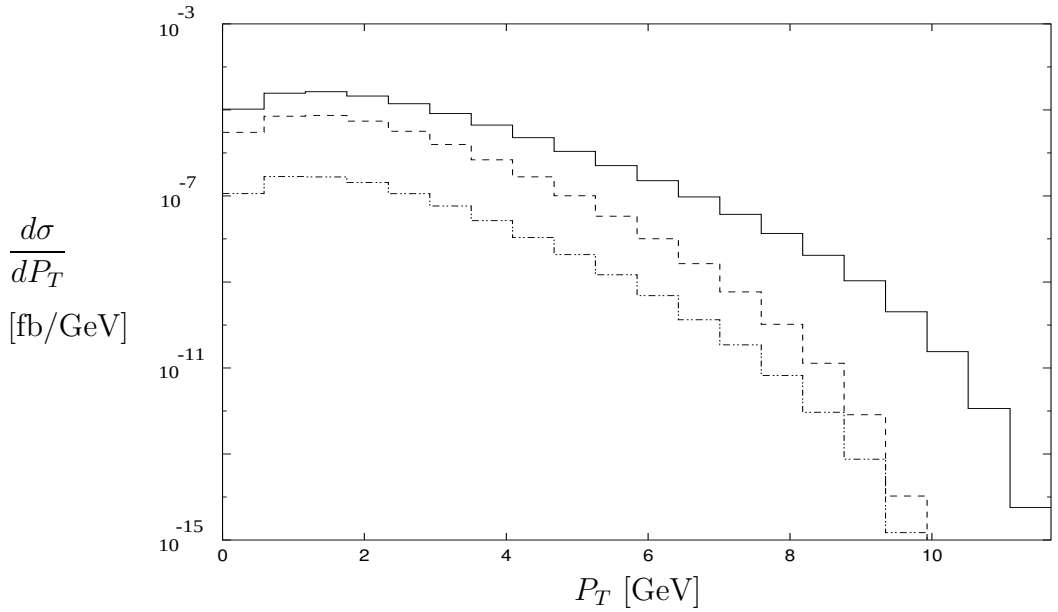

Figure 4.17: NRQCD (upper histogram) and CSM (middle histogram) prediction for the P_T distribution of prompt J/ψ inclusive production in νN charged current DIS appropriate for the CHORUS and NOMAD experiments and the CO contribution (lower histogram) to the NRQCD prediction in case of a charmed jet.

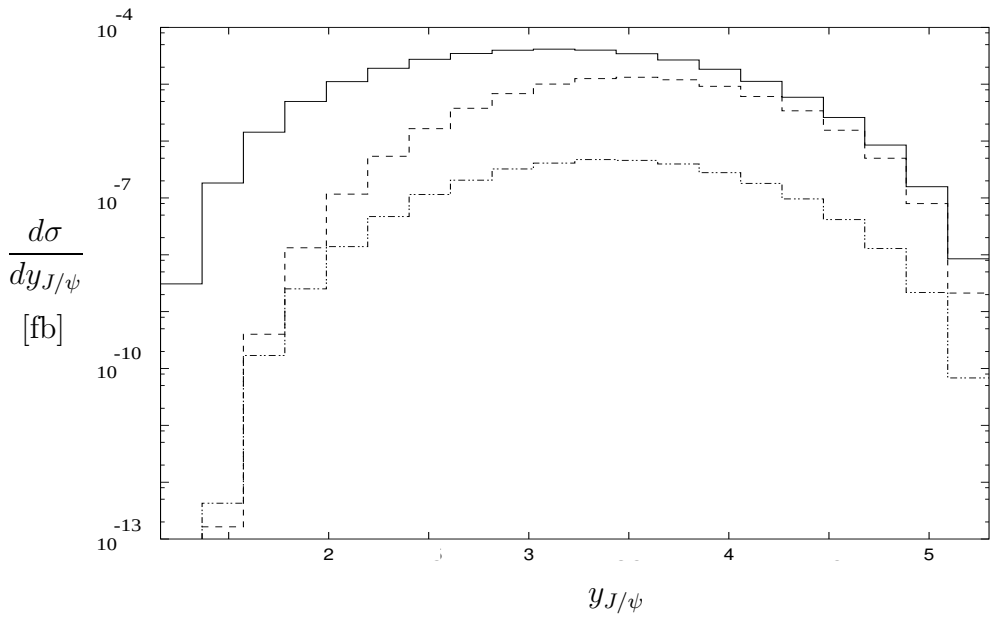

Figure 4.18: NRQCD (upper histogram) and CSM (middle histogram) prediction for the $y_{J/\psi}$ distribution of prompt J/ψ inclusive production in νN charged current DIS appropriate for the CHORUS and NOMAD experiments and the CO contribution (lower histogram) to the NRQCD prediction in case of a charmed jet.

4.2.3 Estimation of the diffractive background in neutral current J/ψ production

We now estimate the contribution of diffractive J/ψ production in νN neutral current DIS. For simplicity, we first focus on direct J/ψ production

$$\nu N \to \nu H N' \ , \tag{4.117}$$

where $H = J/\psi$ and N' denotes the outgoing nucleon or the hadronic system of small invariant mass, respectively, in which the ingoing nucleon turns during the diffraction process. The differential cross section of $\nu N \to \nu J/\psi N'$ may be obtained from the one of $\mu N \to \mu J/\psi N'$ in diffractive DIS via a virtual photon $\gamma^\star$ by adjusting the electroweak couplings and the propagator, as

$$\frac{d\sigma}{dy\,dQ^2}(\nu N \to \nu J/\psi N') = \left[\frac{g^2 v_c Q^2}{e^2 e_c\,(Q^2+m_Z^2)}\right]^2 \frac{d\sigma}{dy\,dQ^2}(\mu N \to \mu J/\psi N'). \tag{4.118}$$

The latter can be decomposed as [58]

$$\begin{aligned}\frac{d\sigma}{dy\,dQ^2}(\mu N \to \mu J/\psi N') = \frac{\alpha}{2\pi}\,\frac{y - Q^2/(2Em_N)}{Q^2(y^2+Q^2/E^2)}\Bigg\{\left[1+(1-y)^2+\frac{Q^2}{2E^2}\right]\sigma_T(\nu,Q^2) \\ + \left[2(1-y)-\frac{Q^2}{2E^2}\right]\sigma_L(\nu,Q^2)\Bigg\},\end{aligned} \tag{4.119}$$

where $\sigma_T(\nu,Q^2)$ and $\sigma_L(\nu,Q^2)$ are the transverse and longitudinal parts of the diffractive cross section of $\gamma^\star N \to J/\psi N'$ in virtual photoproduction, respectively. Here, $E = (S-m_N^2)/(2m_N)$ and $\nu = q_\gamma \cdot P/m_N = yE = q_\gamma^0$ are the incoming lepton and virtual photon energies in the nucleon rest frame, respectively, $\sqrt{S}$ is the lepton nucleon center of mass energy, and the muon mass is neglected. At small values of Q^2, the contribution from longitudinal photons is suppressed, and we may put $\sigma_L(\nu,Q^2) = 0$. We treat $\sigma_T(\nu,Q^2)$ within the Vector Dominance Model. In this model diffractive J/ψ production is assumed to be dominated by fluctuations of the photon or the Z boson into a vector meson $V = J/\psi, \psi', \chi_{c1}, ...$, in direct production case $V = J/\psi$, which then is elastically scattered at the nucleon. Vector dominance implies a relation among $\sigma_T(\nu,Q^2)$ and the cross section $\sigma(\nu)$ for diffractive real photoproduction $\gamma\ N\ \to\ V\ N$ according to

$$\sigma_T(\nu,Q^2) = \frac{\sigma(\nu)}{(1+Q^2/M_V^2)^2}\ , \tag{4.120}$$

where M_V is a phenomenological mass parameter. Fits to experimental data of $\gamma^\star N \to J/\psi N'$ suggest that $M_V = (3.2 \pm 0.6)$ GeV [59]. The measured ν dependence of $\sigma(\nu)$ is well described by the phenomenological parameterization [38, 39, 60, 61, 62]

$$\sigma(\nu) = A \exp\frac{-B}{\nu - C}, \tag{4.121}$$

with $A = 20$ nb, $B = 45$ GeV, and $C = 6$ GeV [62], which is valid for $\nu > C$.

We now generalize our considerations to also include the cases $H = \chi_{c1}, \psi'$. To this end, we exploit, that the strengths of the Z boson vector and axial vector couplings to the S and P wave charmonia are proportional to $v_c f_V$ and $a_c f_A$, where [39]

$$\begin{aligned} f_V^2 &= \frac{3}{8\pi} \frac{|R_S(0)|^2}{m^3}, \\ f_A^2 &= \frac{9}{4\pi} \frac{|R'_P(0)|^2}{m^5}, \end{aligned} \tag{4.122}$$

respectively. Here, $R_S(r)$ and $R_P(r)$ denote the radial wave functions of the S- and P-wave charmonia, respectively. Furthermore, we have [9]

$$\begin{aligned} |R_S(0)|^2 &= \frac{2\pi}{9} \left\langle O^{J/\psi} \left[{}^3S_1^{(1)} \right] \right\rangle \ , \\ |R'_P(0)|^2 &= \frac{2\pi}{9} \frac{\left\langle O^{\chi_{cJ}} \left[{}^3P_J^{(1)} \right] \right\rangle}{2J+1}. \end{aligned} \tag{4.123}$$

Assuming that $\sigma(\psi' N \to \psi' N') \approx \sigma(\chi_{c1} N \to \chi_{c1} N') \approx \sigma(J/\psi N \to J/\psi N')$, we thus conclude that $d\sigma(\nu N \to \nu \psi' N')/(dy\, dQ^2)$ and $d\sigma(\nu N \to \nu \chi_{c1} N')/(dy\, dQ^2)$ may be obtained from $d\sigma(\nu N \to \nu J/\psi N')/(dy\, dQ^2)$ through multiplication with the constant factors

$$\begin{aligned} R_{\psi'} &= \frac{\left\langle O^{\psi'} \left[{}^3S_1^{(1)} \right] \right\rangle}{\left\langle O^{J/\psi} \left[{}^3S_1^{(1)} \right] \right\rangle}, \\ R_{\chi_{c1}} &= \frac{a_c^2}{v_c^2} \frac{6}{m^2} \frac{\left\langle O^{\chi_{c0}} \left[{}^3P_0^{(1)} \right] \right\rangle}{\left\langle O^{J/\psi} \left[{}^3S_1^{(1)} \right] \right\rangle}, \end{aligned} \tag{4.124}$$

respectively. Thus, the effective direct to prompt conversion factor reads

$$R_{(J/\psi)_{\rm prompt}} = 1 + R_{\chi_{c1}} B(\chi_{c1} \to J/\psi\ \gamma) + R_{\psi'} B(\psi' \to J/\psi\ X_{\psi'}). \tag{4.125}$$

Without giving derivations we note the kinematically allowed ranges of E, Q^2, and y to be

$$\begin{aligned} E &> M \left(1 + \frac{M}{2m_N} \right), \\ 0 < Q^2 &< \frac{2E[2Em_N - M(M+2m_N)]}{2E + m_N}, \\ \frac{Q^2 + M(M+2m_N)}{2Em_N} < y &< 1 - \frac{Q^2}{4E^2}, \end{aligned} \tag{4.126}$$

respectively. Here, the N' mass is taken to be m_N. In addition, (4.121) implies the cut $y > C/E$.

As for the numerical result, we find the total cross section of prompt J/ψ production in diffractive νN neutral current DIS to be $3.3^{+1.6}_{-1.4} \times 10^{-3}$ fb. The theoretical uncertainty quoted here is merely parametric; it neither includes the experimental error on $\sigma(\nu)$ as parameterized by (4.121), nor does it reflect the unavoidable lack of rigour of the underlying model assumptions. It is only determined from the errors on the mass parameter M_V, the NRQCD matrix elements $\left\langle O^{J/\psi}\left[{}^3S_1^{(1)}\right]\right\rangle$, $\left\langle O^{\psi'}\left[{}^3S_1^{(1)}\right]\right\rangle$, $\left\langle O^{\chi_{c1}}\left[{}^3P_1^{(1)}\right]\right\rangle$, the branching fractions $B(\psi' \to J/\psi\ X_{\psi'})$, $B(\chi_{c1} \to J/\psi\ \gamma)$ and the parameter α_{coh}. The fractions due to feed down from χ_{c1} and ψ' mesons amount to 19% and 17%, respectively. The corresponding prediction for NOMAD is obtained through multiplication with the scaling factor 0.80, which accounts for the difference in the nuclear correction factors.

The CHORUS Collaboration measured the spectrum averaged total cross section per nucleon of $\nu N \to \nu J/\psi X$ in DIS to be $(6.3 \pm 3.0) \times 10^{-2}$ fb. In Fig. 4.19, this experimental data point is shown together with the theoretical predictions for the diffractive, the color singlet and the color octet contribution with the latter two as given in section 4.2.2. It should be compared with their sum, 6.4×10^{-3} fb. As for the central values, the measurement exceeds the combined prediction by a factor of 10. It should be borne in mind that the theoretical prediction for the nondiffractive cross section is of leading order in α_s and v. The next leading order corrections are expected to lead to a substantial enhancement.

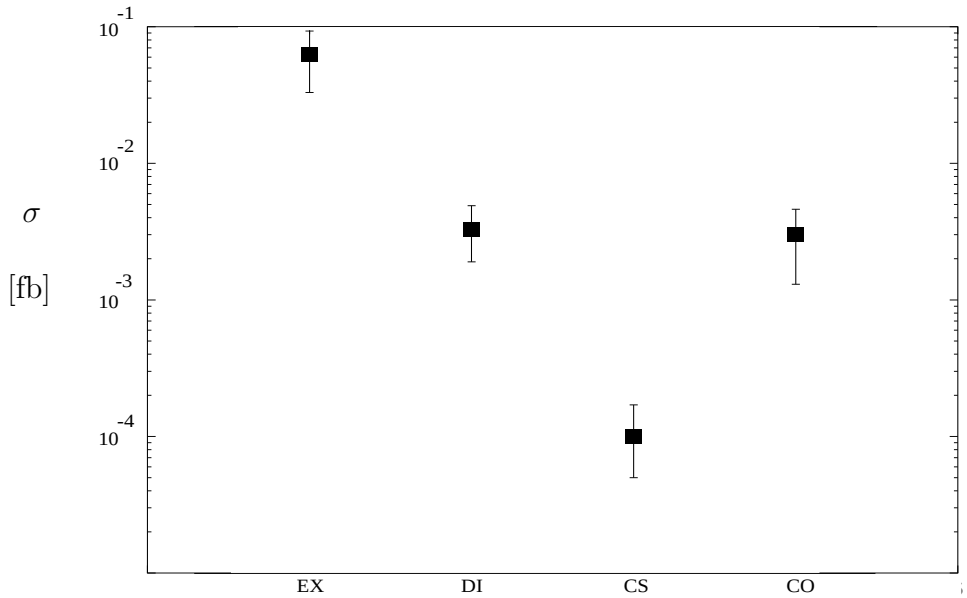

Figure 4.19: The total cross section of $\nu N \to \nu J/\psi X$ measured by CHORUS [51] (EX) is compared with the predicted diffractive (DI), color singlet (CS), and color octet (CO) contributions.

Chapter 5

Single J/ψ inclusive production in $e^{\pm}p$ electromagnetic DIS at next leading order

In order to diminish the uncertainties in our theoretical predictions for J/ψ production it is necessary to calculate the next leading order corrections to the respective cross sections. In fact, it is well known, that at next leading order the scale and scheme dependence of the results will be considerably reduced. In this chapter we calculate the ${}^1S_0^{(8)}$ part of the next leading order corrections to single direct J/ψ inclusive production in electromagnetic $e^{\pm}N$ DIS. The obtained analytical results are then employed for a numerical analysis of this process under HERA conditions.

5.1 The analytical calculation

The ${}^1S_0^{(8)}$ part of the cross section for single direct J/ψ inclusive production in electromagnetic e^-N DIS at next leading order, that is at $o(\alpha^2\alpha_s^2)$, may be written

$$\sigma_{{}^1S_0^{(8)}}\left(e^-N \to e^-J/\psi X'\right) = \sum_{a=g,q}\int d\xi F_N^a(\xi,\mu_F^2)\sigma\left(e^-a \to e^-c\bar{c}\left[{}^1S_0^{(8)}\right]a\right)\left\langle O^{J/\psi}\left[{}^1S_0^{(8)}\right]\right\rangle \ . \tag{5.1}$$

Thereby, we first start with provisional nucleon parton density functions $\hat{F}_N^a(\xi)$, short distance coefficients $\hat{\sigma}_a \equiv \hat{\sigma}\left(e^-a \to e^-c\bar{c}\left[{}^1S_0^{(8)}\right]a\right)$ with $a = g,q$ and $q = u,\bar{u},d,\bar{d},s,\bar{s}$, and a provisional production matrix element $\left\langle \widehat{O}^{J/\psi}\left[{}^1S_0^{(8)}\right]\right\rangle$, which later, as becomes clear below, need to be redefined , the respective redefined quantities being $F_N^a(\xi,\mu_F^2)$, $\sigma\left(e^-a \to e^-c\bar{c}\left[{}^1S_0^{(8)}\right]a\right)$, and $\left\langle O^{J/\psi}\left[{}^1S_0^{(8)}\right]\right\rangle$. The $\hat{\sigma}_g$ and $\hat{\sigma}_q$ can be written up to $o(\alpha^2\alpha_s^2)$

$$\begin{aligned}\hat{\sigma}_g = &\frac{1}{16\xi S}\int dPS_2(p+k;P,k')\ \left(\mu_R^{6\epsilon}\ \overline{\sum}\left|\mathcal{M}_{\rm B}\right|^2 + 2\mu_R^{8\epsilon}\ \overline{\sum}{\rm Re}\left[\mathcal{M}_{\rm B}^{\dagger}\mathcal{M}_{\rm V}\right]\right)\\ &+\frac{1}{16\xi S}\int dPS_3(p+k;P,k',p')\ \mu_R^{8\epsilon}\ \overline{\sum}\left|\mathcal{M}_{\rm R(g)}\right|^2\end{aligned} \tag{5.2}$$

and

$$\hat{\sigma}_q = \frac{1}{16\xi S}\int dPS_3(p+k;P,k',p')\ \mu_R^{8\epsilon}\ \overline{\sum}\left|\mathcal{M}_{\mathrm{R(q)}}\right|^2\ , \tag{5.3}$$

where the factor $1/N_{\mathrm{col}}N_{\mathrm{pol}} = 1/8$ has been taken into account. Here $\mathcal{M}_{\mathrm{B}}$ is the Born amplitude of the partonic subprocess $e^-g \to e^-c\bar{c}\left[{}^1S_0^{(8)}\right]$, $\mathcal{M}_{\mathrm{V}}$ is the amplitude of the corresponding virtual corrections, and $\mathcal{M}_{\mathrm{R(a)}}$ are the amplitudes of the corresponding real corrections due to the partonic subprocesses $e^-a \to e^-c\bar{c}\left[{}^1S_0^{(8)}\right]a$. The integration over $\vec{p}'$ in (5.2), (5.3) is performed over the whole phase space of the outgoing gluon or light quark, respectively. Note, that X' in (5.1) is now understood to also contain the hadronisation products of this outgoing light parton. Furthermore, $\overline{\sum}$ is defined as in (3.17). $\mathcal{M}_{\mathrm{B}}$, $\mathcal{M}_{\mathrm{R(q)}}$, $\mathcal{M}_{\mathrm{R(g)}}$ and $\mathcal{M}_{\mathrm{V}}$ are determined from the Feynman diagrams in Figs. 4.1, 4.2 (or the analogous ones with reversed direction of the light quark line), 4.3 (together with those in Fig. 4.4 for a consistent treatment of the gluon polarization), and Fig. 5.1, respectively. As expressed by (5.2) $\mathcal{M}_{\mathrm{V}}$ contributes at $o(\alpha^2\alpha_s^2)$ only via the interference with $\mathcal{M}_{\mathrm{B}}$. We apply the procedure of dimensional regularization, that is, the space time dimension is taken to be an arbitrary complex number D different from 4, to regularize the infrared and collinear divergences in $\int dPS_3(p+k;P,k',p')\overline{\sum}\left|\mathcal{M}_{\mathrm{R(a)}}\right|^2$ and the infrared, collinear and ultraviolet ones in $\mathcal{M}_{\mathrm{V}}$. Thereby, the renormalization scale μ_R is introduced as an arbitrary mass scale in order to keep the coupling constants g_s and e dimensionless, and ϵ is given by $\epsilon = (4-D)/2$. It seems reasonable to point out, that in D dimensions the number of polarization degrees of freedom of a vector boson (in this concrete case the gluon) changes from 2 to $D-2$, in contrast to a spin 1/2 fermion, for which the number of polarization degrees remains unchanged. Performing the integration over $\vec{P}$ $\hat{\sigma}_g$ and $\hat{\sigma}_q$ become

$$\begin{aligned}\hat{\sigma}_g = \frac{1}{16\xi S}\int \frac{d^{D-1}\vec{k}'}{(2\pi)^{D-2}2k'^0}\mu_R^{6\epsilon}\Big[&\delta(\hat{s}-M^2)\left(\overline{\sum}\left|\mathcal{M}_{\mathrm{B}}\right|^2 + 2\mu_R^{2\epsilon}\ \overline{\sum}\mathrm{Re}\left[\mathcal{M}_{\mathrm{B}}^{\dagger}\mathcal{M}_{\mathrm{V}}\right]\right)\\ &+\int\frac{d^{D-1}\vec{p}'}{(2\pi)^{D-1}2p'^0}\ \delta(\hat{s}+\hat{t}+\hat{u}-M^2+Q^2)\ \mu_R^{2\epsilon}\ \overline{\sum}\left|\mathcal{M}_{\mathrm{R(a)}}\right|^2\Big]\end{aligned} \tag{5.4}$$

and

$$\hat{\sigma}_q = \frac{1}{16\xi S}\int \frac{d^{D-1}\vec{k}'}{(2\pi)^{D-2}2k'^0}\mu_R^{6\epsilon}\int\frac{d^{D-1}\vec{p}'}{(2\pi)^{D-1}2p'^0}\delta(\hat{s}+\hat{t}+\hat{u}-M^2+Q^2)\mu_R^{2\epsilon}\overline{\sum}\left|\mathcal{M}_{\mathrm{R(q)}}\right|^2\ . \tag{5.5}$$

Besides the divergences already quoted $\mathcal{M}_{\mathrm{V}}$ contains additionally a Coulomb divergence. The latter can be traced back to the exchange of a soft gluon between the heavy quark and antiquark in the final state of the partonic subprocess $e^-g \to e^-c\bar{c}\left[{}^1S_0^{(8)}\right]$ and persists even in $D \neq 4$ space time dimensions. As will be later seen, it can be regularized by an infinitesimal heavy quark velocity v in the quarkonium rest frame. According to a general theorem of Kinoshita, Lee and Nauenberg[63] the infrared divergences in the real correction part of $\hat{\sigma}_g$ cancel against the infrared and collinear ones in the virtual correction part of $\hat{\sigma}_g$. The ultraviolet divergences in $\mathcal{M}_{\mathrm{V}}$ are removed by renormalization of the

relevant parameters and fields at the renormalization scale μ_R. Due to the factorization theorem of the QCD improved parton model the only remaining collinear divergences in $\int dPS_3(p+k;P,k',p')\overline{\sum}\left|\mathcal{M}_{\mathrm{R(a)}}\right|^2$ can be factorized at the factorization scale μ_F as universal factors into the nucleon parton density functions, leading to a redefinition of the latters. Finally, the Coulomb divergence can be absorbed as a universal factor into the ${}^1S_0^{(8)}$ production matrix element, which thereby also becomes redefined. Since after this factorization and renormalization procedure the expression in the square brackets in (5.4) as well as the integral over $\vec{p}'$ in (5.5) becomes finite for $D \to 4$ the global factor $\frac{d^{D-1}\vec{k}'}{(2\pi)^{D-2}2k'^0}\mu_R^{6\epsilon}$ in (5.4), (5.5) may be treated in $D=4$ space time dimensions. Furthermore, the γ^5 matrix only appears in the spin projector Π_0, which also plays the role of a global factor. As therefore corrections of order ϵ from the D dimensional generalization of the γ^5 matrix yield no contribution in the limit $D \to 4$ we may treat the γ^5 matrix in the naive scheme. That is, we assume it also in D dimensions to anticommute with all the Dirac matrices γ^μ, $\mu = 0,1,2,...,D-1$ exactly as in 4 dimensions. For similar reasons we may furthermore employ the leptontensor $L_{e^-}^{\mu\nu}$ in its 4 dimensional form as given in (4.38). Making use of (4.30), (4.33) $\hat{\sigma}_g$ and $\hat{\sigma}_q$ become

$$\hat{\sigma}_g = \int dQ^2 dy \left[M_B + \mu_R^{2\epsilon}\left(M_V + M_{R(g)}\right)\right] \ , \tag{5.6}$$

and

$$\hat{\sigma}_q = \int dQ^2 dy \ \mu_R^{2\epsilon} \ M_{R(q)} \tag{5.7}$$

with

$$M_B = \frac{\overline{\sum}\left|\mathcal{M}_{\mathrm{B}}\right|^2}{128\pi\xi\hat{s}S}\delta(1-\mathrm{x}) = M_0\delta(1-\mathrm{x}) \ , \tag{5.8}$$

$$M_V = \frac{\overline{\sum}\mathrm{Re}\left[\mathcal{M}_{\mathrm{B}}^\dagger\mathcal{M}_{\mathrm{V}}\right]}{64\pi\xi\hat{s}S}\delta(1-\mathrm{x}) \ , \tag{5.9}$$

$$M_{R(a)} = \int \frac{d^{D-1}\vec{p}'}{(2\pi)^{D-1}2p'^0}\delta(\hat{s}+\hat{t}+\hat{u}-M^2+Q^2)\frac{\overline{\sum}\left|\mathcal{M}_{\mathrm{R(a)}}\right|^2}{128\pi\xi S} \ . \tag{5.10}$$

Thereby, x is defined as

$$\mathrm{x} = \frac{M^2}{\hat{s}} \tag{5.11}$$

and M_0 is given by

$$M_0 = \frac{1+(1-y)^2}{y}\frac{4\pi^2 e_c^2\alpha^2\alpha_s}{M^3(M^2+Q^2)Q^2}(1-2\epsilon) \ . \tag{5.12}$$

Note, that for $D=4$ the latter formula for M_0 is consistent with (4.48). We refrain from presenting the D dimensional results for $\overline{\sum}\left|\mathcal{M}_{\mathrm{R(a)}}\right|^2$, as they are too lengthy. For $D \to 4$ they have already been calculated in section 4.1.2 and can be extracted in this limit from (A.3), (A.10). $\overline{\sum}\mathrm{Re}\left[\mathcal{M}_{\mathrm{B}}^\dagger\mathcal{M}_{\mathrm{V}}\right]$ will be calculated in section 5.1.2.

5.1.1 The real corrections

For calculating the real corrections we need the D dimensional integration measure $d^{D-1}\vec{p}'/(2\pi)^{D-1}2p'^0$. In appendix B.1 it is derived

$$\frac{d^{D-1}\vec{p}'}{(2\pi)^{D-1}2p'^0} = d\mathrm{x}\; d\mathrm{y}\frac{\hat{s}}{32\pi^2}\left(\frac{16\pi}{\hat{s}}\right)^{\epsilon}\frac{1}{\Gamma(1-\epsilon)}(1-\mathrm{x})^{1-2\epsilon}(1-\mathrm{y}^2)^{-\epsilon}\ . \tag{5.13}$$

Thereby, x will be enforced below by energy momentum conservation to obey (5.11), and y is the cosine of the angle between the momenta $\vec{p}$ and $\vec{p}'$ in the photon parton center of mass system. $\hat{t}$ and $\hat{u}$ read in terms of x and y

$$\hat{t} = -\frac{\hat{s}+Q^2}{2}(1-\mathrm{x})(1-\mathrm{y}) \tag{5.14}$$

$$\hat{u} = -\frac{\hat{s}+Q^2}{2}(1-\mathrm{x})\left(1+\mathrm{y}-\frac{2Q^2}{\hat{s}+Q^2}\right)-Q^2\ . \tag{5.15}$$

It turns out, that in the worst case the $\overline{\sum}\left|\mathcal{M}_{\mathrm{R(a)}}\right|^2$ contain an uncompensated factor $\hat{t}(1-\mathrm{x}) = -(\hat{s}+Q^2)(1-\mathrm{x})(1-\mathrm{y})/2$ in the denominator, making the $\int dPS_3(p+k;P,k',p')\overline{\sum}\left|\mathcal{M}_{\mathrm{R(a)}}\right|^2$ divergent at $\mathrm{x}=1$ or $\mathrm{y}=1$. Obviously the divergences at $\mathrm{x}=1$ are infrared ones, while those at $\mathrm{y}=1$ are collinear ones. Note however, that this classification becomes arbitrary at $\mathrm{x}=\mathrm{y}=1$, where both types of divergences overlap. We write

$$\overline{\sum}\left|\mathcal{M}_{\mathrm{R(a)}}\right|^2 = \frac{\overline{M}_{R(a)}(\mathrm{x},\mathrm{y})}{\hat{t}(1-\mathrm{x})} = -\frac{2}{\hat{s}+Q^2}\frac{1}{(1-\mathrm{x})^2(1-\mathrm{y})}\overline{M}_{R(a)}(\mathrm{x},\mathrm{y})\ , \tag{5.16}$$

where $\overline{M}_{R(a)}(\mathrm{x},\mathrm{y})$ is regular for all x and y. Inserting (5.16) in (5.10), employing (5.13), noting, that

$$\delta(\hat{s}+\hat{t}+\hat{u}-M^2+Q^2) = \frac{1}{\hat{s}}\delta\left(\mathrm{x}-\frac{M^2}{\hat{s}}\right) \tag{5.17}$$

and performing the integration over x, we find

$$M_{R(a)} = -\frac{1}{2048\pi^3\xi S(\hat{s}+Q^2)}\int_{-1}^{1}d\mathrm{y}\left(\frac{16\pi}{\hat{s}}\right)^{\epsilon}\frac{1}{\Gamma(1-\epsilon)}(1-\mathrm{x})^{-1-2\epsilon}(1-\mathrm{y})^{-1-\epsilon}(1+\mathrm{y})^{-\epsilon}\overline{M}_{R(a)}(\mathrm{x},\mathrm{y})\ . \tag{5.18}$$

In appendix B.3 it is derived

$$\begin{aligned}\frac{(16\pi)^{\epsilon}}{\Gamma(1-\epsilon)}(1-\mathrm{x})^{-1-2\epsilon}(1-\mathrm{y})^{-1-\epsilon}(1+\mathrm{y})^{-\epsilon} = {}& \frac{f(\epsilon)}{2\epsilon^2}\left(1-\epsilon^2\frac{\pi^2}{6}\right)\delta(1-\mathrm{x})\delta(1-\mathrm{y})\\ & -\frac{\beta^{-4\epsilon}}{2\bar{\epsilon}}\delta(1-\mathrm{x})\left[\left(\frac{1}{1-\mathrm{y}}\right)_+-\epsilon\left(\frac{\ln\left(\frac{1}{4}(1-\mathrm{y}^2)\right)}{1-\mathrm{y}}\right)_+\right]\\ & -\left[\frac{1}{\bar{\epsilon}}\left(\frac{1}{1-\mathrm{x}}\right)_\rho-2\left(\frac{\ln(1-\mathrm{x})}{1-\mathrm{x}}\right)_\rho\right]\delta(1-\mathrm{y})\\ & +\left(\frac{1}{1-\mathrm{x}}\right)_\rho\left(\frac{1}{1-\mathrm{y}}\right)_+\end{aligned} \tag{5.19}$$

with

$$f(\epsilon) = \frac{(4\pi)^\epsilon \beta^{-4\epsilon}}{\Gamma(1-\epsilon)} \quad , \quad \beta = \sqrt{1-\rho} \quad , \quad \frac{1}{\bar{\epsilon}} = \frac{1}{\epsilon} - \gamma_E + \ln 4\pi \tag{5.20}$$

and the ρ- and +-distributions being defined in appendix B.2. Note the $1/\epsilon^2$-pole, which results from the overlap of the infrared and collinear divergences at $\mathrm{x} = \mathrm{y} = 1$. Furthermore, we find

$$\frac{\overline{M}_{R(a)}(\mathrm{x},1)}{2048\pi^3 \xi S(\hat{s}+Q^2)} = \frac{\alpha_s}{2\pi}(1-\mathrm{x}) K_{ga}(\mathrm{x},Q^2) M_0 \tag{5.21}$$

with

$$K_{gg}(\mathrm{x},Q^2) = \frac{6[Q^4\mathrm{x}^2 + M^2Q^2\mathrm{x}(1+\mathrm{x}) + M^4(1-\mathrm{x}+\mathrm{x}^2)]^2}{(\mathrm{x}-1)(M^2+Q^2)(M^2+Q^2\mathrm{x})^3} \tag{5.22}$$

$$\begin{aligned} K_{gq}(\mathrm{x},Q^2) = &-\frac{4M^2[2M^2Q^2\mathrm{x} + Q^4\mathrm{x}^2 + M^4(2-2\mathrm{x}+\mathrm{x}^2)]}{3(M^2+Q^2)(M^2+Q^2\mathrm{x})^2} \\ &+\epsilon \frac{4M^2(M^2+Q^2)\mathrm{x}^2}{3(M^2+Q^2\mathrm{x})^2} \ . \end{aligned} \tag{5.23}$$

From (5.18),(5.19),(5.21) it follows for $\mu_R^{2\epsilon} M_{R(a)}$

$$\mu_R^{2\epsilon} M_{R(a)} = \mu_R^{2\epsilon} \left(M_{R(a)}^{(\mathrm{x}=1)} + M_{R(a)}^{(\mathrm{y}=1)} + M_{R(a)}^{(\mathrm{finite})} \right) \tag{5.24}$$

with

$$\begin{aligned} \mu_R^{2\epsilon} M_{R(a)}^{(\mathrm{x}=1)} = &\left(\frac{\mu_R^2}{M^2}\right)^\epsilon \frac{f(\epsilon)}{4\epsilon^2} \left(1 - \epsilon^2 \frac{\pi^2}{6}\right) \left[(\mathrm{x}-1) K_{ga}(\mathrm{x},Q^2)\right]_{\mathrm{x}\to 1} \frac{\alpha_s}{\pi} M_B \\ &+ \frac{\beta^{-4\epsilon}}{\bar{\epsilon}} \int_{-1}^{1} \frac{d\mathrm{y}}{4096\pi^3 \xi S(\hat{s}+Q^2)} \left(\frac{\mu_R^2}{M^2}\right)^\epsilon \left[\left(\frac{1}{1-\mathrm{y}}\right)_+ - \epsilon \left(\frac{\ln\left(\frac{1}{4}(1-\mathrm{y}^2)\right)}{1-\mathrm{y}} \right)_+ \right] \\ &\times \overline{M}_{R(a)}(1,\mathrm{y}) \delta(1-\mathrm{x}) + \frac{1}{\bar{\epsilon}} \frac{\alpha_s}{2\pi} \left(\frac{\mu_R^2}{\mu_F^2}\right)^\epsilon b_a M_B \\ = &\begin{cases} \frac{\alpha_s}{\pi} M_B \left[\frac{3C_\epsilon}{2\epsilon^2} + \frac{3C_\epsilon}{2\epsilon} \left(1 - 2\ln(2\beta^2)\right) + 3\left(1 - \ln(2\beta^2) + \ln^2 2 + 4\ln\beta \ln(2\beta) - \frac{\pi^2}{8}\right)\right] \\ + \frac{1}{\bar{\epsilon}} \frac{\alpha_s}{2\pi} \left(\frac{\mu_R^2}{\mu_F^2}\right)^\epsilon b_g M_B \quad , & \text{if} \quad a = g \\ \frac{1}{\bar{\epsilon}} \frac{\alpha_s}{2\pi} \left(\frac{\mu_R^2}{\mu_F^2}\right)^\epsilon b_q M_B \quad , & \text{if} \quad a = q \end{cases} , \end{aligned} \tag{5.25}$$

$$\begin{aligned} \mu_R^{2\epsilon} M_{R(a)}^{(\mathrm{y}=1)} = &\frac{1}{\bar{\epsilon}} \frac{\alpha_s}{2\pi} \left(\frac{\mu_R^2}{\mu_F^2}\right)^\epsilon M_0 \left[\frac{1-\mathrm{x}}{(1-\mathrm{x})_\rho} K_{ga}(\mathrm{x},Q^2) - b_a \delta(1-\mathrm{x}) \right] \\ &+ \frac{\alpha_s}{2\pi} M_0 \left[\ln \frac{\mu_F^2}{\hat{s}} \left(\frac{1}{1-\mathrm{x}}\right)_\rho - 2 \left(\frac{\ln(1-\mathrm{x})}{1-\mathrm{x}} \right)_\rho \right] (1-\mathrm{x}) K_{ga}(\mathrm{x},Q^2) \ , \end{aligned} \tag{5.26}$$

[1]

$$\mu_R^{2\epsilon} M_{R(a)}^{(\mathrm{finite})} = -\left(\frac{1}{1-\mathrm{x}}\right)_\rho \int_{-1}^{1} \frac{d\mathrm{y}}{2048\pi^3 \xi S(\hat{s}+Q^2)} \left(\frac{1}{1-\mathrm{y}}\right)_+ \overline{M}_{R(a)}(\mathrm{x},\mathrm{y}) \ . \tag{5.27}$$

Thereby, C_ϵ is defined as

$$C_\epsilon = \exp(-\epsilon\gamma_E)\left(\frac{16\pi\mu_R^2}{M^2}\right)^\epsilon \ , \tag{5.28}$$

and we neglected terms of the order ϵ. Furthermore, the factorization scale μ_F, which may be different from μ_R, has been introduced by writing

$$\left(\frac{\mu_R^2}{\hat{s}}\right)^\epsilon = \left(\frac{\mu_R^2}{\mu_F^2}\right)^\epsilon \left(\frac{\mu_F^2}{\hat{s}}\right)^\epsilon = \left(\frac{\mu_R^2}{\mu_F^2}\right)^\epsilon \left(1+\epsilon\ln\frac{\mu_F^2}{\hat{s}}\right) + o(\epsilon) \ . \tag{5.29}$$

The parameters b_a, which serve for dividing up the divergent part at $\mathrm{x}=\mathrm{y}=1$ among $M_{R(a)}^{(\mathrm{x}=1)}$ and $M_{R(a)}^{(\mathrm{y}=1)}$, are chosen in such a way, that the (collinear) divergences in $M_{R(a)}^{(\mathrm{y}=1)}$ exhibit the correct factorization behaviour as dictated by the factorization theorem of the QCD improved parton model. The (infrared) divergences in $M_{R(a)}^{(\mathrm{x}=1)}$ should then completely cancel against the infrared and collinear ones in M_V. As no virtual corrections to the light quark initiated subprocesses $e^-q \to e^-c\bar{c}\left[{}^1S_0^{(8)}\right]q$ at $o(\alpha^2\alpha_s^2)$ exist ,which could provide a cancellation of infrared divergences in $M_{R(q)}^{(\mathrm{x}=1)}$, it is clear, that b_q must vanish

$$b_q = 0 \ . \tag{5.30}$$

We will later see, that b_g is given by

$$b_g = \frac{33-2n_f}{6} + 12\ln\beta - 6\ln\frac{M^2+Q^2}{M^2} \ , \tag{5.31}$$

where n_f is the number of active flavours (here $n_f = 3$).

We now come to the factorization of the collinear divergences. First we define a counter term $M_{R(a)}^c$, so that $M_{R(a)}^{(\mathrm{y}=1)} + M_{R(a)}^c$ becomes finite. In the modified minimal subtraction scheme ($\overline{MS}$ scheme) we have

$$\mu_R^{2\epsilon} M_{R(a)}^c = -\frac{1}{\bar{\epsilon}}\frac{\alpha_s}{2\pi}\left(\frac{\mu_R^2}{\mu_F^2}\right)^\epsilon M_0\left[\frac{1-\mathrm{x}}{(1-\mathrm{x})_\rho}\overline{K}_{ga}(\mathrm{x},Q^2) - b_a\delta(1-\mathrm{x})\right] \tag{5.32}$$

with

$$\overline{K}_{gg}(\mathrm{x},Q^2) = K_{gg}(\mathrm{x},Q^2) \ , \tag{5.33}$$

$$\overline{K}_{gq}(\mathrm{x},Q^2) = K_{gq}(\mathrm{x},Q^2) - \epsilon\frac{4M^2(M^2+Q^2)\mathrm{x}^2}{3(M^2+Q^2\mathrm{x})^2} \ . \tag{5.34}$$

We then write the short distance coefficients in the factorized form

$$\frac{d\widehat{\sigma}_a(p,q_\gamma)}{dQ^2dy} = \sum_{b=g,q}\int_0^1 d\xi \frac{d\widehat{\widehat{\sigma}}_a(\xi p,q_\gamma)}{dQ^2dy}\left[\delta_{ba}\delta(1-\xi) - S_{ba}(\xi)\right] \ , \tag{5.35}$$

[1]For reasons of compactness we often write $\frac{1}{(1-\mathrm{x})_\rho}$ instead of $\left(\frac{1}{1-\mathrm{x}}\right)_\rho$ and analogously for +-distributions.

where

$$\frac{d\widehat{\widehat{\sigma}}_a(p,q_\gamma)}{dQ^2dy} = \frac{d\widehat{\sigma}_a(p,q_\gamma)}{dQ^2dy} + M^c_{R(a)}(p,q_\gamma) \tag{5.36}$$

is collinear finite, the collinear divergences being shifted into

$$S_{ba}(\xi) = \frac{1}{\bar{\epsilon}}\frac{\alpha_s}{2\pi}\left(\frac{\mu_R^2}{\mu_F^2}\right)^{\epsilon} P_{ba}(\xi) \tag{5.37}$$

with appropriate splitting functions $P_{ba}(\xi)$, so that (5.35) is valid up to $o(\alpha^2\alpha_s^2)$. Note, that here and in the following we treat $\widehat{\sigma}_a$, $\widehat{\widehat{\sigma}}_a$, M_B, $M_{R(a)}$, M_V and $M^c_{R(a)}$ as functions of p and q_γ. (5.35) is equivalent to

$$\begin{aligned}
&M_B(p,q_\gamma) + \mu_R^{2\epsilon}\left[M_{R(g)}(p,q_\gamma) + M_V(p,q_\gamma)\right] \\
&= \int_0^1 d\xi \left\{\left[M_B(\xi p,q_\gamma) + \mu_R^{2\epsilon}\left(M_{R(g)}(\xi p,q_\gamma) + M_V(\xi p,q_\gamma) + M^c_{R(g)}(\xi p,q_\gamma)\right)\right]\right. \\
&\qquad \times [\delta(1-\xi) - S_{gg}(\xi)] \\
&\qquad \left. -\mu_R^{2\epsilon}\left[M_{R(q)}(\xi p,q_\gamma) + M^c_{R(q)}(\xi p,q_\gamma)\right] S_{gq}(\xi)\right\} \\
&= M_B(p,q_\gamma) + \mu_R^{2\epsilon}\left[M_{R(g)}(p,q_\gamma) + M_V(p,q_\gamma) + M^c_{R(g)}(p,q_\gamma)\right] \\
&\qquad - \int_0^1 d\xi M_B(\xi p,q_\gamma) S_{gg}(\xi) + o(\alpha^2\alpha_s^3)
\end{aligned} \tag{5.38}$$

and

$$\begin{aligned}
\mu_R^{2\epsilon} M_{R(q)}(p,q_\gamma) &= \int_0^1 d\xi \left\{\mu_R^{2\epsilon}\left[M_{R(q)}(\xi p,q_\gamma) + M^c_{R(q)}(\xi p,q_\gamma)\right][\delta(1-\xi) - S_{qq}(\xi)]\right. \\
&\quad - \left[M_B(\xi p,q_\gamma) + \mu_R^{2\epsilon}\left(M_{R(g)}(\xi p,q_\gamma) + M_V(\xi p,q_\gamma) + M^c_{R(g)}(\xi p,q_\gamma)\right)\right] \\
&\quad \left.\times S_{gq}(\xi)\right\} \\
&= \mu_R^{2\epsilon} M_{R(q)}(p,q_\gamma) + \mu_R^{2\epsilon} M^c_{R(q)}(p,q_\gamma) - \int_0^1 d\xi M_B(\xi p,q_\gamma) S_{gq}(\xi) \\
&\quad + o(\alpha^2\alpha_s^3)
\end{aligned} \tag{5.39}$$

resulting in

$$\mu_R^{2\epsilon} M^c_{R(a)}(p,q_\gamma) = \int_0^1 d\xi M_B(\xi p,q_\gamma) S_{ga}(\xi)\ . \tag{5.40}$$

With

$$\begin{aligned}
M_B(\xi p,q_\gamma) &= M_0\delta\left(1 - \frac{M^2}{(\xi p+q_\gamma)^2}\right) \\
&= \frac{M^2\mathrm{x}}{M^2+Q^2\mathrm{x}} M_0\delta\left(\xi - \frac{\mathrm{x}(M^2+Q^2)}{M^2+Q^2\mathrm{x}}\right)\ ,
\end{aligned} \tag{5.41}$$

where

$$\mathrm{x} = \frac{M^2}{\hat{s}} = \frac{M^2}{2pq_\gamma - Q^2} \tag{5.42}$$

or equivalently

$$2pq_\gamma = \frac{M^2 + Q^2\mathrm{x}}{\mathrm{x}} \tag{5.43}$$

has been used, it follows from (5.32), (5.40) for $M^c_{R(a)}$

$$\begin{aligned} P_{ga}(\xi) &= -\frac{M^2+Q^2\mathrm{x}}{M^2\mathrm{x}}\left[\frac{1-\mathrm{x}}{(1-\mathrm{x})_\rho}\overline{K}_{ga}(\mathrm{x},Q^2) - b_a\delta(1-\mathrm{x})\right]\Bigg|_{\mathrm{x}=\mathrm{x}(\xi):=\frac{\xi M^2}{M^2+Q^2(1-\xi)}} \\ &= \frac{1-\mathrm{x}(\xi)}{(1-\mathrm{x}(\xi))_\rho}\overline{P}_{ga}(\xi) + b_a\delta(1-\xi) \end{aligned} \tag{5.44}$$

with

$$\begin{aligned} \overline{P}_{ga}(\xi) &= -\frac{M^2+Q^2\mathrm{x}(\xi)}{M^2\mathrm{x}(\xi)}\overline{K}_{ga}(\mathrm{x}(\xi),Q^2) \\ &= \begin{cases} 6\left[\frac{\xi}{1-\xi} + \frac{1-\xi}{\xi} + \xi(1-\xi)\right] & , \quad \text{if } a = g \\ \frac{4}{3}\frac{1+(1-\xi)^2}{\xi} & , \quad \text{if } a = q\ . \end{cases} \end{aligned} \tag{5.45}$$

Since $\overline{P}_{gq}(\xi)$ is regular at $\xi = 1$ the ρ-distribution in (5.44) for $P_{gq}(\xi)$ can be identified with 1. Using $b_q = 0$ one therefore finds

$$P_{gq}(\xi) = \frac{4}{3}\frac{1+(1-\xi)^2}{\xi}\ . \tag{5.46}$$

As $\overline{P}_{gg}(\xi)$ is singular at $\xi = 1$ the further evaluation of (5.44) is a bit involved. First we convert the ρ-distribution (with respect to x) on the right hand side of (5.44) into a +-distribution (with respect to x), making use of the identity

$$\left(\frac{1}{1-\mathrm{x}}\right)_\rho = \left(\frac{1}{1-\mathrm{x}}\right)_+ - 2\ln\beta\ \delta(1-\mathrm{x})\ . \tag{5.47}$$

In order to verify (5.47) we observe that for any arbitrary regular test function $g(\mathrm{x})$ we have

$$\begin{aligned} &\int_\rho^1 d\mathrm{x}\left(\frac{1}{1-\mathrm{x}}\right)_+ g(\mathrm{x}) = \int_0^1 d\mathrm{x}\left(\frac{1}{1-\mathrm{x}}\right)_+ g(\mathrm{x})\theta(\mathrm{x}-\rho) = \int_0^1 \frac{d\mathrm{x}}{1-\mathrm{x}}\left[g(\mathrm{x})\theta(\mathrm{x}-\rho) - g(1)\right] \\ &= \int_\rho^1 \frac{d\mathrm{x}}{1-\mathrm{x}}\left[g(\mathrm{x}) - g(1)\right] - g(1)\underbrace{\int_0^\rho \frac{d\mathrm{x}}{1-\mathrm{x}}}_{-2\ln\beta} = \int_\rho^1 d\mathrm{x}\left[\left(\frac{1}{1-\mathrm{x}}\right)_\rho + 2\ln\beta\ \delta(1-\mathrm{x})\right] g(\mathrm{x})\ , \end{aligned} \tag{5.48}$$

which proves (5.47). $P_{gg}(\xi)$ then reads

$$P_{gg}(\xi) = \frac{1-\mathrm{x}(\xi)}{(1-\mathrm{x}(\xi))_+}\overline{P}_{gg}(\xi) - 2\ln\beta\ \delta(1-\mathrm{x}(\xi))(1-\mathrm{x}(\xi))\overline{P}_{gg}(\xi) + b_g\ \delta(1-\xi)$$

$$= \frac{1-\mathrm{x}(\xi)}{(1-\mathrm{x}(\xi))_+}\overline{P}_{gg}(\xi) - 2\ln\beta\ \delta(1-\xi)\ \underbrace{\frac{M^2}{M^2+Q^2}\left[(1-\mathrm{x}(\xi))\overline{P}_{gg}(\xi)\right]_{\xi\to 1}}_{6} + b_g\ \delta(1-\xi)$$

$$= \frac{1-\mathrm{x}(\xi)}{(1-\mathrm{x}(\xi))_+}\overline{P}_{gg}(\xi) + (b_g - 12\ln\beta)\ \delta(1-\xi)\ . \tag{5.49}$$

We now have to rewrite the +-distribution with respect to x in terms of distributions with respect to ξ. Let $g(\xi)$ be an arbitrary regular test function. Then we have

$$\begin{aligned}
&\int_0^1 d\xi \frac{1-\mathrm{x}(\xi)}{(1-\mathrm{x}(\xi))_+}\overline{P}_{gg}(\xi)g(\xi) \\
&= \int_0^1 \frac{d\mathrm{x}(\xi)}{\mathrm{x}'(\xi)}\frac{1-\mathrm{x}(\xi)}{(1-\mathrm{x}(\xi))_+}\overline{P}_{gg}(\xi)g(\xi) \\
&= \int_0^1 \frac{d\mathrm{x}(\xi)}{1-\mathrm{x}(\xi)}\left[\frac{1-\mathrm{x}(\xi)}{\mathrm{x}'(\xi)}\overline{P}_{gg}(\xi)g(\xi) - \frac{\left[(1-\mathrm{x}(\xi))\overline{P}_{gg}(\xi)\right]_{\xi\to 1} g(1)}{\mathrm{x}'(1)}\right] \\
&= \int_0^1 \frac{d\mathrm{x}(\xi)}{\mathrm{x}'(\xi)}\left[\overline{P}_{gg}(\xi)g(\xi) - \frac{\mathrm{x}'(\xi)}{\mathrm{x}'(1)}\frac{\left[(1-\mathrm{x}(\xi))\overline{P}_{gg}(\xi)\right]_{\xi\to 1} g(1)}{1-\mathrm{x}(\xi)}\right] \\
&= \int_0^1 \frac{d\xi}{1-\xi}\left[\ (1-\xi)\overline{P}_{gg}(\xi)g(\xi) - \underbrace{\frac{\mathrm{x}'(\xi)(1-\xi)}{\mathrm{x}'(1)(1-\mathrm{x}(\xi))}\left[(1-\mathrm{x}(\xi))\overline{P}_{gg}(\xi)\right]_{\xi\to 1}}_{\frac{6M^2}{M^2+Q^2(1-\xi)}} g(1)\ \right] \\
&= \int_0^1 \frac{d\xi}{1-\xi}\left[\ (1-\xi)\overline{P}_{gg}(\xi)g(\xi) - \frac{M^2}{M^2+Q^2(1-\xi)}\underbrace{\left[(1-\xi)\overline{P}_{gg}(\xi)\right]_{\xi\to 1}}_{6} g(1)\ \right] \\
&= \int_0^1 \frac{d\xi}{1-\xi}\left[(1-\xi)\overline{P}_{gg}(\xi)g(\xi) - \left[(1-\xi)\overline{P}_{gg}(\xi)\right]_{\xi\to 1} g(1)\right] \\
&\quad +6\underbrace{\int_0^1 d\xi \frac{Q^2}{M^2+Q^2(1-\xi)}}_{\ln\frac{M^2+Q^2}{M^2}} g(1) \\
&= \int_0^1 d\xi\left[\frac{1-\xi}{(1-\xi)_+}\overline{P}_{gg}(\xi) + 6\ln\frac{M^2+Q^2}{M^2}\ \delta(1-\xi)\right] g(\xi)\ ,
\end{aligned} \tag{5.50}$$

and consequently

$$\frac{1-\mathrm{x}(\xi)}{(1-\mathrm{x}(\xi))_+}\overline{P}_{gg}(\xi) = \frac{1-\xi}{(1-\xi)_+}\overline{P}_{gg}(\xi) + 6\ln\frac{M^2+Q^2}{M^2}\ \delta(1-\xi)\ . \tag{5.51}$$

Inserting this result in (5.49), using (5.45) for $\overline{P}_{gg}(\xi)$ and choosing b_g as anticipated in (5.31) we find

$$P_{gg}(\xi) = 6\left[\frac{\xi}{(1-\xi)_+} + \frac{1-\xi}{\xi} + \xi(1-\xi)\right] + \frac{33-2n_f}{6}\ \delta(1-\xi)\ . \tag{5.52}$$

The found quark gluon and gluon gluon splitting functions $P_{qg}(\xi)$, $P_{gg}(\xi)$ given in (5.46), (5.52) have the correct universal form, demanded by the factorization theorem of the QCD improved parton model. We complete the factorization of the collinear divergences by absorbing the factor $\delta_{ba}\delta(1-\xi) - S_{ba}(\xi)$ in (5.36) into the parton density functions of the nucleon. Convoluting both sides of (5.36) with $\widehat{F}_N^a(\xi)$ yields

$$\sum_a \int_0^1 d\xi \frac{d\widehat{\sigma}}{dQ^2 dy}(\xi P_N, q_\gamma)\widehat{F}_N^a(\xi) = \sum_a \int_0^1 d\xi \frac{d\widehat{\widehat{\sigma}}}{dQ^2 dy}(\xi P_N, q_\gamma) F_N^a(\xi, \mu_F^2) \ , \tag{5.53}$$

where the redefined (physical) parton density functions $F_N^a(\xi, \mu_F^2)$ are related to the original (unphysical) ones by

$$F_N^a(\xi, \mu_F^2) = \widehat{F}_N^a(\xi) - \frac{1}{\bar{\epsilon}}\frac{\alpha_s}{2\pi}\left(\frac{\mu_R^2}{\mu_F^2}\right)^{\epsilon} \sum_b \int_\xi^1 \frac{d\xi'}{\xi'} P_{ba}(\xi')\widehat{F}_N^a\left(\frac{\xi}{\xi'}\right) \ . \tag{5.54}$$

Applying $\mu_F^2 \frac{\partial}{\partial \mu_F^2}$ on both sides of this equation and neglecting terms of the order ϵ or $\alpha^2\alpha_s^3$ we recover the famous Altarelli Parisi equations

$$\mu_F^2 \frac{\partial}{\partial \mu_F^2} F_N^a(\xi, \mu_F^2) = \frac{\alpha_s}{2\pi} \sum_b \int_\xi^1 \frac{d\xi'}{\xi'} P_{ba}(\xi') F_N^a\left(\frac{\xi}{\xi'}, \mu_F^2\right) \tag{5.55}$$

for the scaling of the $F_N^a(\xi, \mu_F^2)$.

We close this section by summarizing our final results for the real corrections after factorization of the collinear divergences:

$$\begin{aligned}
\mu_R^{2\epsilon}\left(M_{R(g)} + M^c_{R(g)}\right) = \frac{\alpha_s}{\pi} M_0 \Bigg\{ & \left[\frac{3C_\epsilon}{2\epsilon^2} + \frac{3C_\epsilon}{2\epsilon}\left(\frac{51-2n_f}{18} - 2\ln\frac{2(M^2+Q^2)}{M^2}\right)\right. \\
& - \ln\frac{\mu_F^2}{m^2}\left(\frac{33-2n_f}{12} + 6\ln\beta - 3\ln\frac{M^2+Q^2}{M^2}\right) \\
& \left. +3\left(1 - \ln(2\beta^2) + \ln^2 2 + 4\ln\beta\ln(2\beta) - \frac{\pi^2}{8}\right)\right]\delta(1-\mathrm{x}) \\
& + \left[\frac{1}{2}\ln\frac{\mu_F^2}{\hat{s}}\left(\frac{1}{1-\mathrm{x}}\right)_\rho - \left(\frac{\ln(1-\mathrm{x})}{1-\mathrm{x}}\right)_\rho\right](1-\mathrm{x})K_{gg}(\mathrm{x}, Q^2) \\
& + \left(\frac{1}{1-\mathrm{x}}\right)_\rho f_g\left[{}^1S_0^{(8)}\right]\Bigg\}
\end{aligned} \tag{5.56}$$

and

$$\mu_R^{2\epsilon}\left(M_{R(q)} + M^c_{R(q)}\right) = \frac{\alpha_s}{\pi} M_0 \left[\frac{1}{2}\ln\frac{\mu_F^2}{\hat{s}(1-\mathrm{x})^2}K_{gq}(\mathrm{x}, Q^2) + \frac{2M^2(M^2+Q^2)\mathrm{x}^2}{3(M^2+Q^2\mathrm{x})^2} + f_q\left[{}^1S_0^{(8)}\right]\right] \ . \tag{5.57}$$

Thereby, the $f_a\left[{}^1S_0^{(8)}\right]$ are defined by

$$\frac{\alpha_s}{\pi} M_0 f_a\left[{}^1S_0^{(8)}\right] = -\int_{-1}^1 \frac{d\mathrm{y}}{2048\pi^3\xi S(\hat{s}+Q^2)}\left(\frac{1}{1-\mathrm{y}}\right)_+ \overline{M}_{R(a)}(\mathrm{x}, \mathrm{y}) \ . \tag{5.58}$$

The y-integration can be performed analytically, the results being given in (B.31)-(B.35). In (5.57) we exploited, that $K_{gq}(\mathrm{x}, Q^2)$, $\overline{K}_{gq}(\mathrm{x}, Q^2)$ and $f_q\left[{}^1S_0^{(8)}\right]$ are regular at $\mathrm{x} = 1$.

5.1.2 The virtual corrections

As next we turn to the virtual corrections. The diagrams, which contribute to $\mathcal{M}_{\mathrm{V}}$ at order $e^2 g_s^3$, are shown in Fig. 5.1. The diagrams a and b represent the leading order self

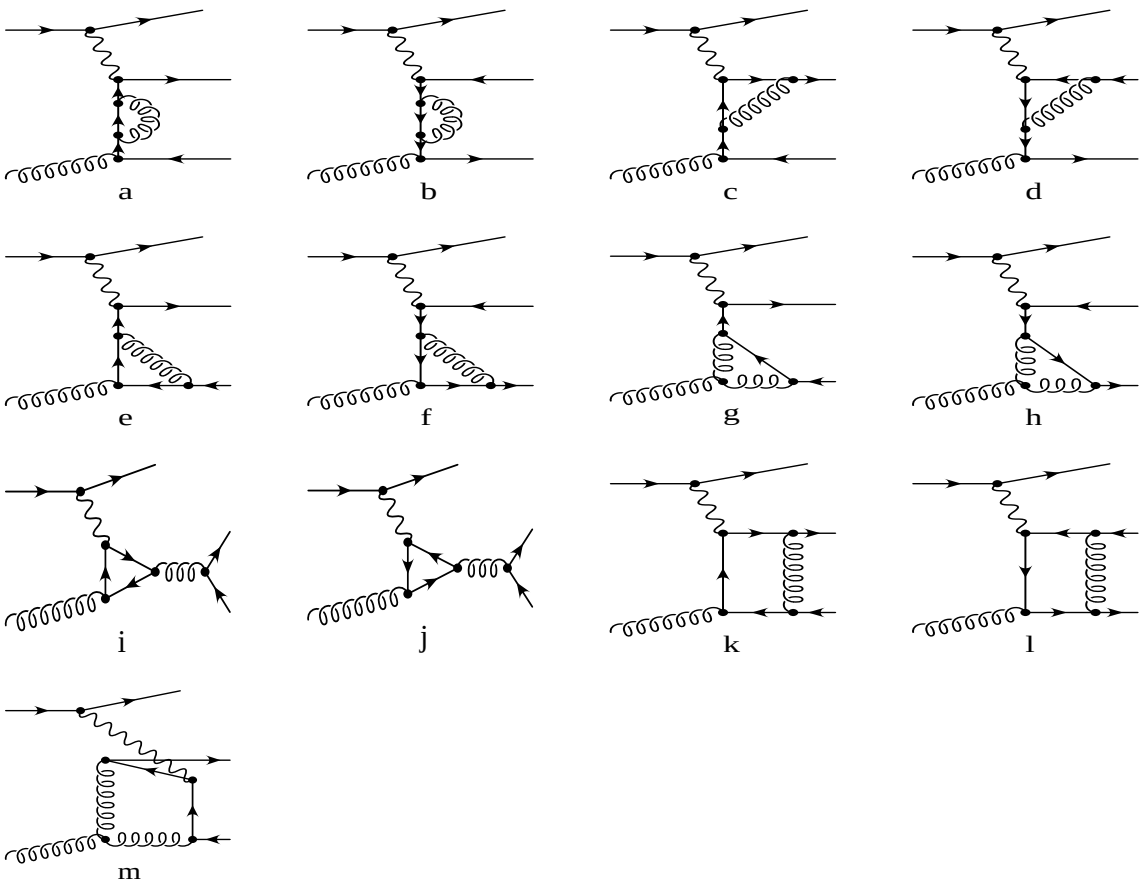

Figure 5.1: Feynman diagrams for the virtual corrections to the partonic subprocess $e^- g \to e^- c\bar{c}$.

energy corrections to the heavy quark mass, while the diagrams c-h represent the leading order vertex corrections. The triangle diagrams i and j with the fermion circulating in the loop being one of the light quarks u,d,s do not contribute, since the gluons in these diagrams behave abelian, so that due to the Furry theorem the corresponding amplitudes add up to zero. As for the occuring divergences, the amplitudes corresponding to the diagrams a-h are all ultraviolet divergent, those belonging to the diagrams g and h being additionally infrared and collinear divergent. The amplitudes corresponding to the box

diagrams k-m are ultraviolet finite but infrared divergent, that belonging to the diagram m being additionally collinear divergent. Finally the amplitudes, which belong to the diagrams k and l, in addition contain a Coulomb divergence. Note, that as a consequence of our choice for the renormalization conditions (see below) self energy corrections to external fields are not considered here.

As already mentioned, the Coulomb divergence is regularized by assigning an infinitesimal velocity v to the heavy quarks in the quarkonium rest frame. This means, that the Coulomb divergent amplitudes corresponding to the diagrams k and l are not calculated for $q = 0$ (with q being the momentum defined in (3.8)) but are calculated under consideration of the identities

$$q^2 = -m^2 v^2 \ , \tag{5.59}$$

$$P^2 = M^2(1 + v^2) \ , \tag{5.60}$$

$$Pq = 0 \ , \tag{5.61}$$

$$pq = -\frac{\hat{s} + Q^2}{2\sqrt{\hat{s}}} m \ v \cos\theta = -\frac{1}{4}(M^2 + Q^2) \ v \ \cos\theta + o(v^3) \ . \tag{5.62}$$

Here θ is the angle between the momenta $\vec{p}$ and $\vec{q} \equiv m\vec{v}$ in the quarkonium rest frame. In accordance with what one expects from rotation symmetry it is later found, that the θ dependence of the total result for M_V completely cancels out. (5.59)-(5.62) are immediately obtained in the quarkonium rest frame, noting, that $\vec{p} + \vec{q}_\gamma = \vec{P} = 0$ and $p_c^2 = \bar{p}_c^2 = m^2$ (with the heavy quark and antiquark momentum now denoted by p_c and $\bar{p}_c$ instead of p and $\bar{p}$ to avoid confusion with the gluon momentum) implies

$$q = \begin{pmatrix} 0 \\ \vec{q} \end{pmatrix} \equiv \begin{pmatrix} 0 \\ m\vec{v} \end{pmatrix} \ , \tag{5.63}$$

$$P = \begin{pmatrix} 2\sqrt{m^2 + \vec{q}^2} \\ \vec{0} \end{pmatrix} \equiv \begin{pmatrix} M\sqrt{1 + v^2} \\ \vec{0} \end{pmatrix} \ , \tag{5.64}$$

$$|\vec{p}| = |\vec{q}_\gamma| = \frac{\hat{s} + Q^2}{2\sqrt{\hat{s}}} \ . \tag{5.65}$$

In connection with the loops in the diagrams contributing to $\mathcal{M}_{\mathrm{V}}$ we have to deal with one loop $n = 2, 3, 4$ point tensor integrals

$$I^{\mu_1 \mu_2 ... \mu_m}(p_1, p_2, ..., p_{n-1}, m_0, m_1, ..., m_{n-1})$$

$$= \int \frac{d^D l}{(2\pi)^D} \frac{l^{\mu_1} l^{\mu_2} ... l^{\mu_m}}{[l^2 - m_0^2 + i\epsilon][(p_1 + l)^2 - m_1^2 + i\epsilon]...[(p_{n-1} + l)^2 - m_{n-1}^2 + i\epsilon]} \ ;$$

$$m = 0, 1, 2, ..., n \ ; \ n = 2, 3, 4 \ , \tag{5.66}$$

which, making use of the method of Passarino and Veltman[64], can be reduced to the one loop 2, 3 and 4 point scalar integrals

$$B_0(p_1, m_0, m_1) = \int \frac{d^D l}{(2\pi)^D} \frac{1}{[l^2 - m_0^2 + i\epsilon][(p_1 + l)^2 - m_1^2 + i\epsilon]} \ , \tag{5.67}$$

$$C_0(p_1, p_2, m_0, m_1, m_2) = \int \frac{d^D l}{(2\pi)^D} \frac{1}{[l^2 - m_0^2 + i\epsilon][(p_1 + l)^2 - m_1^2 + i\epsilon][(p_2 + l)^2 - m_2^2 + i\epsilon]} \ , \tag{5.68}$$

$$D_0(p_1, p_2, p_3, m_0, m_1, m_2, m_3) =$$

$$\int \frac{d^D l}{(2\pi)^D} \frac{1}{[l^2 - m_0^2 + i\epsilon][(p_1 + l)^2 - m_1^2 + i\epsilon][(p_2 + l)^2 - m_2^2 + i\epsilon][(p_3 + l)^2 - m_3^2 + i\epsilon]} \ . \tag{5.69}$$

Here p_1, p_2, p_3 are linear combinations of the four momenta p, q_γ, P, q, furthermore l denotes the loop momentum and m_0, m_1, m_2, m_3 are the masses (and l, $p_1 + l$, $p_2 + l$, $p_3 + l$ the four momenta) of the particles propagating in the loop. For the B_0, C_0 and D_0 functions, which are encountered here, we find the following analytical results (we pass on presenting the corresponding derivations as that would become too lengthy):

$$\mu_R^{2\epsilon} B_0(p, 0, 0) = \frac{i}{16\pi^2} \left(\frac{1}{\bar{\epsilon}_{UV}} - \frac{1}{\bar{\epsilon}} \right) \equiv 0 \ , \tag{5.70}$$

$$\mu_R^{2\epsilon} B_0(p, 0, m) = \frac{i}{16\pi^2} \left(\frac{1}{\bar{\epsilon}_{UV}} + \ln \frac{\mu_R^2}{m^2} + 1 \right) \ , \tag{5.71}$$

$$\mu_R^{2\epsilon} B_0\left(\frac{P}{2}, 0, m\right) = \frac{i}{16\pi^2} \left(\frac{1}{\bar{\epsilon}_{UV}} + \ln \frac{\mu_R^2}{m^2} + 2 \right) \ , \tag{5.72}$$

$$\mu_R^{2\epsilon} B_0(q_\gamma, m, m) = \frac{i}{16\pi^2} \left(\frac{1}{\bar{\epsilon}_{UV}} + \ln \frac{\mu_R^2}{m^2} - 2\sqrt{\frac{M^2 + Q^2}{Q^2}} \ln \frac{\sqrt{M^2 + Q^2} + \sqrt{Q^2}}{M} + 2 \right) \ , \tag{5.73}$$

$$\mu_R^{2\epsilon} B_0\left(\frac{P}{2} - p, 0, m\right) = \frac{i}{16\pi^2} \left(\frac{1}{\bar{\epsilon}_{UV}} + \ln \frac{\mu_R^2}{m^2} - 2\frac{M^2 + Q^2}{M^2 + 2Q^2} \ln \frac{2(M^2 + Q^2)}{M^2} + 2 \right) \ , \tag{5.74}$$

$$\mu_R^{2\epsilon} C_0\left(-p, \frac{P}{2} - p, 0, 0, m\right) = -\frac{iC_\epsilon}{16\pi^2} \frac{1}{M^2 + Q^2} \left[\frac{1}{\epsilon^2} - \frac{2}{\epsilon} \ln \frac{2(M^2 + Q^2)}{M^2} + \ln^2 \frac{2(M^2 + Q^2)}{M^2} - 2\mathrm{Li}_2\left(\frac{M^2 + 2Q^2}{2(M^2 + Q^2)} \right) + \frac{\pi^2}{12} \right] \ , \tag{5.75}$$

$$\mu_R^{2\epsilon} C_0\left(-p, \frac{P}{2} - p, m, m, 0\right) = \frac{i}{8\pi^2} \frac{1}{M^2 + Q^2} \left[\mathrm{Li}_2\left(-\frac{M^2 + 2Q^2}{M^2} \right) - \frac{\pi^2}{6} \right] \ , \tag{5.76}$$

$$\mu_R^{2\epsilon} C_0\left(p,P,m,m,m\right) = \frac{i}{16\pi^2}\frac{1}{M^2+Q^2}\left[\mathrm{Li}_2\left(\frac{2\sqrt{Q^2}}{\sqrt{M^2+Q^2}+\sqrt{Q^2}}\right)\right.$$
$$\left.+\mathrm{Li}_2\left(\frac{-2\sqrt{Q^2}}{\sqrt{M^2+Q^2}-\sqrt{Q^2}}\right)-\frac{\pi^2}{2}\right]\ , \tag{5.77}$$

$$\mu_R^{2\epsilon} C_0\left(p,\frac{P}{2},0,0,m\right) = \mu_R^{2\epsilon} C_0\left(-p,\frac{P}{2}-p,0,0,m\right)$$
$$= -\frac{iC_\epsilon}{16\pi^2}\frac{1}{M^2+Q^2}\left[\frac{1}{\epsilon^2}-\frac{2}{\epsilon}\ln\frac{2(M^2+Q^2)}{M^2}\right.$$
$$\left.+\ln^2\frac{2(M^2+Q^2)}{M^2}-2\mathrm{Li}_2\left(\frac{M^2+2Q^2}{2(M^2+Q^2)}\right)+\frac{\pi^2}{12}\right]\ , \tag{5.78}$$

$$\mu_R^{2\epsilon} C_0\left(p,\frac{P}{2},m,m,0\right) = \mu_R^{2\epsilon} C_0\left(-p,\frac{P}{2}-p,m,m,0\right)$$
$$= \frac{i}{8\pi^2}\frac{1}{M^2+Q^2}\left[\mathrm{Li}_2\left(-\frac{M^2+2Q^2}{M^2}\right)-\frac{\pi^2}{6}\right]\ , \tag{5.79}$$

$$\mu_R^{2\epsilon} C_0\left(P,\frac{P}{2}\pm q,m,m,0\right) = -\frac{iC_\epsilon}{8\pi^2}\frac{1}{M^2}\left(\frac{\pi^2}{2v}+\frac{1}{\epsilon}-2+i\pi\frac{\ln(2v)}{v}\right)\ , \tag{5.80}$$

$$\mu_R^{2\epsilon} C_0\left(q_\gamma,\frac{P}{2},m,m,0\right) = \mu_R^{2\epsilon} C_0\left(-q_\gamma,\frac{P}{2}-q_\gamma,m,m,0\right)$$
$$= \frac{i}{8\pi^2}\frac{1}{M^2+Q^2}\left[\mathrm{Li}_2\left(\frac{2\sqrt{Q^2}}{\sqrt{M^2+Q^2}+\sqrt{Q^2}}\right)\right.$$
$$\left.+\mathrm{Li}_2\left(\frac{-2\sqrt{Q^2}}{\sqrt{M^2+Q^2}-\sqrt{Q^2}}\right)-\mathrm{Li}_2\left(-\frac{M^2+2Q^2}{M^2}\right)-\frac{\pi^2}{3}\right]\ , \tag{5.81}$$

$$\mu_R^{2\epsilon} D_0\left(-p,\frac{P}{2}-p,-\frac{P}{2},0,0,m,m\right) = \frac{iC_\epsilon}{4\pi^2}\frac{1}{(M^2+Q^2)^2}\left[\frac{1}{\epsilon^2}-\frac{2}{\epsilon}\ln\frac{2(M^2+Q^2)}{M^2}\right.$$
$$\left.+2\ln^2\frac{2(M^2+Q^2)}{M^2}-\ln^2\frac{\sqrt{M^2+Q^2}-\sqrt{Q^2}}{\sqrt{M^2+Q^2}+\sqrt{Q^2}}-\frac{7\pi^2}{12}\right]\ , \tag{5.82}$$

$$\mu_R^{2\epsilon} D_0\left(p,P,\frac{P}{2}\pm q,m,m,m,0\right) = \frac{iC_\epsilon}{4\pi^2}\frac{1}{M^2(M^2+Q^2)}\left[\frac{\pi^2}{2v}+\frac{1}{\epsilon}-2+\ln 2\right.$$
$$\left.-2\ln\frac{M^2+Q^2}{m^2}-2\sqrt{\frac{Q^2}{M^2+Q^2}}\ln\frac{\sqrt{M^2+Q^2}-\sqrt{Q^2}}{\sqrt{M^2+Q^2}+\sqrt{Q^2}}\right]\ . \tag{5.83}$$

Thereby, Li_2 denotes the dilogarithm, which is defined by $\mathrm{Li}_2(x)=\int_1^{1-x} dz\frac{\ln z}{1-z}$. Furthermore, poles in ϵ, which originate from UV divergent integrals, have been labelled by 'UV'. The residual unlabelled poles in ϵ then represent the infrared and collinear divergences. By an overlap of the latters the $1/\epsilon^2$ poles in (5.75), (5.78), (5.82) are produced. Note,

that the Coulomb divergence enters the calculation through (5.80), (5.83) in form of a $1/v$ pole.

In order to get rid of the ultraviolet divergences the (full relativistic) heavy quark wave function ψ, the gluon wave function A, the heavy quark mass m and the strong coupling constant g_s require renormalization. This means, ψ, A, m, g_s are redefined according to

$$\psi \to Z_\psi^{\frac{1}{2}} \psi \tag{5.84}$$

$$A \to Z_A^{\frac{1}{2}} A \tag{5.85}$$

$$m \to Z_m \, m \tag{5.86}$$

$$g_s \to Z_g \, g_s \ . \tag{5.87}$$

By the requirement, that all the divergences occurring in QCD are absorbed into the redefined (physical) parameters and fields, the renormalization constants Z_i with $i = \psi, A, m, g$ are uniquely determined up to finite renormalizations. The finite parts of the Z_i are fixed by the special choice for the renormalization scheme. Since the ultraviolet divergent contributions are suppressed by one order in α_s compared to the Born level, the Z_i can be written in the form $Z_i = 1 + \delta Z_i$ with the δZ_i being of the order α_s. We renormalize the heavy quark wave function and mass in the onshell scheme, which is the most natural choice in case of a massive particle, and the gluon wave function and the strong coupling constant in the $\overline{MS}$ scheme. The δZ_i then read

$$\delta Z_\psi = -\frac{\alpha_s}{\pi} \left(\frac{1}{3\bar{\epsilon}_{UV}} + \frac{2}{3\epsilon} + \ln \frac{\mu_R^2}{m^2} + \frac{4}{3} \right) \ , \tag{5.88}$$

$$\delta Z_m = -\frac{\alpha_s}{\pi} \left(\frac{1}{\bar{\epsilon}_{UV}} + \ln \frac{\mu_R^2}{m^2} + \frac{4}{3} \right) \ , \tag{5.89}$$

$$\delta Z_A = \frac{\alpha_s}{\pi} \frac{15 - 2n_f}{12} \left(\frac{1}{\bar{\epsilon}_{UV}} - \frac{1}{\bar{\epsilon}} \right) \equiv 0 \ , \tag{5.90}$$

$$\delta Z_g = -\frac{\alpha_s}{\pi} \frac{33 - 2n_f}{24} \frac{1}{\bar{\epsilon}_{UV}} \ . \tag{5.91}$$

Concerning the renormalization conditions we should go more into detail. Let $i\Sigma(p_c) = i\left(\not{p}_c \Sigma_V(p_c^2) + m\Sigma_S(p_c^2)\right)$ be the heavy quark self energy defined as the amplitude belonging to the Feynman diagram

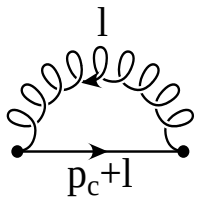

.

The radiatively corrected heavy quark propagator $P = \int \frac{d^D x}{(2\pi)^D} \exp(ip_c x) \langle 0 | T\psi(x)\bar{\psi}(0)|0\rangle$ then reads

$$P = \frac{i}{\not{p}_c - m + \not{p}_c(\Sigma_V(p_c^2) + \delta Z_\psi) + m(\Sigma_S(p_c^2) - \delta Z_\psi - \delta Z_m)} \ . \tag{5.92}$$

In the onshell scheme the pole of P is demanded to be located at the renormalized (physical) mass m, that is

$$\lim_{p_c^2 \to m^2} P^{-1} u(p_c) = 0 \ . \tag{5.93}$$

Due to the Dirac equation

$$\not{p}_c u(p_c) = m u(p_c) \ , \tag{5.94}$$

which holds for $p_c^2 = m^2$, (5.93) is equivalent to

$$\delta Z_m = \Sigma_V(m^2) + \Sigma_S(m^2) \ , \tag{5.95}$$

which after further evaluation yields (5.89). Furthermore in the onshell scheme the residuum of P at $\not{p}_c = m$ is demanded to be i, that is

$$\lim_{p_c^2 \to m^2} \frac{i}{\not{p}_c - m} P^{-1} u(p_c) = u(p_c) \ . \tag{5.96}$$

With (5.94) for $p_c^2 = m^2$ this condition is equivalent to

$$\lim_{p_c^2 \to m^2} \frac{1}{\not{p}_c - m} \left[\not{p}_c (\Sigma_V(p_c^2) + \delta Z_\psi) + m(\Sigma_S(p_c^2) - \delta Z_\psi - \delta Z_m) \right] u(p_c) = 0 \ . \tag{5.97}$$

The left hand side of this equation may be written

$$\begin{aligned}
&\lim_{p_c^2 \to m^2} \frac{\not{p}_c + m}{p_c^2 - m^2} \left[\not{p}_c (\Sigma_V(p_c^2) + \delta Z_\psi) + m(\Sigma_S(p_c^2) - \delta Z_\psi - \delta Z_m) \right] u(p_c) \\
&= \lim_{p_c^2 \to m^2} \frac{1}{p_c^2 - m^2} \Big[\ (p_c^2 - m^2)(\Sigma_V(p_c^2) + \delta Z_\psi) + m(\not{p}_c + m) \Big(\underbrace{\Sigma_V(m^2) + \Sigma_S(m^2) - \delta Z_m}_{=0, \text{ because of (5.95)}} \\
&\quad + (p_c^2 - m^2) \left(\Sigma_V'(m^2) + \Sigma_S'(m^2) \right) + o\left((p_c^2 - m^2)^2 \right) \Big) \Big] u(p_c) \\
&= \lim_{p_c^2 \to m^2} \left[\delta Z_\psi + \Sigma_V(p_c^2) + m(\not{p}_c + m) \left(\Sigma_V'(m^2) + \Sigma_S'(m^2) \right) + o(p_c^2 - m^2) \right] u(p_c) \\
&= \left[\delta Z_\psi + \Sigma_V(m^2) + 2m^2 \left(\Sigma_V'(m^2) + \Sigma_S'(m^2) \right) \right] u(p_c) \ ,
\end{aligned} \tag{5.98}$$

where in the last line we again exploited the Dirac equation. Hence it follows

$$\delta Z_\psi = -\Sigma_V(m^2) - 2m^2 \left(\Sigma_V'(m^2) + \Sigma_S'(m^2) \right) \ , \tag{5.99}$$

which after further evaluation yields (5.88). (5.97) can also be written

$$\lim_{p_c^2 \to m^2} \left[\frac{i}{\not{p}_c - m} i\Sigma(p_c) u(p_c) + \frac{i}{\not{p}_c - m} \left(i\delta Z_\psi (\not{p}_c - m) - i\delta Z_m m \right) u(p_c) \right] = 0 \tag{5.100}$$

or diagramatically

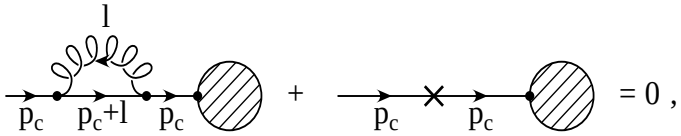

(5.101)

where the hatched circle stands for the rest of the process. This means, that in the onshell scheme the self energy correction to an external heavy quark line is exactly compensated by the additional counter term contributions, which arise from the heavy quark wave function and mass renormalization and which are symbolized by the cross in the second diagram in (5.101). This is the reason, why we ignore diagrams with self energy corrections to the outgoing heavy quark or antiquark in our calculation. As for the renormalization of the gluon wave function in the $\overline{MS}$ scheme, δZ_A in (5.90) should in principle only contain the $1/\bar{\epsilon}_{UV}$ pole term. But since per definition diagrams containing self energy corrections to the external gluon leg are excluded from the calculation the gluon wave function is per definition not renormalized.Thus the ultraviolet finite part of δZ_A is chosen to exactly compensate the $1/\bar{\epsilon}_{UV}$ pole, as is the case in (5.90). Finally, δZ_g is minimally defined in the original sense of $\overline{MS}$ subtraction[2].

It is interesting to study the scaling behaviour of g_s, m and ψ induced by our renormalization conditions. Due to (5.91) the unrenormalized (dimensionfull) coupling $\hat{g}_s$ is related to the renormalized (dimensionless) one according to

$$\hat{g}_s = \left[1 - \beta g_s^2 \frac{1}{\bar{\epsilon}}\right] g_s \mu_R^{\epsilon} \qquad \text{with} \qquad \beta = \frac{33 - 2n_f}{96\pi^2} \ , \tag{5.102}$$

where we now refrain from the label 'UV'. Applying $\mu_R \frac{\partial}{\partial \mu_R}$ on both sides of this equation and noting, that $\hat{g}_s$ is independent of μ_R, it is obtained

$$0 = \mu_R \frac{\partial g_s}{\partial \mu_R} + \epsilon g_s - 3\beta g_s^2 \mu_R \frac{\partial g_s}{\partial \mu_R} \frac{1}{\bar{\epsilon}} - \beta g_s^3 \frac{\epsilon}{\bar{\epsilon}} \ , \tag{5.103}$$

or equivalently

$$\mu_R \frac{\partial g_s}{\partial \mu_R} = -\epsilon g_s + 3\beta g_s^2 \mu_R \frac{\partial g_s}{\partial \mu_R} \frac{1}{\bar{\epsilon}} + \beta g_s^3 \frac{\epsilon}{\bar{\epsilon}} \ . \tag{5.104}$$

Inserting this equation in itself and neglecting terms of order higher than g_s^3 we obtain the leading order renormalization group equation for g_s

$$\begin{aligned} \mu_R \frac{\partial g_s}{\partial \mu_R} &= -\epsilon g_s - 2\beta g_s^3 (1 - \epsilon\gamma_E + \epsilon \ln 4\pi) \\ &= -2\beta g_s^3 \ . \end{aligned} \tag{5.105}$$

As solution of this differential equation it is found as leading order formula for the running coupling constant

$$\alpha_s(\mu_R) = \frac{12\pi}{(33 - 2n_f) \ln \frac{\mu_R^2}{\Lambda_{QCD}^2}} \ , \tag{5.106}$$

where Λ_{QCD} plays the role of the integration constant. Due to (5.89) the unrenormalized mass $\widehat{m}$ is related to the renormalized mass m by

$$\widehat{m} = \left[1 - \frac{g_s^2}{4\pi^2} \left(\frac{1}{\bar{\epsilon}} + \ln \frac{\mu_R^2}{m^2} + \frac{4}{3}\right)\right] m \ . \tag{5.107}$$

[2]The calculation of the renormalization constants in the $\overline{MS}$ scheme may be found in standard textbooks, see for example [65].

Applying again $\mu_R \frac{\partial}{\partial \mu_R}$ on both sides of this equation and noting, that $\widehat{m}$ does not depend on μ_R, it follows

$$0 = \mu_R \frac{\partial m}{\partial \mu_R} \left[1 - \frac{g_s^2}{4\pi} \left(\frac{1}{\bar{\epsilon}} + \ln \frac{\mu_R^2}{m^2} + \frac{4}{3} \right) \right] - \frac{g_s}{2\pi^2} \, \mu_R \frac{\partial g_s}{\partial \mu_R} \left(\frac{1}{\bar{\epsilon}} + \ln \frac{\mu_R^2}{m^2} + \frac{4}{3} \right) m - \frac{g_s^2}{2\pi^2} m \ . \tag{5.108}$$

Inserting the first line of (5.105) and neglecting terms of order higher than g_s^3 and terms of order ϵ, we get

$$\mu_R \frac{\partial m}{\partial \mu_R} \left[1 - \frac{g_s^2}{4\pi^2} \left(\frac{1}{\bar{\epsilon}} + \ln \frac{\mu_R^2}{m^2} + \frac{4}{3} \right) \right] = 0 \tag{5.109}$$

and consequently

$$\mu_R \frac{\partial m}{\partial \mu_R} = 0 \ . \tag{5.110}$$

Analogously it is found

$$\mu_R \frac{\partial \psi}{\partial \mu_R} = 0 \ . \tag{5.111}$$

Thus in the onshell renormalization scheme the renormalized heavy quark mass and wave function turn out to be scale independent. For completeness it should be mentioned, that, for the trivial reason, that the gluon wave function A is not renormalized, A is also scale independent.

The net effect of the renormalizations given in (5.84)-(5.87) consists in adding a total counter term $\mathcal{M}_{\rm V}^{\rm c}$ to $\mathcal{M}_{\rm V}$ or equivalently $M_V^c = 2{\rm Re}\left[\mathcal{M}_{\rm B}^{\dagger}\mathcal{M}_{\rm V}^{\rm c}\right]$ to M_V with $\mathcal{M}_{\rm V}^{\rm c}$ given by

$$\mathcal{M}_{\rm V}^{\rm c} = \left(1 + \delta Z_\psi + \frac{1}{2}\delta Z_A + \delta Z_g\right) \mathcal{M}_{\rm B} \Big|_{m \to m(1+\delta Z_m)} - \mathcal{M}_{\rm B} \ . \tag{5.112}$$

Our final result for the virtual corrections reads

$$\mu_R^{2\epsilon} \left(M_V + M_V^c\right) = \frac{\alpha_s}{\pi} M_B \left[\frac{\mathcal{C}\pi^2}{2v} - \frac{3C_\epsilon}{2\epsilon^2} - \frac{3C_\epsilon}{2\epsilon} \left(\frac{51 - 2n_f}{18} - 2 \ln \frac{2(M^2+Q^2)}{M^2} \right) \right] + \text{finite terms} \ , \tag{5.113}$$

where the finite part will be explicitly presented within the analytical total result in the next section, and $\mathcal{C}$ is here, and in general always when the $c\bar{c}$ pair is produced in a color octet state[9], given by

$$\mathcal{C} = C_F - \frac{C_A}{2} = -\frac{1}{6} \ . \tag{5.114}$$

Thereby, $C_F = 4/3$, $C_A = 3$ are the Casimir operators of the fundamental and the adjoint representation of the $SU(3)$ color group, respectively. Note, that $\mu_R^{2\epsilon}\left(M_V + M_V^c\right)$ is in fact free of ultraviolet divergences. Furthermore, in acordance with the Kinoshita Lee Nauenberg theorem the infrared and collinear divergences in (5.113) agree up to the sign

with the infrared divergences in the real corrections given in (5.56). Adding the virtual corrections $\mu_R^{2\epsilon}\left(M_V + M_V^c\right)$ to the Born part M_B we see, that the Coulomb divergence occurs as factor $1 + \frac{\alpha_s \mathcal{C}\pi}{2v}$, which multiplies M_B. Thus we can factorize the Coulomb divergence into the ${}^1S_0^{(8)}$ production matrix element according to

$$\frac{d\widehat{\widehat{\sigma}}_a}{dQ^2dy}\left\langle \widehat{O}^{J/\psi}\left[{}^1S_0^{(8)}\right]\right\rangle = \frac{d\sigma_a}{dQ^2dy}\left\langle O^{J/\psi}\left[{}^1S_0^{(8)}\right]\right\rangle + o(\alpha^2\alpha_s^3)\ , \tag{5.115}$$

where the redefined $\sigma_g \equiv \sigma\left(e^- g \to e^- c\bar{c}\left[{}^1S_0^{(8)}\right] g\right)$ is obtained from $\widehat{\widehat{\sigma}}_g$ defined in (5.36) by deleting the $1/v$ pole term, furthermore $\sigma_q \equiv \sigma\left(e^- q \to e^- c\bar{c}\left[{}^1S_0^{(8)}\right]\right) = \widehat{\widehat{\sigma}}_q$, and the redefined matrix element is related to the original one by

$$\left\langle O^{J/\psi}\left[{}^1S_0^{(8)}\right]\right\rangle = \left(1 + \frac{\alpha_s \mathcal{C}\pi}{2v}\right)\left\langle \widehat{O}^{J/\psi}\left[{}^1S_0^{(8)}\right]\right\rangle\ . \tag{5.116}$$

5.1.3 The analytical total result

The total result for the short distance coefficients $\sigma\left(e^- a \to e^- c\bar{c}\left[{}^1S_0^{(8)}\right] a\right)$ in (5.1) given as the sum of the Born, real correction and virtual correction part can finally be summarized by

$$\begin{aligned}\frac{d\sigma\left(e^- g \to e^- c\bar{c}\left[{}^1S_0^{(8)}\right] g\right)}{dQ^2dy} &= M_0\left\{\left(1 + \frac{\alpha_s}{\pi} g\left[{}^1S_0^{(8)}\right]\right)\delta(1-\mathrm{x})\right.\\ &+ \frac{\alpha_s}{\pi}\left[\left[\frac{1}{2}\ln\frac{\mu_F^2}{\hat{s}}\left(\frac{1}{1-\mathrm{x}}\right)_\rho - \left(\frac{\ln(1-\mathrm{x})}{1-\mathrm{x}}\right)_\rho\right](1-\mathrm{x})K_{gg}(\mathrm{x},Q^2)\right.\\ &\left.\left.+ \left(\frac{1}{1-\mathrm{x}}\right)_\rho f_g\left[{}^1S_0^{(8)}\right]\right]\right\}\end{aligned} \tag{5.117}$$

and

$$\begin{aligned}&\frac{d\sigma\left(e^- q \to e^- c\bar{c}\left[{}^1S_0^{(8)}\right] q\right)}{dQ^2dy}\\ &= \frac{\alpha_s}{\pi} M_0\left[\frac{1}{2}\ln\frac{\mu_F^2}{\hat{s}(1-\mathrm{x})^2}K_{gq}(\mathrm{x},Q^2) + \frac{2M^2(M^2+Q^2)\mathrm{x}^2}{3(M^2+Q^2\mathrm{x})^2} + f_q\left[{}^1S_0^{(8)}\right]\right]\end{aligned} \tag{5.118}$$

with the $f_a\left[{}^1S_0^{(8)}\right]$ and $g\left[{}^1S_0^{(8)}\right]$ given in (B.31)-(B.35) and (B.36), respectively, M_0 given in (5.12) (with $\epsilon = 0$) and the $K_{ga}(\mathrm{x},Q^2)$ given in (5.22), (5.23) (with $\epsilon = 0$). This result for the next leading order corrected production cross section does not change, if the electron is replaced by a positron, muon, antimuon, tauon or antitauon. In the photoproduction limit $Q^2 \to 0$ it is found agreement with Ref.[23].

Finally, some remark on the arbitrary parameter ρ is indicated. (5.1) contains an integration over ξ, which extends from $\frac{M^2+Q^2}{yS}$ to 1. It is comfortable to change the integration variable from ξ to x according to

$$\int_{\frac{M^2+Q^2}{yS}}^{1} d\xi = \frac{M^2}{yS} \int_{\frac{M^2}{W^2}}^{1} \frac{d\mathrm{x}}{\mathrm{x}^2} \ . \tag{5.119}$$

The ρ distributions then become easy to handle with if we choose

$$\rho = \frac{M^2}{W^2} \ . \tag{5.120}$$

5.2 Numerical analysis

Based on the analytical results of the last section we numerically calculate the ${}^1S_0^{(8)}$ contribution to a variety of differential distributions. As input we use the next leading order formula for $\alpha_s(\mu_R)$ with $n_f = 3$ active flavours and we employ the next leading order set of proton parton density functions by the CTEQ Collaboration (CTEQ5M) with asymptotic scale parameter $\Lambda_{\mathrm{QCD}}^{(n_f=4)} = 326$ MeV, which corresponds to $\Lambda_{\mathrm{QCD}}^{(n_f=3)} = 380$ MeV. In calculating distributions referring to the Born level for comparison we switch to the leading order formula for $\alpha_s(\mu_R)$ with $n_f = 3$ and to the leading order set of proton parton density functions by the CTEQ Collaboration (CTEQ5L) with asymptotic scale parameter $\Lambda_{\mathrm{QCD}}^{(n_f=4)} = 192$ MeV, which corresponds to $\Lambda_{\mathrm{QCD}}^{(n_f=3)} = 224$ MeV. Due to the lack of next leading order fit results for the NRQCD matrix elements we use both in connection with the CTEQ5L as well as with the CTEQ5M parton densities $\left\langle O^{J/\psi}\left[{}^1S_0^{(8)}\right]\right\rangle = \kappa_{J/\psi} M_{3.4}^{J/\psi}$ with $\kappa_{J/\psi} = 1/2$ and $M_{3.4}^{J/\psi} = (6.6 \pm 0.7) \times 10^{-2}\mathrm{GeV}^3$. If not said otherwise we choose the renormalization and factorization scale to be $\mu_R = \mu_F = \sqrt{M^2 + Q^2}$. The residual input agrees with that used in the analysis of J/ψ production under HERA conditions in section 4.2.1, except for the kinematical cut on z, which here is left out. Due to the fact, that the P wave contributions are not yet taken into account, the here produced results don't allow for a comparison with the experiment. Because of this preliminary character of this analysis we here refrain from error estimations. We now present our numerical results. In Figs. 5.2, 5.4, 5.6 the ${}^1S_0^{(8)}$ contribution to the Q^2, y and W distributions are shown. In each case the next leading order result (solid line) is compared with the Born result (dashed dotted line). Furthermore in Figs. 5.3, 5.5, 5.7 the corresponding K factors defined as the ratio of the respective next leading order corrected result and the Born result are shown for each distribution. In Figs. 5.8, 5.9, 5.10 the scale dependence of the next leading order corrected result (solid line) and the Born result (dashed dotted line) for $\frac{d\sigma}{dQ^2}$ is demonstrated for low, medium and large Q^2, $Q^2 = 2, 20, 80\mathrm{GeV}^2$. As was expected, in all three cases the variation of $\frac{d\sigma}{dQ^2}$ as function of $\mu_R = \mu_F$ is considerably flatten if the next leading order corrections are taken into account. After adequate adaptation of

the input we find in the photoproduction limit numerical agreement with Ref.[23] for the total cross section. Finally it should be emphasised again, that the here presented curves are in principle without explanatory power, since, due to the non-consideration of the P wave contributions, this calculation is incomplete.

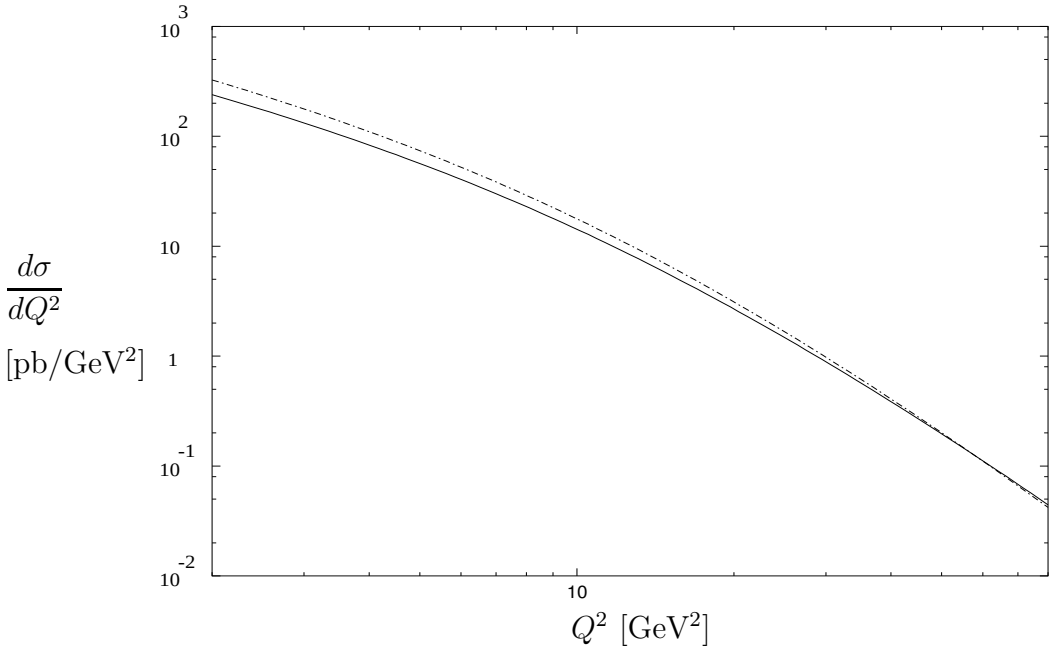

Figure 5.2: The ${}^1S_0^{(8)}$ contribution to the Q^2 distribution of J/ψ inclusive production in $e^{\pm}p$ DIS. The next leading order corrected result (solid line) is compared with the Born result (dashed dotted line).

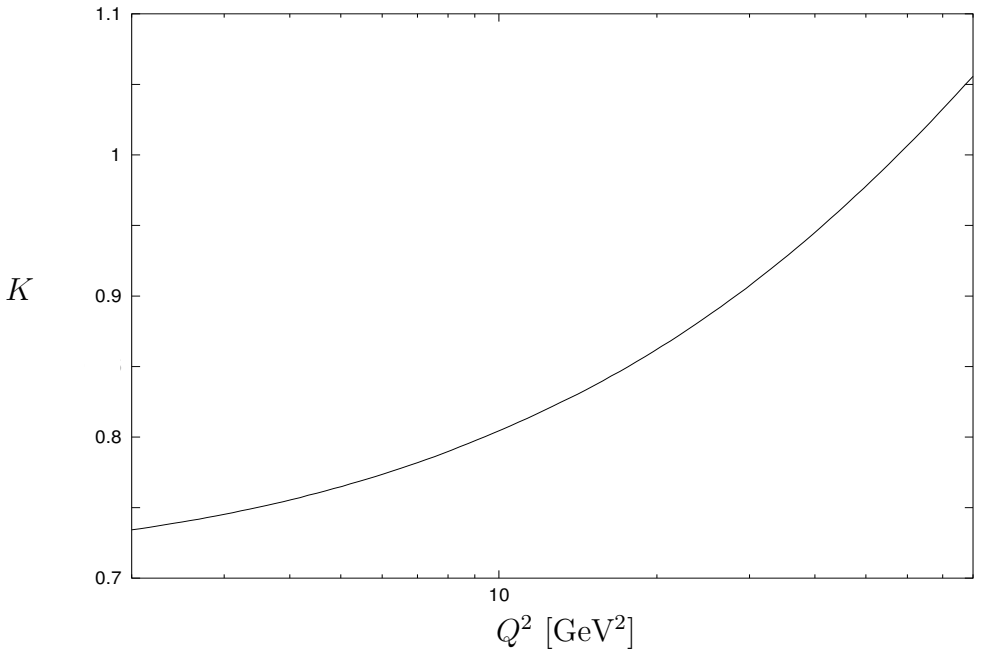

Figure 5.3: The K factor of the ${}^1S_0^{(8)}$ contribution to the Q^2 distribution of J/ψ inclusive production in $e^{\pm}p$ DIS defined as the ratio of the next leading order corrected result and the Born result.

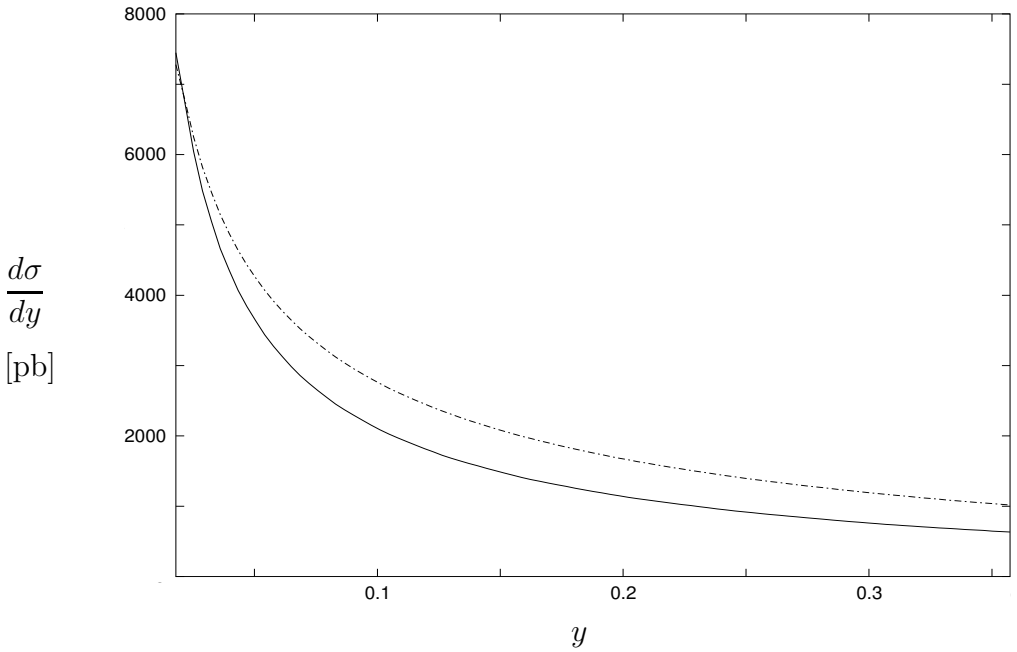

Figure 5.4: The ${}^1S_0^{(8)}$ contribution to the y differential distribution of J/ψ inclusive production in $e^{\pm}p$ DIS. The next leading order corrected result (solid line) is compared with the Born result (dashed dotted line).

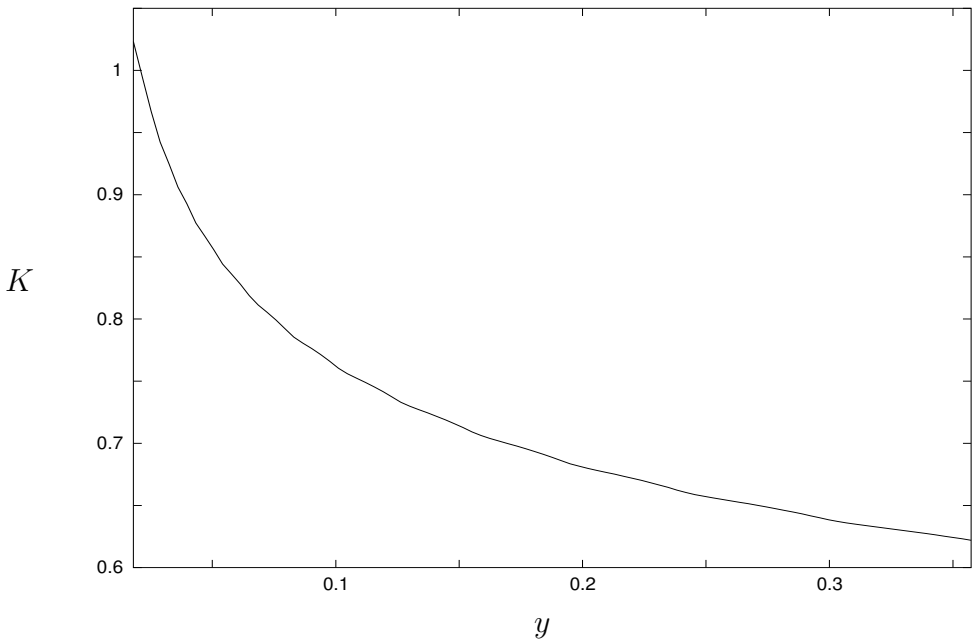

Figure 5.5: The K factor of the ${}^1S_0^{(8)}$ contribution to the y distribution of J/ψ inclusive production in $e^{\pm}p$ DIS defined as the ratio of the next leading order corrected result and the Born result.

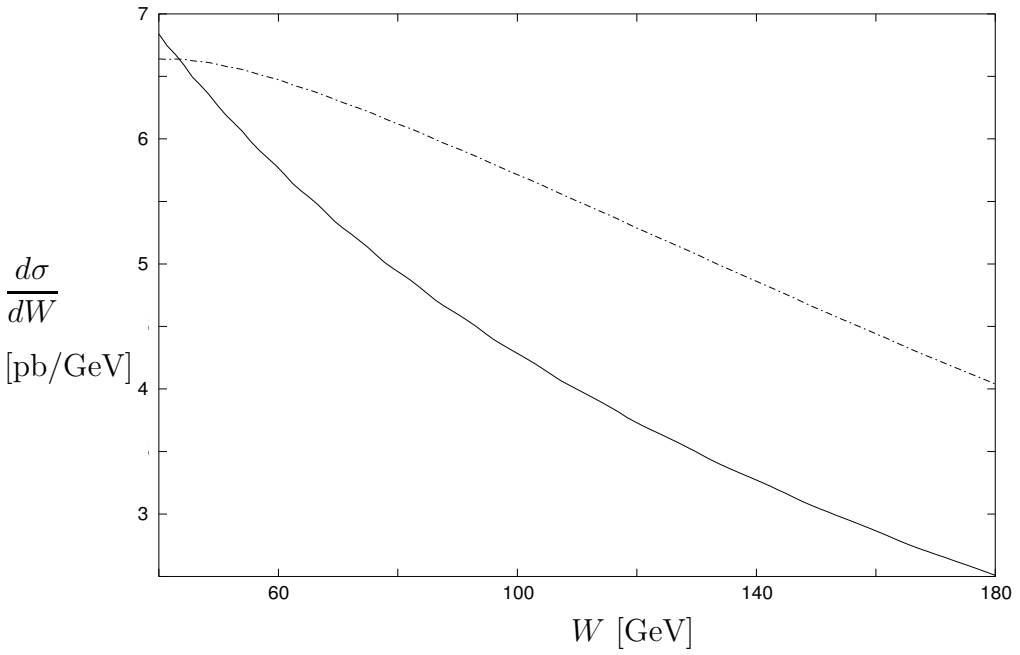

Figure 5.6: The ${}^1S_0^{(8)}$ contribution to the W differential distribution of J/ψ inclusive production in $e^{\pm}p$ DIS. The next leading order corrected result (solid line) is compared with the Born result (dashed dotted line).

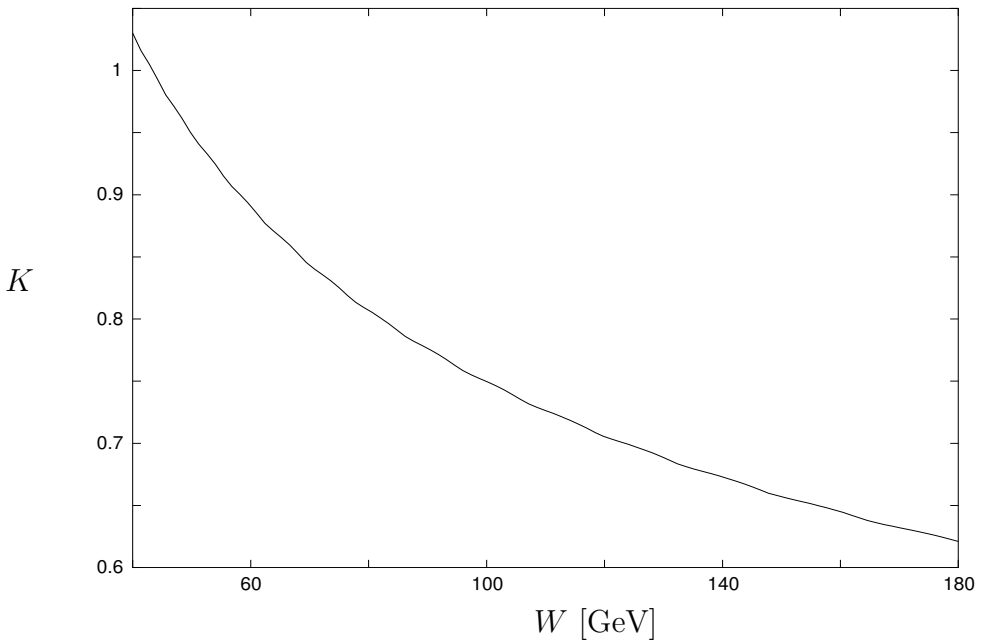

Figure 5.7: The K factor of the ${}^1S_0^{(8)}$ contribution to the W distribution of J/ψ inclusive production in $e^{\pm}p$ DIS defined as the ratio of the next leading order corrected result and the Born result.

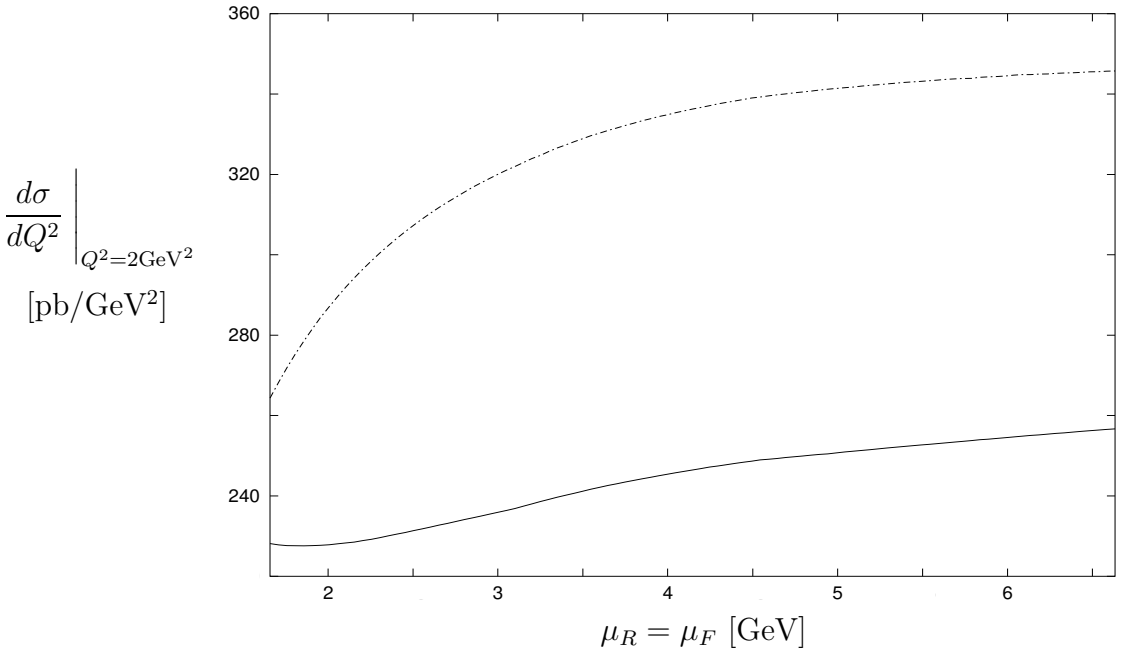

Figure 5.8: The next leading order corrected result (solid line) and the Born result (dashed dotted line) for $\frac{d\sigma}{dQ^2}$ at $Q^2 = 2GeV^2$ are shown as function of $\mu_R = \mu_F$.

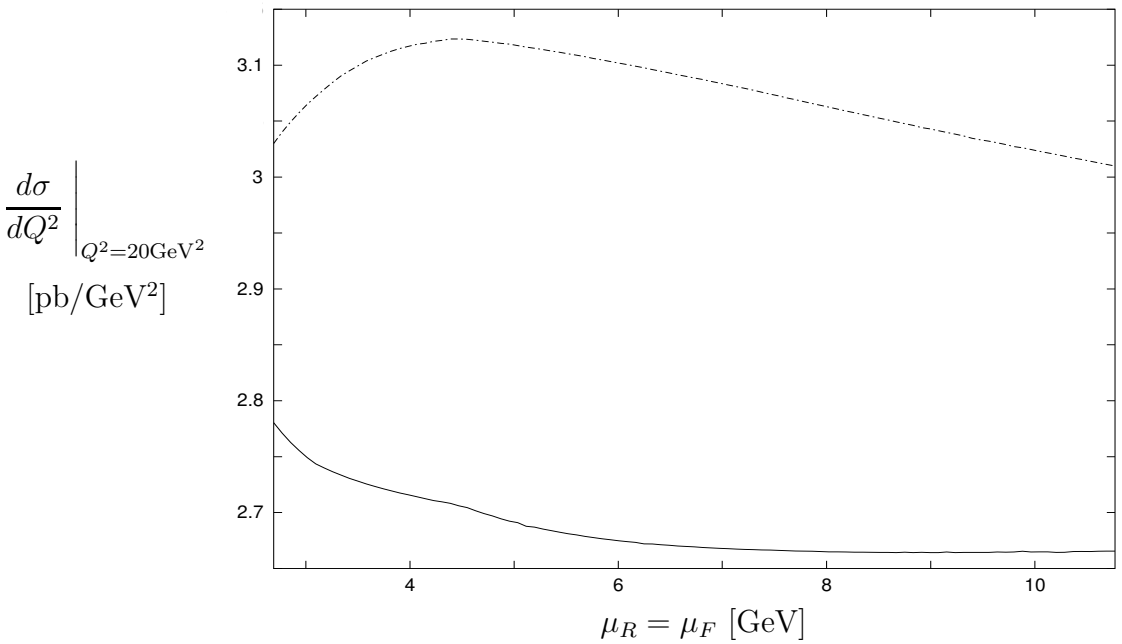

Figure 5.9: The next leading order corrected result (solid line) and the Born result (dashed dotted line) for $\frac{d\sigma}{dQ^2}$ at $Q^2 = 20GeV^2$ are shown as function of $\mu_R = \mu_F$.

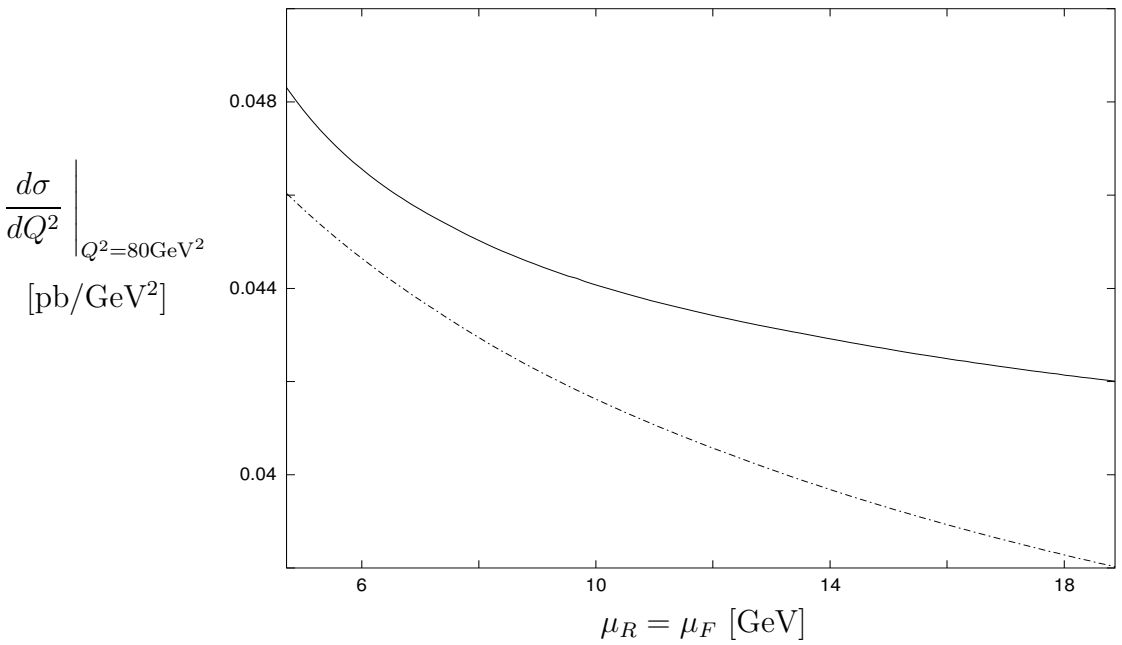

Figure 5.10: The next leading order corrected result (solid line) and the Born result (dashed dotted line) for $\frac{d\sigma}{dQ^2}$ at $Q^2 = 80GeV^2$ are shown as function of $\mu_R = \mu_F$.

Chapter 6

Summary and outlook

In this work we theoretically investigated, at Born level, J/ψ inclusive production in $e^{\pm}p$ DIS through the electromagnetic interaction in the H1 experiment at DESY HERA as well as in νN DIS both through the neutral and through the charged current interaction in the CHORUS and NOMAD experiments at CERN. As for the H1 experiment we calculated CSM and NRQCD predictions for distributions with respect to the photon virtuality Q^2, the photon proton center of mass energy W, the inelasticity variable z as well as the J/ψ transverse momentum P_T (P_T^*) and rapidity $y_{J/\psi}$ ($y^*_{J/\psi}$) in the HERA laboratory frame (photon proton center of mass frame). For all these distributions, except for those with respect to P_T^* and $y_{J/\psi}$, data exists to compare with. It was found, that the H1 data tend to prefer the NRQCD rather than the CSM predictions. As for the CHORUS and NOMAD experiments we calculated distributions with respect to the J/ψ transverse momentum P_T and rapidity $y_{J/\psi}$ in the CHORUS and NOMAD laboratory frame, both within the CSM as well as within NRQCD. In case of J/ψ production in νN neutral current DIS only a measurement of the total production cross section exists. In addition to calculating the corresponding NRQCD and CSM predictions we also estimated the contribution from diffraction within the vector dominance model. The NRQCD result turned out to exceed the CSM result by more than one order of magnitude, and it was found to be comparable in magnitude with the diffractive contribution. Although the diffractive and the NRQCD contribution to the total production cross section together were found to come much nearer to the measurement than the CSM prediction together with the contribution from diffraction they turned out to still undershoot the measurement by a factor of 10. However, it should be noted, that due to kinematical reasons in case of J/ψ production through the neutral current interaction we were forced to restrict our NRQCD analysis to leading order. It is expected, that the inclusion of the next leading order corrections will improve the relation between the theoretical prediction and the measurement. As for J/ψ production in νN charged current DIS at CHORUS and NOMAD no data is available until now to confront our predictions with. Finally, we calculated the ${}^1S_0^{(8)}$ part of the next leading order corrections to the cross section of the process $e^{\pm}p \to e^{\pm}J/\psi X'$. It was found, that at next leading order the scale dependence is considerably reduced compared to the Born level. But in order to make this calculation

meaningful also the ${}^3P_J^{(8)}$ part of the next leading order corrections needs to be calculated. This task is left for future work.

Appendix A

The short distance coefficients of the Born processes

In this appendix we present analytic expressions for the coefficients $F_{la}[n]$, $T_{la}[n]$, $L_{la}[n]$ and $A_{la}[n]$ appearing in (4.77), (4.88). In order to compactify the expressions, the Lorentz invariants $s = 2pq_B$, $t = -2pp'$, and $u = -2q_Bp'$ are introduced, which are related to the partonic Mandelstam variables defined in (4.17), (4.58), (4.59) by $s = \hat{s} + Q^2$, $t = \hat{t} - m'^2$, and $u = \hat{u} + Q^2 - m'^2$, respectively, where $m'^2 = p'^2$.

A.1 The processes $lN \to l(J/\psi)_{\text{prompt}} jX$ with $l = \nu_e, \overline{\nu}_e, e^{\pm}$

We here explicitly present only the coefficients $F_{la}[n]$, $T_{la}[n]$, $L_{la}[n]$ and $A_{la}[n]$ occurring in (4.77) for $l = \nu_e$ and $l = \overline{\nu}_e$. The coefficients $F_{la}[n]$, $T_{la}[n]$ and $L_{la}[n]$ relevant for the process with $l = e^{\pm}$ are obtained from the here given ones in the limit $a_q \to 0$ (inclusively $a_c \to 0$), $v_q \to e_q$ (inclusively $v_c \to e_c$), $g \to e$ and $m_Z \to 0$.

$\nu_e(\overline{\nu}_e)\ q(\overline{q}) \to \nu_e(\overline{\nu}_e)\ c\overline{c}\left[{}^3S_1^{(1)}\right]\ q(\overline{q})$:

$$F = T = L = A = 0. \tag{A.1}$$

$\nu_e(\overline{\nu}_e)\ q(\overline{q}) \to \nu_e(\overline{\nu}_e)\ c\overline{c}\left[{}^3P_J^{(1)}\right]\ q(\overline{q})$:

$$F = T = L = A = 0. \tag{A.2}$$

$\nu_e(\overline{\nu}_e)\ q(\overline{q}) \to \nu_e(\overline{\nu}_e)\ c\overline{c}\left[{}^1S_0^{(8)}\right]\ q(\overline{q})$:

$$\begin{aligned} F &= \frac{-g^4\alpha_s^2 v_c^2 Q^2}{6\pi M(Q^2+m_Z^2)^2 s^4 t(s+u)^2}, \\ T &= 2Q^4t^2 + 2Q^2st(s+u) + s^4 + s^2u^2, \\ L &= -2Q^2t(Q^2t+su), \\ A &= 0. \end{aligned} \tag{A.3}$$

$\nu_e(\overline{\nu}_e)\ q(\overline{q}) \to \nu_e(\overline{\nu}_e)\ c\overline{c}\left[^3S_1^{(8)}\right]\ q(\overline{q})$:

$$F = \frac{g^4\alpha_s^2}{36\pi M^3(Q^2+m_Z^2)^2(Q^2-s)^2(Q^2-u)^2s^4t(s+u)^2},$$
$$\begin{aligned}
T = &-(a_q^2+v_q^2)Q^2t(s+u)^2\{2Q^6t^2(2s+t)+2Q^4s[s^2u-st(3t-2u)-2t^3]+Q^2s^2[s^2(t\\
&-2u)+2s(t^2-4tu-u^2)+t(2t^2-2tu-u^2)]+s^3u(s^2+2st+2t^2+2tu+u^2)\}\\
&+4a_qa_cQ^2t(s+u)(Q^2-s)(Q^2-u)\{Q^6t(s+2t)+Q^4[s^3-s^2(t-2u)-5st^2-2t^2(t\\
&+u)]-Q^2s[s^3+s^2(t+5u)-s(2t^2-5tu-3u^2)-t(2t^2+tu-u^2)]+s^2u[2s^2+s(4t\\
&+3u)+2t^2+3tu+u^2]\}-2a_c^2Q^2(Q^2-s)^2(Q^2-u)^2\{2Q^6t^2+2Q^4t[s^2-s(3t-u)-3t(t\\
&+u)]-Q^2[s^4+6s^3t+s^2(2t^2+12tu+u^2)-2st(4t^2+tu-3u^2)-4t^2(t+u)^2]+s^5\\
&+s^4(5t+u)+s^3(8t^2+12tu+u^2)+s^2(4t^3+16t^2u+13tu^2+u^3)+4stu(t+u)^2\},\\
L = &\,2(a_q^2+v_q^2)Q^4(Q^2-s)^2t^2(s+t)^2(s+u)^2-4a_qa_cQ^2(Q^2-s)^2(Q^2-u)t(s+u)[Q^4t(s\\
&+2t)-Q^2(s^3+2s^2t+3st^2+2t^3+2t^2u)+s^4+s^3(2t+u)+s^2t^2-stu(t+u)]+2a_c^2(Q^2\\
&-s)^2(Q^2-u)^2\{2Q^8t^2-2Q^6t[s^2+s(3t-u)+3t(t+u)]+Q^4[s^4+4s^3t+s^2(8t^2-2tu\\
&+u^2)+2st(4t^2+tu-3u^2)+4t^2(t+u)^2]-2Q^2s[s^4+s^3(2t+u)+s^2(2t^2+u^2)+s(t^3\\
&-2t^2u-2tu^2+u^3)-2tu(t+u)^2]+s^2(s+t+u)^2(s^2+u^2)\},\\
A = &\pm 2v_qQ^2st(s+u)\{a_q(s+u)[2Q^6st-2Q^4t(2s^2+st-tu)\\
&+Q^2s(s^2(t-2u)+2s(t^2+u^2)-tu(2t-u))+s^2u(s-u)(s+2t+u)]\\
&-2a_c(Q^2-s)(Q^2-u)[Q^6t-Q^4(s^2+3st+t^2)\\
&+Q^2(s^3+s^2(3t+u)+s(2t^2+tu+u^2)-tu(t+u))-su^2(s+t+u)]\},
\end{aligned} \tag{A.4}$$

where the plus (minus) sign refers to a $\nu_e\ q$ or $\overline{\nu}_e\ \overline{q}$ ($\nu_e\ \overline{q}$ or $\overline{\nu}_e\ q$) initial state.

$\nu_e(\overline{\nu}_e)\ q(\overline{q}) \to \nu_e(\overline{\nu}_e)\ c\overline{c}\left[^3P_J^{(8)}\right]\ q(\overline{q})$:

$$\begin{aligned}
F = &\frac{2g^4\alpha_s^2v_c^2Q^2}{3\pi M^3(Q^2+m_Z^2)^2s^4t(s+u)^4},\\
T = &\,8Q^6t[2s^2+st+t(2t+u)]-2Q^4[4s^4+12s^3t+s^2(19t^2+8tu+4u^2)+2st(6t^2\\
&+tu-2u^2)+t^2(8t^2+12tu+7u^2)]+2Q^2s[6s^4+s^3(7t+6u)+s^2(4t^2+3tu\\
&+6u^2)-su(8t^2+3tu-6u^2)-tu(8t^2+12tu+7u^2)]-s^2(s+u)[7s^3+s^2(12t\\
&+7u)+s(8t^2+16tu+7u^2)+u(8t^2+12tu+7u^2)],\\
L = &\,8Q^6t[s^2-st-t(2t+u)]-2Q^4[2s^4+4s^3t+s^2(5t^2+8tu+2u^2)-2st(6t^2\\
&+tu-2u^2)-t^2(8t^2+12tu+7u^2)]+2Q^2s(s+u)[2s^3+2s^2t+s(8t^2+5tu\\
&+2u^2)+t(8t^2+12tu+7u^2)],\\
A = &\,0.
\end{aligned} \tag{A.5}$$

$\nu_e(\overline{\nu}_e)\ g \to \nu_e(\overline{\nu}_e)\ c\overline{c}\left[^3S_1^{(1)}\right]\ g$:

$$F = \frac{-2g^4\alpha_s^2v_c^2Q^2}{27\pi M(Q^2+m_Z^2)^2s^4(s+t)^2(s+u)^2(t+u)^2},$$

$$
\begin{aligned}
T &= 4Q^6t^2(s^2+t^2) - 2Q^4t[s^3(3t-2u) + 3s^2t(t+u) + 2st^2(t-u) + 2t^3(t+u)] \\
&\quad + 2Q^2s[s^3(t-u)^2 - 2s^2tu(t+u) - st^2u(2t-u) - 2t^3u(t+u)] - 2s^2[s^3(t^2 \\
&\quad + tu+u^2) + s^2(t+u)^3 + stu(t^2+3tu+u^2) + t^2u^2(t+u)], \\
L &= 2Q^6t^2(s^2-2t^2) - 2Q^4t(s^2-2t^2)[s(t-u) + t(t+u)] + Q^2s[s^3(t^2+u^2) \\
&\quad + 2s^2t^2(t+u) + st^2(t^2+6tu+u^2) + 4t^3u(t+u)], \\
A &= 0.
\end{aligned} \tag{A.6}
$$

$\nu_e(\overline{\nu}_e)\ g \to \nu_e(\overline{\nu}_e)\ c\overline{c}\left[{}^3P_0^{(1)}\right]\ g$:

$$
\begin{aligned}
F &= \frac{8g^4\alpha_s^2a_c^2(Q^2+M^2)^2}{27\pi M^3(Q^2+m_Z^2)^2s^4(s+t)^4(s+u)^4(t+u)^4}, \\
T &= 4Q^8t^2[s^6 - 2s^4u^2 + s^3(t^3-tu^2) + s^2(2t^4+4t^3u+2t^2u^2+u^4) + st(2t^4+6t^3u+5t^2u^2 \\
&\quad +2tu^3+u^4) + t^2(t+u)^2(t^2+u^2)] - 4Q^6t[s^7(2t-u) + s^6t(t+u) - 2s^5(t^3+t^2u+2tu^2 \\
&\quad -u^3) - s^4t(t^3+6t^2u+7tu^2+2u^3) + s^3(t^5-3t^4u-7t^3u^2-3t^2u^3+2tu^4-u^5) + s^2t(t^5 \\
&\quad +4t^4u+3t^3u^2+2t^2u^3+3tu^4+u^5) + st^2u(t+u)^2(2t^2+5tu+u^2) + 2t^3u^2(t+u)^3] \\
&\quad +2Q^4t[2s^8(t-2u) + 2s^7(t^2-u^2) - s^6(3t^3-2t^2u-tu^2-8u^3) - 2s^5(2t^4+4t^3u+t^2u^2 \\
&\quad -4tu^3-3u^4) + s^4(t^5-6t^4u-6t^3u^2+2t^2u^3+3tu^4-4u^5) + 2s^3(t+u)^2(2t^4+2t^3u \\
&\quad -t^2u^2+tu^3-2u^4) + s^2t(t+u)^2(2t^4+12t^3u+9t^2u^2-4tu^3-2u^4) + 2st^2u(t+u)^3(2t^2 \\
&\quad +4tu-u^2) + 2t^3u^2(t+u)^4] + 2Q^2stu[2s^8 + 2s^7(t+u) - s^6(3t^2+2tu+3u^2) - 2s^5(2t^3 \\
&\quad +5t^2u+6tu^2+3u^3) + s^4(t^4-4t^3u-8t^2u^2-4tu^3+u^4) + 2s^3(2t^5+7t^4u+11t^3u^2 \\
&\quad +10t^2u^3+6tu^4+2u^5) + s^2(t+u)^2(2t^4+12t^3u+15t^2u^2+6tu^3+2u^4) + 2stu(t+u)^3(2t^2 \\
&\quad +4tu+u^2) + 2t^2u^2(t+u)^4], \\
L &= -2Q^8t^2[s^6 - 2s^4u^2 + 2s^3(t^3-tu^2) + s^2(4t^4+8t^3u+4t^2u^2+u^4) + 2st(2t^4+6t^3u+5t^2u^2 \\
&\quad +2tu^3+u^4) + 2t^2(t+u)^2(t^2+u^2)] + 2Q^6t[s^7(3t-u) + 3s^6t(t+u) - 2s^5(2t^3+3t^2u \\
&\quad +4tu^2-u^3) - 2s^4t(t^3+8t^2u+9tu^2+2u^3) + s^3(6t^5-2t^4u-18t^3u^2-8t^2u^3+5tu^4-u^5) \\
&\quad +s^2t(4t^5+12t^4u+6t^3u^2+4t^2u^3+7tu^4+u^5) + 2st^2u(t+u)^2(2t^2+5tu+u^2) + 4t^3u^2(t \\
&\quad +u)^3] - Q^4[s^8(7t^2-4tu+u^2) + 2s^7t(7t^2+5tu-2u^2) - s^6(5t^4-6t^3u-t^2u^2-12tu^3 \\
&\quad +2u^4) - 8s^5t(3t-u)(t+u)^3 - s^4(8t^6+76t^5u+110t^4u^2+40t^3u^3-5t^2u^4+8tu^5-u^6) \\
&\quad +2s^3t(4t^6+2t^5u-22t^4u^2-22t^3u^3-t^2u^4-tu^5-2u^6) + s^2t^2(t+u)^2(4t^4+24t^3u+8t^2u^2 \\
&\quad -4tu^3-u^4) + 4st^3u(t+u)^3(2t^2+4tu-u^2) + 4t^4u^2(t+u)^4] + 2Q^2s(s+u)[s^7(2t^2-tu \\
&\quad +u^2) + 2s^6t^2(3t+u) + s^5(4t^4+9t^3u+6t^2u^2+3tu^3-2u^4) - s^4t(4t^4-11t^2u^2-12tu^3 \\
&\quad -u^4) - s^3(6t^6+18t^5u+12t^4u^2-t^3u^3+2t^2u^4+2tu^5-u^6) - s^2t(t+u)^2(2t^4+12t^3u \\
&\quad +6t^2u^2+2tu^3+u^4) - 2st^3u(t+u)^3(2t+3u) - 2t^3u^2(t+u)^4] - s^2(s+u)^2(s+t+u)^2[s^4 \\
&\quad (t^2+u^2) + 2s^3(t^3-u^3) + s^2(t^4+2t^3u+2t^2u^2+u^4) + 2st^3u(t+u) + t^2u^2(t+u)^2], \\
A &= 0.
\end{aligned} \tag{A.7}
$$

$\nu_e(\overline{\nu}_e)\ g \to \nu_e(\overline{\nu}_e)\ c\overline{c}\left[^3P_1^{(1)}\right]\ g$:

$$F = \frac{4g^4\alpha_s^2 a_c^2}{27\pi M^3(Q^2+m_Z^2)^2 s^4(s+t)^4(s+u)^4(t+u)^4},$$

$$\begin{aligned}
T = {} & -8Q^{10}t^4(s+t)(t+u)[3s^3+s^2(7t+10u)+s(5t^2+15tu+9u^2)+t^3+5t^2u+7tu^2 \\
& +2u^3] - 4Q^8t^2[s^8+7s^7(t+u)+s^6(24t^2+48tu+22u^2)+2s^5(17t^3+62t^2u+60tu^2 \\
& +15u^3)+s^4(7t^4+112t^3u+219t^2u^2+130tu^3+17u^4)-s^3(30t^5+37t^4u-91t^3u^2 \\
& -151t^2u^3-56tu^4-3u^5)-s^2t(t+u)^2(31t^3+62t^2u-18tu^2-4u^3)-st(11t^6+69t^5u \\
& +144t^4u^2+123t^3u^3+42t^2u^4+6tu^5+u^6)-t^3(t+u)^2(t^3+9t^2u+17tu^2+7u^3)] \\
& +2Q^6t[s^9(4t-2u)+2s^8(16t^2+9tu-7u^2)+s^7(125t^3+206t^2u+25tu^2-44u^3) \\
& +s^6(239t^4+695t^3u+507t^2u^2-9tu^3-60u^4)+s^5(221t^5+1022t^4u+1410t^3u^2 \\
& +602t^2u^3-35tu^4-34u^5)+s^4(91t^6+689t^5u+1548t^4u^2+1318t^3u^3+361t^2u^4 \\
& -13tu^5-6u^6)+s^3t(t+u)^2(16t^4+156t^3u+357t^2u^2+78tu^3+2u^4)+s^2t^2(10t^6 \\
& +24t^5u+57t^4u^2+127t^3u^3+99t^2u^4-tu^5-16u^6)+2st^2(t+u)^2(4t^5+2t^4u \\
& -17t^3u^2-19t^2u^3-12tu^4-4u^5)+2t^3(t+u)^4(t^3-4tu^2-u^3)]-2Q^4[s^{10}(3t^2 \\
& -2tu+u^2)+s^9(25t^3+7t^2u-11tu^2+7u^3)+s^8(100t^4+132t^3u-25t^2u^2-22tu^3 \\
& +23u^4)+s^7(208t^5+539t^4u+277t^3u^2-93t^2u^3-5tu^4+34u^5)+s^6(217t^6 \\
& +935t^5u+1162t^4u^2+366t^3u^3-66t^2u^4+29tu^5+23u^6)+s^5(87t^7+688t^6u \\
& +1545t^5u^2+1320t^4u^3+406t^3u^4+59t^2u^5+36tu^6+7u^7)-s^4(t+u)^2(22t^6-119t^5u \\
& -396t^4u^2-184t^3u^3-72t^2u^4-17tu^5-u^6)-s^3t(28t^8+152t^7u+257t^6u^2+100t^5u^3 \\
& -163t^4u^4-241t^3u^5-158t^2u^6-51tu^7-4u^8)-s^2t^2(t+u)^2(6t^6+52t^5u+132t^4u^2 \\
& +125t^3u^3+47t^2u^4-5tu^5-7u^6)-2st^3u(t+u)^4(3t^3+12t^2u+8tu^2+2u^3)-2t^4u^2(t \\
& +u)^6]+2Q^2s[s^{10}(t^2+u^2)+s^9(8t^3+6t^2u+6tu^2+8u^3)+s^8(32t^4+56t^3u+42t^2u^2 \\
& +52tu^3+30u^4)+s^7(75t^5+232t^4u+261t^3u^2+221t^2u^3+174tu^4+57u^5)+s^6(105t^6 \\
& +508t^5u+888t^4u^2+836t^3u^3+576t^2u^4+280tu^5+57u^6)+2s^5(43t^7+308t^6u+791t^5u^2 \\
& +1015t^4u^3+774t^3u^4+389t^2u^5+119tu^6+15u^7)+s^4(t+u)^2(38t^6+332t^5u+799t^4u^2 \\
& +754t^3u^3+389t^2u^4+96tu^5+8u^6)+s^3(7t^9+134t^8u+734t^7u^2+1847t^6u^3+2546t^5u^4 \\
& +2066t^4u^5+993t^3u^6+262t^2u^7+30tu^8+u^9)+2s^2tu(t+u)^2(8t^6+65t^5u+167t^4u^2 \\
& +193t^3u^3+111t^2u^4+29tu^5+2u^6)+st^2u^2(t+u)^4(11t^3+34t^2u+28tu^2+7u^3) \\
& +2t^3u^3(t+u)^6],
\end{aligned}$$

$$\begin{aligned}
L = {} & 8Q^{10}t^4(s+t)(t+u)[3s^3+s^2(7t+10u)+s(5t^2+15tu+9u^2)+t^3+5t^2u+7tu^2+2u^3] \\
& +2Q^8t^2[s^8-2s^7(t+u)-s^6(21t^2+42tu+23u^2)-2s^5(29t^3+62t^2u+55tu^2+22u^3) \\
& -s^4(98t^4+218t^3u+176t^2u^2+90tu^3+33u^4)-2s^3(54t^5+157t^4u+130t^3u^2+35t^2u^3 \\
& +13tu^4+5u^5)-s^2(t+u)^2(70t^4+156t^3u+4t^2u^2+6tu^3+u^4)-2st(11t^6+69t^5u \\
& +144t^4u^2+123t^3u^3+42t^2u^4+6tu^5+u^6)-2t^3(t+u)^2(t^3+9t^2u+17tu^2+7u^3)] \\
& -2Q^6t[s^9(3t-u)+s^8(t^2+3tu+2u^2)-s^7(35t^3+47t^2u-3tu^2-23u^3)-s^6(101t^4
\end{aligned}$$

$+233t^3u + 167t^2u^2 - 9tu^3 - 44u^4) - s^5(134t^5 + 422t^4u + 528t^3u^2 + 294t^2u^3 + 17tu^4$
$-33u^5) - s^4(96t^6 + 392t^5u + 648t^4u^2 + 620t^3u^3 + 313t^2u^4 + 35tu^5 - 10u^6) - s^3(t+u)^2$
$(30t^5 + 126t^4u + 114t^3u^2 + 142t^2u^3 + 15tu^4 - u^5) + s^2t(6t^7 - 22t^6u - 130t^5u^2 - 228t^4u^3$
$-241t^3u^4 - 161t^2u^5 - 47tu^6 - u^7) + 2st^2(t+u)^2(4t^5 + 2t^4u - 17t^3u^2 - 19t^2u^3 - 12tu^4$
$-4u^5) + 2t^3(t+u)^4(t^3 - 4tu^2 - u^3)] + Q^4[s^{10}(5t^2 - 8tu - u^2) + 2s^9(4t^3 - 6t^2u - 15tu^2$
$-5u^3) - s^8(32t^4 + 48t^3u + 59t^2u^2 + 54tu^3 + 35u^4) - 4s^7(30t^5 + 63t^4u + 45t^3u^2 + 10t^2u^3$
$+11tu^4 + 13u^5) - s^6(179t^6 + 596t^5u + 694t^4u^2 + 228t^3u^3 - 120t^2u^4 - 24tu^5 + 35u^6)$
$-2s^5(78t^7 + 404t^6u + 756t^5u^2 + 600t^4u^3 + 74t^3u^4 - 132t^2u^5 - 31tu^6 + 5u^7) - s^4(t+u)^2$
$(86t^6 + 516t^5u + 768t^4u^2 + 360t^3u^3 - 142t^2u^4 - 32tu^5 + u^6) - 4s^3t(7t^8 + 89t^7u + 338t^6u^2$
$+596t^5u^3 + 535t^4u^4 + 212t^3u^5 - t^2u^6 - 19tu^7 - u^8) - s^2t^2(t+u)^2(4t^6 + 92t^5u + 338t^4u^2$
$+444t^3u^3 + 245t^2u^4 + 30tu^5 - 13u^6) - 4st^3u(t+u)^4(3t^3 + 12t^2u + 8tu^2 + 2u^3) - 4t^4u^2(t$
$+u)^6] + 2Q^2s(s+t+u)^2[s^8u(5t+u) + s^7(2t^3 + 16t^2u + 21tu^2 + 7u^3) + s^6(5t^4 + 24t^3u$
$+57t^2u^2 + 46tu^3 + 16u^4) + s^5(3t^5 + 13t^4u + 55t^3u^2 + 79t^2u^3 + 50tu^4 + 16u^5) - s^4(t^6 + 11t^5u$
$+22t^4u^2 + 4t^3u^3 - 19t^2u^4 - 22tu^5 - 7u^6) - s^3(t^7 + 15t^6u + 70t^5u^2 + 128t^4u^3 + 113t^3u^4$
$+37t^2u^5 - 5tu^6 - u^7) - s^2tu(t+u)^2(4t^4 + 27t^3u + 49t^2u^2 + 26tu^3 - u^4) - st^2u^2(t+u)^2$
$(5t^3 + 19t^2u + 18tu^2 + 6u^3) - 2t^3u^3(t+u)^4] - s^2(s+u)(s+t+u)^2[s^7(t^2 + 4tu + u^2)$
$+s^6(4t^3 + 19t^2u + 18tu^2 + 5u^3) + 2s^5(3t^4 + 19t^3u + 33t^2u^2 + 21tu^3 + 5u^4) + 2s^4(2t^5$
$+20t^4u + 56t^3u^2 + 58t^2u^3 + 26tu^4 + 5u^5) + s^3(t^6 + 22t^5u + 98t^4u^2 + 156t^3u^3 + 116t^2u^4$
$+42tu^5 + 5u^6) + s^2u(t+u)^2(5t^4 + 30t^3u + 33t^2u^2 + 16tu^3 + u^4) + stu^2(t+u)^3(5t^2$
$+7tu + 4u^2) + t^2u^3(t+u)^4],$

$$A = 0. \tag{A.8}$$

$\nu_e(\overline{\nu}_e)\ g \to \nu_e(\overline{\nu}_e)\ c\overline{c}\left[{}^3P_2^{(1)}\right]\ g$:

$$F = \frac{4g^4\alpha_s^2 a_c^2}{135\pi M^3(Q^2+m_Z^2)^2 s^4(s+t)^4(s+u)^4(t+u)^4},$$

$T = -24Q^{10}t^4(s+t)(t+u)[s^3 + s^2(3t+4u) + s(3t^2 + 7tu + 5u^2) + t^3 + 3t^2u + 3tu^2 + 2u^3]$
$+4Q^8t^2[s^8 + 5s^7(t+u) + 2s^6(8t^2 + 16tu + 7u^2) + s^5(28t^3 + 84t^2u + 82tu^2 + 26u^3)$
$+s^4(61t^4 + 168t^3u + 181t^2u^2 + 102tu^3 + 29u^4) + s^3(112t^5 + 365t^4u + 443t^3u^2 + 241t^2u^3$
$+68tu^4 + 17u^5) + s^2(t+u)^2(103t^4 + 234t^3u + 146t^2u^2 + 20tu^3 + 4u^4) + st(43t^6 + 229t^5u$
$+498t^4u^2 + 551t^3u^3 + 298t^2u^4 + 66tu^5 + 7u^6) + t^2(t+u)^2(7t^4 + 29t^3u + 47t^2u^2 + 47tu^3$
$+4u^4)] - 2Q^6t[s^9(4t-2u) + 2s^8(8t^2 + 3tu - 5u^2) + s^7(61t^3 + 94t^2u - 7tu^2 - 28u^3)$
$+s^6(151t^4 + 443t^3u + 319t^2u^2 - 25tu^3 - 52u^4) + s^5(225t^5 + 842t^4u + 1102t^3u^2 + 518t^2u^3$
$-19tu^4 - 58u^5) + s^4(247t^6 + 1025t^5u + 1648t^4u^2 + 1210t^3u^3 + 385t^2u^4 + 11tu^5 - 34u^6)$
$+s^3(t+u)^2(180t^5 + 628t^4u + 545t^3u^2 + 106t^2u^3 + 38tu^4 - 8u^5) + s^2t(50t^7 + 548t^6u$
$+1725t^5u^2 + 2371t^4u^3 + 1543t^3u^4 + 483t^2u^5 + 92tu^6 + 8u^7) - 2st^2(t+u)^2(6t^5 - 56t^4u$
$-229t^3u^2 - 255t^2u^3 - 68tu^4 - 16u^5) - 2t^3(t+u)^3(3t^4 - 3t^3u - 32t^2u^2 - 49tu^3 - 11u^4)]$

$$
\begin{aligned}
&-2Q^4[s^{10}(t^2+10tu+3u^2)+s^9(9t^3+55t^2u+61tu^2+15u^3)+3s^8(4t^4+48t^3u+99t^2u^2\\
&+62tu^3+11u^4)-s^7(64t^5-27t^4u-581t^3u^2-803t^2u^3-355tu^4-42u^5)-s^6(221t^6\\
&+557t^5u-54t^4u^2-1270t^3u^3-1278t^2u^4-437tu^5-33u^6)-s^5(317t^7+1180t^6u\\
&+1263t^5u^2-400t^4u^3-1694t^3u^4-1215t^2u^5-336tu^6-15u^7)-s^4(t+u)^2(266t^6+745t^5u\\
&+340t^4u^2-464t^3u^3-408t^2u^4-141tu^5-3u^6)-s^3t(128t^8+840t^7u+1933t^6u^2+1756t^5u^3\\
&+69t^4u^4-969t^3u^5-694t^2u^6-219tu^7-28u^8)-s^2t^2(t+u)^2(26t^6+240t^5u+540t^4u^2\\
&+321t^3u^3-111t^2u^4-81tu^5-29u^6)-2st^3u(t+u)^3(17t^4+73t^3u+76t^2u^2+10tu^3+2u^4)\\
&-14t^4u^2(t+u)^6]+2Q^2s[s^{10}(3t^2+8tu+3u^2)+6s^9(3t^3+10t^2u+10tu^2+3u^3)+s^8(54t^4\\
&+228t^3u+346t^2u^2+216tu^3+48u^4)+s^7(93t^5+526t^4u+1105t^3u^2+1061t^2u^3+464tu^4\\
&+75u^5)+s^6(99t^6+764t^5u+2132t^4u^2+2872t^3u^3+1980t^2u^4+652tu^5+75u^6)+s^5(72t^7\\
&+734t^6u+2618t^5u^2+4630t^4u^3+4480t^3u^4+2370t^2u^5+612tu^6+48u^7)+s^4(t+u)^2(36t^6\\
&+404t^5u+1297t^4u^2+1774t^3u^3+1143t^2u^4+332tu^5+18u^6)+s^3(9t^9+188t^8u+1142t^7u^2\\
&+3251t^6u^3+5142t^5u^4+4834t^4u^5+2729t^3u^6+874t^2u^7+128tu^8+3u^9)+2s^2tu(t+u)^2(16t^6\\
&+138t^5u+387t^4u^2+495t^3u^3+311t^2u^4+100tu^5+10u^6)+st^2u^2(t+u)^3(37t^4+161t^3u\\
&+234t^2u^2+127tu^3+29u^4)+14t^3u^3(t+u)^6],\\
L=\;&24Q^{10}t^4(s+t)(t+u)[s^3+s^2(3t+4u)+s(3t^2+7tu+5u^2)+t^3+3t^2u+3tu^2+2u^3]\\
&-2Q^8t^2[s^8+14s^7(t+u)+s^6(55t^2+110tu+53u^2)+2s^5(67t^3+162t^2u+141tu^2+46u^3)\\
&+s^4(254t^4+666t^3u+652t^2u^2+322tu^3+83u^4)+2s^3(160t^5+521t^4u+608t^3u^2+319t^2u^3\\
&+91tu^4+19u^5)+s^2(t+u)^2(230t^4+516t^3u+304t^2u^2+46tu^3+7u^4)+2st(43t^6+229t^5u\\
&+498t^4u^2+551t^3u^3+298t^2u^4+66tu^5+7u^6)+2t^2(t+u)^2(7t^4+29t^3u+47t^2u^2+47tu^3\\
&+4u^4)]+2Q^6t[s^9(3t-u)+s^8(51t^2+37tu-14u^2)+s^7(221t^3+389t^2u+107tu^2-53u^3)\\
&+s^6(467t^4+1269t^3u+1049t^2u^2+155tu^3-92u^4)+s^5(610t^5+2090t^4u+2674t^3u^2\\
&+1434t^2u^3+161tu^4-83u^5)+s^4(542t^6+2196t^5u+3484t^4u^2+2782t^3u^3+1115t^2u^4\\
&+125tu^5-38u^6)+s^3(t+u)^2(302t^5+990t^4u+870t^3u^2+342t^2u^3+67tu^4-7u^5)+s^2t(70t^7\\
&+670t^6u+2020t^5u^2+2756t^4u^3+1859t^3u^4+643t^2u^5+127tu^6+7u^7)-2st^2(t+u)^2(6t^5\\
&-56t^4u-229t^3u^2-255t^2u^3-68tu^4-16u^5)-2t^3(t+u)^3(3t^4-3t^3u-32t^2u^2-49tu^3\\
&-11u^4)]-Q^4[s^{10}(13t^2+8tu+7u^2)+2s^9(74t^3+56t^2u+tu^2+19u^3)+s^8(588t^4+880t^3u\\
&+61t^2u^2-118tu^3+89u^4)+4s^7(298t^5+750t^4u+413t^3u^2-161t^2u^3-93tu^4+29u^5)\\
&+s^6(1421t^6+5216t^5u+5998t^4u^2+1312t^3u^3-1504t^2u^4-536tu^5+89u^6)+2s^5(536t^7\\
&+2616t^6u+4606t^5u^2+3264t^4u^3+232t^3u^4-734t^2u^5-209tu^6+19u^7)+s^4(t+u)^2(534t^6\\
&+2328t^5u+2692t^4u^2+896t^3u^3-370t^2u^4-184tu^5+7u^6)+4s^3t(43t^8+397t^7u+1177t^6u^2\\
&+1596t^5u^3+1060t^4u^4+279t^3u^5-55t^2u^6-54tu^7-7u^8)+s^2t^2(t+u)^2(28t^6+444t^5u\\
&+1178t^4u^2+920t^3u^3+103t^2u^4-26tu^5-43u^6)+4st^3u(t+u)^3(17t^4+73t^3u+76t^2u^2\\
&+10tu^3+2u^4)+28t^4u^2(t+u)^6]+2Q^2s[s^{10}(8t^2+11tu+7u^2)+s^9(58t^3+78t^2u+65tu^2\\
&+45u^3)+s^8(177t^4+287t^3u+162t^2u^2+187tu^3+127u^4)+s^7(295t^5+655t^4u+232t^3u^2\\
&-20t^2u^3+313tu^4+205u^5)+s^6(290t^6+925t^5u+438t^4u^2-844t^3u^3-540t^2u^4+308tu^5
\end{aligned}
$$

$$
\begin{aligned}
&+205u^6) + s^5(168t^7 + 776t^6u + 692t^5u^2 - 1164t^4u^3 - 2216t^3u^4 - 930t^2u^5 + 165tu^6 + 127u^7)\\
&+s^4(t+u)^2(53t^6 + 247t^5u - 61t^4u^2 - 871t^3u^3 - 719t^2u^4 - 55tu^5 + 45u^6) + s^3(t+u)^2(7t^7\\
&+53t^6u - 73t^5u^2 - 531t^4u^3 - 697t^3u^4 - 339t^2u^5 - 17tu^6 + 7u^7) - s^2tu^2(t+u)^3(85t^4 + 274t^3u\\
&+227t^2u^2 + 99tu^3 + u^4) - 3st^2u^2(t+u)^4(7t^3 + 33t^2u + 22tu^2 + 6u^3) - 14t^3u^3(t+u)^6]\\
&-s^2(s+u)(s+t+u)^2[s^7(7t^2 + 12tu + 7u^2) + s^6(28t^3 + 45t^2u + 50tu^2 + 31u^3) + 2s^5(21t^4\\
&+33t^3u + 51t^2u^2 + 69tu^3 + 29u^4) + 2s^4(14t^5 + 24t^4u + 34t^3u^2 + 90t^2u^3 + 94tu^4 + 29u^5)\\
&+s^3(7t^6 + 18t^5u - 2t^4u^2 + 60t^3u^3 + 180t^2u^4 + 138tu^5 + 31u^6) + s^2u(t+u)^2(3t^4 - 14t^3u\\
&+23t^2u^2 + 36tu^3 + 7u^4) + 3stu^2(t+u)^3(t^2 + 3tu + 4u^2) + 7t^2u^3(t+u)^4],\\
A &= 0. \qquad \text{(A.9)}
\end{aligned}
$$

$\nu_e(\overline{\nu}_e)\ g \to \nu_e(\overline{\nu}_e)\ c\overline{c}\left[{}^1S_0^{(8)}\right]\ g$:

$$
\begin{aligned}
F &= \frac{g^4\alpha_s^2}{12\pi M(Q^2+m_Z^2)^2 s^4 t(s+t)^2(s+u)^2(t+u)^2},\\
T &= 9v_c^2Q^2(Q^2t+su)[2Q^4t^2u^2 + 2Q^2stu(st+su+t^2+tu+u^2) + s^6\\
&\quad + 2s^5(t+u) + 3s^4(t+u)^2 + 2s^3(t+u)^3 + s^2(t^4 + 2t^3u + 3t^2u^2 + 2tu^3 + u^4)]\\
&\quad + 10a_c^2Q^2s^2t^2(Q^2t+su)(s+t+u)^2,\\
L &= -9v_c^2Q^4t[2Q^4t^2u^2 + 2Q^2stu(st+su+t^2+tu+2u^2) + s^4(t+u)^2\\
&\quad + 2s^3(t^3 + 2t^2u + 2tu^2 + u^3) + s^2(t^4 + 2t^3u + 3t^2u^2 + 2tu^3 + 2u^4)]\\
&\quad - 5a_c^2s^2t(Q^2t+su)^2(s+t+u)^2,\\
A &= 0. \qquad \text{(A.10)}
\end{aligned}
$$

$\nu_e(\overline{\nu}_e)\ g \to \nu_e(\overline{\nu}_e)\ c\overline{c}\left[{}^3S_1^{(8)}\right]\ g$:

$$
\begin{aligned}
F &= \frac{-g^4\alpha_s^2}{36\pi M(Q^2+m_Z^2)^2 s^4 t(s+t)^2(s+u)^2(t+u)^2},\\
T &= 10v_c^2Q^2t\{2Q^6t^2(s^2+t^2) - Q^4t[s^3(3t-2u) + 3s^2t(t+u) + 2st^2(t-u) + 2t^3(t+u)]\\
&\quad + Q^2s[s^3(t-u)^2 - 2s^2tu(t+u) - st^2u(2t-u) - 2t^3u(t+u)] - s^5(t^2+tu+u^2)\\
&\quad - s^4(t+u)^3 - s^3tu(t^2+3tu+u^2) - s^2t^2u^2(t+u)\} + 9a_c^2Q^2\{2Q^6t^3u^2 - 2Q^4t^2u[s^3\\
&\quad - s^2(t+u) + s(t^2+tu-2u^2) + 2tu(t+u)] - Q^2st[s^5 + 2s^4(t+u) + s^3(t^2+2tu\\
&\quad + 3u^2) + 2s^2t(t^2+3tu+2u^2) + s(t^4+6t^3u+15t^2u^2+12tu^3-u^4) + 4tu^2(t^2+3tu\\
&\quad + 2u^2)] - s^7u - 2s^6u(t+u) - s^5(2t^3+5t^2u+6tu^2+3u^3) - 2s^4(t^4+4t^3u+7t^2u^2\\
&\quad + 5tu^3+u^4) - s^3u(3t^4+12t^3u+17t^2u^2+10tu^3+u^4) - 2s^2tu^2(t^3+3t^2u+4tu^2\\
&\quad + 2u^3)\},\\
L &= 5v_c^2Q^4t\{2Q^4t^2(s^2-2t^2) - 2Q^2t(s^2-2t^2)[s(t-u)+t(t+u)] + s^4(t^2+u^2)\\
&\quad + 2s^3t^2(t+u) + s^2t^2(t^2+6tu+u^2) + 4st^3u(t+u)\} - 9a_c^2\{2Q^8t^3u^2 + 2Q^6t^2u[s^3\\
&\quad + s^2(t+u) - s(t^2+tu-2u^2) - 2tu(t+u)] + Q^4st[s^5 + 2s^4(t+u) + s^3u(t+5u)\\
&\quad - s^2(2t^3+7t^2u+tu^2-4u^3) - s(t^4+6t^3u+14t^2u^2+8tu^3-3u^4) - 4tu^2(t^2+3tu
\end{aligned}
$$

$$+ 2u^2)] - Q^2s^2[s^5(t-u) + s^4(3t^2+tu-2u^2) + s^3(3t^3+8t^2u+4tu^2-3u^3) + s^2(t^4 + 9t^3u + 18t^2u^2 + 8tu^3 - 2u^4) + su(3t^4+13t^3u+20t^2u^2+9tu^3-u^4) + tu^2(t + u)^2(t+5u)] - s^3u(s+t+u)[s^2+s(t+u)+u(t+u)]^2\},$$

$$A = 0. \tag{A.11}$$

$\nu_e(\overline{\nu}_e)\ g \to \nu_e(\overline{\nu}_e)\ c\overline{c}\left[{}^3P_J^{(8)}\right]\ g$:

$$F = \frac{-g^4\alpha_s^2}{3\pi M^3(Q^2+m_Z^2)^2s^4t(s+t)^3(s+u)^4(t+u)^3},$$

$$T = 9v_c^2Q^2\{8Q^8t^2[2s^5t - 2s^4u^2 + s^3t^2(2t-3u) - s^2tu(t^2+3tu-3u^2) - stu(2t^3+t^2u - tu^2 - u^3) + t^2u^3(2t+u)] - 2Q^6t[4s^7(t+u) + 4s^6(5t^2+2u^2) + 4s^5(5t^3+6t^2u - 2tu^2 + 4u^3) + 2s^4(9t^4 - 9t^3u + 4t^2u^2 - 6tu^3 + 4u^4) + s^3(12t^5 - 2t^4u - 29t^3u^2 + 33t^2u^3 - 12tu^4 + 4u^5) - s^2t(2t^5 + 20t^4u + 25t^3u^2 - t^2u^3 - 16tu^4 + 4u^5) - st^2u \times (12t^4 + 26t^3u + 2t^2u^2 + tu^3 + u^4) - t^3u^2(2t^3 - 6t^2u - 15tu^2 - 7u^3)] + 2Q^4[2s^8 \times (3t^2+tu-2u^2) + s^7(21t^3+3t^2u+10tu^2-8u^3) + s^6(28t^4+15t^3u-15t^2u^2+22tu^3 - 12u^4) + s^5(27t^5+11t^4u+8t^3u^2-20t^2u^3+26tu^4-8u^5) + s^4(16t^6+17t^5u-20t^4u^2 + 2t^3u^3 - 33t^2u^4 + 18tu^5 - 4u^6) + s^3t(2t^6+8t^5u-3t^4u^2-19t^3u^3-19t^2u^4-17tu^5 + 6u^6) - s^2t^2(2t^6+14t^5u+30t^4u^2+33t^3u^3+46t^2u^4+21tu^5+4u^6) - 2st^3u(2t^5 + 10t^4u + 16t^3u^2 + 20t^2u^3 + 19tu^4 + 7u^5) - 2t^6u^2(t+u)^2] - Q^2s[s^8(7t^2-5tu-12u^2) + s^7(25t^3+3t^2u-18tu^2-36u^3) + s^6(37t^4+25t^3u-12t^2u^2-20tu^3-60u^4) + s^5(39t^5 + 39t^4u + 16t^3u^2 - 18t^2u^3 - 6tu^4 - 60u^5) + s^4(29t^6+83t^5u+72t^4u^2+88t^3u^3+40t^2u^4 + 22tu^5 - 36u^6) + s^3(9t^7+75t^6u+148t^5u^2+176t^4u^3+178t^3u^4+102t^2u^5+22tu^6 - 12u^7) + s^2tu(22t^6+107t^5u+199t^4u^2+211t^3u^3+177t^2u^4+73tu^5+9u^6) + st^2u^2(17t^5 + 69t^4u + 107t^3u^2 + 105t^2u^3 + 71tu^4 + 21u^5) + 4t^5u^3(t+u)^2] - s^2(s+u)[7s^7u(t+u) + s^6u(25t^2+38tu+21u^2) + s^5(2t^4+47t^3u+88t^2u^2+78tu^3+35u^4) + s^4(4t^5+63t^4u + 132t^3u^2 + 156t^2u^3 + 98tu^4 + 35u^5) + s^3(2t^6+47t^5u+136t^4u^2+190t^3u^3+156t^2u^4 + 78tu^5 + 21u^6) + s^2u(13t^6+70t^5u+136t^4u^2+132t^3u^3+88t^2u^4+38tu^5+7u^6) + stu^2 \times (13t^5+47t^4u+63t^3u^2+47t^2u^3+25tu^4+7u^5) + 2t^4u^3(t+u)^2]\} + 10a_c^2Q^2t\{4Q^8t^4 \times [2s^3+s^2(5t+7u)+s(4t^2+11tu+7u^2)+(t+u)^2(t+2u)] + 2Q^6t^2[2s^6+s^5(7t + 9u) + s^4(5t^2+27tu+12u^2) - s^3(13t^3-7t^2u-34tu^2-4u^3) - s^2(23t^4+57t^3u + 18t^2u^2 - 14tu^3 + 2u^4) - s(12t^5+52t^4u+73t^3u^2+33t^2u^3+tu^4+u^5) - t(2t^5 + 12t^4u + 27t^3u^2 + 29t^2u^3 + 13tu^4 + u^5)] - Q^4t[2s^7(5t-2u) + s^6(41t^2+37tu-18u^2) + s^5(56t^3+147t^2u+45tu^2-24u^3) + s^4(19t^4+164t^3u+194t^2u^2+19tu^3-8u^4) - s^3(16t^5-12t^4u-154t^3u^2-117t^2u^3+5tu^4-4u^5) - s^2(8t^6+66t^5u+95t^4u^2 + 8t^3u^3 - 17t^2u^4 + 10tu^5 - 2u^6) + 2st(2t^6-8t^5u-53t^4u^2-82t^3u^3-45t^2u^4 - 8tu^5 - 2u^6) + 2t^2(t+u)^2(t^4-8t^2u^2-12tu^3-3u^4)] + Q^2[s^9(t+u) + s^8(11t^2 + tu + 6u^2) + s^7(40t^3+36t^2u-3tu^2+17u^3) + s^6(56t^4+144t^3u+57t^2u^2+9tu^3$$

$$
\begin{aligned}
&+ 24u^4) + s^5(19t^5 + 167t^4u + 230t^3u^2 + 90t^2u^3 + 41tu^4 + 17u^5) - s^4(29t^6 + 5t^5u \\
&- 182t^4u^2 - 228t^3u^3 - 117t^2u^4 - 53tu^5 - 6u^6) - s^3(30t^7 + 126t^6u + 115t^5u^2 \\
&- 81t^4u^3 - 158t^3u^4 - 88t^2u^5 - 31tu^6 - u^7) - s^2t(8t^7 + 72t^6u + 191t^5u^2 + 181t^4u^3 \\
&+ 16t^3u^4 - 60t^2u^5 - 29tu^6 - 7u^7) - 2st^2u(t+u)^2(5t^4 + 21t^3u + 21t^2u^2 + 2tu^3 \\
&- u^4) - 4t^3u^2(t+u)^5] - s(s+u)[s^8(t+u) + 6s^7(t^2 + tu + u^2) + s^6(19t^3 + 29t^2u \\
&+ 27tu^2 + 17u^3) + 2s^5(17t^4 + 47t^3u + 50t^2u^2 + 35tu^3 + 12u^4) + s^4(35t^5 + 162t^4u \\
&+ 254t^3u^2 + 202t^2u^3 + 92tu^4 + 17u^5) + s^3(20t^6 + 145t^5u + 338t^4u^2 + 370t^3u^3 \\
&+ 216t^2u^4 + 65tu^5 + 6u^6) + s^2(5t^7 + 62t^6u + 217t^5u^2 + 346t^4u^3 + 286t^3u^4 + 125t^2u^5 \\
&+ 26tu^6 + u^7) + stu(t+u)^2(9t^4 + 40t^3u + 56t^2u^2 + 28tu^3 + 5u^4) + 4t^2u^2(t+u)^5]\},
\end{aligned}
$$

$$
\begin{aligned}
L = 18v_c^2Q^4\{&4Q^6t^2[s^5t - s^4u^2 - 2s^3t^3 + s^2t^2u(t+3u) + stu(2t^3 + t^2u - tu^2 - u^3) \\
&- t^2u^3(2t+u)] - Q^4t[2s^7(t+u) + 4s^6(2t^2 + u^2) - s^5(t^3 - t^2u + 2tu^2 - 8u^3) - s^4(21t^4 \\
&+ 13t^3u + 18t^2u^2 - 2tu^3 - 4u^4) - 2s^3(6t^5 + 10t^4u + t^3u^2 + 4t^2u^3 - 6tu^4 - u^5) + 2s^2t \\
&\times (t^5 + 10t^4u + 11t^3u^2 + 9t^2u^3 + 6tu^4 + 5u^5) + st^2u(12t^4 + 26t^3u + 2t^2u^2 + tu^3 + u^4) \\
&+ t^3u^2(2t^3 - 6t^2u - 15tu^2 - 7u^3)] + 2Q^2[s^8(t^2 - u^2) + s^7(3t^3 + tu^2 - 2u^3) - s^6(2t^4 \\
&+ 2t^3u + 2t^2u^2 - tu^3 + 3u^4) - s^5(12t^5 + 16t^4u + 16t^3u^2 - t^2u^3 + tu^4 + 2u^5) - s^4(10t^6 \\
&+ 28t^5u + 28t^4u^2 + 13t^3u^3 - 7t^2u^4 + 3tu^5 + u^6) - s^3t(t^6 + 9t^5u + 18t^4u^2 + t^3u^3 \\
&- 15t^2u^4 - 10tu^5 + 2u^6) + s^2t^2(t^6 + 7t^5u + 13t^4u^2 + 18t^3u^3 + 35t^2u^4 + 24tu^5 + 6u^6) \\
&+ st^3u(2t^5 + 10t^4u + 16t^3u^2 + 20t^2u^3 + 19tu^4 + 7u^5) + t^6u^2(t+u)^2] + s(s+u)[2s^7u(t \\
&+ u) + 2s^6u(3t^2 + 3tu + 2u^2) + s^5(5t^4 + 15t^3u + 18t^2u^2 + 14tu^3 + 6u^4) + s^4(15t^5 \\
&+ 38t^4u + 53t^3u^2 + 40t^2u^3 + 22tu^4 + 4u^5) + s^3(15t^6 + 52t^5u + 88t^4u^2 + 81t^3u^3 + 47t^2u^4 \\
&+ 19tu^5 + 2u^6) + s^2t(5t^6 + 32t^5u + 78t^4u^2 + 90t^3u^3 + 68t^2u^4 + 34tu^5 + 9u^6) + st^2u(7t^5 \\
&+ 31t^4u + 47t^3u^2 + 39t^2u^3 + 23tu^4 + 7u^5) + 2t^5u^2(t+u)^2]\} - 10a_c^2t\{4Q^{10}t^4[2s^3 \\
&+ s^2(5t + 7u) + s(4t^2 + 11tu + 7u^2) + (t+u)^2(t+2u)] - 2Q^8t^2[2s^6 + 2s^5(4t + 5u) \\
&+ 2s^4(9t^2 + 11tu + 9u^2) + s^3(29t^3 + 43t^2u + 15tu^2 + 15u^3) + s^2(27t^4 + 73t^3u + 41t^2u^2 \\
&+ tu^3 + 6u^4) + s(12t^5 + 52t^4u + 73t^3u^2 + 33t^2u^3 + tu^4 + u^5) + t(2t^5 + 12t^4u + 27t^3u^2 \\
&+ 29t^2u^3 + 13tu^4 + u^5)] + Q^6t[s^7(11t - 4u) + 5s^6(9t^2 + 8tu - 4u^2) + s^5(81t^3 + 153t^2u \\
&+ 73tu^2 - 36u^3) + s^4(87t^4 + 221t^3u + 226t^2u^2 + 99tu^3 - 30u^4) + s^3(56t^5 + 198t^4u \\
&+ 231t^3u^2 + 183t^2u^3 + 82tu^4 - 12u^5) + s^2(14t^6 + 106t^5u + 201t^4u^2 + 145t^3u^3 + 69t^2u^4 \\
&+ 31tu^5 - 2u^6) - 2st(2t^6 - 8t^5u - 53t^4u^2 - 82t^3u^3 - 45t^2u^4 - 8tu^5 - 2u^6) - 2t^2(t+u)^2 \\
&\times (t^4 - 8t^2u^2 - 12tu^3 - 3u^4)] - Q^4[s^9(t+u) + s^8(14t^2 - tu + 6u^2) + s^7(48t^3 + 35t^2u \\
&- 18tu^2 + 16u^3) + s^6(78t^4 + 148t^3u + 17t^2u^2 - 54tu^3 + 22u^4) + s^5(75t^5 + 240t^4u + 214t^3u^2 \\
&- 30t^2u^3 - 86tu^4 + 16u^5) + s^4(48t^6 + 229t^5u + 360t^4u^2 + 216t^3u^3 - 43t^2u^4 - 74tu^5 \\
&+ 6u^6) + s^3(20t^7 + 152t^6u + 339t^5u^2 + 326t^4u^3 + 134t^3u^4 - 17t^2u^5 - 31tu^6 + u^7) + s^2t(4t^7 \\
&+ 62t^6u + 210t^5u^2 + 275t^4u^3 + 150t^3u^4 + 28t^2u^5 - 4tu^6 - 5u^7) + 2st^2u(t+u)^2(5t^4 + 21t^3u \\
&+ 21t^2u^2 + 2tu^3 - u^4) + 4t^3u^2(t+u)^5] + Q^2s[2s^9(t+u) + s^8(12t^2 + 12tu + 13u^2) + s^7(28t^3 \\
&+ 41t^2u + 37tu^2 + 37u^3) + s^6(32t^4 + 73t^3u + 50t^2u^2 + 62tu^3 + 60u^4) + s^5(18t^5 + 59t^4u
\end{aligned}
$$

$$+ 29t^3u^2 - 17t^2u^3 + 48tu^4 + 60u^5) + s^4(4t^6 + 11t^5u - 41t^4u^2 - 146t^3u^3 - 133t^2u^4 + 2tu^5 + 37u^6) - s^3u(10t^6 + 84t^5u + 225t^4u^2 + 279t^3u^3 + 162t^2u^4 + 21tu^5 - 13u^6) - s^2u(t+u)^2 \times (4t^5 + 40t^4u + 87t^3u^2 + 57t^2u^3 + 16tu^4 - 2u^5) - 2stu^2(t+u)^3(4t^3 + 15t^2u + 9tu^2 + u^3) - 4t^2u^3(t+u)^5] - s^2(s+u)(s+t+u)^2[s^6(t+u) + s^5(3t^2 + 4tu + 4u^2) + s^4(3t^3 + 7t^2u + 11tu^2 + 7u^3) + s^3(t^4 + 6t^3u + 13t^2u^2 + 14tu^3 + 7u^4) + s^2u(2t^4 + 8t^3u + 13t^2u^2 + 11tu^3 + 4u^4) + su^2(t+u)^2(2t^2 + 2tu + u^2) + tu^3(t+u)^3]\},$$

$$A = 0. \tag{A.12}$$

A.2 The process $\nu_e N \to e^-(J/\psi)_{\text{prompt}} jX$

In this section we present the coefficients $F_{\nu_e a}[n]$, $T_{\nu_e a}[n]$, $L_{\nu_e a}[n]$ and $A_{\nu_e a}[n]$ occurring in (4.88). For completeness we here include also the relevant Cabbibo Kobayashi Maskawa mixing matrix elements in the formulae. Note, that in our numerical analysis these matrix elements are set equal to one.

$\nu_e\ d(\bar{u}) \to e^-\ c\overline{c}\left[{}^3S_1^{(1)}\right]\ u(\bar{d})$:

$$F = T = L = A = 0$$

$\nu_e\ d(\bar{u}) \to e^-\ c\overline{c}\left[{}^3P_0^{(1)}\right]\ u(\bar{d})$:

$$F = T = L = A = 0$$

$\nu_e\ d(\bar{u}) \to e^-\ c\overline{c}\left[{}^3P_1^{(1)}\right]\ u(\bar{d})$:

$$F = T = L = A = 0$$

$\nu_e\ d(\bar{u}) \to e^-\ c\overline{c}\left[{}^3P_2^{(1)}\right]\ u(\bar{d})$:

$$F = T = L = A = 0$$

$\nu_e\ d(\bar{u}) \to e^-\ c\overline{c}\left[{}^1S_0^{(8)}\right]\ u(\bar{d})$:

$$F = T = L = A = 0$$

$\nu_e\ d(\bar{u}) \to e^-\ c\overline{c}\left[{}^3S_1^{(8)}\right]\ u(\bar{d})$:

$$F = \frac{g'^4\alpha_s^2 Q^2 |V_{ud}|^2}{72\pi M^3 s^4 (Q^2 + m_W^2)^2 (Q^2 - s)^2 (Q^2 - u)^2},$$

$$T = -2Q^6t^2(2s+t) - 2Q^4s[s^2u - st(3t-2u) - 2t^3] - Q^2s^2[s^2(t-2u) + 2s(t^2 - 4tu - u^2) + t(2t^2 - 2tu - u^2)] - s^3u(s^2 + 2st + 2t^2 + 2tu + u^2),$$

$$L = 2Q^2t(Q^2 - s)^2(s+t)^2,$$

$$A = \pm\{2Q^6s^2t - 2Q^4st(2s^2 + st - tu) + Q^2s^2[s^2(t-2u) + 2s(t^2 + u^2) - tu(2t-u)] + s^3u(s-u)(s+2t+u)\}\ , \tag{A.13}$$

where the plus (minus) sign refers to the $\nu_e d$ ($\nu_e \bar{u}$) initial state.

$\nu_e\ d(\bar{u}) \to e^-\ c\overline{c}\left[^3P_J^{(8)}\right]\ u(\bar{d})$:

$$F = T = L = A = 0$$

$\nu_e\ s \to e^-\ c\overline{c}\left[^3S_1^{(1)}\right]\ c$:

$$
\begin{aligned}
F &= \frac{g'^4\alpha_s^2|V_{cs}|^2}{27\pi M s^4(Q^2+m_W^2)^2(2Q^2+s-2t+u)^2(2Q^2-2s+t+u)^4},\\
T &= 32Q^{10}(2s^3+14s^2t+18st^2-39t^3)-16Q^8[31s^4-s^3(133t+50u)+s^2t(328t+u)\\
&\quad -3st^2(33t-32u)+81t^3(t+u)]+24Q^6[46s^5-s^4(201t+4u)+2s^3(66t^2-97tu-u^2)\\
&\quad -s^2t(104t^2+40tu+53u^2)+12st^2(t+u)(3t-7u)-15t^3(t+u)^2]-4Q^4[244s^6\\
&\quad -4s^5(173t-57u)-3s^4(61t^2+168tu-73u^2)-s^3(677t^3-72t^2u-591tu^2-154u^3)\\
&\quad +s^2t(t+u)(52t^2-283tu+259u^2)-9st^2(t+u)^2(3t-16u)+3t^3(t+u)^3]+2Q^2s[152s^6\\
&\quad -52s^5(5t-2u)-2s^4(131t^2-16tu+93u^2)-s^3(469t^3-456t^2u-531tu^2+238u^3)\\
&\quad +4s^2(t+u)(25t^3+7t^2u+56tu^2-25u^3)-st(t+u)^2(10t^2-46tu+115u^2)\\
&\quad -6t^2u(t+u)^3],\\
L &= -16Q^{10}(4s^3-47s^2t+36st^2-78t^3)+16Q^8[30s^4-s^3(73t-44u)+s^2t(55t-38u)\\
&\quad -3st^2(33t-32u)+81t^3(t+u)]-4Q^6[260s^5+s^4(119t+348u)+2s^3(144t^2-31tu\\
&\quad -4u^2)+3s^2t(11t^2+166tu+12u^2)+72st^2(t+u)(3t-7u)-90t^3(t+u)^2]\\
&\quad +4Q^4[220s^6+s^5(391t+150u)+18s^4(23t^2-10u^2)+s^3(295t^3+132t^2u+18tu^2-92u^3)\\
&\quad +s^2t(t+u)(40t^2-271tu+175u^2)-9st^2(t+u)^2(3t-16u)+3t^3(t+u)^3]-Q^2s[240s^6\\
&\quad +4s^5(197t-40u)+4s^4(277t^2-116tu-183u^2)+3s^3(293t^3-110t^2u-143tu^2-104u^3)\\
&\quad +2s^2(t+u)(130t^3-81t^2u+15tu^2+10u^3)-st(t+u)^2(32t^2-104tu+269u^2)\\
&\quad -12t^2u(t+u)^3]-s^2[16s^6-4s^5(29t-18u)-4s^4(75t^2-26tu-11u^2)-s^3(215t^3\\
&\quad -258t^2u-213tu^2+104u^3)-s^2(t+u)(47t^3-224t^2u-67tu^2+132u^3)\\
&\quad -su(t+u)^2(22t^2-19tu+40u^2)-3tu^2(t+u)^3],\\
A &= -32Q^{10}s(15s^2-43st+33t^2)+16Q^8s[105s^3-s^2(86t-63u)+st(43t-38u)-9t^2(22t+9u)]\\
&\quad -24Q^6s[90s^4-5s^3(t-6u)+s^2(5t+3u)(37t-5u)-st(155t^2-116tu-76u^2)\\
&\quad +21t^2(t+u)(3t+u)]+4Q^4s[300s^5-8s^4(10t+9u)+3s^3(389t^2-116tu-141u^2)\\
&\quad -3s^2(40t^3-215t^2u+110tu^2+53u^3)+st(t+u)(253t^2-295tu-170u^2)-3t^2(t+u)^2(8t\\
&\quad +5u)]-2Q^2s^2[120s^5-100s^4t+2s^3(289t^2-368tu-9u^2)+3s^2(77t^3+62t^2u-95tu^2\\
&\quad +76u^3)-2s(t+u)(2t^3+175t^2u-16tu^2-63u^3)-t(t+u)^2(4t^2-28tu-23u^2)]
\end{aligned}
\tag{A.14}
$$

$\nu_e\ s \to e^-\ c\overline{c}\left[^3P_0^{(1)}\right]\ c$:

$$F = \frac{4g'^4\alpha_s^2|V_{cs}|^2}{27\pi M^3 s^4(Q^2+m_W^2)^2(2Q^2+s-2t+u)^4(2Q^2-2s+t+u)^5},$$

$$
\begin{aligned}
T = {} & 256Q^{16}t(94s^2+36st-39t^2)+128Q^{14}[237s^4+s^3(193t+294u)+s^2t(58t+637u)\\
& -3st^2(39t+8u)+18t^3(8t-3u)]-192Q^{12}[330s^5+s^4(668t-57u)+s^3(883t^2\\
& +271tu-426u^2)+s^2t(437t^2+1039tu-220u^2)+3st^2(137t^2-25tu+30u^2)\\
& +3t^3(14t^2-11u^2)]+32Q^{10}[729s^6+s^5(1805t-3492u)+6s^4(1234t^2-1673tu\\
& -450u^2)-6s^3(108t^3+958t^2u+1907tu^2-132u^3)+s^2t(6314t^3-5349t^2u-7635tu^2\\
& -1885u^3)-9st^2(101t^3+146t^2u+54tu^2+30u^3)-12t^3(t+u)(38t^2+70tu-13u^2)]\\
& +16Q^8[384s^7+s^6(5636t+813u)-s^5(5617t^2-22685tu+6822u^2)\\
& +6s^4(978t^3+1160t^2u-1498tu^2-1763u^3)-2s^3(410t^4-13320t^3u+1257t^2u^2\\
& +12083tu^3+1866u^4)+s^2t(1568t^4+4703t^3u+1866t^2u^2-5446tu^3-4690u^4)\\
& +3st^2(t+u)(339t^3+86t^2u-1166tu^2-40u^3)-9t^3(t+u)^2(59t^2+50tu\\
& +9u^2)]+24Q^6[840s^8-2s^7(1954t-1545u)-s^6(1024t^2+3229tu-3243u^2)\\
& -s^5(2423t^3-536t^2u-7177tu^2+2274u^3)-s^4(2897t^4+4662t^3u-7860t^2u^2\\
& -1816tu^3+5793u^4)-s^3(715t^5-2492t^4u-9804t^3u^2-3932t^2u^3+4957tu^4\\
& +2526u^5)-s^2t(t+u)(1832t^4+2228t^3u-2727t^2u^2-391tu^3+1247u^4)\\
& +3st^2(t+u)^2(286t^3+92t^2u-365tu^2-36u^3)-6t^3(t+u)^3(64t^2-39tu+11u^2)]\\
& -4Q^4[4320s^9-4s^8(664t-1305u)-24s^7(454t^2-107tu+441u^2)+3s^6(1112t^3\\
& +6299t^2u+5326tu^2-5709u^3)-s^5(14699t^4+249t^3u-17283t^2u^2-6325tu^3\\
& -2196u^4)-3s^4(2312t^5+1739t^4u+3900t^3u^2+11648t^2u^3+2576tu^4-4419u^5)\\
& +3s^3(t+u)(1785t^5+6260t^4u+5462t^3u^2-4586t^2u^3-2543tu^4+1806u^5)\\
& -s^2t(t+u)^2(4141t^4+1480t^3u+1815t^2u^2-1229tu^3-1088u^4)-9st^2(t+u)^3(192t^3\\
& -182t^2u+51tu^2-46u^3)+3t^3(t+u)^4(16t-5u)^2]+2Q^2s[336s^9+40s^8(184t-39u)\\
& -4s^7(1646t^2-2065tu+801u^2)-6s^6(1326t^3+2625t^2u+832tu^2-571u^3)+s^5(4835t^4\\
& +18963t^3u-6609t^2u^2-10807tu^3+7482u^4)-2s^4(998t^5-7945t^4u-13506t^3u^2\\
& -814t^2u^3+3488tu^4-153u^5)-6s^3(t+u)(473t^5+1925t^4u+1679t^3u^2-962t^2u^3-858tu^4\\
& +637u^5)+2s^2(t+u)^2(128t^5+983t^4u-4764t^3u^2-334t^2u^3+3056tu^4\\
& -690u^5)-st(t+u)^3(272t^4-5728t^3u-78t^2u^2+1718tu^3+35u^4)\\
& -6t^2u(t+u)^4(16t-5u)^2],\\
L = {} & -128Q^{16}(12s^3-59s^2t+72st^2-78t^3)+64Q^{14}[226s^4-2s^3(17t-126u)+s^2t(431t-55u)\\
& +6st^2(39t+8u)-36t^3(8t-3u)]-32Q^{12}[1040s^5+10s^4(137t+59u)+12s^3(89t^2\\
& +21tu-69u^2)+3s^2t(1009t^2-652tu+245u^2)-18st^2(137t^2-25tu+30u^2)\\
& -18t^3(14t^2-11u^2)]+16Q^{10}[1122s^6+2s^5(2615t-1518u)-6s^4(317t^2-225tu+826u^2)\\
& +12s^3(789t^3-1381t^2u-11tu^2-29u^3)-s^2t(7547t^3-7545t^2u-2559tu^2+419u^3)\\
& +18st^2(101t^3+146t^2u+54tu^2+30u^3)+24t^3(t+u)(38t^2+70tu-13u^2)]\\
& +8Q^8[3176s^7-s^6(10037t-12174u)+2s^5(8093t^2-2803tu+2982u^2)-2s^4(10451t^3\\
& -19740t^2u+336tu^2+3146u^3)+2s^3(10685t^4-5025t^3u-1929t^2u^2+1145tu^3\\
& -1602u^4)-s^2t(10778t^4+4106t^3u-8970t^2u^2-4120tu^3-2659u^4)-6st^2(t+u)(339t^3
\end{aligned}
$$

$$
\begin{aligned}
&+86t^2u-1166tu^2-40u^3)+18t^3(t+u)^2(59t^2+50tu+9u^2)]\\
&-4Q^6[8944s^8-8s^7(1612t-1673u)+3s^6(9355t^2-6847tu-3274u^2)-2s^5(12211t^3\\
&-23634t^2u+3837tu^2+10282u^3)+2s^4(13886t^4-9175t^3u-9240t^2u^2+212tu^3\\
&-2017u^4)+6s^3(943t^5+5888t^4u+1572t^3u^2-4856t^2u^3-1069tu^4+378u^5)\\
&-3s^2t(t+u)(3608t^4-268t^3u-5828t^2u^2+1462tu^3+1785u^4)\\
&+18st^2(t+u)^2(286t^3+92t^2u-365tu^2-36u^3)-36t^3(t+u)^3(64t^2-39tu+11u^2)]\\
&+2Q^4[6912s^9-8s^8(1121t-408u)+6s^7(2257t^2-4629tu-3094u^2)-3s^6(655t^3\\
&-12272t^2u+779tu^2+3226u^3)+2s^5(3611t^4-12591t^3u-4287t^2u^2+12773tu^3\\
&+8490u^4)+6s^4(5158t^5+5319t^4u-7411t^3u^2-7604t^2u^3+2031tu^4+2315u^5)\\
&-6s^3(t+u)(2059t^5+892t^4u+804t^3u^2-186t^2u^3-850tu^4-358u^5)\\
&+s^2t(t+u)^2(6110t^4+7808t^3u-16386t^2u^2+1526tu^3+4139u^4)-18st^2(t+u)^3(192t^3\\
&-182t^2u+51tu^2-46u^3)+6t^3(t+u)^4(16t-5u)^2]-Q^2s[992s^9-32s^8(55t+39u)\\
&-4s^7(629t^2+2255tu+762u^2)+4s^6(1480t^3+141t^2u-1146tu^2+1873u^3)+s^5(173t^4\\
&-9t^3u+1887t^2u^2+6293tu^3+10272u^4)+4s^4(2459t^5-3733t^4u-5061t^3u^2+2339t^2u^3\\
&-490tu^4-1266u^5)+2s^3(t+u)(4822t^5-928t^4u-8213t^3u^2+12406t^2u^3+1091tu^4\\
&-5084u^5)-4s^2(t+u)^2(716t^5-295t^4u+2937t^3u^2-3040t^2u^3-616tu^4\\
&+783u^5)+st(t+u)^3(3568t^4+592t^3u-876t^2u^2+1384tu^3-1391u^4)\\
&-12t^2u(t+u)^4(16t-5u)^2]-s^2[64s^9+8s^8(41t+38u)+12s^7(49t^2+67tu+10u^2)\\
&+2s^6(103t^3+174t^2u-201tu^2-248u^3)-s^5(169t^4+283t^3u+1995t^2u^2+1441tu^3\\
&-152u^4)-3s^4(137t^5-240t^4u+494t^3u^2+896t^2u^3-351tu^4-304u^5)-2s^3(t+u)(820t^5\\
&-922t^4u+49t^3u^2+1420t^2u^3-1441tu^4+172u^5)-2s^2(t+u)^2(640t^5\\
&-1288t^4u-239t^3u^2+1396t^2u^3-1540tu^4+616u^5)+3su(t+u)^3(464t^4-216t^3u\\
&-180t^2u^2+377tu^3-168u^4)-3tu^2(t+u)^4(16t-5u)^2],\\
A=\;&256Q^{16}s(35s^2+107st+141t^2)-128Q^{14}s[115s^3-s^2(t+260u)+st(862t-839u)\\
&+81t^2(5t-2u)]+192Q^{12}s[143s^4-115s^3(3t-u)+s^2(192t^2-901tu+359u^2)\\
&-st(178t^2+1529tu-269u^2)-3t^2(13t^2+101tu+61u^2)]-32Q^{10}s[2141s^5+s^4(329t\\
&+3516u)-6s^3(255t^2-537tu-205u^2)+2s^2(826t^3+765t^2u+6279tu^2-437u^3)\\
&-st(2710t^3-33t^2u-7305tu^2-2645u^3)+3t^2(485t^3+384t^2u+258tu^2+332u^3)]\\
&+16Q^8s[3304s^6+s^5(7388t-515u)+s^4(559t^2+11005tu-10758u^2)+2s^3(3551t^3\\
&+1506t^2u-2277tu^2-5281u^3)+s^2(4661t^4+14932t^3u-108t^2u^2-19618tu^3\\
&-3299u^4)+st(1783t^4+2947t^3u+3624t^2u^2-3722tu^3-5615u^4)-27t^2(t+u)(4t^3\\
&+87t^2u+27tu^2+7u^3)]+24Q^6s[440s^7-2s^6(1866t-2009u)-s^5(2304t^2+157tu\\
&-4715u^2)-s^4(3041t^3+290t^2u-4019tu^2+2728u^3)-s^3(3933t^4-430t^3u-6696t^2u^2\\
&+1020tu^3+6377u^4)-s^2(351t^5-3614t^4u-9248t^3u^2-4764t^2u^3+3517tu^4+2512u^5)\\
&-st(t+u)(2140t^4+1426t^3u+51t^2u^2-989tu^3+1081u^4)+3t^2(t+u)^2(4t-5u)(20t^2\\
&+37tu-10u^2)]-4Q^4s[4336s^8-4s^7(332t-1761u)-24s^6(488t^2-207tu
\end{aligned}
$$

$$
\begin{aligned}
&+383u^2) + s^5(2936t^3 + 14697t^2u + 7338tu^2 - 19759u^3) - s^4(15136t^4 - 9795t^3u \\
&-19941t^2u^2 - 2225tu^3 - 303u^4) - 3s^3(2535t^5 + 2685t^4u + 4606t^3u^2 + 8496t^2u^3 \\
&-57tu^4 - 4637u^5) + s^2(t+u)(2488t^5 + 21065t^4u + 4390t^3u^2 - 13118t^2u^3 - 6790tu^4 \\
&+5749u^5) - st(t+u)^2(4952t^4 - 1612t^3u - 933t^2u^2 - 901tu^3 + 29u^4) \\
&+3t^2(t+u)^3(352t^3 - 528t^2u + 372tu^2 - 71u^3)] + 2Q^2s^2[368s^8 + 8s^7(956t - 179u) \\
&-4s^6(1510t^2 - 2033tu + 921u^2) - 2s^5(3286t^3 + 7503t^2u + 3348tu^2 - 1085u^3) \\
&+s^4(3713t^4 + 19387t^3u - 2925t^2u^2 - 9199tu^3 + 7240u^4) - 4s^3(1274t^5 - 1579t^4u \\
&-4845t^3u^2 - 1150t^2u^3 + 737tu^4 - 267u^5) - 2s^2(t+u)(932t^5 + 2224t^4u + 7253t^3u^2 \\
&-1354t^2u^3 - 2087tu^4 + 1826u^5) + 2s(t+u)^2(800t^5 + 3504t^4u - 3020t^3u^2 - 322t^2u^3 \\
&+2448tu^4 - 767u^5) - t(t+u)^3(784t^4 + 544t^3u - 1992t^2u^2 + 1840tu^3 - 377u^4)] \qquad \text{(A.15)}
\end{aligned}
$$

$\nu_e\ s \to e^-\ c\overline{c}\left[{}^3P_1^{(1)}\right]\ c$:

$$
\begin{aligned}
F &= \frac{-8g'^4\alpha_s^2|V_{cs}|^2}{27\pi M^3 s^4(Q^2+m_W^2)^2(2Q^2+s-2t+u)^4(2Q^2-2s+t+u)^5}, \\
T &= 256Q^{16}(2s^3 + 18s^2t - 57st^2 + 78t^3) - 128Q^{14}[4s^4 + s^3(352t + 13u) - 3s^2t(53t - 60u) \\
&+3st^2(108t - 19u) - 9t^3(16t + 29u)] - 192Q^{12}[28s^5 - s^4(451t - 53u) + s^3(67t^2 + 152tu \\
&+97u^2) - 3s^2t(261t^2 + 104tu - 35u^2) + 6st^2(17t^2 + 19tu - 40u^2) - 3t^3(28t^2 + 55tu \\
&+33u^2)] + 32Q^{10}[466s^6 - 3s^5(467t - 247u) + 3s^4(209t^2 + 1163tu + 46u^2) - s^3(2735t^3 \\
&-4422t^2u - 3189tu^2 + 488u^3) - 27s^2t(10t^3 - 153t^2u - 100tu^2 - 35u^3) - 3st^2(176t^3 \\
&+81t^2u - 381tu^2 - 412u^3) + 3t^3(t+u)(106t^2 + 161tu + 46u^2)] - 16Q^8[929s^7 \\
&+s^6(1181t + 539u) + 3s^5(735t^2 + 1277tu - 680u^2) + s^4(2573t^3 + 6228t^2u - 4521tu^2 \\
&-2440u^3) + s^3(3920t^4 + 11969t^3u - 6441t^2u^2 - 8791tu^3 - 628u^4) - 3s^2t(148t^4 - 498t^3u \\
&+201t^2u^2 + 1405tu^3 + 900u^4) + 3st^2(t+u)(225t^3 + 55t^2u - 454tu^2 - 293u^3) \\
&-9t^3(t+u)^2(22t^2 + 21tu + 8u^2)] + 24Q^6[242s^8 + 2s^7(485t - 109u) + s^6(1373t^2 - 467tu \\
&-772u^2) + s^5(1709t^3 - 1833t^2u - 2817tu^2 + 629u^3) + s^4(2965t^4 + 1147t^3u - 5271t^2u^2 \\
&+487tu^3 + 1654u^4) + s^3(107t^5 - 1925t^4u - 5218t^3u^2 - 778t^2u^3 + 2653tu^4 + 713u^5) \\
&+3s^2t(t+u)(303t^4 + 134t^3u - 250t^2u^2 + 118tu^3 + 262u^4) - 3st^2(t+u)^3(22t^2 - 22tu \\
&-41u^2) + 3t^3(t+u)^3(22t^2 - 20tu + 9u^2)] - 4Q^4[76s^9 + 12s^8(113t - 49u) + 3s^7(879t^2 \\
&-1226tu - u^2) + s^6(2963t^3 - 8481t^2u - 1443tu^2 + 1745u^3) + 3s^5(695t^4 - 4291t^3u \\
&-1113t^2u^2 + 2915tu^3 - 346u^4) + 3s^4(2320t^5 + 493t^4u - 250t^3u^2 + 4396t^2u^3 + 1150tu^4 \\
&-1309u^5) + s^3(t+u)(847t^5 - 5620t^4u - 566t^3u^2 + 5962t^2u^3 - 664tu^4 - 1805u^5) \\
&+9s^2t(t+u)^2(119t^4 - 88t^3u - 39t^2u^2 + 29tu^3 - 85u^4) + 3st^2(t+u)^3(4t^3 - 138t^2u \\
&+111tu^2 - 62u^3) - 33t^3(t+u)^4(2t-u)^2] - 2Q^2s[88s^9 + 8s^8(17t + 23u) + 6s^7(7t^2 \\
&+136tu - 7u^2) - 4s^6(265t^3 - 588t^2u + 237tu^2 - 14u^3) - s^5(499t^4 - 2141t^3u + 5307t^2u^2 \\
&+1393tu^3 - 434u^4) - 6s^4(180t^5 - 937t^4u + 94t^3u^2 + 768t^2u^3 - 454tu^4 + 61u^5) \\
&-2s^3(t+u)(1411t^5 - 169t^4u + 769t^3u^2 - 296t^2u^3 - 1819tu^4 + 556u^5)
\end{aligned}
$$

$$
\begin{aligned}
&+2s^2(t+u)^2(452t^5+889t^4u-658t^3u^2-178t^2u^3+502tu^4-253u^5)-3st(t+u)^3(32t^4\\
&-120t^3u+150t^2u^2+2tu^3+15u^4)-66t^2u(t+u)^4(2t-u)^2],\\
L=\;&128Q^{16}(21s^3-52s^2t+114st^2-156t^3)-64Q^{14}[196s^4-2s^3(142t-31u)+5s^2t(179t\\
&-7u)-6st^2(108t-19u)+18t^3(16t+29u)]+32Q^{12}[740s^5-2s^4(314t-75u)+s^3(2217t^2\\
&-956tu-401u^2)+6s^2t(76t^2+68tu+53u^2)+36st^2(17t^2+19tu-40u^2)-18t^3(28t^2\\
&+55tu+33u^2)]-16Q^{10}[1428s^6-4s^5(259t+123u)+6s^4(58t^2-689tu-293u^2)\\
&+6s^3(586t^3-609t^2u+213tu^2+42u^3)+s^2t(317t^3-2109t^2u-4809tu^2+281u^3)\\
&-6st^2(176t^3+81t^2u-381tu^2-412u^3)+6t^3(t+u)(106t^2+161tu+46u^2)]\\
&+8Q^8[1429s^7-2s^6(526t+827u)-2s^5(3841t^2+2623tu+855u^2)-2s^4(151t^3\\
&+6021t^2u-3543tu^2-1217u^3)-s^3(1718t^4+7180t^3u+1764t^2u^2-3364tu^3-791u^4)\\
&+2s^2t(116t^4+107t^3u+1245t^2u^2+1166tu^3-925u^4)+6st^2(t+u)(225t^3+55t^2u-454tu^2\\
&-293u^3)-18t^3(t+u)^2(22t^2+21tu+8u^2)]-4Q^6[584s^8+2s^7(847t-489u)\\
&-s^6(13833t^2-2389tu-1102u^2)-8s^5(1412t^3+1143t^2u-1827tu^2-430u^3)\\
&-2s^4(3692t^4-615t^3u-9552t^2u^2-2788tu^3+117u^4)-2s^3(1581t^5+4291t^4u-1571t^3u^2\\
&-3201t^2u^3+1801tu^4+505u^5)+3s^2t(t+u)(10t^4-1160t^3u-694t^2u^2+662tu^3+789u^4)\\
&-18st^2(t+u)^3(22t^2-22tu-41u^2)+18t^3(t+u)^3(22t^2-20tu+9u^2)]\\
&-2Q^4[72s^9-44s^8(127t+3u)+3s^7(2743t^2-3472tu-247u^2)+12s^6(1199t^3+261t^2u\\
&-471tu^2+139u^3)+2s^5(5731t^4-9729t^3u-9186t^2u^2+5461tu^3+2391u^4)+6s^4(1729t^5\\
&-92t^4u-4442t^3u^2-530t^2u^3+2035tu^4+448u^5)+3s^3(t+u)(978t^5+1200t^4u-1464t^3u^2\\
&+604t^2u^3+581tu^4+37u^5)-2s^2t(t+u)^2(205t^4+352t^3u+1428t^2u^2-548tu^3\\
&-695u^4)-6st^2(t+u)^3(4t^3-138t^2u+111tu^2-62u^3)+66t^3(t+u)^4(2t-u)^2]+Q^2s[32s^9\\
&-56s^8(83t-5u)-4s^7(214t^2+1993tu-333u^2)+8s^6(785t^3+363t^2u+195tu^2+209u^3)\\
&+s^5(8713t^4-12949t^3u+5931t^2u^2+8161tu^3-1288u^4)+4s^4(2149t^5-3863t^4u-4827t^3u^2\\
&+3439t^2u^3+364tu^4-1026u^5)+2s^3(t+u)(1810t^5-2224t^4u-1073t^3u^2+6574t^2u^3\\
&-463tu^4-1430u^5)+4s^2(t+u)^2(224t^5-207t^4u-539t^3u^2+740t^2u^3-282tu^4-158u^5)\\
&+st(t+u)^3(344t^4-592t^3u-60t^2u^2+584tu^3-427u^4)-132t^2u(t+u)^4(2t-u)^2]\\
&+s^2[40s^9+8s^8(83t+9u)+2s^7(375t^2+436tu-11u^2)-16s^6(7t^3+69t^2u+51tu^2+u^3)\\
&-s^5(1171t^4-129t^3u+4071t^2u^2+469tu^3-78u^4)-s^4(1545t^5-2824t^4u-934t^3u^2\\
&+1440t^2u^3-2179tu^4+248u^5)-2s^3(t+u)(400t^5-1450t^4u+79t^3u^2+646t^2u^3-1336tu^4\\
&+325u^5)-2s^2(t+u)^2(94t^5-518t^4u+489t^3u^2+574t^2u^3-611tu^4+240u^5)\\
&+su(t+u)^3(80t^4-184t^3u+12t^2u^2+185tu^3-118u^4)-33tu^2(t+u)^4(2t-u)^2],\\
A=\;&-768Q^{16}s(s^2+10st+14t^2)+384Q^{14}s[11s^3+s^2(54t+u)-st(20t+107u)+3t^2(60t+7u)]\\
&-576Q^{12}s[17s^4+2s^3(44t+13u)-2s^2(41t^2+36tu-14u^2)+2st(65t^2-73tu+15u^2)\\
&-t^2(76t^2+202tu+69u^2)]+96Q^{10}s[112s^5+s^4(943t+237u)-s^3(187t^2-102tu+39u^2)\\
&+s^2(1213t^3+552t^2u+957tu^2-182u^3)-st(782t^3+711t^2u-1560tu^2-481u^3)+t^2(236t^3\\
&+603t^2u+759tu^2+338u^3)]-48Q^8s[83s^6+s^5(1527t-47u)+s^4(1195t^2-35tu-852u^2)
\end{aligned}
$$

$$
\begin{aligned}
&+s^3(2387t^3+57t^2u-1557tu^2-835u^3)+s^2(951t^4+805t^3u+153t^2u^2-2199tu^3-167u^4)\\
&+st(664t^4+1522t^3u+405t^2u^2-1865tu^3-1034u^4)-3t^2(t+u)(72t^3+118t^2u+83tu^2\\
&+64u^3)]-72Q^6s[26s^7-2s^6(127t-103u)-s^5(919t^2-345tu-268u^2)-s^4(645t^3-943t^2u\\
&-741tu^2+271u^3)-2s^3(540t^4-440t^3u-495t^2u^2+205tu^3+299u^4)-s^2(361t^5-279t^4u\\
&-1294t^3u^2-482t^2u^3+735tu^4+239u^5)-st(t+u)(62t^4-12t^3u-108t^2u^2+68tu^3+237u^4)\\
&-t^2(t+u)^2(46t^3+26t^2u+37tu^2+3u^3)]+12Q^4s[140s^8+4s^7(83t+93u)\\
&-s^6(1487t^2-1290tu+255u^2)-s^5(1337t^3-1623t^2u+303tu^2+959u^3)-s^4(1124t^4\\
&-7059t^3u-903t^2u^2+2507tu^3-273u^4)-s^3(2821t^5+663t^4u+900t^3u^2+3844t^2u^3\\
&+483tu^4-1383u^5)+s^2(t+u)(224t^5+2029t^4u-154t^3u^2-1702t^2u^3+247tu^4+638u^5)\\
&-st(t+u)^2(484t^4-320t^3u-117t^2u^2+79tu^3-122u^4)+t^2(t+u)^3(124t^3-84t^2u\\
&+72tu^2-17u^3)]-6Q^2s^2[40s^8+8s^7(39t+u)+2s^6(151t^2+208tu-111u^2)-4s^5(205t^3\\
&+12t^2u+81tu^2+34u^3)-s^4(663t^4-643t^3u+1881t^2u^2-129tu^3-220u^4)-4s^3(29t^5\\
&-757t^4u-57t^3u^2+317t^2u^3-298tu^4+6u^5)-2s^2(t+u)(376t^5-118t^4u+379t^3u^2\\
&+76t^2u^3-448tu^4+187u^5)+4s(t+u)^2(60t^5+122t^4u-115t^3u^2+21t^2u^3+71tu^4-46u^5)\\
&-t(t+u)^3(40t^4+112t^3u-96t^2u^2+100tu^3-29u^4)] \qquad \text{(A.16)}
\end{aligned}
$$

$\nu_e\ s \to e^-\ c\overline{c}\left[{}^3P_2^{(1)}\right]\ c$:

$$
F=\frac{-8g'^4\alpha_s^2|V_{cs}|^2}{135\pi M^3s^4(Q^2+m_W^2)^2(2Q^2+s-2t+u)^4(2Q^2-2s+t+u)^5},
$$

$$
\begin{aligned}
T=\;&256Q^{16}(30s^3+2s^2t+117st^2-384t^3)-128Q^{14}[306s^4-s^3(608t+87u)+s^2t(2167t-62u)\\
&-3st^2(336t-337u)-9t^3(188t-57u)]+192Q^{12}[432s^5-s^4(859t-39u)+s^3(421t^2\\
&-1574tu-99u^2)+s^2t(3755t^2+1186tu-223u^2)-12st^2(151t^2-200tu+60u^2)+3t^3(272t^2\\
&+729tu+217u^2)]-32Q^{10}[2784s^6-s^5(1573t-999u)-3s^4(6355t^2+2101tu-102u^2)\\
&+3s^3(7219t^3-8714t^2u+875tu^2+292u^3)-s^2t(6874t^3+6951t^2u+26382tu^2-911u^3)\\
&+9st^2(444t^3+475t^2u-2109tu^2-460u^3)+3t^3(t+u)(346t^2-1507tu-1754u^2)]\\
&+16Q^8[2673s^7+s^6(6973t-1239u)-s^5(44033t^2-13345tu+4104u^2)-3s^4(3193t^3\\
&+10588t^2u-12485tu^2+228u^3)-s^3(27296t^4+39099t^3u-21243t^2u^2-26065tu^3-156u^4)\\
&-s^2t(3176t^4+11324t^3u+15915t^2u^2-37489tu^3-4216u^4)+3st^2(t+u)(1551t^3-2225t^2u\\
&+3494tu^2+4615u^3)-9t^3(t+u)^2(52t^2+277tu-522u^2)]+24Q^6[126s^8-2s^7(2477t\\
&-1167u)+s^6(12919t^2-6887tu+3942u^2)+s^5(9191t^3-9857t^2u-3607tu^2+2889u^3)\\
&+s^4(16733t^4-11163t^3u-34293t^2u^2+9293tu^3+1848u^4)+s^3(10549t^5-521t^4u\\
&-15282t^3u^2-11090t^2u^3+12535tu^4+693u^5)-s^2t(t+u)(1033t^4-2882t^3u+7380t^2u^2\\
&-3908tu^3-3512u^4)+3st^2(t+u)^2(62t^3+460t^2u-1051tu^2+1413u^3)\\
&+3t^3(t+u)^3(134t^2-312tu+187u^2)]-4Q^4[2868s^9-4s^8(3491t-1809u)+3s^7(3113t^2\\
&-5398tu-87u^2)+3s^6(3359t^3-5663t^2u+8093tu^2-5429u^3)+s^5(22193t^4-83613t^3u\\
&-6195t^2u^2+50309tu^3-19170u^4)+3s^4(19832t^5-11011t^4u-8238t^3u^2+17540t^2u^3
\end{aligned}
$$

$$
\begin{aligned}
&+6170tu^4-3165u^5)+3s^3(t+u)(1493t^5-2368t^4u-4062t^3u^2+14602t^2u^3-3930tu^4\\
&-661u^5)-s^2t(t+u)^2(5225t^4-2788t^3u+10263t^2u^2-10177tu^3+8483u^4)\\
&+9st^2(t+u)^3(196t^3-662t^2u+909tu^2-486u^3)-3t^3(t+u)^4(88t^2-136tu+55u^2)]\\
&+2Q^2s[1656s^9-8s^8(767t-381u)-2s^7(2915t^2+5108tu+297u^2)+12s^6(305t^3\\
&+873t^2u-409tu^2-105u^3)+s^5(5623t^4+2463t^3u+43455t^2u^2-13547tu^3+6006u^4)\\
&+2s^4(9500t^5-26299t^4u+6042t^3u^2+14996t^2u^3-13858tu^4+4347u^5)+6s^3(t+u)(1585t^5\\
&-3807t^4u-2069t^3u^2+3540t^2u^3-3635tu^4+666u^5)-2s^2(t+u)^2(3368t^5\\
&-6583t^4u+1098t^3u^2-154t^2u^3+818tu^4-291u^5)+st(t+u)^3(1016t^4-4048t^3u\\
&+7194t^2u^2-5674tu^3+2345u^4)+6t^2u(t+u)^4(88t^2-136tu+55u^2)],\\
L=&-128Q^{16}(9s^3-286s^2t+234st^2-768t^3)+64Q^{14}[302s^4-2s^3(892t-201u)-s^2t(329t\\
&+653u)-6st^2(336t-337u)-18t^3(188t-57u)]-32Q^{12}[2164s^5-26s^4(61t-104u)\\
&-3s^3(1565t^2-456tu-81u^2)+6s^2t(304t^2+917tu+140u^2)-72st^2(151t^2-200tu\\
&+60u^2)+18t^3(272t^2+729tu+217u^2)]+16Q^{10}[6378s^6+4s^5(3266t+1281u)\\
&-6s^4(208t^2-2373tu+671u^2)+6s^3(3044t^3+965t^2u+877tu^2-438u^3)-s^2t(4111t^3\\
&-34593t^2u+18147tu^2-4367u^3)+18st^2(444t^3+475t^2u-2109tu^2-460u^3)\\
&+6t^3(t+u)(346t^2-1507tu-1754u^2)]-8Q^8[7745s^7+4s^6(10507t-726u)+2s^5(16919t^2\\
&+7391tu-10689u^2)+2s^4(27235t^3-7197t^2u-8715tu^2-4997u^3)+s^3(35626t^4\\
&+25776t^3u-17340t^2u^2+40tu^3+627u^4)+2s^2t(5453t^4-7960t^3u-31227t^2u^2\\
&+14432tu^3-1234u^4)+6st^2(t+u)(1551t^3-2225t^2u+3494tu^2+4615u^3)\\
&-18t^3(t+u)^2(52t^2+277tu-522u^2)]+4Q^6[88s^8+2s^7(23351t-10201u)+3s^6(25513t^2\\
&-6487tu-9136u^2)+4s^5(23401t^3-21672t^2u-16431tu^2+1690u^3)+2s^4(47681t^4\\
&-16807t^3u-15504t^2u^2-6196tu^3+9008u^4)+6s^3(8257t^5-3337t^4u-4869t^3u^2+5617t^2u^3\\
&-3265tu^4+723u^5)+3s^2t(t+u)(6034t^4-10736t^3u+10784t^2u^2-5524tu^3-3909u^4)\\
&-18st^2(t+u)^2(62t^3+460t^2u-1051tu^2+1413u^3)-18t^3(t+u)^3(134t^2-312tu+187u^2)]\\
&+2Q^4[7656s^9-4s^8(2741t-5403u)-3s^7(21617t^2-12420tu-197u^2)-6s^6(15638t^3\\
&-19355t^2u-4408tu^2+6329u^3)-2s^5(55853t^4-72369t^3u-33240t^2u^2+19817tu^3\\
&+13359u^4)-6s^4(14998t^5-13515t^4u-6616t^3u^2+6070t^2u^3+4212tu^4-121u^5)\\
&-3s^3(t+u)(10778t^5-24948t^4u+5428t^3u^2-12752t^2u^3+8563tu^4-945u^5)\\
&+2s^2t(t+u)^2(1109t^4-856t^3u-9375t^2u^2+6659tu^3-7720u^4)+18st^2(t+u)^3(196t^3\\
&-662t^2u+909tu^2-486u^3)-6t^3(t+u)^4(88t^2-136tu+55u^2)]-Q^2s[4672s^9\\
&+8s^8(1867t+675u)-4s^7(2290t^2-6581tu+2793u^2)-8s^6(6407t^3-5820t^2u+2055tu^2\\
&+1442u^3)-s^5(72785t^4-122829t^3u+7539t^2u^2+47513tu^3-17400u^4)-4s^4(16577t^5\\
&-32131t^4u-2523t^3u^2+22739t^2u^3+4412tu^4-6702u^5)-2s^3(t+u)(14446t^5-40612t^4u\\
&+33235t^3u^2+9898t^2u^3+2753tu^4-5414u^5)-4s^2(t+u)^2(76t^5-1283t^4u\\
&-1347t^3u^2+1924t^2u^3-1754tu^4-264u^5)+st(t+u)^3(2504t^4-9568t^3u+14628t^2u^2\\
&-11872tu^3+5843u^4)+12t^2u(t+u)^4(88t^2-136tu+55u^2)]-s^2[8s^9-8s^8(509t-79u)
\end{aligned}
$$

$-6s^7(971t^2+944tu-259u^2)+4s^6(1348t^3+21t^2u+798tu^2+133u^3)+s^5(14551t^4$
$-2921t^3u+22191t^2u^2+973tu^3-602u^4)+3s^4(3143t^5-9528t^4u+1430t^3u^2+3848t^2u^3$
$-3933tu^4+560u^5)+2s^3(t+u)(1072t^5-12622t^4u+7303t^3u^2+70t^2u^3-6706tu^4+1855u^5)$
$+2s^2(t+u)^2(64t^5-748t^4u+3199t^3u^2+1036t^2u^3-2971tu^4+1138u^5)$
$+3su(t+u)^3(616t^4-1080t^3u+828t^2u^2-287tu^3+150u^4)+3tu^2(t+u)^4(88t^2$
$-136tu+55u^2)],$

$A=-256Q^{16}s(47s^2-160st+168t^2)+128Q^{14}s[481s^3-s^2(394t-223u)-st(608t+329u)$
$-297t^2u]-192Q^{12}s[623s^4+2s^3(255t+92u)-2s^2(147t^2-379tu+35u^2)-2st(641t^2$
$+46tu-280u^2)-3t^2(922t^2+512tu+121u^2)]+32Q^{10}s[3206s^5+s^4(8171t-1281u)$
$+3s^3(1611t^2+678tu-1441u^2)+s^2(16361t^3+22752t^2u+2829tu^2-1294u^3)$
$-st(30490t^3-16863t^2u-11742tu^2-623u^3)+3t^2(332t^3+6279t^2u+5109tu^2+1322u^3)]$
$-16Q^8s[1447s^6+11s^5(1441t-547u)+s^4(5425t^2-10841tu-7104u^2)+s^3(72799t^3$
$-4863t^2u-25425tu^2+721u^3)-s^2(5911t^4-62125t^3u+37611t^2u^2+19939tu^3-1171u^4)$
$-st(10766t^4-37108t^3u+19803t^2u^2+29429tu^3+7112u^4)+27t^2(t+u)(164t^3+56t^2u$
$-497tu^2-182u^3)]-24Q^6s[866s^7-2s^6(2379t-1481u)+s^5(1161t^2+1727tu-142u^2)$
$-s^4(22889t^3-28777t^2u+595tu^2+5245u^3)-2s^3(10917t^4-3350t^3u-14283t^2u^2+5145tu^3$
$+1840u^4)+s^2(3411t^5-8839t^4u+33722t^3u^2-906t^2u^3-8671tu^4-673u^5)-st(t+u)(2542t^4$
$+2224t^3u-5790t^2u^2+6874tu^3+3031u^4)-3t^2(t+u)^2(478t^3-1050t^2u+399tu^2$
$+307u^3)]+4Q^4s[3388s^8-4s^7(497t-1419u)+3s^6(3527t^2+54tu-217u^2)-s^5(17365t^3$
$-38457t^2u+23991tu^2-1835u^3)-s^4(58828t^4-103125t^3u+42771t^2u^2+32773tu^3$
$-14379u^4)-3s^3(8829t^5-1689t^4u-27392t^3u^2+30108t^2u^3-417tu^4-4199u^5)+$
$s^2(t+u)(388t^5+2699t^4u+10138t^3u^2-30338t^2u^3+9539tu^4+2992u^5)-st(t+u)^2(6512t^4$
$-21184t^3u+16905t^2u^2-3787tu^3-4648u^4)+3t^2(t+u)^3(532t^3-600t^2u-96tu^2+199u^3)]$
$-2Q^2s^2[1064s^8+8s^7(419t+7u)+2s^6(4483t^2+2524tu-2607u^2)-4s^5(1025t^3+3783t^2u$
$-3645tu^2+1589u^3)-s^4(18649t^4-14389t^3u+71991t^2u^2-36119tu^3+4220u^4)$
$-4s^3(2465t^5-12601t^4u-5511t^3u^2+13253t^2u^3-7972tu^4+1290u^5)-2s^2(t+u)(1988t^5$
$-4358t^4u-5875t^3u^2+3644t^2u^3-5942tu^4+2063u^5)+4s(t+u)^2(136t^5$
$+942t^4u-4783t^3u^2+2041t^2u^3+81tu^4-259u^5)+t(t+u)^3(344t^4-1792t^3u+1848t^2u^2$
$+620tu^3-853u^4)]$ (A.17)

$\nu_e\ s\to e^-\ c\overline{c}\left[{}^1S_0^{(8)}\right]\ c$:

$$F=\frac{g'^4\alpha_s^2|V_{cs}|^2}{96\pi Ms^4(Q^2+m_W^2)^2(2Q^2+s-2t+u)^2(2Q^2-2s+t+u)^4},$$

$T=32Q^{10}(2s^3+10s^2t-6st^2-3t^3)+16Q^8[5s^4-s^3(15t-26u)-s^2t(44t+17u)$
$-3st^2(3t+8u)-9t^3(t+u)]-24Q^6[14s^5+s^4(17t+16u)+2s^3(2t^2+27tu+u^2)$
$+s^2t(2t+5u)^2+12st^2u(t+u)+3t^3(t+u)^2]+4Q^4[44s^6+8s^5(17t-6u)$

$+3s^4(49t^2+20tu-49u^2)+s^3(89t^3+12t^2u-135tu^2-82u^3)+s^2t(t+u)(40t^2+35tu$
$-59u^2)+3st^2(t+u)^2(t-8u)-3t^3(t+u)^3]+2Q^2s[8s^6-4s^5(27t-20u)$
$-2s^4(43t^2-44tu-15u^2)-s^3(61t^3-48t^2u-3tu^2+94u^3)-4s^2(t+u)(3t^3-17t^2u$
$-16tu^2+13u^3)-st(t+u)^2(2t^2-14tu+11u^2)-6t^2u(t+u)^3],$

$L = 16Q^{10}(4s^3-s^2t+12st^2+6t^3)-16Q^8[10s^4-s^3(15t+8u)+s^2t(17t-10u)$
$-3st^2(3t+8u)-9t^3(t+u)]+12Q^6[8s^5-s^4(41t+20u)-10s^3t(2t+3u)$
$+s^2t(t^2+26tu+36u^2)+24st^2u(t+u)+6t^3(t+u)^2]+4Q^4[8s^6+s^5(85t+24u)$
$+6s^4(2t+u)(11t-2u)+s^3(5t^3-42t^2u-18tu^2+8u^3)-s^2t(t+u)(2t^2-41tu-79u^2)$
$-3st^2(t+u)^2(t-8u)+3t^3(t+u)^3]-Q^2s[32s^6+4s^5(21t-4u)+4s^4(61t^2$
$-8tu-15u^2)+s^3(215t^3+150t^2u-69tu^2-88u^3)+2s^2(t+u)^2(18t^2-11tu-38u^2)$
$+st(t+u)^2(40t^2+8tu-77u^2)-12t^2u(t+u)^3]+3s^2[4s^5t+4s^4(3t^2-u^2)$
$+s^3t(21t^2-6tu-23u^2)+s^2(t+u)^2(13t^2-29tu+12u^2)-su(t+u)^2(6t^2+tu-8u^2)$
$+tu^2(t+u)^3],$

$A = 32Q^{10}s(s^2+11st-9t^2)+16Q^8s[13s^3-s^2(18t-31u)-st(25t+22u)-9t^2(2t+u)]$
$-24Q^6s[22s^4+s^3(19t+26u)+s^2(17t^2+42tu+u^2)+5st(t^2+8tu+4u^2)+3t^2(t^2-u^2)]$
$+4Q^4s[76s^5+4s^4(41t+3u)+3s^3(57t^2-8tu-53u^2)+s^2(100t^3+33t^2u-234tu^2-95u^3)$
$+st(t+u)(17t^2-47tu-10u^2)+9t^2u(t+u)^2]-2Q^2s^2[8s^5+4s^4(33t-10u)+2s^3(41t^2$
$-76tu-21u^2)+s^2(47t^3-126t^2u-141tu^2+68u^3)+2s(t+u)(6t^3-11t^2u+32tu^2+31u^3)$
$+t(t+u)^2(4t^2-4tu-17u^2)]$ (A.18)

$\nu_e\ s \to e^-\ c\overline{c}\left[{}^3S_1^{(8)}\right]\ c$:

$$F = \frac{g'^4\alpha_s^2|V_{cs}|^2}{432\pi M^3 s^4(Q^2+m_W^2)^2(2Q^2+s-2t+u)^2(2Q^2-2s+t+u)^4(-4Q^2+s+t+4u)^2},$$

$T = -256Q^{16}(68s^3-100s^2t+81st^2-129t^3)+128Q^{14}[754s^4-s^3(262t-337u)$
$+s^2t(1303t-323u)-3st^2(243t-74u)-18t^3(8t+43u)]-192Q^{12}[1058s^5+s^4(201t$
$+814u)+s^3(1686t^2-1297tu+134u^2)+s^2t(485t^2+2350tu+476u^2)-9st^2(23t^2$
$+119tu-115u^2)+3t^3(31t^2+76tu+33u^2)]+32Q^{10}[6323s^6+26s^5(121t+309u)$
$+3s^4(2281t^2-5643tu+482u^2)+s^3(5849t^3+12807t^2u-11175tu^2-3397u^3)$
$-s^2t(1594t^3+1497t^2u-21309tu^2+1171u^3)+18st^2(2t+u)(18t^2+43tu-17u^2)$
$+3t^3(t+u)(77t^2+736tu+344u^2)]-16Q^8[5698s^7+2s^6(2839t+7232u)$
$+s^5(2665t^2-30689tu+4128u^2)+s^4(1819t^3-4218t^2u-46863tu^2-5648u^3)$
$-2s^3(3065t^4+7486t^3u-5454t^2u^2+17027tu^3+2044u^4)-4s^2t(758t^4+2174t^3u$
$+3540t^2u^2+2411tu^3+800u^4)+3st^2(t+u)(270t^3+2297t^2u-1223tu^2-1783u^3)$
$+9t^3(t+u)^2(4t^2-174tu+101u^2)]+24Q^6[364s^8+s^7(2043t+4031u)+s^6(126t^2$
$-6647tu+3871u^2)-4s^5(1090t^3+3820t^2u+6803tu^2-28u^3)-s^4(1161t^4+5383t^3u$
$-4443t^2u^2+10389tu^3-2834u^4)-s^3(4647t^5+15326t^4u+18464t^3u^2+6726t^2u^3$

$$
\begin{aligned}
&-2320tu^4-2197u^5)+s^2t(t+u)(37t^4+973t^3u-7686t^2u^2-5822tu^3+505u^4)\\
&+9st^2(t+u)^2(41t^3-128t^2u+129tu^2-98u^3)-3t^3(t+u)^3(43t^2+10tu+162u^2)]\\
&+4Q^4[1288s^9-4s^8(827t+309u)-24s^7(28t^2+78tu+581u^2)+2s^6(4735t^3+16281t^2u\\
&+20409tu^2-9989u^3)+s^5(9605t^4+51879t^3u+52413t^2u^2+48737tu^3-8922u^4)\\
&+6s^4(581t^5-513t^4u-6977t^3u^2-11518t^2u^3-6696tu^4-1421u^5)+s^3(t+u)(7366t^5\\
&+27743t^4u+47203t^3u^2-10811t^2u^3-40831tu^4-8162u^5)\\
&-s^2t(t+u)^2(3773t^4+1034t^3u+4305t^2u^2-3214tu^3+6752u^4)+9st^2(t+u)^3(144t^3\\
&+28t^2u-6tu^2-571u^3)-3t^3(t+u)^4(38t^2-20tu+41u^2)]-2Q^2s[512s^9-4s^8(113t\\
&-539u)-4s^7(124t^2+1255tu+1047u^2)+s^6(1267t^3+5985t^2u+2457tu^2-15461u^3)\\
&+s^5(4181t^4+21109t^3u+22725t^2u^2+7343tu^3-12422u^4)+2s^4(1088t^5+4721t^4u\\
&+5460t^3u^2+2156t^2u^3+3338tu^4+2577u^5)-2s^3(t+u)(203t^5+4561t^4u+11810t^3u^2\\
&+20702t^2u^3+3997tu^4-8011u^5)+s^2(t+u)^2(772t^5+10902t^4u+10004t^3u^2\\
&-6440t^2u^3-9579tu^4+8075u^5)-st(t+u)^3(28t^4+2464t^3u+1554t^2u^2+346tu^3\\
&-4901u^4)+6t^2u(t+u)^4(38t^2-20tu+41u^2)],\\
L=&-128Q^{16}(41s^3-73s^2t-162st^2+258t^3)+64Q^{14}[321s^4+s^3(53t+311u)-s^2t(722t\\
&-1243u)+6st^2(243t-74u)+36t^3(8t+43u)]-32Q^{12}[841s^5+7s^4(388t+189u)\\
&-s^3(846t^2-8636tu+991u^2)+3s^2t(1331t^2+49tu+853u^2)+54st^2(23t^2+119tu-115u^2)\\
&-18t^3(31t^2+76tu+33u^2)]+16Q^{10}[245s^6+14s^5(628t-129u)-18s^4(26t^2-1213tu\\
&+531u^2)+s^3(5597t^3-1041t^2u+5769tu^2-5131u^3)+s^2t(4562t^3+15765t^2u-26229tu^2\\
&+5273u^3)-36st^2(2t+u)(18t^2+43tu-17u^2)-6t^3(t+u)(77t^2+736tu+344u^2)]\\
&+8Q^8[3348s^7-s^6(9239t-19819u)+2s^5(1279t^2-9989tu+18843u^2)-6s^4(144t^3\\
&-3613t^2u-382tu^2-3980u^3)-s^3(6371t^4+11822t^3u-75102t^2u^2+4946tu^3-2395u^4)\\
&+s^2t(2060t^4+10469t^3u+6942t^2u^2+5018tu^3+3137u^4)+6st^2(t+u)(270t^3\\
&+2297t^2u-1223tu^2-1783u^3)+18t^3(t+u)^2(4t^2-174tu+101u^2)]-4Q^6[8312s^8\\
&+s^7(113t+45201u)+s^6(5844t^2+8461tu+75577u^2)+4s^5(2702t^3+14361t^2u\\
&+3267tu^2+9992u^3)+s^4(4607t^4+30858t^3u+141126t^2u^2-5122tu^3-7605u^4)\\
&+s^3(3960t^5+33346t^4u+54082t^3u^2+42090t^2u^3+7969tu^4-8561u^5)+3s^2t(t+u)(1646t^4\\
&+9812t^3u-3941t^2u^2-5333tu^3+4713u^4)+54st^2(t+u)^2(41t^3-128t^2u\\
&+129tu^2-98u^3)-18t^3(t+u)^3(43t^2+10tu+162u^2)]+2Q^4[9520s^9+2s^8(2231t\\
&+24279u)+18s^7(335t^2+1501tu+4382u^2)+s^6(20915t^3+73623t^2u+14013tu^2\\
&+25049u^3)+s^5(14459t^4+66834t^3u+140442t^2u^2-51646tu^3-46257u^4)+9s^4(424t^5\\
&+5105t^4u+9228t^3u^2+4392t^2u^3-3902tu^4-4419u^5)+s^3(t+u)(12028t^5+49382t^4u\\
&+2989t^3u^2-33221t^2u^3+15791tu^4-8303u^5)+s^2t(t+u)^2(5650t^4\\
&+1756t^3u+13398t^2u^2-5237tu^3+3391u^4)-18st^2(t+u)^3(144t^3+28t^2u-6tu^2\\
&-571u^3)+6t^3(t+u)^4(38t^2-20tu+41u^2)]-Q^2s[5424s^9+4s^8(307t+6715u)\\
&+4s^7(818t^2+3179tu+10041u^2)+3s^6(5167t^3+15237t^2u+13tu^2-2217u^3)
\end{aligned}
$$

$$
\begin{aligned}
&+s^5(8507t^4+55445t^3u+87069t^2u^2-68617tu^3-64252u^4)+2s^4(2522t^5+16451t^4u\\
&+24828t^3u^2+1754t^2u^3-28708tu^4-23019u^5)+6s^3(t+u)(1591t^5+5269t^4u-1673t^3u^2\\
&-9487t^2u^3+1194tu^4-592u^5)+s^2(t+u)^2(3976t^5+11984t^4u+7492t^3u^2\\
&-27182t^2u^3-15277tu^4+3613u^5)-st(t+u)^3(1000t^4-1136t^3u-4314t^2u^2-3362tu^3\\
&+11911u^4)-12t^2u(t+u)^4(38t^2-20tu+41u^2)]+s^2[544s^9+4s^8(43t+831u)+4s^7(3t^2\\
&-49tu+1112u^2)+s^6(1751t^3+4593t^2u-4467tu^2-5821u^3)+s^5(1490t^4+10845t^3u\\
&+15927t^2u^2-13873tu^3-17133u^4)+s^4(741t^5+3982t^4u+8470t^3u^2+4356t^2u^3-7895tu^4\\
&-7886u^5)+2s^3(t+u)(590t^5+1567t^4u-4234t^3u^2-8668t^2u^3+3472tu^4+4391u^5)\\
&+s^2(t+u)^2(562t^5+2464t^4u-894t^3u^2-13070t^2u^3+589tu^4+9567u^5)+su(t+u)^3(524t^4\\
&+848t^3u-1230t^2u^2-1630tu^3+2543u^4)+3tu^2(t+u)^4(38t^2-20tu+41u^2)],\\
A=\;&256Q^{16}s(72s^2+59st+249t^2)-128Q^{14}s[678s^3-s^2(32t-69u)+st(1333t-983u)\\
&-9t^2(5t-76u)]+192Q^{12}s[909s^4-s^3(277t-594u)+s^2(1018t^2-2285tu+138u^2)\\
&-st(616t^2-346tu+889u^2)-9t^2(50t^2+111tu+13u^2)]-32Q^{10}s[5967s^5+s^4(347t\\
&+9459u)+6s^3(884t^2-2756tu+927u^2)-3s^2(349t^3-3067t^2u+1579tu^2-933u^3)\\
&-st(5674t^3+12369t^2u-2715tu^2+337u^3)-3t^2(61t^3+1299t^2u+2334tu^2+988u^3)]\\
&+16Q^8s[7302s^6+2s^5(3653t+10740u)+s^4(7738t^2-14657tu+20043u^2)+6s^3(1062t^3\\
&+2918t^2u-2711tu^2+890u^3)-2s^2(1498t^4-6786t^3u-30543t^2u^2-9941tu^3-1884u^4)\\
&+st(247t^4-9788t^3u-10128t^2u^2+11500tu^3+9325u^4)+9t^2(t+u)(83t^3+402t^2u+231tu^2\\
&+263u^3)]-24Q^6s[1476s^7+s^6(4237t+8073u)+s^5(2864t^2+1595tu+10167u^2)\\
&+s^4(4117t^3+6737t^2u-7049tu^2+3303u^3)+2s^3(170t^4+5100t^3u+9969t^2u^2-3700tu^3\\
&-2043u^4)+s^2(2531t^5+8522t^4u+20322t^3u^2+22976t^2u^3+3530tu^4-3171u^5)\\
&+st(t+u)(463t^4+1795t^3u-2562t^2u^2+928tu^3-443u^4)+9t^2(t+u)^2(10t^3\\
&+101t^2u+277tu^2+24u^3)]+4Q^4s[792s^8+4s^7(2045t+3123u)+12s^6(699t^2\\
&+1642tu+1953u^2)+6s^5(425t^3+289t^2u-3805tu^2+927u^3)+s^4(8161t^4+36723t^3u\\
&+38145t^2u^2-37163tu^3-18666u^4)+3s^3(629t^5+3358t^4u+7056t^3u^2-736t^2u^3\\
&-13541tu^4-6318u^5)+3s^2(t+u)(2236t^5+8557t^4u+3573t^3u^2-1745t^2u^3-9575tu^4\\
&-2154u^5)-st(t+u)^2(1378t^4+1228t^3u-6141t^2u^2+12280tu^3+5149u^4)\\
&+3t^2(t+u)^3(104t^3+186t^2u-426tu^2-211u^3)]+2Q^2s^2[96s^8-4s^7(355t+303u)\\
&-4s^6(934t^2+2785tu+2367u^2)+3s^5(171t^3-623t^2u+1265tu^2-581u^3)-s^4(569t^4\\
&-5535t^3u-18687t^2u^2-40237tu^3-19446u^4)-4s^3(890t^5+5930t^4u+9786t^3u^2\\
&+2525t^2u^3-3877tu^4-1008u^5)-6s^2(t+u)(79t^5-261t^4u-2086t^3u^2-1178t^2u^3\\
&+1437tu^4+2975u^5)-s(t+u)^2(256t^5+3316t^4u+2856t^3u^2-19172t^2u^3-1367tu^4\\
&+8853u^5)-t(t+u)^3(40t^4-248t^3u-966t^2u^2+1294tu^3+1081u^4)]
\end{aligned}
\tag{A.19}
$$

$\nu_e\ s \to e^-\ c\overline{c}\left[{}^3P_J^{(8)}\right]\ c$:

$$F = \frac{g'^4\alpha_s^2|V_{cs}|^2}{24\pi M^3 s^4(Q^2+m_W^2)^2(2Q^2+s-2t+u)^4(2Q^2-2s+t+u)^5},$$

$$\begin{aligned}
T = &-768Q^{16}(8s^3+2s^2t-16st^2-29t^3)+384Q^{14}[97s^4+11s^3(11t+2u)+s^2t(382t+177u)\\
&-st^2(21t-184u)-6t^3(76t+11u)]-576Q^{12}[114s^5+s^4(184t-33u)+s^3(147t^2-421tu\\
&-134u^2)+s^2t(1405t^2+587tu-144u^2)-st^2(425t^2-449tu-10u^2)+t^3(242t^2+596tu\\
&+207u^2)]+96Q^{10}[389s^6+5s^5(157t-132u)-2s^4(1916t^2+2421tu+162u^2)+2s^3(3282t^3\\
&-4698t^2u-1407tu^2+304u^3)-s^2t(646t^3+4893t^2u+8511tu^2+637u^3)+st^2(1139t^3\\
&+966t^2u-5034tu^2-1774u^3)-4t^3(t+u)(8t^2+355tu+311u^2)]+48Q^8[68s^7\\
&-s^6(136t-725u)+s^5(10631t^2+2109tu-1206u^2)+2s^4(2248t^3+5992t^2u-6168tu^2\\
&-1325u^3)+2s^3(4294t^4+9814t^3u-4647t^2u^2-7169tu^3-434u^4)+s^2t(584t^4+4035t^3u\\
&+3342t^2u^2-11746tu^3-3258u^4)-st^2(t+u)(471t^3-1622t^2u+3626tu^2+3676u^3)\\
&-3t^3(t+u)^2(29t^2-126tu+367u^2)]-72Q^6[96s^8-10s^7(2t-3u)+s^6(3900t^2-1483tu\\
&+u^2)+s^5(3451t^3-3472t^2u-3477tu^2+1314u^3)+s^4(6017t^4-1198t^3u-12008t^2u^2\\
&+2188tu^3+2157u^4)+s^3(2495t^5-1676t^4u-7964t^3u^2-3420t^2u^3+5105tu^4+910u^5)\\
&+s^2t(t+u)(580t^4+1156t^3u-2443t^2u^2+1061tu^3+1443u^4)-st^2(t+u)^2(98t^3\\
&-276t^2u+453tu^2-1036u^3)+2t^3(t+u)^3(88t^2-137tu+75u^2)]+12Q^4[208s^9\\
&-4s^8(476t-159u)+4s^7(1261t^2-1584tu+279u^2)+s^6(3844t^3-11529t^2u+2658tu^2\\
&-553u^3)+s^5(7955t^4-27135t^3u-5523t^2u^2+16307tu^3-5196u^4)+s^4(18632t^5-5775t^4u\\
&-4692t^3u^2+24368t^2u^3+7272tu^4-6201u^5)+s^3(t+u)(965t^5-7412t^4u-4906t^3u^2\\
&+15238t^2u^3-2215tu^4-2246u^5)+s^2t(t+u)^2(13t^4+256t^3u-2313t^2u^2+2299tu^3-2516u^4)\\
&+st^2(t+u)^3(592t^3-1782t^2u+2091tu^2-1142u^3)-t^3(t+u)^4(232t^2-232tu+67u^2)]\\
&-6Q^2s[272s^9-8s^8(284t-91u)-4s^7(148t^2+933tu-63u^2)+2s^6(1202t^3+1255t^2u\\
&+48tu^2-349u^3)+s^5(1045t^4-2987t^3u+13929t^2u^2-881tu^3+214u^4)+2s^4(2582t^5\\
&-8601t^4u+30t^3u^2+4778t^2u^3-3600tu^4+1071u^5)+2s^3(t+u)(2155t^5-2009t^4u-307t^3u^2\\
&+1842t^2u^3-3922tu^4+1027u^5)-2s^2(t+u)^2(1064t^5-761t^4u-724t^3u^2\\
&-190t^2u^3+856tu^4-310u^5)+st(t+u)^3(320t^4-1776t^3u+1890t^2u^2-1066tu^3\\
&+555u^4)+2t^2u(t+u)^4(232t^2-232tu+67u^2)],\\
L = &-128Q^{16}(40s^3+67s^2t+96st^2+174t^3)+64Q^{14}[266s^4+10s^3(61t-6u)+s^2t(2153t\\
&+347u)+6st^2(21t-184u)+36t^3(76t+11u)]-32Q^{12}[384s^5+2s^4(129t-653u)\\
&+20s^3(396t^2-137tu-62u^2)+3s^2t(235t^2-1168tu+107u^2)+18st^2(425t^2-449tu\\
&-10u^2)-18t^3(242t^2+596tu+207u^2)]-16Q^{10}[1022s^6+2s^5(4519t+2706u)\\
&-6s^4(149t^2-2885tu-414u^2)+4s^3(497t^3+4173t^2u+249tu^2-535u^3)-s^2t(859t^3\\
&-24765t^2u+3333tu^2-2489u^3)+6st^2(1139t^3+966t^2u-5034tu^2-1774u^3)\\
&-24t^3(t+u)(8t^2+355tu+311u^2)]+8Q^8[3364s^7+s^6(26777t+5430u)+2s^5(21659t^2\\
&+9239tu-4422u^2)+2s^4(14975t^3+13824t^2u-13008tu^2-6814u^3)+2s^3(17155t^4
\end{aligned}$$

$+14097t^3u - 4659t^2u^2 - 2969tu^3 - 1116u^4) + s^2t(3214t^4 - 12410t^3u - 43626t^2u^2 + 15952tu^3$
$+2941u^4) + 6st^2(t+u)(471t^3 - 1622t^2u + 3626tu^2 + 3676u^3) + 18t^3(t+u)^2(29t^2$
$-126tu + 367u^2)] - 4Q^6[1872s^8 + 8s^7(2931t - 898u) + s^6(88047t^2 - 24599tu$
$-23750u^2) + 6s^5(12809t^3 - 3958t^2u - 12601tu^2 - 1538u^3) + 2s^4(43800t^4 - 15493t^3u$
$-32520t^2u^2 - 9636tu^3 + 5567u^4) + 2s^3(20619t^5 + 7796t^4u - 11308t^3u^2 - 24t^2u^3$
$-3997tu^4 + 2834u^5) + 3s^2t(t+u)(2800t^4 - 4748t^3u + 10520t^2u^2 - 5494tu^3 - 4779u^4)$
$+18st^2(t+u)^2(98t^3 - 276t^2u + 453tu^2 - 1036u^3) - 36t^3(t+u)^3(88t^2$
$-137tu + 75u^2)] - 2Q^4[2656s^9 + 8s^8(857t + 1698u) - 6s^7(10701t^2 - 9155tu - 1344u^2)$
$-s^6(90673t^3 - 58884t^2u - 29715tu^2 + 25426u^3) - 2s^5(49901t^4 - 71901t^3u - 41961t^2u^2$
$+28391tu^3 + 16518u^4) - 6s^4(15176t^5 - 7421t^4u - 15765t^3u^2 + 452t^2u^3 + 7555tu^4$
$+1587u^5) - 2s^3(t+u)(11653t^5 - 22240t^4u + 232t^3u^2 - 10754t^2u^3 + 11156tu^4 - 476u^5)$
$+s^2t(t+u)^2(262t^4 - 2336t^3u - 1326t^2u^2 + 6178tu^3 - 14453u^4)$
$+6st^2(t+u)^3(592t^3 - 1782t^2u + 2091tu^2 - 1142u^3) - 6t^3(t+u)^4(232t^2 - 232tu + 67u^2)]$
$+Q^2s[2720s^9 + 128s^8(155t + 27u) - 4s^7(889t^2 - 9125tu + 2274u^2) - 4s^6(12176t^3$
$-6261t^2u + 3138tu^2 + 3383u^3) - s^5(66007t^4 - 107787t^3u + 17517t^2u^2 + 50095tu^3$
$-10752u^4) - 4s^4(16169t^5 - 30391t^4u - 13023t^3u^2 + 22817t^2u^3 + 3506tu^4 - 6942u^5)$
$-2s^3(t+u)(14858t^5 - 31832t^4u + 17273t^3u^2 + 23882t^2u^3 + 1273tu^4 - 8164u^5)$
$-4s^2(t+u)^2(260t^5 - 1171t^4u - 2955t^3u^2 + 3776t^2u^3 - 1528tu^4 - 753u^5) - st(t+u)^3(208t^4$
$+5392t^3u - 10164t^2u^2 + 9544tu^3 - 5213u^4) + 12t^2u(t+u)^4(232t^2 - 232tu + 67u^2)]$
$-s^2[96s^9 + 8s^8(519t - 22u) + 4s^7(1395t^2 + 1447tu - 260u^2) - 6s^6(625t^3 + 358t^2u$
$+649tu^2 + 92u^3) - s^5(12099t^4 - 2111t^3u + 23601t^2u^2 + 2067tu^3 - 608u^4) - s^4(9513t^5$
$-24944t^4u + 1486t^3u^2 + 11472t^2u^3 - 12575tu^4 + 1312u^5) - 6s^3(t+u)(596t^5 - 3874t^4u$
$+1681t^3u^2 + 604t^2u^3 - 2541tu^4 + 648u^5) - 2s^2(t+u)^2(444t^5 - 1964t^4u$
$+3031t^3u^2 + 2304t^2u^3 - 3716tu^4 + 1444u^5) - su(t+u)^3(608t^4 - 1576t^3u + 1812t^2u^2$
$-1321tu^3 + 704u^4) - 3tu^2(t+u)^4(232t^2 - 232tu + 67u^2)],$

$A = 256Q^{16}s(49s^2 - 11st + 243t^2) - 128Q^{14}s[425s^3 + s^2(61t + 68u) - 7st(34t + 163u)$
$+9t^2(135t - 14u)] + 192Q^{12}s[565s^4 + s^3(753t + 317u) - s^2(624t^2 + 227tu - 241u^2)$
$-st(134t^2 + 1447tu - 643u^2) - 3t^2(771t^2 + 779tu + 239u^2)] - 32Q^{10}s[3523s^5$
$+5s^4(2243t + 348u) + 6s^3(265t^2 + 507tu - 451u^2) + 2s^2(9368t^3 + 9495t^2u + 5907tu^2$
$-1123u^3) - st(25922t^3 - 6987t^2u - 19623tu^2 - 4183u^3) + 9t^2(285t^3 + 1840t^2u$
$+1670tu^2 + 556u^3)] + 16Q^8s[2564s^6 + 19s^5(1168t - 235u) + s^4(10973t^2 - 3769tu$
$-13434u^2) + 2s^3(32611t^3 - 948t^2u - 13905tu^2 - 4025u^3) + s^2(3319t^4 + 51224t^3u$
$-24192t^2u^2 - 33026tu^3 - 1321u^4) - st(2599t^4 - 34853t^3u + 9564t^2u^2 + 32050tu^3$
$+12817u^4) + 9t^2(t+u)(180t^3 - 211t^2u - 1187tu^2 - 499u^3)] + 24Q^6s[880s^7$
$-10s^6(594t - 455u) - s^5(5508t^2 - 3169tu - 3085u^2) - s^4(20143t^3 - 24746t^2u$
$-5389tu^2 + 6032u^3) - s^3(22347t^4 - 9890t^3u - 27216t^2u^2 + 9660tu^3 + 8167u^4)$

$$
\begin{aligned}
&-s^2(9t^5+3014t^4u-33328t^3u^2-3876t^2u^3+11363tu^4+2720u^5)-st(t+u)(2780t^4\\
&+1886t^3u-4491t^2u^2+4661tu^3+3803u^4)-3t^2(t+u)^2(384t^3-664t^2u\\
&+415tu^2+194u^3)]-4Q^4s[4544s^8+4s^7(56t+2091u)-12s^6(481t^2-792tu\\
&+419u^2)-s^5(18620t^3-40275t^2u+15366tu^2+11117u^3)-s^4(51008t^4-114369t^3u\\
&+16449t^2u^2+36149tu^3-11325u^4)-3s^3(12373t^5+1095t^4u-14926t^3u^2+30592t^2u^3\\
&+669tu^4-7111u^5)+s^2(t+u)(2432t^5+20995t^4u+7298t^3u^2-34810t^2u^3+5578tu^4\\
&+7739u^5)-st(t+u)^2(8896t^4-16580t^3u+10257t^2u^2-2351tu^3-3821u^4)\\
&+9t^2(t+u)^3(240t^3-248t^2u+68tu^2+25u^3)]+2Q^2s^2[1072s^8+8s^7(832t-49u)\\
&+4s^6(1444t^2+2143tu-1509u^2)-2s^5(4922t^3+7689t^2u-2772tu^2+2165u^3)\\
&-s^4(15173t^4-19913t^3u+60255t^2u^2-21787tu^3-920u^4)-4s^3(2242t^5-13469t^4u\\
&-5631t^3u^2+10354t^2u^3-6857tu^4+807u^5)-2s^2(t+u)(3892t^5-2872t^4u+775t^3u^2\\
&+2434t^2u^3-7345tu^4+3106u^5)+2s(t+u)^2(1168t^5+3888t^4u-8764t^3u^2\\
&+2866t^2u^3+1776tu^4-1153u^5)-t(t+u)^3(272t^4+2048t^3u-2472t^2u^2\\
&+800tu^3+269u^4)]
\end{aligned}
\tag{A.20}
$$

Appendix B

Formulae concerning the calculation of $\sigma\left(e^{\pm}p \to e^{\pm}J/\psi X'\right)$ at $o(\alpha^2\alpha_s^2)$

B.1 The integration measure $\frac{d^{D-1}\vec{p}'}{(2\pi)^{D-1}2p'^0}$

In order to express $\frac{d^{D-1}\vec{p}'}{(2\pi)^{D-1}2p'^0}$ in terms of invariants we first have to express $d^{D-1}\vec{p}'$ in polar coordinates. Therefore we need to generalize the concept of polar coordinates from 3 to an arbitrary number $D-1$ of (spatial) dimensions. In $D-1=3$ dimensions polar coordinates are generally known to be defined by

$$\begin{aligned} p'^1 &= |\vec{p}'|\sin\theta_2\sin\theta_1 \ , \\ p'^2 &= |\vec{p}'|\sin\theta_2\cos\theta_1 \ , \\ p'^3 &= |\vec{p}'|\cos\theta_2 \end{aligned} \tag{B.1}$$

with $0 \le \theta_1 \le 2\pi$, $0 \le \theta_2 \le \pi$. As for the changeover to $D-1=4$ dimensions, we decompose the four dimensional vector $\vec{p}'$ into one component in 4-direction, which is given by $p'^4 = |\vec{p}'|\cos\theta_3$ with uniquely determined $\theta_3 \in [0,\pi]$, and one component of length $|\vec{p}'|\sin\theta_3$ in the three dimensional subspace spanned by the 1-, 2- and 3-directions. Parametrizing the latter component according to (B.1) we find as result for polar coordiantes in four dimensions

$$\begin{aligned} p'^1 &= |\vec{p}'|\sin\theta_3\sin\theta_2\sin\theta_1 \ , \\ p'^2 &= |\vec{p}'|\sin\theta_3\sin\theta_2\cos\theta_1 \ , \\ p'^3 &= |\vec{p}'|\sin\theta_3\cos\theta_2 \ , \\ p'^4 &= |\vec{p}'|\cos\theta_3 \ , \end{aligned} \tag{B.2}$$

where $0 \le \theta_1 \le 2\pi$, $0 \le \theta_2, \theta_3 \le \pi$. Continuating this construction procedure inductively to higher dimensions we end up with

$$p'^1 = |\vec{p}'|\prod_{j=1}^{D-2}\sin\theta_j \quad , \quad p'^{i>1} = |\vec{p}'|\cos\theta_{i-1}\prod_{j=i}^{D-2}\sin\theta_j \ ;$$

$$0 \leq \theta_1 \leq 2\pi \quad , \quad 0 \leq \theta_2, \theta_3, ..., \theta_{D-2} \leq \pi \tag{B.3}$$

as general result for polar coordinates in $D-1$ dimensions. Utilizing (B.3) we may write for $d^{D-1}\vec{p}'$

$$d^{D-1}\vec{p}' = |J_{D-1}| d\,|\vec{p}'| \prod_{i=1}^{D-2} d\theta_i \ , \tag{B.4}$$

where it follows for the Jacobi determinant J_{D-1}

$$J_{D-1} = \begin{vmatrix} \frac{\partial p'^1}{\partial|\vec{p}'|} & \frac{\partial p'^1}{\partial\theta_{D-2}} & \frac{\partial p'^1}{\partial\theta_{D-3}} & \cdots & \frac{\partial p'^1}{\partial\theta_1} \\ \frac{\partial p'^2}{\partial|\vec{p}'|} & \frac{\partial p'^2}{\partial\theta_{D-2}} & \frac{\partial p'^2}{\partial\theta_{D-3}} & \cdots & \frac{\partial p'^2}{\partial\theta_1} \\ \vdots & \vdots & \vdots & & \vdots \\ \frac{\partial p'^{D-1}}{\partial|\vec{p}'|} & \frac{\partial p'^{D-1}}{\partial\theta_{D-2}} & \frac{\partial p'^{D-1}}{\partial\theta_{D-3}} & \cdots & \frac{\partial p'^{D-1}}{\partial\theta_1} \end{vmatrix}$$

$$= \begin{vmatrix} \prod_{j=1}^{D-2}\sin\theta_j & |\vec{p}'|\cos\theta_{D-2}\prod_{j=1}^{D-3}\sin\theta_j & |\vec{p}'|\sin\theta_{D-2}\cos\theta_{D-3}\prod_{j=1}^{D-4}\sin\theta_j & ... & |\vec{p}'|\cos\theta_1\prod_{j=2}^{D-2}\sin\theta_j \\ \cos\theta_1\prod_{j=2}^{D-2}\sin\theta_j & |\vec{p}'|\cos\theta_1\cos\theta_{D-2}\prod_{j=2}^{D-3}\sin\theta_j & |\vec{p}'|\cos\theta_1\sin\theta_{D-2}\cos\theta_{D-3}\prod_{j=2}^{D-4}\sin\theta_j & ... & -\prod_{j=1}^{D-2}\sin\theta_j \\ \cos\theta_2\prod_{j=3}^{D-2}\sin\theta_j & |\vec{p}'|\cos\theta_2\cos\theta_{D-2}\prod_{j=3}^{D-3}\sin\theta_j & |\vec{p}'|\cos\theta_2\sin\theta_{D-2}\cos\theta_{D-3}\prod_{j=3}^{D-4}\sin\theta_j & ... & 0 \\ \vdots & \vdots & \vdots & & \vdots \\ \cos\theta_{D-3}\sin\theta_{D-2} & |\vec{p}'|\cos\theta_{D-2}\cos\theta_{D-3} & -|\vec{p}'|\sin\theta_{D-2}\sin\theta_{D-3} & ... & 0 \\ \cos\theta_{D-2} & -|\vec{p}'|\sin\theta_{D-2} & 0 & ... & 0 \end{vmatrix}$$

$$= \pm\,|\vec{p}'|\cos^2\theta_{D-2}\sin^{D-3}\theta_{D-2} \underbrace{\begin{vmatrix} \prod_{j=1}^{D-3}\sin\theta_j & |\vec{p}'|\cos\theta_{D-3}\prod_{j=1}^{D-4}\sin\theta_j & ... & |\vec{p}'|\cos\theta_1\prod_{j=2}^{D-3}\sin\theta_j \\ \cos\theta_1\prod_{j=2}^{D-3}\sin\theta_j & |\vec{p}'|\cos\theta_1\cos\theta_{D-3}\prod_{j=2}^{D-4}\sin\theta_j & ... & -\prod_{j=1}^{D-3}\sin\theta_j \\ \cos\theta_2\prod_{j=3}^{D-3}\sin\theta_j & |\vec{p}'|\cos\theta_2\cos\theta_{D-3}\prod_{j=3}^{D-4}\sin\theta_j & ... & 0 \\ \vdots & \vdots & & \vdots \\ \cos\theta_{D-3} & -|\vec{p}'|\sin\theta_{D-3} & ... & 0 \end{vmatrix}}_{J_{D-2}}$$

$$\pm\,|\vec{p}'|\sin^{D-1}\theta_{D-2} \underbrace{\begin{vmatrix} \prod_{j=1}^{D-3}\sin\theta_j & |\vec{p}'|\cos\theta_{D-3}\prod_{j=1}^{D-4}\sin\theta_j & ... & |\vec{p}'|\cos\theta_1\prod_{j=2}^{D-3}\sin\theta_j \\ \cos\theta_1\prod_{j=2}^{D-3}\sin\theta_j & |\vec{p}'|\cos\theta_1\cos\theta_{D-3}\prod_{j=2}^{D-4}\sin\theta_j & ... & -\prod_{j=1}^{D-3}\sin\theta_j \\ \cos\theta_2\prod_{j=3}^{D-3}\sin\theta_j & |\vec{p}'|\cos\theta_2\cos\theta_{D-3}\prod_{j=3}^{D-4}\sin\theta_j & ... & 0 \\ \vdots & \vdots & & \vdots \\ \cos\theta_{D-3} & -|\vec{p}'|\sin\theta_{D-3} & ... & 0 \end{vmatrix}}_{J_{D-2}} \ . \tag{B.5}$$

Thereby we have expanded the determinant in the second line with respect to its bottom row. Thus we have found the recursion formula

$$J_{D-1} = \pm\,|\vec{p}'|\sin^{D-3}\theta_{D-2} J_{D-2} \ . \tag{B.6}$$

Noting, that $|J_2| = |\vec{p}'|$, we find by induction the general formula

$$|J_{D-1}| = |\vec{p}'|^{D-2} \sin^{D-3}\theta_{D-2} \sin^{D-4}\theta_{D-3} ... \sin^2\theta_3 \sin\theta_2 \ . \tag{B.7}$$

Inserting (B.7) in (B.4) we obtain

$$d^{D-1}\vec{p}' = d\,|\vec{p}'|\,|\vec{p}'|^{D-2}\, d\theta_1 d\theta_2 \sin\theta_2 ... d\theta_{D-2} \sin^{D-3}\theta_{D-2} \ . \tag{B.8}$$

In the following we will assume, that $d^{D-1}\vec{p}'$ stands with an integrand, which only depends on θ_{D-2} and $|\vec{p}'|$. The integration over the residual variables θ_1, θ_2,..., θ_{D-3} then yields the surface

$$S_{D-2} = \frac{2\pi^{\frac{D-2}{2}}}{\Gamma\left(\frac{D-2}{2}\right)} \tag{B.9}$$

of the $D-2$ dimensional unit sphere. The proof of (B.9) is the following. For any arbitrary spherical symmetric function $f = f(|\vec{x}|)$ with $\vec{x} \in R^n$ it holds $\int d^n\vec{x} f(|\vec{x}|) = S_n \int d\,|\vec{x}|\,|\vec{x}|^{n-1} f(|\vec{x}|)$. Specifying f to be $\exp(-\vec{x}^2)$ the left hand side of this equation becomes $\pi^{n/2}$, while the right hand side becomes $S_n\Gamma(n/2)/2$ with the Euler Gamma function being defined by $\Gamma(z) = \int_0^\infty dt t^{z-1}\exp(-t)$. Thus it follows $S_n = 2\pi^{n/2}/\Gamma(n/2)$, which for $n = D-2$ yields (B.9). $d^{D-1}\vec{p}'$ then takes the form

$$d^{D-1}\vec{p}' = \frac{2\pi^{\frac{D-2}{2}}}{\Gamma\left(\frac{D-2}{2}\right)} d\,|\vec{p}'|\,|\vec{p}'|^{D-2}\, d\cos\theta \sin^{D-4}\theta \ , \tag{B.10}$$

where we renamed θ_{D-2} as θ. With (B.10) we may now write

$$\frac{d^{D-1}\vec{p}'}{(2\pi)^{D-1}2p'^0} = \frac{d\,|\vec{p}'|\,|\vec{p}'|\,d\cos\theta}{8\pi^2\Gamma\left(\frac{D-2}{2}\right)} \left(\frac{|\vec{p}'|^2\sin^2\theta}{4\pi}\right)^{\frac{D-4}{2}} \ , \tag{B.11}$$

where here and in the following we assume $p'^0 = |\vec{p}'|$. Specifying the photon parton center of mass system and choosing θ to be the angle between the momenta of the in and outgoing parton, $\theta = \angle(\vec{p},\vec{p}')$, we may apply (4.73) to express $d\,|\vec{p}'|\,|\vec{p}'|\,d\cos\theta$ in terms of $\hat{s}$, $\hat{t}$, $\hat{u}$ and Q^2, and we can identify $|\vec{p}'|^2\sin^2\theta$ with the square of P_T^* given in (4.96) (with $m' = 0$). This yields

$$\frac{d^{D-1}\vec{p}'}{(2\pi)^{D-1}2p'^0} = \frac{d\hat{t}d\hat{u}}{16\pi^2(\hat{s}+Q^2)\Gamma\left(\frac{D-2}{2}\right)} \left(\frac{\hat{t}(M^2Q^2+\hat{s}\hat{u})}{4\pi(\hat{s}+Q^2)^2}\right)^{\frac{D-4}{2}} \ . \tag{B.12}$$

After changing the variables from $\hat{t}$ and $\hat{u}$ to x and y according to (5.14), (5.15) we finally obtain

$$\frac{d^{D-1}\vec{p}'}{(2\pi)^{D-1}2p'^0} = d\mathrm{x}\ d\mathrm{y} \frac{\hat{s}}{32\pi^2}\left(\frac{16\pi}{\hat{s}}\right)^\epsilon \frac{1}{\Gamma(1-\epsilon)} (1-\mathrm{x})^{1-2\epsilon}(1-\mathrm{y}^2)^{-\epsilon} \ , \tag{B.13}$$

where $\epsilon = (4-D)/2$.

B.2 ρ- and +-distributions

A ρ-distribution $\left(f(z)\right)_\rho$ to an arbitrary function $f(z)$ is defined by the property, that

$$\int_\rho^1 dz(f(z))_\rho g(z) = \int_\rho^1 dz f(z)[g(z) - g(1)] \tag{B.14}$$

for any arbitrary regular function $g(z)$. Furthermore, we define a +-distribution by

$$(f(z))_+ = (f(z))_{\rho=0}, \tag{B.15}$$

if the variable z is x (as in (5.47)) or ξ (as in (5.52) or by

$$(f(z))_+ = (f(z))_{\rho=-1}, \tag{B.16}$$

if the variable z is y (as in the second line of (5.19)).

B.3 ϵ-expansion of $\frac{(16\pi)^\epsilon}{\Gamma(1-\epsilon)}(1-\mathrm{x})^{-1-2\epsilon}(1-\mathrm{y})^{-1-\epsilon}(1+\mathrm{y})^{-\epsilon}$

Let in the following $g(\mathrm{x})$ or $g(\mathrm{y})$, respectively, be an arbitrary regular test function. Furthermore let δ be an infinitesimal real positive number with $\delta \ll |\epsilon|$. Consider first the integral

$$\int_\rho^1 d\mathrm{x}(1-\mathrm{x})^{-1-2\epsilon} g(\mathrm{x}) = \underbrace{\int_{1-\delta}^1 d\mathrm{x}\frac{g(\mathrm{x})}{(1-\mathrm{x})^{1+2\epsilon}}}_{I_1} + \underbrace{\int_\rho^{1-\delta} d\mathrm{x}\frac{g(\mathrm{x})}{(1-\mathrm{x})^{1+2\epsilon}}}_{I_2} . \tag{B.17}$$

For I_1 we find

$$I_1 = \int_{1-\delta}^1 d\mathrm{x}\frac{1}{(1-\mathrm{x})^{1+2\epsilon}} \underbrace{g(\mathrm{x})}_{g(1)+o(\delta)} = g(1)\int_{1-\delta}^1 \frac{d\mathrm{x}}{(1-\mathrm{x})^{1+2\epsilon}}(1+o(\delta)) = -\frac{1}{2\epsilon}\delta^{-2\epsilon} g(1)(1+o(\delta))$$
$$= g(1)\left[-\frac{1}{2\epsilon} + \ln\delta - \epsilon\ln^2\delta + o(\epsilon^2)\right](1+o(\delta)) . \tag{B.18}$$

For I_2 we find

$$I_2 = \int_\rho^{1-\delta} d\mathrm{x}\frac{g(\mathrm{x})}{(1-\mathrm{x})^{1+2\epsilon}}$$
$$= \underbrace{\int_\rho^{1-\delta} d\mathrm{x}\frac{g(\mathrm{x})}{1-\mathrm{x}}}_{I_{21}} - 2\epsilon \underbrace{\int_\rho^{1-\delta} d\mathrm{x}\frac{\ln(1-\mathrm{x})}{1-\mathrm{x}} g(\mathrm{x})}_{I_{22}} + o(\epsilon^2) \tag{B.19}$$

with

$$I_{21} = \int_\rho^{1-\delta} d\mathrm{x}\frac{g(\mathrm{x}) - g(1)}{1-\mathrm{x}} + g(1)\int_\rho^{1-\delta}\frac{d\mathrm{x}}{1-\mathrm{x}}$$

$$= \int_\rho^1 d\mathrm{x}\frac{g(\mathrm{x})-g(1)}{1-\mathrm{x}} - \underbrace{\int_{1-\delta}^1 d\mathrm{x}\frac{g(\mathrm{x})-g(1)}{1-\mathrm{x}}}_{\int_{1-\delta}^1 d\mathrm{x}\frac{g'(1)(\mathrm{x}-1)+o\left((\mathrm{x}-1)^2\right)}{1-\mathrm{x}}=o(\delta)} + g(1)(2\ln\beta - \ln\delta)$$

$$= \int_\rho^1 d\mathrm{x}\left(\frac{1}{1-\mathrm{x}}\right)_\rho g(\mathrm{x}) + g(1)(2\ln\beta - \ln\delta) + o(\delta) \tag{B.20}$$

and

$$I_{22} = \int_\rho^{1-\delta} d\mathrm{x}\frac{\ln(1-\mathrm{x})}{1-\mathrm{x}}\left[g(\mathrm{x})-g(1)\right] + g(1)\int_\rho^{1-\delta} d\mathrm{x}\frac{\ln(1-\mathrm{x})}{1-\mathrm{x}}$$

$$= \int_\rho^1 d\mathrm{x}\frac{\ln(1-\mathrm{x})}{1-\mathrm{x}}\left[g(\mathrm{x})-g(1)\right] - \underbrace{\int_{1-\delta}^1 d\mathrm{x}\frac{\ln(1-\mathrm{x})}{1-\mathrm{x}}\left[g(\mathrm{x})-g(1)\right]}_{\int_{1-\delta}^1 d\mathrm{x}\frac{\ln(1-\mathrm{x})}{1-\mathrm{x}}[g'(1)(\mathrm{x}-1)+o((\mathrm{x}-1)^2)]=o(\delta\ln\delta)} + g(1)\left(2\ln^2\beta - \frac{1}{2}\ln^2\delta\right)$$

$$= \int_\rho^1 d\mathrm{x}\left(\frac{\ln(1-\mathrm{x})}{1-\mathrm{x}}\right)_\rho g(\mathrm{x}) + g(1)\left(2\ln^2\beta - \frac{1}{2}\ln^2\delta\right) + o(\delta\ln\delta)\ , \tag{B.21}$$

where $\beta = \sqrt{1-\rho}$. Putting all pieces together and performing the limit $\delta \to 0$ we obtain

$$\int_\rho^1 d\mathrm{x}(1-\mathrm{x})^{-1-2\epsilon}g(\mathrm{x}) = I_1 + I_{21} - 2\epsilon I_{22} + o(\epsilon^2)$$

$$= \int_\rho^1 \left[\delta(1-x)\underbrace{\left(-\frac{1}{2\epsilon} + \ln\beta^2 - \epsilon\ln^2\beta^2\right)}_{-\frac{\beta-4\epsilon}{2\epsilon}+o(\epsilon^2)} + \left(\frac{1}{1-\mathrm{x}}\right)_\rho - 2\epsilon\left(\frac{\ln(1-\mathrm{x})}{1-\mathrm{x}}\right)_\rho\right] g(\mathrm{x}) + o(\epsilon^2) \tag{B.22}$$

or equivalently

$$(1-\mathrm{x})^{-1-2\epsilon} = -\frac{\beta-4\epsilon}{2\epsilon}\delta(1-x) + \left(\frac{1}{1-\mathrm{x}}\right)_\rho - 2\epsilon\left(\frac{\ln(1-\mathrm{x})}{1-\mathrm{x}}\right)_\rho + o(\epsilon^2)\ . \tag{B.23}$$

Now turn to the integral

$$\int_{-1}^1 d\mathrm{y}(1-\mathrm{y})^{-1-\epsilon}(1+\mathrm{y})^{-\epsilon}g(\mathrm{y}) = \int_{-1}^1 d\mathrm{y}\frac{1}{1-\mathrm{y}}\left[\frac{1}{2}\left(\frac{1}{1+\mathrm{y}} + \frac{1}{1-\mathrm{y}}\right)\right]^\epsilon g(\mathrm{y})\ . \tag{B.24}$$

We decompose the integral on the right hand side into the sum of three integrals I_1, I_2 and I_3. Thereby I_1 is given by

$$I_1 = \int_{-1}^{-1+\delta} d\mathrm{y}\frac{1}{1-\mathrm{y}}\left[\frac{1}{2}\left(\frac{1}{1+\mathrm{y}} + \frac{1}{1-\mathrm{y}}\right)\right]^\epsilon g(\mathrm{y})$$

$$= \frac{1}{2^{1+\epsilon}}\int_{-1}^{-1+\delta} d\mathrm{y}\ \underbrace{\frac{1}{1-\frac{1+\mathrm{y}}{2}}}_{1+o(\delta)}\underbrace{\left(1+\frac{1+\mathrm{y}}{1-\mathrm{y}}\right)^\epsilon}_{1+\epsilon o(\delta)}(1+\mathrm{y})^{-\epsilon}\ \underbrace{g(\mathrm{y})}_{g(-1)+o(\delta)}$$

$$
\begin{aligned}
&= \frac{g(-1)}{2^{1+\epsilon}} \int_{-1}^{-1+\delta} d\mathrm{y}(1+\mathrm{y})^{-\epsilon}(1+o(\delta)) \\
&= \frac{g(-1)}{2^{1+\epsilon}} \frac{1}{1-\epsilon}\delta^{1-\epsilon}(1+o(\delta)) \ , \qquad \text{(B.25)}
\end{aligned}
$$

that is

$$
I_1 = 0 \qquad \text{(B.26)}
$$

in the limit $\delta \to 0$. I_2 is given by

$$
\begin{aligned}
I_2 &= \int_{-1+\delta}^{1-\delta} d\mathrm{y} \frac{1}{1-\mathrm{y}}(1-\mathrm{y}^2)^{-\epsilon} g(\mathrm{y}) \\
&= \int_{-1}^{1-\delta} d\mathrm{y} \frac{1}{1-\mathrm{y}} g(\mathrm{y}) - \epsilon \int_{-1}^{1-\delta} d\mathrm{y} \frac{\ln(1-\mathrm{y}^2)}{1-\mathrm{y}} g(\mathrm{y}) + o(\delta) \\
&= \int_{-1}^{1} d\mathrm{y} \frac{g(\mathrm{y})-g(1)}{1-\mathrm{y}} + g(1) \int_{-1}^{1-\delta} \frac{d\mathrm{y}}{1-\mathrm{y}} \\
&\quad -\epsilon \left[\int_{-1}^{1} d\mathrm{y} \frac{\ln(1-\mathrm{y}^2)}{1-\mathrm{y}} [g(\mathrm{y})-g(1)] + g(1) \int_{-1}^{1-\delta} d\mathrm{y} \frac{\ln(1-\mathrm{y}^2)}{1-\mathrm{y}} \right] + o(\delta) \\
&= \int_{-1}^{1} d\mathrm{y} \left(\frac{1}{1-\mathrm{y}} \right)_+ g(\mathrm{y}) - \epsilon \int_{-1}^{1} d\mathrm{y} \left(\frac{\ln(1-\mathrm{y}^2)}{1-\mathrm{y}} \right)_+ g(\mathrm{y}) \\
&\quad -g(1) \left[\ln \frac{\delta}{2} - \epsilon \left(\frac{\pi^2}{6} - \frac{3}{2} \ln^2 2 + \frac{1}{2} \ln \delta \ln 4\delta \right) \right] + o(\delta) \ . \qquad \text{(B.27)}
\end{aligned}
$$

I_3 finally is given by

$$
\begin{aligned}
I_3 &= \int_{1-\delta}^{1} d\mathrm{y} \frac{1}{1-\mathrm{y}} \left[\frac{1}{2} \left(\frac{1}{1+\mathrm{y}} + \frac{1}{1-\mathrm{y}} \right) \right]^{\epsilon} g(\mathrm{y}) \\
&= \frac{1}{2^{\epsilon}} \int_{1-\delta}^{1} d\mathrm{y} (1-\mathrm{y})^{-1-\epsilon} \underbrace{\left(1 + \frac{1-\mathrm{y}}{1+\mathrm{y}} \right)^{\epsilon}}_{1+\epsilon o(\delta)} \underbrace{g(\mathrm{y})}_{g(1)+o(\delta)} \\
&= \frac{g(1)}{2^{\epsilon}} \int_{1-\delta}^{1} d\mathrm{y} (1-\mathrm{y})^{-1-\epsilon} (1+o(\delta)) \\
&= -g(1) \frac{(2\delta)^{-\epsilon}}{\epsilon} (1+o(\delta)) \\
&= -g(1) \left[\frac{1}{\epsilon} - \ln(2\delta) + \frac{\epsilon}{2} \ln^2(2\delta) + o(\epsilon^2) \right] (1+o(\delta)) \ . \qquad \text{(B.28)}
\end{aligned}
$$

Putting all parts together we obtain in the limit $\delta \to 0$

$$
\begin{aligned}
&\int_{-1}^{1} d\mathrm{y} (1-\mathrm{y})^{-1-\epsilon} (1+\mathrm{y})^{-\epsilon} g(\mathrm{y}) = I_1 + I_2 + I_3 \\
&= \int_{-1}^{1} d\mathrm{y} \left[\left(\frac{1}{1-\mathrm{y}} \right)_+ - \epsilon \left(\frac{\ln(1-\mathrm{y}^2)}{1-\mathrm{y}} \right)_+ - \delta(1-\mathrm{y}) \left(\underbrace{\frac{1}{\epsilon} - \ln 4 + \frac{\epsilon}{2} \ln^2 4}_{\frac{4-\epsilon}{\epsilon} + o(\epsilon^2)} - \epsilon \frac{\pi^2}{6} \right) \right] g(\mathrm{y}) \\
&\quad + o(\epsilon^2) \qquad \text{(B.29)}
\end{aligned}
$$

or equivalently

$$(1-\mathrm{y})^{-1-\epsilon}(1+\mathrm{y})^{-\epsilon} = -4^{-\epsilon}\left\{\frac{1}{\epsilon}\delta(1-\mathrm{y}) - \left(\frac{1}{1-\mathrm{y}}\right)_+ - \epsilon\left[\frac{\pi^2}{6}\delta(1-\mathrm{y}) - \left(\frac{\ln\left(\frac{1}{4}(1-\mathrm{y}^2)\right)}{1-\mathrm{y}}\right)_+\right]\right\} + o(\epsilon^2)\ . \tag{B.30}$$

With (B.23) and (B.30) we immediately obtain (5.19) for the expansion of $\frac{(16\pi)^\epsilon}{\Gamma(1-\epsilon)}(1-\mathrm{x})^{-1-2\epsilon}(1-\mathrm{y})^{-1-\epsilon}(1+\mathrm{y})^{-\epsilon}$ up to order ϵ^0.

B.4 $f_a\left[{}^1S_0^{(8)}\right]$ and $g\left[{}^1S_0^{(8)}\right]$

The $f_a\left[{}^1S_0^{(8)}\right]$ defined in (5.58) can be decomposed into transverse and longitudinal parts according to

$$f_a\left[{}^1S_0^{(8)}\right] = T_a\left[{}^1S_0^{(8)}\right] - \frac{4(1-y)}{1+(1-y)^2}L_a\left[{}^1S_0^{(8)}\right] \tag{B.31}$$

with

$$\begin{aligned}
T_g\left[{}^1S_0^{(8)}\right] = {}& \frac{-3}{(1-\mathrm{x})(M^2+Q^2)(M^2+Q^2\mathrm{x})^3(M^2(1+\mathrm{x})+2Q^2\mathrm{x})^3} \\
& \times\Big\{16Q^{14}\mathrm{x}^7(1-\mathrm{x}) + 8M^2Q^{12}\mathrm{x}^6(5+\mathrm{x}-6\mathrm{x}^2) + 2M^4Q^{10}\mathrm{x}^5(35+5\mathrm{x}-7\mathrm{x}^2-33\mathrm{x}^3) \\
& + M^6Q^8\mathrm{x}^4(83+22\mathrm{x}-28\mathrm{x}^2-22\mathrm{x}^3-55\mathrm{x}^4) + 2M^8Q^6\mathrm{x}^3(31+15\mathrm{x}-2\mathrm{x}^2-22\mathrm{x}^3 \\
& - 5\mathrm{x}^4-17\mathrm{x}^5) + M^{10}Q^4\mathrm{x}^2(29+14\mathrm{x}+21\mathrm{x}^2-20\mathrm{x}^3-25\mathrm{x}^4-2\mathrm{x}^5-17\mathrm{x}^6) \\
& + 2M^{12}Q^2\mathrm{x}(4+\mathrm{x}+5\mathrm{x}^2+2\mathrm{x}^3-5\mathrm{x}^4-4\mathrm{x}^5-3\mathrm{x}^7) + M^{14}(1+\mathrm{x}^2+2\mathrm{x}^3-2\mathrm{x}^5-\mathrm{x}^6 \\
& - \mathrm{x}^8) + \Big[8Q^{14}\mathrm{x}^7 + 4M^2Q^{12}\mathrm{x}^6(1+8\mathrm{x}-\mathrm{x}^2) - 8M^4Q^{10}\mathrm{x}^5(1-6\mathrm{x}-2\mathrm{x}^2+\mathrm{x}^3) \\
& - 8M^6Q^8\mathrm{x}^4(3-10\mathrm{x}+2\mathrm{x}^4) - 2M^8Q^6\mathrm{x}^3(17-44\mathrm{x}-10\mathrm{x}^2+8\mathrm{x}^3-3\mathrm{x}^4+12\mathrm{x}^5) \\
& - 4M^{10}Q^4\mathrm{x}^2(6-11\mathrm{x}-10\mathrm{x}^2+2\mathrm{x}^3-\mathrm{x}^4-3\mathrm{x}^5+5\mathrm{x}^6) - 2M^{12}Q^2\mathrm{x}(4-4\mathrm{x}-11\mathrm{x}^2 \\
& - 2\mathrm{x}^4-4\mathrm{x}^5-3\mathrm{x}^6+4\mathrm{x}^7) - M^{14}(1-4\mathrm{x}^2-2\mathrm{x}^4-4\mathrm{x}^6+\mathrm{x}^8)\Big]\ln\mathrm{x} + \Big[4Q^{14}\mathrm{x}^7 \\
& - 2M^2Q^{12}\mathrm{x}^6(3-12\mathrm{x}+\mathrm{x}^2) - 4M^4Q^{10}\mathrm{x}^5(6-8\mathrm{x}-3\mathrm{x}^2-\mathrm{x}^3) - 2M^6Q^8\mathrm{x}^4(19-25\mathrm{x} \\
& + \mathrm{x}^2+\mathrm{x}^3-6\mathrm{x}^4) - 2M^8Q^6\mathrm{x}^3(20-30\mathrm{x}-3\mathrm{x}^2+7\mathrm{x}^3+\mathrm{x}^4-5\mathrm{x}^5) - M^{14}(1-3\mathrm{x}^2 \\
& - \mathrm{x}^4-\mathrm{x}^6) - 2M^{12}Q^2\mathrm{x}(4-3\mathrm{x}-8\mathrm{x}^2+\mathrm{x}^3-\mathrm{x}^4-\mathrm{x}^6) - M^{10}Q^4\mathrm{x}^2(25-32\mathrm{x}-25\mathrm{x}^2 \\
& + 10\mathrm{x}^3+3\mathrm{x}^4-2\mathrm{x}^5-3\mathrm{x}^6)\Big]\ln\frac{M^2+Q^2}{M^2+Q^2\mathrm{x}(2-\mathrm{x})}\Big\}\ ,
\end{aligned} \tag{B.32}$$

$$\begin{aligned}
L_g\left[{}^1S_0^{(8)}\right] = {}& \frac{-3M^2Q^2\mathrm{x}^2}{(1-\mathrm{x})(M^2+Q^2\mathrm{x})^3(M^2+Q^2\mathrm{x}(2-\mathrm{x}))(M^2(1+\mathrm{x})+2Q^2\mathrm{x})^3} \\
& \times\Big\{8Q^{10}\mathrm{x}^5(5-7\mathrm{x}+2\mathrm{x}^2) + 4M^2Q^8\mathrm{x}^4(23-12\mathrm{x}-13\mathrm{x}^2+2\mathrm{x}^4) + 2M^4Q^6\mathrm{x}^3(43+13\mathrm{x} \\
& - 32\mathrm{x}^2-20\mathrm{x}^3-11\mathrm{x}^4+7\mathrm{x}^5) + M^{10}(1+2\mathrm{x}+3\mathrm{x}^2-\mathrm{x}^4-2\mathrm{x}^5-3\mathrm{x}^6) + M^6Q^4\mathrm{x}^2(41 \\
& + 42\mathrm{x}-5\mathrm{x}^2-40\mathrm{x}^3-29\mathrm{x}^4-18\mathrm{x}^5+9\mathrm{x}^6) + 2M^8Q^2\mathrm{x}(5+8\mathrm{x}+6\mathrm{x}^2-5\mathrm{x}^3-5\mathrm{x}^4-8\mathrm{x}^5
\end{aligned}$$

$$
\begin{aligned}
&- 2\mathrm{x}^6 + \mathrm{x}^7) + 2(M^2+Q^2)\mathrm{x}\Big[4Q^8\mathrm{x}^4(4-\mathrm{x}^2) + 2M^2Q^6\mathrm{x}^3(16+6\mathrm{x}+11\mathrm{x}^2-10\mathrm{x}^3+\mathrm{x}^4)\\
&+ M^8(1+2\mathrm{x}+2\mathrm{x}^2+6\mathrm{x}^3+\mathrm{x}^4) + M^6Q^2\mathrm{x}(8+11\mathrm{x}+14\mathrm{x}^2+22\mathrm{x}^3-6\mathrm{x}^4-\mathrm{x}^5)\\
&+ 2M^4Q^4\mathrm{x}^2(12+10\mathrm{x}+16\mathrm{x}^2+5\mathrm{x}^3-8\mathrm{x}^4+\mathrm{x}^5)\Big]\ln\mathrm{x} + 2(M^2+Q^2)\mathrm{x}\Big[2Q^8\mathrm{x}^4(8-6\mathrm{x}\\
&+ \mathrm{x}^2) + M^8(1+2\mathrm{x}+\mathrm{x}^2+2\mathrm{x}^3) + M^6Q^2\mathrm{x}(8+10\mathrm{x}+3\mathrm{x}^2+6\mathrm{x}^3-3\mathrm{x}^4) + M^2Q^6\mathrm{x}^3(32\\
&- 4\mathrm{x}-\mathrm{x}^2-4\mathrm{x}^3+\mathrm{x}^4) + M^4Q^4\mathrm{x}^2(24+13\mathrm{x}+\mathrm{x}^2+2\mathrm{x}^3-5\mathrm{x}^4+\mathrm{x}^5)\Big]\\
&\times \ln\frac{M^2+Q^2}{M^2+Q^2\mathrm{x}(2-\mathrm{x})}\Bigg\}\ , \qquad \text{(B.33)}
\end{aligned}
$$

$$
\begin{aligned}
T_q\left[{}^1S_0^{(8)}\right] &= \frac{-4M^2}{3(M^2+Q^2)(M^2+Q^2\mathrm{x})^4(M^2+Q^2\mathrm{x}(2-\mathrm{x}))}\\
&\times\Big[M^{10}(1-\mathrm{x}) + 5M^8Q^2\mathrm{x}(1-\mathrm{x}) + 2Q^{10}\mathrm{x}^5(1-\mathrm{x}) + 2M^2Q^8\mathrm{x}^4(1-\mathrm{x})(3+\mathrm{x})\\
&+ M^6Q^4\mathrm{x}^2(1-\mathrm{x})(10+\mathrm{x}^2) + M^4Q^6\mathrm{x}^3(1-\mathrm{x})(10+2\mathrm{x}+\mathrm{x}^2) - M^2\Big(M^2\\
&+ Q^2\mathrm{x}(2-\mathrm{x})\Big)^2\Big(M^4(1-\mathrm{x}) + M^2Q^2\mathrm{x} + Q^4\mathrm{x}^2\Big)\ln\frac{(M^2+Q^2)\mathrm{x}}{M^2+Q^2\mathrm{x}(2-\mathrm{x})}\Big]\ , \qquad \text{(B.34)}
\end{aligned}
$$

$$
L_q\left[{}^1S_0^{(8)}\right] = \frac{-4M^4Q^2\mathrm{x}^2}{3(M^2+Q^2\mathrm{x})^4}\left[(M^2+Q^2\mathrm{x})(1-\mathrm{x}) + (M^2+Q^2)\mathrm{x}\ln\frac{(M^2+Q^2)\mathrm{x}}{M^2+Q^2\mathrm{x}(2-\mathrm{x})}\right]\ . \qquad \text{(B.35)}
$$

$g\left[{}^1S_0^{(8)}\right]$ introduced in (5.117) is given by

$$
\begin{aligned}
g\left[{}^1S_0^{(8)}\right] &= \frac{1}{36(M^2+Q^2)(M^2+2Q^2)^2}\\
&\times\Bigg\{3(49M^6+247M^4Q^2+416M^2Q^4+236Q^6)\ln\frac{\mu_R^2}{m^2} - 6(8M^6+41M^4Q^2\\
&+ 76M^2Q^4+52Q^6)\ln\frac{2\mu_R^2}{M^2+Q^2} + 6(10M^6+35M^4Q^2+42M^2Q^4+8Q^6)\\
&\times\ln\frac{2(M^2+Q^2)}{M^2} - \frac{3}{4}(M^2+Q^2)(M^2+2Q^2)^2\Bigg[8n_f\ln\frac{\mu_R^2}{\mu_F^2} + 288\ln\beta\,(1-2\ln\beta\\
&+ \ln\frac{\mu_F^2}{M^2}\Big) + 3\left(48\ln 2(1-\ln 2) + 4\ln\frac{\mu_F^2}{m^2}\left(11-12\ln\frac{M^2+Q^2}{M^2}\right)\right.\\
&+ \left.39\ln^2\frac{2(M^2+Q^2)}{M^2}\right)\Bigg] + 12\sqrt{Q^2(M^2+Q^2)}(M^2+2Q^2)^2\ln\frac{M(\sqrt{M^2+Q^2}-\sqrt{Q^2})}{(\sqrt{M^2+Q^2}+\sqrt{Q^2})^2}\\
&+ \frac{3}{2}(M^2+2Q^2)^2(17M^2+2Q^2)\ln^2\frac{\sqrt{M^2+Q^2}-\sqrt{Q^2}}{\sqrt{M^2+Q^2}+\sqrt{Q^2}}\\
&+ \frac{1}{2}\,(M^2+2Q^2)\Big(3(20-\pi^2)M^4 + 2(138-19\pi^2)M^2Q^2 + 8(27-8\pi^2)Q^4\\
&+ 81(M^4+3M^2Q^2+2Q^4)\mathrm{Li}_2\frac{M^2+2Q^2}{2(M^2+Q^2)}
\end{aligned}
$$

$$- \ 3(9M^4+59M^2Q^2+82Q^4)\mathrm{Li}_2\frac{-M^2-2Q^2}{M^2}\Bigg)\Bigg\} \ . \tag{B.36}$$

Bibliography

[1] H. Fritzsch, M. Gell-Mann, and H. Leutwyler, Phys. Lett. B 47 (1973) 365.

[2] J.J. Aubert et. al., Phys. Rev. Lett. 33 (1974) 1404;
J.-E. Augustin et. al., Phys. Rev. Lett. 33 (1974) 1406.

[3] Particle Data Group, D.E. Groom et. al., Eur. Phys. J. C 15 (2000) 1.

[4] H. Fritzsch, Phys. Lett. B 67 (1977) 217;
F. Halzen, Phys. Lett. B 69 (1977) 105;
F. Halzen and S. Matsuda, Phys. Rev. D 17 (1978) 1344;
M. Gluck, J. Owens, and E. Reya, Phys. Rev. D 17 (1978) 2324.

[5] R. Baier and R. Rückl, Phys. Lett. 102 B (1981) 364;
R. Baier and R. Rückl, Z. Phys. C 19 (1983) 251;
B. Humpert, Phys. Lett. B 184 (1987) 105;
R. Gastmans and W. Troost, T.T. Wu, Phys. Lett. B 184 (1987) 257;
R. Gastmans and W. Troost, T.T. Wu, Nucl. Phys. B 291 (1987) 731.

[6] E.L. Berger and D. Jones, Phys. Rev. D 23 (1981) 1521.

[7] R. Barbieri, M. Caffo, R.Gatto, and E. Remiddi, Phys. Lett. 95 B (1980) 93;
Nucl. Phys. B 192 (1981) 61;
R. Barbieri, M. Caffo, and E. Remiddi, Nucl. Phys. B 162 (1980) 220;
R. Barbieri, R.Gatto, and E. Remiddi, Phys. Lett. 61 B (1976) 465.

[8] B.A. Kniehl and L. Zwirner, Nucl. Phys. B 637 (2002).

[9] G.T. Bodwin, E. Braaten, G.P. Lepage, Phys. Rev. D 51 (1995) 1125;
G.T. Bodwin, E. Braaten, and G.P. Lepage, Phys. Rev. D 55 (1997) 5853, Erratum.

[10] S. Fleming and I.Maksymyk, Phys. Rev. D 54 (1996) 3608;
E. Braaten and Y.-Q.Chen, Phys. Rev. D 54 (1996) 3216.

[11] G.T. Bodwin, E. Braaten, and G.P. Lepage, Phys. Rev. D 46 (1992) R1914

[12] CDF Collaboration, F. Abe et al., Phys. Rev. Lett. 69 (1992) 3704;
CDF Collaboration, F. Abe et al., Phys. Rev. Lett. 71 (1993) 2537;

CDF Collaboration, F. Abe et al., Phys. Rev. Lett. 79 (1997) 572;
CDF Collaboration, F. Abe et al., Phys. Rev. Lett. 79 (1997) 578;
D0 Collaboration, S. Abachi et al., Phys. Lett. B 370 (1996) 239;
D0 Collaboration, B. Abbott et al., Phys. Rev. Lett. 82 (1999) 35.

[13] E. Braaten, S. Fleming, Phys. Rev. Lett. 74 (1995) 3327;
P. Cho, A.K. Leibovich, Phys. Rev. D 53 (1996) 150,
Phys. Rev. D 53 (1996) 6203.

[14] E. Braaten and T.C. Yuan, Phys. Rev. D 52 (1995) 6627,
Phys. Rev. Lett. 71 (1993) 1673.

[15] A. Petrelli, M.Cacciari, M. Greco, F. Maltoni, and M.L. Mangano,
Nucl. Phys. B 514 (1998) 245.

[16] B.A. Kniehl, C. Palisoc, and L. Zwirner, Phys. Rev. D 66 (2002) 114002.

[17] S. Fleming and I. Maksymyk, Phys. Rev. D 54 (1996) 3608,
C.S. Kim, J. Lee, and H.S. Song, Phys. Rev. D 55 (1997) 5429;
E. Braaten, M.A. Doncheski, S. Fleming, and M.L. Mangano,
Phys. Lett. B 333 (1994) 548;
D.P. Roy and K. Sridhar, Phys. Lett. B 339 (1994) 141;
M. Cacciari and M. Greco, Phys. Rev. Lett. 73 (1994) 1586;
S Gupta and K. Sridhar, Phys. Rev. D 54 (1996) 5545.

[18] M. Beneke and M. Krämer, Phys. Rev. D 55 (1997) 5269;
A.K. Leibovich, Phys. Rev. D 56 (1997) 4412;
B.A. Kniehl and J. Lee, Phys. Rev. D 62 (2000) 114027;
S. Fleming, A.K. Leibovich, I.Z. Rothstein,
Phys. Rev. D 64 (2001) 036002;
W.-K. Tang and M. Vänttinen, Phys. Rev. D 53 (1996) 4851;
Phys. Rev. D 54 (1996) 4349;
M. Beneke and I.Z. Rothstein, Phys. Rev. D 54 (1996) 2005.

[19] E. Braaten, B.A. Kniehl and J. Lee, Phys. Rev. D 62 (2000) 094005.

[20] B.A. Kniehl, C. Palisoc, and L. Zwirner, in preparation.

[21] P. Ko, J. Lee and H.S. Song, Phys. Rev. D 54 (1996) 4312,
Phys. Rev. D 60 (1999) 119902, Erratum.

[22] J. Amundson, S. Fleming, and I. Maksymyk, Phys.Rev.D 56 (1997) 5844;
T. Mehen, Phys. Rev. D 55 (1997) 4338;
B.A. Kniehl, G. Kramer, Phys. Lett. B 413 (1997) 416.

[23] F. Maltoni, M.L. Mangano and A. Petrelli,
Nucl. Phys. B 519 (1998) 361.

[24] M. Cacciari and M.Krämer, Phys. Rev. Lett. 76 (1996) 4128.

[25] M. Beneke, M. Krämer and M. Vänttinnen,
Phys. Rev. D 57 (1998) 4258.

[26] J.P. Ma, Nucl. Phys. B 460 (1996) 109.

[27] E. Braaten and Y.-Q. Chen, Phys. Rev. Lett. 76 (1996) 730.

[28] M. Klasen, B.A. Kniehl, L. Mihaila, and M. Steinhauser,
Nucl. Phys. B 609 (2001) 518;
M. Klasen, B.A. Kniehl, L. Mihaila, and M. Steinhauser,
hep-ph/0112259;
J.P. Ma, B.H.J. McKellar, and C.B. Paranavitane,
Phys. Rev. D 57 (1997) 606.

[29] K. Cheung, W.-Y. Keung, and T.C. Yuan,
Phys. Rev. Lett. 76 (1996) 877;
P. Cho, Phys. Lett. B 368 (1996) 171;
C.-F. Qiao, F. Yuan, and K.-T. Chao, Phys. Rev. D 55 (1997) 4001.

[30] P. Ko, J. Lee, and H.S. Song, Phys. Rev. D 53 (1996) 1409;
S. Fleming, O.F. Hernandez, I. Maksymyk, and H. Nadeau,
Phys. Rev. D 55 (1997) 4098.

[31] S. Fleming and T. Mehen, Phys. Rev. D 57 (1998) 1846;
S. Fleming, private communication.

[32] F. Yuan and K.-T. Chao, Phys. Rev. D 63 (2001) 034017.

[33] A.A. Petrov and T. Torma, Phys. Rev. D 60 (1999) 093009.

[34] B.A. Kniehl and L. Zwirner, Nucl. Phys. B 621 (2002) 337, L. Zwirner, J. Phys. G 28 (2002) 1011 (proceeding of the workshop "New Trends in HERA Physics 2001", Ringberg Castle, Tegernsee, Germany, 17-22 Jun 2001).

[35] B.A. Kniehl and L. Zwirner, hep-ph/0308164.

[36] E. Braaten, S. Fleming and T.C. Yuan, Ann. Rev. Nucl. Part. Sci. 46 (1996) 197;
M. Krämer, Prog. Part. Nucl. Phys. 47 (2001) 141.

[37] M.K. Gaillard, S.A. Jackson, and D.V. Nanopoulos, Nucl. Phys. B 102 (1976) 326;
M.K. Gaillard, S.A. Jackson, and D.V. Nanopoulos, Nucl. Phys. B 112 (1976) 545, Erratum.

[38] J.H. Kühn and R. Rückl, Phys. Lett. 95 B (1980) 431.

[39] J.H. Kühn, Acta Phys. Polon. B 12 (1981) 347.

[40] O. Nachtmann, Elementarteilchenphysik, Vieweg

[41] J.G. Körner, J. Cleymans, M. Kuroda, G.J. Gounaris, Phys. Lett. 114B (1982) 195.

[42] J.-Ph. Guillet, Z. Phys. C 39 (1988) 75.

[43] H. Merabet, J.F. Mathiot, R. Mendez-Galain, Z. Phys. C 62 (1994) 639.

[44] D. Krücker, PhD Thesis, RWTH Aachen, 1995.

[45] A.D. Martin, R.G. Roberts, W.J. Stirling, R.S. Thorne, Eur. Phys. J. C 4 (1998) 463.

[46] CTEQ Collaboration, H.L. Lai et al., Eur. Phys. J. C 12 (2000) 375.

[47] A. Meyer, PhD Thesis, Universität Hamburg, 1998, Report No. DESY-THESIS-1998-012;
A. Meyer, private communication;
S. Mohrdieck, private communication.

[48] H1 Collaboration, C. Adloff et al., Eur. Phys. J. C 25 (2002) 41;
H1 Collaboration, C. Adloff et al., Eur. Phys. J. C 10 (1999) 373;
B. Naroska, on behalf of the H1 and ZEUS Collaborations, in: S. Söldner-Rembold (Ed.), Photon 99: Proceedings of the International Conference on the Structure and Interactions of the Photon, including the 12th International Workshop on Photon-Photon Collisions, Freiburg, Germany, 23–27 May 1999, Nucl. Phys. B (Proc. Suppl.) 82 (2000) 187;
B. Naroska, on behalf of the H1 and ZEUS Collaborations, in: G. Grindhammer, B.A. Kniehl, G. Kramer, W. Ochs (Eds.), Proceedings of the Ringberg Workshop on New Trends in HERA Physics 2001, Tegernsee, Germany, 17–22 June 2001, J. Phys. G (to appear);
A. Bertolin, on behalf of the H1 and ZEUS Collaborations, in: K. Huitu, H. Kurki-Suonio, J. Maalampi (Eds.), High Energy Physics 99: Proceedings of the International Europhysics Conference on High Energy Physics, Tampere, Finland, 15–21 July 1999, Institute of Physics Publishing, Bristol and Philadelphia, 2000, p. 580.

[49] M. Beneke, I.Z. Rothstein, and M.B. Wise, Phys.Lett.B 408 (1997) 373.

[50] M. Glück, E. Reya, A. Vogt, Z. Phys. C 67 (1995) 433.

[51] CHORUS Collaboration, E. Eskut et al., Phys. Lett. B 503 (2001) 1.

[52] M. Mezzetto, on behalf of the NOMAD Collaboration, Nucl. Phys. B (Proc. Suppl.) 91 (2001) 184;
K. Zuber, private communication.

[53] R.L. Anderson et al., Phys. Rev. Lett. 38 (1977) 263.

[54] Tagged-Photon Spectrometer Collaboration, M.D. Sokoloff et al., Phys. Rev. Lett. 57 (1986) 3003.

[55] European Muon Collaboration, J.J. Aubert et al., Phys. Lett. 152 B (1985) 433.

[56] New Muon Collaboration, P. Amaudruz et al., Nucl. Phys. B 371 (1992) 553.

[57] Fermilab E706 Collaboration, L. Apanasevich et al., Phys. Rev. Lett. 81 (1998) 2642.

[58] L.N. Hand, Phys. Rev. 129 (1963) 1834.

[59] New Muon Collaboration, M. Arneodo et al., Phys. Lett. B 332 (1994) 195.

[60] Fermilab E203 Collaboration, A.R. Clark et al., Phys. Rev. Lett. 43 (1979) 187.

[61] T. Weiler, Phys. Rev. Lett. 44 (1980) 304.

[62] M. de Jong, PhD Thesis, Free University of Amsterdam, 1991.

[63] T. Kinoshita, J. Math. Phys. 3 (1962) 650;
T.D. Lee and M. Nauenberg, Phys. Rev. B 133 (1964) 1549.

[64] G. Passarino and M. Veltman, Nucl. Phys. B 160 (1979) 151.

[65] F.J.Yndurain, The Theory of Quark and Gluon Interactions, Springer Verlag.